

**A MULTI-COMPARTMENT PHARMACOKINETIC MODEL OF  
5-FLUOROURACIL AND DIHYDROFLUOROURACIL**

**OLUSOJI OLATUNDE OSUNBIYI**  
**Bachelor of Technology, Federal University of Technology, Minna, 2012**

A thesis/project submitted  
in partial fulfilment of the requirements for the degree of

**MASTER OF SCIENCE**

in

**PHYSICS**

Department of Physics and Astronomy  
University of Lethbridge  
LETHBRIDGE, ALBERTA, CANADA

© Olusoji Olatunde Osunbiyi, 2020

A MULTI-COMPARTMENT PHARMACOKINETIC MODEL OF 5-FLUOROURACIL  
AND DIHYDROFLUOROURACIL

OLUSOJI OLATUNDE OSUNBIYI

Date of Defence: November 22, 2019

Dr. Kenneth J. E. Vos Supervisor	Associate Professor	Ph.D.
Dr. Steve Patitsas Thesis Examination Committee Member	Associate Professor	Ph.D.
Dr. Stacey Wetmore Thesis Examination Committee Member	Professor	Ph.D.
Dr. Arundhati Dasgupta Chair, Thesis Examination Com- mittee	Associate Professor	Ph.D.

# Dedication

To God Almighty who is the source of all wisdom. To my late mother, Maria Taiwo Osunbiyi, and my late father, Chief Amos Oladiti Osunbiyi.

# Abstract

5-Fluorouracil (5-FU) is extensively biotransformed to dihydrofluorouracil (DHFU) by the dihydropyrimidine dehydrogenase enzyme (DPD) that catalyzes the reduction of uracil and thymine. This research involves the development of intensive quantitative compartment models that predict the time course of 5-FU and DHFU in the body using the Runge-Kutta fourth order method. The parameters within our system of nonlinear differential equations were determined by fitting the models to the clinical data. We showed that the one-compartment model was insufficient to describe the kinetics of 5-FU and that a minimum of two compartments is needed. The area under the curve (AUC), maximum concentration ( $C_{max}$ ), and half-life ( $t_{1/2}$ ) were obtained from the theoretical solutions to our models. Further work was done on how age and gender influence the drug's interaction with the body. It was determined that age reduces the rate of elimination and women are more prone to toxic effects.

# Acknowledgments

I would like to acknowledge the efforts of my supervisor that made it possible for me to achieve the level of master degree. My sincere thanks goes to Dr. Ken Vos, who has been the brain and the motivation behind my success. I remember the first day I received a response mail from him to be part of his research team, it was a testimony. What an amazing opportunity for me to pursue my long term interest with western world professionals. The letter was timely to receive because I almost lost interest in furthering applying for the master degree program in Alberta universities. I see Dr. Ken Vos as a person that revived my hope to pursue my ambitions. Since I resumed my program almost three years ago, working with him prepared me for handling multi-tasked assignments at a steady pace and to never accept the words "it is impossible". I am so privileged to have this opportunity to work with him. All I can say is a big "*thank you*" for the professional support and insights he rendered to me.

My academic pursuits at the University of Lethbridge led me to meet several people of high reputation, who have contributed to my success in one way or the other. I extend my gratitude to Dr. Steve Patitsas and Dr. Stacey Wetmore, they have opened my eyes to several precautions that helped me through the research work. It is a privilege to have them as my supervisory committee members. I also acknowledge the administrative supports and contributions received from every member of the physics and astronomy department. Thank you all.

This research was enabled in part by support provided by WestGrid ([www.westgrid.ca](http://www.westgrid.ca)) and Compute Canada ([www.computecanada.ca](http://www.computecanada.ca)). Thank you for the access we were given to the graham and cedar servers. These facilities speeded up the numerical calculations

involved.

My sincere appreciation also goes to my brother, Samuel Oludele Olubiyi, for the countless support, motivation and encouragement. He made me realize that if I could see it then I can be it. I now realize the little push, little encouragement and support birthed my great success. I can never thank you enough for believing in me all this time. *Thank you a million times.*

Thank you.

# Contents

<b>Contents</b>	<b>vii</b>
<b>List of Tables</b>	<b>x</b>
<b>List of Figures</b>	<b>xiii</b>
<b>List of Abbreviations</b>	<b>1</b>
<b>List of Symbols</b>	<b>4</b>
<b>1 Introduction</b>	<b>6</b>
1.1 Background . . . . .	6
1.2 Pharmacokinetics . . . . .	9
1.2.1 History of Pharmacokinetics . . . . .	9
1.2.2 The Principles of PK . . . . .	11
1.2.3 PK Models . . . . .	18
1.2.4 Michaelis-Menten Kinetics Model Equation . . . . .	20
1.3 5-FU and Its Metabolites . . . . .	21
1.3.1 Mechanism Pathway of 5-FU and Its Metabolites . . . . .	21
1.3.2 5-FU Related Severe Toxicity . . . . .	22
1.3.3 The Quality of Life During and After Treatment with 5-FU . . . . .	24
1.3.4 Technique of 5-FU Administration . . . . .	24
1.4 Specific Aims . . . . .	25
1.5 Overview . . . . .	26
<b>2 Methodology</b>	<b>28</b>
2.1 Methods . . . . .	28
2.1.1 Four-Compartment Model Analysis of 5-FU . . . . .	28
2.1.2 Model . . . . .	31
2.1.3 PK Modelling Parameters . . . . .	39
2.1.4 Numerical Modelling Tools . . . . .	40
2.2 Summary . . . . .	46
<b>3 Model Sampling Design and Analysis for 5-FU</b>	<b>48</b>
3.1 One-Compartment Model . . . . .	49
3.1.1 Optimisation with Fixed Degree Exponents . . . . .	50
3.1.2 Optimisation with Variable Exponents . . . . .	52
3.2 Two-Compartment Model . . . . .	56

3.2.1	Fixed Exponents with Elimination from Compartment 1 . . . . .	56
3.2.2	Fixed Exponents with Elimination from Compartment 2 . . . . .	59
3.2.3	Variable Exponents with Elimination from Compartment 1 . . . . .	63
3.2.4	Variable Exponents with Elimination from Compartment 2 . . . . .	66
3.2.5	Variable Exponents and Saturation Limiting Interaction . . . . .	69
3.3	Three-Compartment Model . . . . .	75
3.3.1	Fixed Exponents Minimisation for the Three-Compartment Model .	76
3.3.2	Variable Exponents' Minimisation for the Three-Compartment Model	80
3.4	Summary . . . . .	83
<b>4</b>	<b>Model Sampling Design and Analysis for DHFU</b>	<b>84</b>
4.1	One-Compartment DHFU Model . . . . .	85
4.1.1	Fixed Degree Exponents, One-Molecule Model . . . . .	85
4.1.2	Variable Exponents, One-Molecule, One-Compartment Model . . .	88
4.2	Variable Exponents, the Two-Molecule One-Compartment Model . . . . .	91
4.3	(1+2) Two-Compartment DHFU Model . . . . .	94
4.3.1	Fixed Exponents, One-Molecule Two-Compartment Model . . . . .	94
4.3.2	Variable Exponents, One-Molecule Two-Compartment Model . . .	96
4.4	Two-Molecule (1+2) Two-Compartment DHFU Model . . . . .	99
4.5	Summary . . . . .	101
<b>5</b>	<b>Results and Applications</b>	<b>103</b>
5.1	AUC, $C_{max}$ , and Half-life for 5-FU . . . . .	104
5.2	AUC, $C_{max}$ , and Half-life for DHFU . . . . .	107
5.3	The Theoretical Solutions Compared to the Clinical Data for 5-FU . . . . .	110
5.3.1	Comparison to the 5-FU Results From G. Bocci et al. [81] . . . . .	110
5.3.2	Comparison to the 5-FU Results From J. G. Maring et al. [84] . . .	112
5.4	Comparison to the DHFU Results from J. G. Maring et al. [84] . . . . .	114
5.5	The Influence of Gender and Age . . . . .	116
5.5.1	The PK Parameters Responsible for Gender Influence on 5-FU . . .	117
5.5.2	AUC, $C_{max}$ , and Half-life for Gender Differences . . . . .	119
5.5.3	The PK Parameters Responsible for Gender Influence on DHFU . .	119
5.5.4	The PK Parameters Responsible for Age Influence on 5-FU . . . . .	123
5.5.5	The PK Parameters Responsible for Age Influence on DHFU . . . . .	126
5.6	Summary . . . . .	129
<b>6</b>	<b>Conclusion</b>	<b>130</b>
	<b>Bibliography</b>	<b>134</b>
<b>A</b>	<b>Dictionary</b>	<b>144</b>
<b>B</b>	<b>Weighted Variance</b>	<b>150</b>
B.1	Effects of $S_{\sigma}$ Results Compared to the $S_p$ Results . . . . .	150
B.1.1	One-Compartment Model Optimization with $S_{\sigma}$ . . . . .	150
B.1.2	(1+2) Two-Compartment Model with $S_{\sigma}$ Minimization . . . . .	151

---

B.1.3	Three-Compartment Model with $S_\sigma$ Minimization . . . . .	154
B.2	$AUC$ , $C_{max}$ , and $t_{1/2}$ for 5-FU . . . . .	154
B.3	Minimization of the Weighted Variance ( $S_\sigma$ ) for DHFU . . . . .	155
B.3.1	$S_\sigma$ Minimization for Case 2 of the One-Compartment Model . . . . .	155
<b>C</b>	<b>Graphs</b>	<b>159</b>
<b>D</b>	<b>Tables</b>	<b>168</b>

# List of Tables

1.1	Common Terminology Criteria for Adverse Effects (CTCAE) [61] . . . . .	16
2.1	Groups of molecules and their accessible compartments. . . . .	31
3.1	The clinical datasets . . . . .	49
3.2	5-FU parameters for the one-compartment model with fixed exponents . . .	50
3.3	5-FU transition parameters for the one-compartment model with fixed exponents. . . . .	52
3.4	5-FU parameters for the one-compartment model with variable exponents .	52
3.5	5-FU transition times for the one-compartment model with variable exponents. . . . .	54
3.6	5-FU parameters for the (1+3) two-compartment model with fixed exponents	57
3.7	5-FU transition parameters for the (1+3) two-compartment model with fixed exponents. . . . .	59
3.8	5-FU parameters for the (1+2) two-compartment model with fixed exponents	60
3.9	5-FU transition parameters for the (1+2) two-compartment model with fixed exponents. . . . .	62
3.10	5-FU parameters for the (1+3) two-compartment model with variable exponents . . . . .	63
3.11	5-FU transition parameters for the (1+3) two-compartment model with variable exponents. . . . .	65
3.12	5-FU transition parameters for the (1+3) two-compartment model with variable exponents. . . . .	65
3.13	5-FU parameters for the (1+2) two-compartment model with variable exponents . . . . .	66
3.14	5-FU transition parameters for the (1+2) two-compartment model with variable exponents. . . . .	68
3.15	5-FU parameters at the maximum elimination rate for the (1+2) two-compartment model with variable exponents. . . . .	69
3.16	5-FU parameters for the (1+2) two-compartment model with saturation limiting function . . . . .	70
3.17	5-FU transition parameters for the (1+2) two-compartment model with variable exponents. . . . .	74
3.18	5-FU parameters at the maximum elimination rate for the (1+2) two-compartment model with variable exponents. . . . .	75
3.19	5-FU parameters for the three-compartment model with fixed exponents . .	77
3.20	5-FU transition parameters for the three-compartment model with fixed exponents. . . . .	79

3.21	5-FU parameters for the three-compartment model with variable exponents.	80
3.22	5-FU transition parameters for the three-compartment model with variable exponents. . . . .	82
3.23	5-FU transition parameters for the three-compartment model with variable exponents. . . . .	82
4.1	The clinical datasets of DHFU . . . . .	85
4.2	DHFU parameters for the one-molecule one-compartment model with fixed exponents . . . . .	86
4.3	DHFU transition parameters for the one-compartment model with fixed exponents. . . . .	88
4.4	DHFU parameters for the one-molecule one-compartment model with variable exponents . . . . .	89
4.5	DHFU transition parameters for the one molecule one-compartment model with variable exponents. . . . .	91
4.6	DHFU parameters for the two-molecule one-compartment model with variable exponents . . . . .	92
4.7	DHFU transition times for the two-molecule one-compartment models with variable exponents. . . . .	94
4.8	DHFU parameters for the one-molecule two-compartment model with fixed exponents. . . . .	95
4.9	DHFU parameters for the one-molecule two-compartment model with variable exponents. . . . .	97
4.10	DHFU transition times for the one-molecule two-compartment models with variable exponents. . . . .	98
4.11	5-FU and DHFU PK parameters for the two-molecule two-compartment model with variable exponents. . . . .	99
4.12	DHFU transition times for the two-molecule two-compartment models with variable exponents. . . . .	100
4.13	DHFU maximum elimination times for the two-molecule two-compartment models. . . . .	101
5.1	Comparison of the <i>AUC</i> of the 5-FU theoretical models to clinical estimates	104
5.2	Comparison of the $C_{max}$ of the 5-FU theoretical models to the clinical estimates . . . . .	105
5.3	Comparison of the $t_{1/2}$ of the theoretical models to the clinical estimates . . . . .	106
5.4	Comparison of the <i>AUC</i> of the DHFU theoretical models to the clinical estimates . . . . .	107
5.5	Comparison of the $C_{max}$ of the theoretical models to the clinical estimates for DHFU. . . . .	109
5.6	Comparison of the $t_{1/2}$ of the theoretical models to the clinical estimates for DHFU. . . . .	110
5.7	Comparison of the theoretical models to G. Bocci et al. [81] . . . . .	111
5.8	Comparison of the <i>AUC</i> of the 5-FU theoretical models to J. G. Maring et al. [84]. . . . .	113

---

5.9	The quantities of the theoretical models compared to the clinical results for DHFU. . . . .	115
5.10	PK values for gender influence on 5-FU . . . . .	117
5.11	Comparison of the theoretical results and clinical results for gender difference	120
5.12	PK values for gender influence on DHFU . . . . .	121
5.13	PK values for age influence on 5-FU . . . . .	123
5.14	Comparison of the theoretical results and clinical estimates for age difference. . . . .	125
5.15	PK values for age influence on DHFU . . . . .	127
B.1	The PK values for cases 1, 1.4, 2, and 2.2, one-compartment model with $S_{\sigma}$ minimization. . . . .	150
B.2	Cases 1, 1.4, 2, and 3.3 of the (1+2) two-compartment model with $S_{\sigma}$ minimized . . . . .	151
B.3	The PK values for case 2 of the three-compartment model . . . . .	154
B.4	The observable quantities in comparing $S_p$ and $S_{\sigma}$ . . . . .	155
B.5	The DHFU PK values for case 2, one-compartment model . . . . .	156
B.6	PK values for gender influence on 5-FU . . . . .	156
B.7	PK values for gender influence on DHFU . . . . .	157
B.8	PK values for age influence on 5-FU . . . . .	157
B.9	PK values for age influence on DHFU . . . . .	157
D.1	Digitized clinical datasets for 5-Fu . . . . .	168
D.2	Digitized clinical datasets for DHFU . . . . .	169
D.3	Digitized clinical datasets for 5-Fu comparison . . . . .	170
D.4	Digitized clinical datasets for DHFU comparison from Maring J. G. et al.[79]	170

# List of Figures

1.1	Chemical structure of 5-FU [6]. . . . .	8
1.2	Metabolic pathways of 5-FU [67]. . . . .	23
2.1	Systemic inter-flows for the one- to four-compartment PK models. . . . .	29
2.2	Summarised metabolic pathways of 5-FU. . . . .	30
2.3	Kinetic flows of molecule $d1$ between compartments $c1$ and $c2$ . . . . .	33
2.4	Change of molecule $d1$ to molecule $d2$ in compartment $c1$ . . . . .	36
2.5	Change of molecule $d1$ into two molecules $d2$ and $d3$ in compartment $c1$ . . . . .	37
2.6	The binding of molecules $d1$ and $d2$ to create molecule $d3$ in compartment $c1$ . . . . .	39
2.7	Schematic drawing of the model algorithm. . . . .	44
3.1	5-FU concentration for case 1.3 of the one-compartment model . . . . .	51
3.2	5-FU concentration for the one-compartment model with variable exponents . . . . .	55
3.3	5-FU concentration for case 1.3 of the two-compartment models. . . . .	58
3.4	5-FU concentration for case 2 of the (1+3) two-compartment model . . . . .	64
3.5	5-FU concentration for case 2 of the (1+2) two-compartment model . . . . .	69
3.6	5-FU concentration for case 3.1 of the (1+2) two-compartment models . . . . .	72
3.7	5-FU concentration for case 1.3 of the three-compartment model . . . . .	78
3.8	5-FU concentration for case 2 of the three-compartment model . . . . .	81
4.1	DHFU concentration for the fixed exponents of the one-molecule one-compartment model . . . . .	87
4.2	DHFU concentration for case 2 of the one-compartment model . . . . .	90
4.3	DHFU concentration for case 2.2 of the two-molecule one-compartment model . . . . .	93
4.4	DHFU concentration for case 1 of the one-molecule (1+2) two-compartment model . . . . .	96
4.5	DHFU concentration for case 2 of the one-molecule two-compartment model . . . . .	97
4.6	DHFU concentration for case 2 of the two-molecule two-compartment model . . . . .	100
5.1	Comparison of the theoretical models to G. Bocci et al. [1] for 5-FU results. . . . .	112
5.2	Comparison of the theoretical models to J. G. Maring et al. [2] for 5-FU results. . . . .	114
5.3	Comparison of the theoretical solution to J. G. Maring et al. DHFU results. . . . .	115
5.4	Concentration versus time curve for 5-FU comparing the effects of gender. . . . .	118
5.5	Concentration versus time curve for DHFU comparing the effect of gender. . . . .	122
5.6	Concentration versus time curve for 5-FU comparing the effects of age. . . . .	124
5.7	Concentration curve for DHFU illustrating the effects of age . . . . .	128

---

B.1	5-FU concentration for case 1.4 (Part A) and case 2.2 (Part B) of the one-compartment model with $S_G$ minimized . . . . .	152
B.2	5-FU concentration for cases 2 and 3.3 of the (1+2) two-compartment model with $S_G$ minimized . . . . .	153
B.3	5-FU concentration for case 2 of the three-compartment model with $S_G$ minimized . . . . .	155
B.4	DHFU concentration for case 2 of the one-compartment model . . . . .	156
C.1	5-Fu concentration curve for case 1.3, one-compartment model . . . . .	159
C.2	5-Fu concentration for case 2.2, one-compartment model . . . . .	160
C.3	5-Fu concentration for case 1.3, (1+3) two-compartment model . . . . .	160
C.4	5-Fu concentration for case 1.3, (1+2) two-compartment model . . . . .	161
C.5	5-Fu concentration for case 2 of the (1+3) two-compartment model . . . . .	161
C.6	5-Fu concentration for case 2 of the (1+2) two-compartment model . . . . .	162
C.7	5-Fu concentration for case 3.3, (1+2) two-compartment model . . . . .	162
C.8	5-Fu concentration for case 1.3, three-compartment model . . . . .	163
C.9	5-Fu concentration for case 2, three-compartment model optimization . . . . .	163
C.10	DHFU concentration for cases 1 and 1.3, one-molecule one-compartment model . . . . .	164
C.11	DHFU concentration for cases 2 and 2.2, one-molecule one-compartment model . . . . .	165
C.12	DHFU concentration for cases 2 and 2.2 of two-molecule one-compartment model . . . . .	166
C.13	DHFU concentration for case 2, two-molecule two-compartment model . . . . .	167

# List of Abbreviations

5-Fu	5-fluorouracil
ADMB	AD Model Builder
ADME	Absorption, Distribution, Metabolism, and Elimination
AUC	Area Under Curve
BSD	Berkeley Software Distribution
BOBYQA	Bound Optimization BY Quadratic Approximation
CERN	European Organization for Nuclear Research
COBYLA	Constrained optimization by linear approximation
CPR	Cytochrome P450-Reductase
CYP	Cytochrome P450
cytb5	Cytochrome b5
DHFU	Dihydrofluorouracil
DNA	Deoxyribonucleic Acid
DPYD	Dihydropyrimidine Dehydrogenase
DPYS	Dihydropyrimidinase
FBAL	Alpha-fluoro-beta-alanine
F-dUMP	5-fluoro-deoxyuridine monophosphate
F-dUTP	5-fluorodeoxyuridine triphosphate

F-UMP	5-fluoroxuridine monophosphate
FUPA	Fluoro-beta-ureidopropionate
FUR	Fluorouridine
F-UTP	5-fluorouridine triphosphate
GPL	General Public License
GI	Gastrointestinal
ISO	International Standards Organization
LGPL	Library General Public License
LINCOA	LINearly Constrained Optimization Algorithm
MRT	Mean Residence Time
NEWUOA	Numerical Unconstrained Optimization Algorithm
NCI	National Cancer Institute
NIH	National Institutes of Health
NLopt	Nonlinear optimization Library
PPAT	Glutamine Phosphoribosylpyrophosphate Amino Transferase
RNA	Ribonucleic Acid
RPMI	Roswell Park Memorial Institute
TK1	Thymidine Kinase
TOLMIN	Numerical Linear Constrained Optimization Algorithm
TYMP	Thymidylate Phosphorylase
UCK	Uridine-Cytidine Kinase

UMPS	Uridine Monophosphate Synthase
UOBYQA	Unconstrained Optimization BY Quadratic Approximation
UPB1	Beta-Ureidopropionase
UPP	Uridine Phosphorylase
USPHS	United States Public Health Service
WHO	World Health Organization

# List of Symbols

$V_d$	the volume of distribution
$k$	the rate constant
$\lambda$	terminal exponential coefficient
$V_{\lambda z}$	the volume of distribution at pseudo-distribution equilibrium
$d$	amount of molecule
$c$	compartment
$\frac{dX}{dt}$	The rate of change of the amount of molecule
$I_{d1,c1}$	the infusion of molecule $d1$ into compartment $c1$
$A$	exponent with kinetic rate coefficient
$B$	exponent with saturation coefficient
$H$	the Heaviside step function
$\bar{k}$	the effective rate constant
$\Gamma$	the saturation parameter
	the change from one type of molecule to another type of molecule
	separation of the molecules involved in the reaction from the molecules interfering with the reaction
$X$	the amount of molecules
$\delta$	the parameter that enforces conservation of mass

$\alpha$	the saturation limiting numerator factor
$\beta$	the saturation limiting denominator factor
$C_{max}$	peak plasma concentration
$t_{max}$	time of peak plasma concentration
$t_{1/2}$	half-life
$p$	the order process
$C$	the concentration of molecule
$S_p$	the weighted percentage variance
$S_\sigma$	the weighted variance
$N_p$	the total weight of the patients
$j, k$	the flows or conversion from compartment $j$ to compartment $k$

# Chapter 1

## Introduction

---

*A chemical cannot be a drug, no matter how active nor how specific its action,  
unless it is also taken appropriately into the body (absorption),  
distributed to the right parts of the body,  
metabolized in a way that does not instantly remove its activity,  
and eliminated in a suitable manner.*

*A compound must get in, move about, hang around, and then get out.*

–John Hodgson

---

### 1.1 Background

The first significant breakthrough in pharmacokinetics (PK) occurred in the 1910s when the tumour systems in rodents were transplanted by George Clowes of Roswell Park Memorial Institute (RPMI) in Buffalo. Dr. Clowes used these tumour systems for chemotherapeutic tests and later conceived the idea of standardized model systems and the testing of chemicals [3]. Their work encouraged many researchers to focus on the development of models that would minimize the cost of severe side-effects that sprung up as a result of the increasing trend of chemotherapy treatments [4]. The outcome of these great works from Dr. Clowes [3] on model development enhanced the production of chemotherapy for various treatments. In 1937, the Office of Cancer Investigations of the United States Public Health Service (USPHS) collaborated with the National Institutes of Health (NIH) Laboratory of Pharmacology to form the National Cancer Institute (NCI). One of their primary

objectives was to jointly work on a program (murine-S37) implemented as a model system for cancer drug screening. It was primarily developed by Murray Shear, at the Office of Cancer Investigations of the USPHS, to test a broad array of compounds. From this, they were able to screen over 3000 compounds for cancer treatment [3].

The age of chemotherapy to treat cancer began in the 1960s. Surgery and radiotherapy used to dominate the field of cancer therapy, but cure rates after treatment reached a plateau of approximately 33% due to the presence of micrometastases [3]. Chemotherapy as a treatment for cancer was discovered to be one of the most effective means of treating cancers, and has grown to transform the procedure of cancer treatments over time. Adjuvant chemotherapy is an additional treatment using drugs to reduce the reoccurrence of cancer after the primary treatment of surgery or radiation has been carried out [5]. The current data shows that the adjuvant chemotherapy treatment, especially in their combinations, is effective in reducing the recurrence of cancers that grow from the micrometastases after surgery or radiotherapy treatment. This maximizes the antitumor effect and improves the remission and cure rate of the cancer [6, 7].

In the middle of the 1950s, Charles Heidelberger worked together with his colleagues at the University of Wisconsin on hepatoma metabolism in rats. They were able to observe the uptake of uracil in healthy tissues. This work suggested to develop the fluoropyrimidine 5-fluorouracil (5-FU) synthesis by attaching a fluorine atom to the fifth C-position of the uracil pyrimidine base along the pathway [8]. 5-FU chemical structure is  $C_4H_3FN_2O_2$  and the molecular weight is  $130.0772 \frac{g}{mol}$  [9, 10]. Diasio et al. [11] reported that 5-FU has a rapid distribution and elimination from the body with a terminal half-life of 8 to 20 minutes. The chemical structure of 5-FU is shown in Figure 1.1.

5-FU was developed as an antimetabolite analogue of uracil and is currently in use for the treatment of various cancers, such as pancreatic, neck, breast, bladder, and liver tumours [12]. 5-FU is known to be an effective chemotherapy agent in combination with other drugs, such as methotrexate, cyclophosphamide, and leucovorin. 5-FU-based chemother-

apy has been proven to be one of the superior antitumour antineoplastic agents. However, the damage 5-FU cost to the healthy cells is inevitable; the resulting toxicity from the drug can lead to leukopenia, diarrhea, stomatitis, nausea, and hand-foot syndrome [13, 14]. Cardiac toxicities that were identified in the patients treated with 5-FU have shown that the drug is one of the most common sources of chemotherapy-induced cardiotoxicity [13]. Up to 3.5% of patients treated with the medication were reported to have died as a result of heart failure during the first cycle of their treatment with the drug [15]. The study has shown that 29 out of 100 patients treated with 5-FU ended up having cardiac toxic effects [15], and recurrence of the side-effects after first treatment reported to be in the range of 20-100% [13, 16]. The chemical reaction that is responsible for more than 80% of the toxic effect received from administration of 5-FU comes from the improper conversion of 5-FU to Alpha-fluoro-beta-alanine (FBAL) that is excreted out of the body [17].

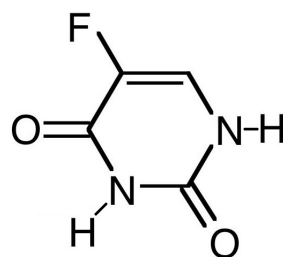


Figure 1.1: Chemical structure of 5-FU [6].

Further discoveries into the potential uses of 5-FU were confirmed in its combination with other drugs. One example developed in 1975 is cyclophosphamide and methotrexate, which was identified and approved to be the first effective adjuvant chemotherapy combination that increases the cure rates for node-positive early-stage breast cancer [18, 19]. Cyclophosphamide and methotrexate are immune system suppressant, while 5-FU is an antimetabolite and antineoplastic agent. Even with the effectiveness of 5-FU in its combinations with other drugs, the cost of toxicity that shows up due to the interactions with cells in the body is still a threat. A combined medication for treatment has a more toxic effect on the body's cells than monotherapy [20]. Due to several reports on the unavoidable

cost of toxicity from chemotherapy, some level of distrust was emphasized on the potential of chemotherapy. There are still ongoing demands for research on the safe prediction and administration of chemotherapy that will maintain the anti-tumour effects but eradicate the collective damage on healthy cells. The area under the curve ( $AUC$ ) is needed to be maximized while we maintain lower maximum concentration ( $C_{max}$ ) in the body. The joint efforts on pharmacology (pharmacodynamic and PK analyses) have brought tremendous advancement in the methodological analysis in the field of drug development in general, especially in PK, and enables the detailed prediction of the time course of molecules in the body that involves molecule-molecule and molecule-enzyme interactions, and also enhances the compartmentalizing of the functional connectivity.

## 1.2 Pharmacokinetics

### 1.2.1 History of Pharmacokinetics

The word pharmacokinetics (PK) comes from ancient Greek; the prefix "pharmaco-" is derived from the word "pharmakon" that implies "drug" and the suffix "kinetics" comes from the word "kinetikos" which means "moving, putting in motion" [21]. The first review of PK was published in 1961 [22]. It was defined to be the kinetics of drug absorption, distribution, metabolism, and excretion [22, 23]. The origins of PK are seen to be both multinational and multidisciplinary [22]. In 1913, German biochemist Leonor Michaelis and Canadian physician Maud Menten derived the Michaelis-Menten equation for the analysis of enzyme kinetics and the elimination kinetics for the drugs [24]. In 1924, Widmark and Tandberg [22] made a significant contribution from Sweden; they published two equations on a one-compartment open model: (*a*) with intravenous bolus injection and multiple doses administered at uniform time intervals, and (*b*) with constant rate intravenous infusion [25]. In 1932, Widmark hypothesized the elimination of ethyl alcohol from the blood as zero-order elimination; "the concept that ethyl alcohol eliminated at a fixed rate independent of its concentration within the body" [26]. While Lundquist et

al. [27] and Wagner et al. [26] revealed that with moderate doses of alcohol, its elimination from human blood obeyed Michaelis-Menten kinetics, most likely when the plasma is saturated [22, 26, 27, 28]; other than the zero-order kinetics that implies the elimination rate of ethanol to be independent of the concentration of alcohol in the blood regardless of the dose administered [29]. Ramon Paniague-Dominquez from the United States also made a contribution to the concept of PK. During the period 1939 to 1950, he introduced the concept of volume of distribution to derive the rate of absorption of a substance as a function of time [22, 30, 31, 32, 33, 34, 35, 36, 37, 38]. He theorized the equation as

$$\frac{dA}{dt} = V_d \frac{dC}{dt} + V_d k C, \quad (1.1)$$

where  $dA/dt$  is the rate of absorption at time  $t$ ,  $V_d$  is the volume of distribution,  $C$  is the plasma drug concentration at time  $t$  and  $k$  is the first-order elimination rate constant. In 1937, Teorell from Sweden published two ground-breaking articles that ended up becoming the foundation of modern PK [39, 40]. In these articles, Teorell designed a physiologically-based PK model that comprises a five-compartment scheme that represents grouping functions in the body; circulatory system, drug depot, fluid volume, kidney elimination, and tissue inactivation. Each grouping has a physiological volume with similar blood perfusion rate [22].

In 1963, Wagner and Nelson published their work on biopharmaceutics [22, 41]. They developed a method of estimating the amount of drug absorbed per millilitre of the volume of distribution versus time from either blood concentration-time data or urinary excretion data for the one-compartment open model. Later a method was developed for the two-compartment open model by Loo-Riegelman in 1968 [42, 43]. Another landmark was the work of Beckett and Rowland that related diurnal urine pH variations with the pH-dependent renal clearance of a drug [22, 44]. This helped in the area of drug production evaluation using urinary excretion data to test for doping in the body.

In 1965, a simple equation was developed by Wagner et al. [22]; the one-compartment

open model to estimate the time-average steady-state concentration ( $C$ ) was given as:

$$C = \frac{FD}{V_d k \tau}, \quad (1.2)$$

where  $F$  is the availability factor,  $D$  is the dose,  $\tau$  is step size,  $V_d$  is the volume of distribution, and  $k$  is the apparent elimination rate constant. Gibaldi and Weintraub later worked on this equation to solve a multi-compartment system by changing the apparent elimination rate constant to a terminal exponential coefficient ( $\lambda$ ) [45], given as:

$$C = \frac{FD}{V_d \lambda \tau}. \quad (1.3)$$

### 1.2.2 The Principles of PK

PK is best defined as the study of the time course of a drug's absorption, distribution, metabolism, and elimination (ADME) in humans and animals [46]. It determines what happens to a drug after administration as it travels through the body, metabolizes, and is eliminated from the body. There are five distinct ways that drugs can be administered: (1) topical administration, (2) inhalation, (3) oral administration, (4) injection, and (5) rectal administration [47, 48]. PK modelling concepts are known to be cost effective compared to clinical trials, using the numerical solution as a compelling technique to predict the time course of a drug or different molecules within the human body before the use of clinical trials. It is a way to determine what can happen or go wrong with the drug in the course while within the body. Furthermore, it can be used to analyse different dosages as to produce a better prediction without any cost of life or toxic effects. We shall now discuss in detail each of the four fundamental processes ADME [49] that make up PK modelling.

The intravenous route of administration does not involve the absorption process, because the drugs are injected into the bloodstream directly. The drug absorption process occurs when there are drugs transferred from the site of administration into the bloodstream via the gastrointestinal tract. Panakanti and Narang [50] revealed the factors that affect the

rate of drug absorption and bioavailability, which includes: "the potency and dose of the drug, therapeutic window, site of absorption, rate limiting factor in drug absorption (e.g., permeability or solubility limited), or whether drug metabolism, efflux, complexation, or degradation at the site of absorption play a role in determining its bioavailability" [50]. Oral administration reduces the amount of the drug that gets to the bloodstream; therefore, to obtain a certain concentration of the drug in the systemic circulation, it has to be administered at a higher dosage, because all of the drug does not enter the bloodstream contrary to intravenous injection.

When a drug is administered via routes different from the intravenous, there will be an amount of the drug that will not get into the bloodstream due to the factors that have to do with the transportation. The factors include: (i.) The dissolution rate that comes from the manufacturing processes, drug particle sizes, and water solubility. (ii.) The absorption by a passive diffusion mechanism that is governed by cell concentration gradients. This process is non-saturable which does not involve any transporter except passive diffusion. (iii.) The drug passage that involves carrier-mediated transporters (active proteins) to cross the membranes. This process is saturable on the account of the limited number of active proteins that are available at any given time [51]. Kodama et al. [52] conducted an experiment to study the absorption rate of 5-FU on the kidney and liver surfaces. The study recorded that 69.1% of 5-FU was absorbed in 360 minutes after its application to the liver surface [52]. From this, Kodama et al. [52] determined that diffusion of 5-FU followed a first-order process. Furthermore, the kidney is the main distributor of 5-FU and the concentration of the drug is lower in the liver compared to the kidney [52].

Distribution of a drug starts when it enters the bloodstream after the absorption process. The bloodstream is the part of the circulatory system that carries drugs (or other compounds) through the liver for metabolism and to the site of action. With the bloodstream are several active proteins that affect the distribution of drugs to the target sites. Binding to the plasma proteins prevents drugs from binding to receptors at the site of action. The

binding becomes weak when the drug has strong affinity to the active protein at the target site. At the site of action, free drugs are able to bind to the receptors. This process of drugs binding to receptors helps more plasma-bound drugs to be released into the bloodstream as free drugs to balance the concentration of bound and free drugs in the bloodstream. Plasma albumin has the greatest influence on drug binding capacity when the drug enters the bloodstream [49]. Plasma proteins bind to the drugs, at a rate dependent on the drug affinity and concentration. Drug-protein binding affinity and dissociation can be expressed using the law of mass action. It expresses the equilibrium constant,  $k_{binding}$ , conventionally as the ratio of the equilibrium concentrations of the products (drug-protein bound complex)  $[XP]$  to that of the reactants (drug concentration  $[X]$  and total protein concentration  $[P]$ ). Binding affinity can also be typically measured using the equilibrium dissociation constant ( $k_{diss}$ ) which is its inverse. The greater the binding affinity of the drug molecules to its target the smaller the  $k_{diss}$  value, and vice versa.

$$k_{binding} = \frac{[XP]}{[X][P]} = \frac{1}{k_{diss}}. \quad (1.4)$$

The volume of distribution ( $V_d(t)$ ) explains the extent to which compounds distribute throughout the body. It can be estimated as a proportionality constant between the amount of compound present in the body (X) and the concentration (C) of a compound in the body fluid where it is being measured at any given time (t) [49]:

$$V_d(t) = \frac{X(t)}{C(t)}. \quad (1.5)$$

According to the analysis by Jianghong et al. [49], the volume of distribution is separated into three quantitative expressions. The first says, the volume of distribution of the central compartment ( $V_c$ ) is expressed as the ratio between the intravenous dose ( $Dose^{iv}$ ) and the concentration at time zero,  $C_o$  [49]:

$$V_c = \frac{Dose^{iv}}{C_o}. \quad (1.6)$$

The second expression provides the volume of distribution at steady-state ( $V_{ss}$ ) as the product of the systemic clearance of a compound,  $CL_s$ , and the mean residence time,  $MRT^{iv}$ .  $CL_s$  can be calculated from the ratio of intravenous dose  $Dose^{iv}$  to the area under the curve ( $AUC$ ) from the time of dosing and extrapolated to infinity  $AUC_{0-\infty}^{iv}$  [49]. Therefore, the steady-state volume distribution is

$$V_{ss} = CL_s \times MRT^{iv} = \frac{Dose^{iv}}{AUC_{0-\infty}^{iv}} \times MRT^{iv}. \quad (1.7)$$

The third expression interprets volume of distribution at pseudo-distribution equilibrium ( $V_{\lambda_z}$ ) where the compound exhibits bi-exponential decay. It is formulated as the ratio of the clearance to the rate constant obtained from the terminal elimination phase ( $\lambda_z$ ) after intravenous dosing [49]:

$$V_{\lambda_z} = \frac{CL_s}{\lambda_z}. \quad (1.8)$$

Membranes also play an essential role in influencing the movement of a drug in the body. Some layers are so active in protecting a cell from external factors that they obstruct a certain amount of the drug from moving into the cell [48]. There are six routes that compounds can use for their movement into cells. First, diffusion, the movement of molecules from a higher concentration region to a lower concentration region. Second, pores, openings in the surface or integument of a cell that molecules pass through into the cell. Third, vesicular transport endocytosis, the transfer of molecules into the cell by in-folding of the cell membrane to internalize the molecules. Fourth, receptor mediated active transport, the proteins that allow specific types of molecules outside the cell to attach to them as a medium to get transferred into the cell. Fifth, p-glycoprotein, an ATP-powered efflux pump which can transport hundreds of structurally unrelated hydrophobic amphipathic compounds, including therapeutic drugs, peptides and lipid-like compounds [53]. Finally, transcellular,

the passing of molecules from a particular cell to another via adjacent cell membranes [48].

Metabolism, also known as biotransformation, takes place primarily in the liver; however, it can also occur at the site of action [54]. There are usually two phases involved in metabolism, but some drugs have only one phase metabolism. For instance, 5-FU has one phase metabolism which occurs in the liver. Phase one reactions are oxidation, reduction and hydrolysis that principally react with hepatic metabolic enzymes, the family of cytochrome P450 [54]. Phase one metabolism involves adding a polar functional group to a drug, which slightly increases water solubility of the drug and become more active. Phase two metabolic reactions are conjugation reactions, adding another substance (glucuronic acid, sulfuric acid, or amino acid) to a drug to produce one or more metabolites [54].

Cytochrome P450 (CYP) is a superfamily of heme-containing enzymes, and it accounts for 57 genes and 13 isoforms in humans that are responsible for the metabolism of more than 80% of the clinically used drugs [55]. CYP catalyses the insertion of molecular oxygen into inactivated carbon-hydrogen and carbon-carbon bonds [55, 56]. The reaction occurs by the sequential donation of two electrons by cytochrome P450-reductase (CPR) and cytochrome b5 (cytb5) [57]. The proteins increase the rate of reaction until all the enzymes are bound [58].

Many factors affect drug metabolism in the body. One of these is deficiency of some drug metabolizing enzymes which is genetic. These people have poor tolerance for certain drugs. For instance, homozygous and heterozygous mutation carriers can build up critical toxicity after the administration of the antineoplastic drug 5-FU, which is also catabolized by the dihydropyrimidine dehydrogenase (DPYD) gene that encodes the enzyme of the same name dihydropyrimidine dehydrogenase (DPD) [59]. Etienne-Grimaldi et al. [60] recorded the life-threatening (grade 3-4) toxicity of 5-FU associated with the DPYP variant. Grade indicates the intensity of the adverse effects caused by therapies. The grade criteria for adverse effects shown in Table 1.1 were made by the U.S. Department of Health and Human Services [61] and published in 2017.

Table 1.1: Common Terminology Criteria for Adverse Effects (CTCAE) [61]

Grades	Intensity	Clinical Description
1	Mild	Asymptomatic or mild symptoms; clinical or diagnostic observations only; intervention not indicated.
2	Moderate	Minimal, local or noninvasive intervention indicated; limiting age-appropriate instrumental activities of daily living.
3	Severe	Severe or medically significant but not immediately life-threatening; hospitalization or prolongation of hospitalization indicated; disabling; limiting self care activities of daily living.
4	Life-threatening	Life-threatening consequences; urgent intervention indicated.
5	Deadly	Death related to adverse effects.

Age is another factor that influences drug metabolism [17]. As people age from young adult, there is a gradual reduction in the activeness of the genes. Likewise, infants also are susceptible to the effect of inadequate metabolism of drugs because of immature genes that interact with the molecules. Both elderly and little children are more susceptible to the toxic effects of 5-FU [17].

Another factor contributing to the drug metabolism is the combination of drugs that share a metabolism pathway and undergo the same type of enzymatic reaction. Under this condition, the one that has a higher affinity to the protein will be preferentially metabolised over the other. This can lead to abnormal metabolism of the one with lower affinity and may cause increased toxicity in the body.

Elimination is the last of the four fundamental PK activities and is complete when the administered drug and the metabolites are completely removed from the blood plasma. A drug can be eliminated from the plasma either unchanged or metabolized. The rate of elim-

ination of a drug depends on the composition of the drug. For instance, polar compounds (e.g. water, ammonia, and ethanol ) can more easily be eliminated from the system than non-polar substances (benzene, methane, ethylene, and most organic molecules) [62]. The drug elimination can occur through renal excretion, biliary and fecal excretion, and other routes. Renal excretion is when the drugs and metabolites are excreted via urination. The three main processes involved are: glomerular filtration, active tubular secretion, and passive tubular reabsorption. The amount of drug that is reabsorbed into the tubular lumen depends on the extent at which the plasma binds to the drug, and the glomerular filtration rate of the unbound drug to get filtered. Filtration is affected by changes in plasma protein binding to drugs as a result of saturation of protein binding or fluctuations in pH. About 10% of total cardiac output is filtered through the kidneys, the rate at which this occurs can be obtained by determining the glomerular blood flow and the unbound drug concentration [63]. The biliary and fecal excretion involves the protein transporters that secrete drugs and metabolites into bile. The phase two conjugation metabolism occurs in this process of digestion and makes metabolites become polar conjugate. Therefore, the drug is most likely inactive and readily gets excreted in urine and feces. The conjugated metabolites of the drug can also be reabsorbed into the bloodstream by the intestines.

Analysis of a drug in the urine can be used to measure the time course of the renal clearance of a drug, using the simple equation [48]

$$CL_r = \frac{C \times Q}{C_{urine}}, \quad (1.9)$$

where  $CL_r$  is renal clearance,  $C$  is the concentration of the drug in plasma,  $Q$  is the urine flow rate, and  $C_{urine}$  is the concentration of the drug in the urine.

Moreover, the total clearance of the drug from various compartments can be estimated as the summation of the clearance of the different tissues [48];

$$CL = CL_h + CL_g + CL_r, \quad (1.10)$$

where  $CL_h$  and  $CL_g$  are the clearance through the liver and gastrointestinal (GI) tract.

Bioavailability is not a fundamental PK process in determining the fate of a drug in the body. Bioavailability describes the quantity of the drug that is available in the bloodstream for the target site. It is a mathematical formulation that estimates the rate at which drug gets to the bloodstream using the ratio of the area under the curve (AUC) for administration via oral routes (or non-intravenous routes) to that of intravenous [48]:

$$\text{Bioavailability} = \frac{AUC_{\text{oral}}}{AUC_{\text{intravenous}}} \times 100. \quad (1.11)$$

### 1.2.3 PK Models

PK modelling is a mathematical technique or tool structured in a bio-systematic way to understand and describe the kinetics of molecules in the body. It provides an understanding about the fate of molecules in a biological system, and can be used to minimize the cost of life involved in clinical treatments and trials. PK models analyse the movement, the impact, and the concentration of the molecules in the body by combining input and disposition models. PK modelling exploits the sum of exponentials or differential equations based on mass-action principles (i.e. maintaining constant proportionality for the ratio of reagents to products of the reaction) to analyse the interaction of molecules within the time frame of the PK processes [20].

The model can incorporate zeroth-, first-, second- and mixed-order kinetics. These can be distinguished by the factors that affect the movement of molecules in all the compartments. It is termed a zeroth-order process when the molecules' movement rate across the membrane is independent of its concentration on both sides. For instance, if the concentration of molecule A is decreasing at a constant rate that is independent of its instantaneous concentration, then the rate of molecule A's elimination from the body can be described as:

$$\frac{dC}{dt} = -k^{(0)}, \quad (1.12)$$

where  $k^{(0)}$  is the zeroth order rate constant. The concentration driven process of the movement of molecules is a first order process, it is expressed as [63]:

$$\frac{dC}{dt} = -k^{(1)}C, \quad (1.13)$$

where  $C$  is the concentration of the molecules.  $k^{(1)}$  is the first order rate constant. Lastly, the mathematical expression for the  $n^{th}$  order kinetic process of molecules [63] is

$$\frac{dC}{dt} = -k^{(n)}C^n, \quad (1.14)$$

where  $n$  is the order of process.  $k^{(n)}$  is the  $n$ th order rate constant.

PK models can be analysed in two ways: non-compartmental models and compartmental models. Non-compartment PK analysis are model-independent, and does not involve the assumption of compartment analysis. It provides solution to the PK parameter estimation by using algebraic equations [64]. Compartmental models can be analysed using two modelling methods; population compartmental models and physiologically based models [65]. Population compartmental models depend on the rate of molecule distribution across different interconnected compartments that are kinetically homogenous in the body [65]. Physiologically based modelling is a compartment model in which each of the compartments represent a physiologically discrete entity, such as an organ or tissue, and the blood flow into and out of those entities [65]. In the compartment models, the number of compartments indicate the different rates of molecule distribution categorized in the system. For instance, a single compartment that represents the one-compartment model explains a single flow rate in molecule distribution across the whole body system; a two-compartment model involves three flow rates that depend on the version of the model; the three, and four-compartment models can also be analysed based on the different number of molecule distribution rates categorized in the systemic circulations. This analysis will look at one to three-compartment models with an extra compartment representing the environ-

ment exterior to the body. The interior compartments are the plasma for distribution, liver for metabolism, healthy cells, and tumour cells for target sites within the four-compartment model.

#### 1.2.4 Michaelis-Menten Kinetics Model Equation

Victor Henri, a French physical chemist, discovered an enzyme-substrate reaction in the year 1903 [66]. Ten years later the Michaelis-Menten kinetics equation [24] was derived from



where  $E$  stands for the enzymes in the body,  $S$  is the substrate,  $P$  is the product. This was applied to the model in terms of the drug components and the corresponding enzymes, shown in Equation 1.16 below:



Double arrows between the substrate and the complex substrate indicate a reversible reaction. The complex either undergoes the forward reaction to form DHFU and the enzyme DPYD, or the backward reaction to form 5-FU and DPYD. The rate that DHFU ( $v$ ) is formed can be represented by:

$$v = \frac{d[DHFU]}{dt} = V_{max} \frac{[5FU]}{K_M + [5FU]} = k_{cat} [DPYD]_0 \frac{[5FU]}{K_M + [5FU]}, \quad (1.17)$$

where  $\frac{d[DHFU]}{dt}$  is the rate at which DHFU is formed;  $V_{max}$  is the maximum velocity of the reaction;  $K_M$  is the Michaelis-Menten constant that describes the concentration of the substrate when the reaction velocity is one half the maximum velocity;  $k_{cat}$  is the catalytic rate constant that explains the maximum number of 5-FU molecules converted to DHFU per DPYD per second;  $[DPYD]_0$  is the initial DPYD concentration. The order of the reaction depends on the ratio between  $K_M$  and  $[5FU]$ . When  $[5FU] \ll K_M$ , the reaction is a first order

kinetic process, linearly dependent on the concentration of the substrate. On the other hand, if  $[5FU] \gg K_M$ , it is known as a zeroth order process, where the reaction is independent of the substrate concentration. At this point, the rate of reaction is at its maximum value, because all the enzymes are involved in the reaction. The Michaelis-Menten constant is derived from the ratio of  $k_{cat}$  to  $K_M$  ( $k_{cat}/K_M$ ) where  $K_M$  is defined as:

$$K_M = \frac{k_r + k_{cat}}{k_f}. \quad (1.18)$$

The rate constant  $k_r$  is for unbinding 5-FU from DPYD,  $k_f$  is for 5-FU binding to DPYD, and  $k_{cat}$  is for converting the complex-substrate (5-FU + DPYD) to DHFU.

### 1.3 5-FU and Its Metabolites

#### 1.3.1 Mechanism Pathway of 5-FU and Its Metabolites

5-FU is an antineoplastic and antimetabolite drug. 5-FU exerts cytotoxic effects on the cancer cells when it reacts with the ribonucleoside-diphosphate reductase. It incorporates into the DNA and RNA, and also inhibits thymidylate synthase, preventing the enzymes to react with uracil that produces deoxythymidine monophosphate (dTMP), which is an essential metabolite in cell replication. 7 – 20% of 5-FU is excreted unchanged within six hours of administration [9, 10]. The rest of the 5-FU is metabolized through four pathways as shown in Figure 1.2 [67]. One pathway is the interaction of 5-FU with the enzyme DPYD to form inactive DHFU; which is further converted to fluoro-beta-ureidopropionate (FUPA) by dihydropyrimidinase (DPYS), and FUPA turns to alpha-fluoro-beta-alanine (FBAL) by beta-ureidopropionase (UPB1) [67]. Up to 80% of the 5-FU is degraded to the inactive end product FBAL by the three enzymes.

The imbalance in conversion rates between the three enzymes along the DPYD pathway can cause DHFU to accumulate in the body and interact with healthy cells that leads to toxic effects [67]. The second pathway shows the strong affinity of 5-fluorodeoxyuridine

monophosphate (F-dUMP) has over dUMP in reacting with thymidylate synthase (TS). The reaction prevents TS from interacting with folate which catalyses the reductive methylation that involves the transfer of the methylene group of 5,10-methylenetetrahydrofolate to the carbon-5 position of dUMP and a two electron reduction of the methylene group to a methyl group [68]. The inhibition of TS causes increased levels of dUMP and an imbalance of dTMP eventually leading to DNA damage. The uniqueness between the third and fourth pathways are indicated from 5-FU to 5-fluorouridine monophosphate (F-UMP) in Figure 1.2; one is direct conversion by interacting with uridine monophosphate synthase and glutamine phosphoribosylpyrophosphate amino transferase (UMPS/P-PAT). The other conversion occurs from 5-FU to fluorouridine (FUR) by the interaction of 5-FU with uridine phosphorylase 1 and 2 (UPP1/UPP2), then to F-UMP by the FUR interaction with uridine-cytidine kinase 1 and 2 (UCK1/UCK2) [67]. The cytotoxic effects on the tumour cells and normal tissue through anabolic actions is between 1-3% of 5-FU [69], which is largely converted to F-UMP. From here, F-UMP is metabolized through one of three pathways: (i.) 5-fluorouridine triphosphate (F-UTP) that incorporates into RNA, (ii.) 5-fluorodeoxyuridine triphosphate (F-dUTP) that incorporates into DNA, and (iii.) 5-fluorodeoxyuridine monophosphate (F-dUMP) that inhibites thymidylate synthase. F-dUMP can also be obtained on an alternate pathway for minor conversion from 5-FU via 5-fluoro-deoxyuridine (FUDR) catalysed by two enzymes: thymidylate phosphorylase (TYMP) and thymidine kinase (TK1) respectively. Figure 1.2 follows the information given in the interactive version of fluoropyrimidine pathways available online at PharmGKB by Thorn et al. [67], it shows the detailed metabolic pathways of 5-FU and the metabolites.

### **1.3.2 5-FU Related Severe Toxicity**

Despite many studies on the PK of 5-FU and its metabolites, there is still more to discover about the mechanism of the drug, especially in the area of toxic effects and bioavailability. This project will numerically solve the Boisdron Celle et al. [70] developed clinical

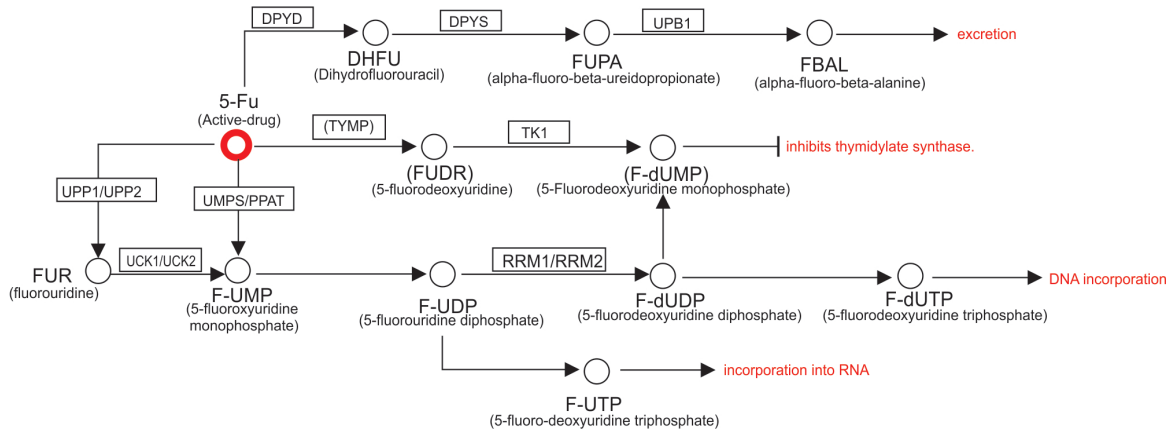


Figure 1.2: Metabolic pathways of 5-FU [67].

methods that determined the correlation between the correlation between DPYD deficiency and 5-FU. The studies found no correlation between the dihydrouracil/uracil ratio and 5-FU plasma clearance. Also, no relationship was found between mRNA expression and 5-FU plasma clearance, uracil concentration, or toxicity, but a significant correlation was found between dihydrouracil/uracil ratio and treatment toxicity [70]. Bocci et al. [17] also validated the influence of DPYD deficiency. This was done by separating the plasma concentration of 5-FU from its metabolites and observing the individual plasma concentration of each. The DPYD deficiency was examined in two categories of its deficiency (complete and partial). In the general population the contributed estimate to severe toxicity of DHFU are 0.1% and 3% respectively [17]. Statistically, no significant correlation was found between DPYD deficiency and 5-FU toxic effect. With their studies on the metabolite DHFU, it was shown that DPYD activity possesses a significant correlation with both the maximum concentration ( $C_{max}$ ) and the area under the curve ( $AUC$ ) of DHFU. The plasma level of DHFU may be the signpost for DPYD activity in the body. These studies shed light on the previous belief about 5-FU toxicity, that it occurs as a result of DPYD deficiency. From this, the studies conclude that being deficient in DPYD can lead to toxic effects from DHFU.

### 1.3.3 The Quality of Life During and After Treatment with 5-FU

The palliative care of patients undergoing chemotherapy for cancer is important for proper treatment. The caring for patients as a whole is critical, not just the aim to cure the disease. Glimelius et al. [71] looked at information about the quality of life after cancer treatment with chemotherapy. They studied the proportion of patients who experience an improved quality of life after treatment with 5-FU in two different chemotherapy combinations: MFL (Methotrexate, 5-FU, and Leucovorin) and FLv (5-FU and Leucovorin). Two hundred and two patients were given the questionnaires and interviewed at random. The evaluation of response from patients showed that between 23% and 52% of the patients were considered to have improved quality of life and 11 – 38% had consistent quality of life [71]. The proportion of patients found to have an improved quality of life was shown to be greater in the 5-FU bolus injection group (15 of 33; 45%) than in the group who had a short-term infusion of 5-FU (10 of 37; 27%) [71]. The study validated the technique of 5-FU administration as a useful means for improving the quality of life after treatment.

### 1.3.4 Technique of 5-FU Administration

The studies of Per-Anders et al. [72] investigated the PK of 5-FU with two adaptable techniques of intravenous administration: 20 min. infusion and 2 min. bolus (push) injection of the drug ( $500 \frac{mg}{m^2}$ ) with the combination of Leucovorin 50 mg in 14 colorectal cancer (liver metastases) patients. The differences between the PK behaviour of the two administration techniques were analysed by comparing their plasma peak levels and AUC. They were able to evaluate the clinical response rates and frequency of adverse side-effects in patients after administration of the two different methods. Bolus dose clearance was found to be 0.5-1.4  $min^{-1}$ , while clearance rates after prolonged infusions were 10- to 60-fold higher [72]. Even though prolonged infusions recorded a higher  $C_{max}$  compared with the bolus injection ( $341 \pm 34 \mu M$  vs.  $161 \pm 17 \mu M$ ), the average AUC after bolus was found to be  $6158 \pm 874 \frac{\mu mol}{min}$  compared to  $3355 \pm 428 \frac{\mu mol}{min}$  for prolonged infusions [72]. Prolonged

infusion administration is more susceptible to the toxic effects than bolus injection, which is also validated by Glimelius et al. [71].

## 1.4 Specific Aims

Our goal is to analyse the average concentration of drug in the blood for distribution to cancer cells, healthy cells, and liver for metabolism and elimination. This research involves the development of an intensive quantitative model that describes the interactions between 5-FU, its metabolite, DHFU, and the metabolic enzyme of DPYD, within the body. It will enhance our ability to predict how 5-FU and DHFU interact with each other and with the body.

The study involves the optimization of the model by comparing it to experimental data in order to obtain the PK parameters within the model. This allows for the easy calculation of the quantities:  $AUC$ ,  $C_{max}$ , and half-life of 5-FU and DHFU. The PK parameters will also be optimized for gender differences between men and women, and age differences between  $< 70$  years old (young adult) and  $\geq 70$  years old. These optimizations will help us to determine how each demographic is affected by the drug. This will enable us to use the theoretical solution for the prediction of the activity of the drug within the body.

This model is analysed based on the four fundamental PK processes the molecules undergo in the body; from the moment of administration to the distribution and metabolism, to the point of complete elimination from the body. One of the essential tools needed for this numerical modelling is the signalling pathway of the drugs, the metabolites and the enzymes involved. It helps to analyse the likely interaction between the molecules and the corresponding enzymes, the affinity between two substrates, and the elimination path of the molecules from the body. Furthermore, our model can be individualized enhancing its accuracy.

## 1.5 Overview

Chapter two explains the methods that were adopted to achieve the aims of the research. It includes knowing the pathways for the molecules involved, providing numerical solutions to the nonlinear differential equations using the Runge-Kutta (RK) method, and the optimization of the PK parameters using Powell's algorithm for minimizing the variance.

Chapter three involves the analysis of 5-FU, taking the modelling from the one-compartment model to the three-compartment model. Both fixed and variable exponents impact was considered on the fitness of numerical solutions to the clinical data. Also, we further examined the impact of combining the degrees of exponents to fit the solution to the clinical data better. The impact of saturation limiting functions on the 5-FU flow rates were also examined. The models obtained allow for the calculation of the observable quantities  $AUC$ ,  $C_{max}$ , and half-life.

Chapter four has the same objectives as we have in chapter three. The significant difference is the molecules that were studied. In this chapter, the molecule we will focus on is DHFU, the metabolite of 5-FU. The analysis includes one- and two-compartment models as well as two methods of optimizing the PK parameters. The one-molecule model method involves optimizing the 5-FU PK parameters and then holding them fixed while the DHFU PK parameters are optimized. The second method involves optimizing both 5-FU and DHFU PK parameters simultaneously. Lastly, we examine the effect of combining the degrees of exponents to fit the experimental data.

Chapter five contains the results and applications of the model to both 5-FU and DHFU. The influences of age and gender are examined using the numerical solutions of the model and compared them with the clinical data. Moreover, this chapter analyses the responsible PK parameters for the variations observed between the groups. The  $AUC$ ,  $C_{max}$  and half-life were examined for both molecules.

Chapter six is the conclusion and highlights the general results that achieve the aims of the research. A discussion of potential applications and future research based on this work

will conclude the chapter.

Lastly, the appendices used to accommodate the extra information in the thesis, such as the tables, graphs, dictionary, and the code for modelling. The appendices were sectioned based on these categories, respectively.

# Chapter 2

## Methodology

---

*to the human body it makes a great difference whether the bread be fine or coarse;  
with or without the hull, whether mixed with much or little water,  
strongly wrought or scarcely at all, baked or raw.*

*Whoever pays no attention to these things, or, paying attention,  
does not comprehend them, how can he understand the diseases which befall man ?*

– Hippocrates 400 B.C.

---

### 2.1 Methods

The quantitative multi-compartment PK model developed used a system of nonlinear differential equations that were solved numerically with RK fourth order method. The optimized PK parameters for the models provided predictions about the influence of the body on the drug's ADME. The numerical work was done using the C++ programming language.

#### 2.1.1 Four-Compartment Model Analysis of 5-FU

The PK model of 5-FU and its metabolites was designed based on a four-compartment model. The compartments are: (i.) Blood plasma for distribution of the molecules in the body and denoted by compartment 1. (ii.) Liver for elimination of the molecules in the body, denoted by compartment 2. (iii.) Healthy cells that represent the functional body cells, denoted by compartment 3. (iv.) Tumour cells that are the target sites, denoted by

compartment 4. The four-compartment model consists of not only the four compartments within the body but also one compartment external to the body. The exterior environment to the body is denoted by compartment 0. The one to four compartments accessible by 5-FU and its metabolites within the body are illustrated in Figure 2.1.

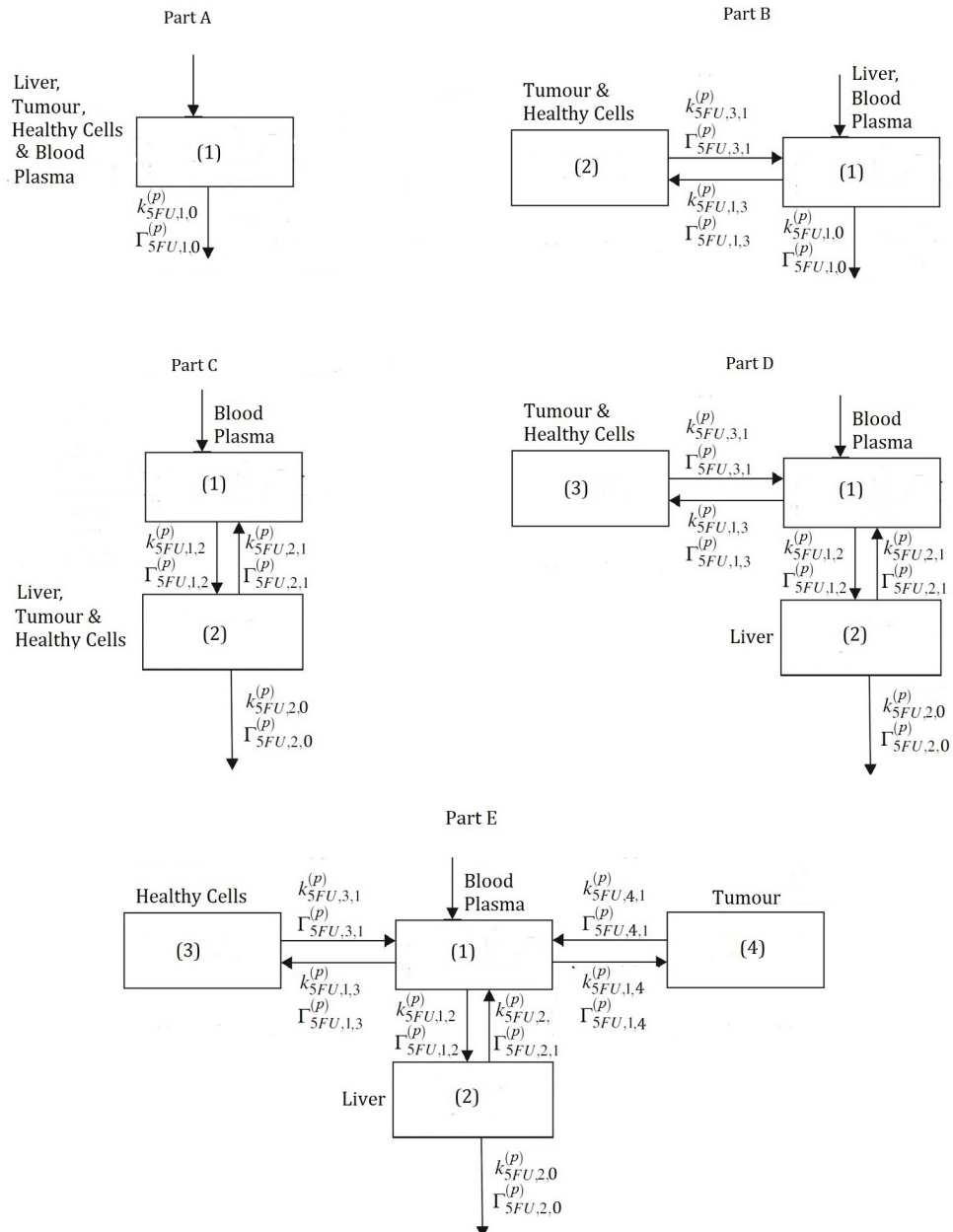


Figure 2.1: Systemic inter-flows for the one- to four-compartment PK models.

The metabolism pathways of the molecules that were detailed in Figure 1.2 can be sum-

marized and compressed to reduce the computational workload. It is important to recognize that the number of important metabolite pathways appropriate for the proper interpretation of molecules derived from 5-FU is two. The two metabolism pathways of 5-FU are denoted as DHFU and F-UMP. The F-UMP pathway leads to the incorporation of the metabolites into RNA and DNA, which obstructs replication of the cells. The DHFU pathway represents the elimination of the molecules. This is summarised in Figure 2.2. Table 2.1 shows that

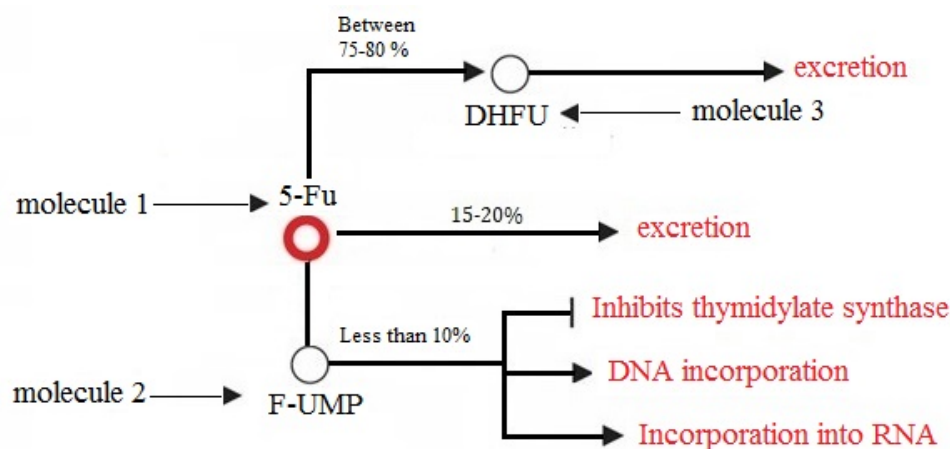


Figure 2.2: Summarised metabolic pathways of 5-FU.

the molecules have been separated into eight groups. The first group (ID No. 1) represents the parent drug 5-FU. The second group (ID No. 2) represents the first metabolite group F-UMP, the third group represents the second metabolite group DHFU. The fourth and fifth groups (ID No. 4 and 5) represent the corresponding enzymes that interact with 5-FU to produce the two metabolites as the end products respectively. The sixth and seventh groups (ID No. 6 and 7) describe the intermediate formation of 5-FU and enzyme complexes that lead to F-UMP and DHFU. The last group (ID No. 8) describes the clinically prepared form of 5-FU; such as oral pills or encapsulated drug.

The last column of Table 2.1 shows the compartments that are accessed by each group of molecules within the four-compartment model. The number of different types of molecules in each compartment is used for determining the number of nonlinear differential equations involved in the model. According to Table 2.1, there are thirteen nonlinear differential equa-

Table 2.1: Groups of molecules and their accessible compartments.

<b>ID No.</b>	<b>Name of molecules</b>	<b>Accessible compartments</b>
1	5-FU (Parent drug)	0,1,2
2	F-UMP (Active metabolite)	1,2,3,4
3	DHFU (Inactive metabolite)	1,2,3
4	Enzymes group 1	2
5	Enzymes group 2	2
6	Complex substrate (5-FU + group 1)	2
7	Complex substrate (5-FU + group 2)	2
8	5-FU (Oral administration)	0,1,2

tions required for the four-compartment model of 5-FU and its metabolites in the body by intravenous administration. In the case of oral administration, there are an extra two nonlinear differential equations that represent the clinically prepared form of the drug for oral administration treatment. Hence, there are fifteen coupled nonlinear differential equations to be used for oral administration.

### 2.1.2 Model

The M-compartment N-molecule model can be split into two parts. The first part is the number of compartments and their representation. The molecules were modelled in reduced compartment models in addition to the four-compartment model: one-, two-, and three-compartment models. Figure 2.1 shows all the compartment models used. In all of the compartment models, the zeroth compartment represents the environment external to the body. In the one-compartment model, the first compartment unifies all the rate constants involved in all four PK processes and treats the body as a homogenous system. This is shown in Figure 2.1 A.

In the two-compartment model there are two possibilities; The first case corresponds to the first compartment representing the distribution event, which is carried out by the blood plasma; as well as the liver and the organs that metabolize the drugs and eliminates the molecules from the body. The second compartment represents the healthy and tumour cells that are affected by the molecules within the body. Figure 2.1 B shows the two-

compartment model that has its route of elimination via the central compartment. The second case illustrated in Figure 2.1 C shows the first compartment is the distribution event only, which is carried out by the blood plasma. The second compartment represents the liver and the organs that metabolize the drugs and eliminates the molecules from the body, as well as the healthy and tumour cells that are affected by the molecules within the body.

The model that consists of three compartments splits the whole kinetic process into three compartments: (i.) the first compartment is the blood/plasma that represents distribution, (ii.) the second compartment represents the liver and the organs that metabolize the drugs and eliminates the molecules from the body, and (iii.) the third compartment represents the molecules' interaction with the healthy and tumour cells. This is shown in Figure 2.1 D.

The model that consists of four compartments has: (i.) the blood/plasma compartment for distribution from one compartment to another, (ii.) the elimination organs compartment for both metabolites and the drugs, (iii.) the healthy cells compartment representing the interaction of the healthy cells with the molecules, and (iv.) the tumour cells compartment representing the interaction of the cancer cells with the molecules. This is illustrated in Figure 2.1 E.

The second part of the model is the set of nonlinear differential equations that describe the rate of change of the number of each type of molecule in each compartment. The rate of change of the amount of molecule  $d1$  in compartment  $c1$  is given by

$$\frac{dX_{d1,c1}}{dt} = I_{d1,c1}(t) + \frac{dX_{d1,c1}^{(1)}}{dt} + \frac{dX_{d1,c1}^{(2)}}{dt} + \frac{dX_{d1,c1}^{(3)}}{dt} + \frac{dX_{d1,c1}^{(4)}}{dt}, \quad (2.1)$$

where the amount of molecule  $d1$  in compartment  $c1$  is  $X_{d1,c1}$ . In compartment  $c1$  the concentration of the molecule  $d1$  is

$$C_{d1,c1} = \frac{X_{d1,c1}}{V_{d,d1,c1}}, \quad (2.2)$$

where  $V_{d,d1,c1}$  is the volume of distribution of molecule  $d1$  within compartment  $c1$ .

The right-hand side of equation 2.1 has been split into five terms:

1. The first term on the right-hand side of equation 2.1 represents the infusion of molecule  $d1$  into compartment  $c1$ . This can be the IV infusion of 5-FU into compartment 1, or the body producing more proteins, or the intake of prepared drugs such as oral drugs.
2. The second term on the right-hand side of the differential equation in equation 2.1 describes the flow of molecule  $d1$  from compartment  $c1$  into another compartment and vice versa as illustrated in Figure 2.3. The differential equation is;

$$\frac{dX_{d1,c1}^{(1)}}{dt} = \sum_{p1=0}^2 \sum_{c2=0}^M \left\{ \frac{\bar{k}_{d1,c2,c1}^{(1,p1)} X_{d1,c2}^{A_{d1,c2,c1}^{(1,p1)}}}{1 + \Gamma_{d1,c2,c1}^{(1,p1)} X_{d1,c2}^{B_{d1,c2,c1}^{(1,p1)}}} - \frac{\bar{k}_{d1,c1,c2}^{(1,p1)} X_{d1,c1}^{A_{d1,c1,c2}^{(1,p1)}}}{1 + \Gamma_{d1,c1,c2}^{(1,p1)} X_{d1,c1}^{B_{d1,c1,c2}^{(1,p1)}}} \right\}, \quad (2.3)$$

where  $p1$  represents the process, which determines the exponents A and B. That is the zeroth order process,  $p1 = 0$ , is  $A_{d1,c1,c2}^{(1,0)} = B_{d1,c1,c2}^{(1,0)} = 0$ ; the first order process,  $p1 = 1$ , is  $A_{d1,c1,c2}^{(1,1)} = B_{d1,c1,c2}^{(1,1)} = 1$ ; and the second order process,  $p1 = 2$ , is  $A_{d1,c1,c2}^{(1,2)} = B_{d1,c1,c2}^{(1,2)} = 2$ . The exponents  $A_{d1,c1,c2}^{(1,p1)}$  and  $B_{d1,c1,c2}^{(1,p1)}$  will be allowed to vary from these values when the model is fitted to the clinical data. The compartments  $c2 = 1$  to  $M$  represent the body with the number  $M$  varying from one for the one-compartment model to four in the four-compartment model.

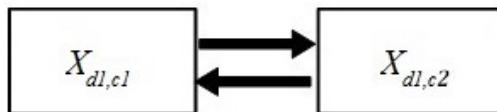


Figure 2.3: Kinetic flows of molecule  $d1$  between compartments  $c1$  and  $c2$ .

The parameters in equation 2.3 have three subscripts  $d1$ ,  $c1$  and  $c2$ . This indicates that the process is for molecule  $d1$  moving from compartment  $c1$  to compartment  $c2$  ( $d1, c1, c2$ ) or vice versa ( $d1, c2, c1$ ). Besides the exponents A and B, the  $\Gamma$ 's are the

saturation parameters and the effective rate constant is defined as;

$$\begin{aligned} \bar{k}_{d1,c1,c2}^{(1,p1)} &= k_{d1,c1,c2}^{(1,p1)} \left[ 1 + \sum_{d2=1}^N \sum_{c3=1}^M \sum_{p2=0}^2 \frac{\alpha_{d1,c1,c2||d2,c3}^{(1,p1,p2)} X_{d1,c1,c2||d2,c3}^C X_{d2,c3}^{(1,p1,p2)}}{1 + \beta_{d1,c1,c2||d2,c3}^{(1,p1,p2)} X_{d1,c1,c2||d2,c3}^D X_{d2,c3}^{(1,p1,p2)}} \right] H(X_{d1,c1}) \\ &\times H \left( 1 + \sum_{d2=1}^N \sum_{c3=1}^M \sum_{p2=0}^2 \frac{\alpha_{d1,c1,c2||d2,c3}^{(1,p1,p2)} X_{d1,c1,c2||d2,c3}^C X_{d2,c3}^{(1,p1,p2)}}{1 + \beta_{d1,c1,c2||d2,c3}^{(1,p1,p2)} X_{d1,c1,c2||d2,c3}^D X_{d2,c3}^{(1,p1,p2)}} \right), \end{aligned} \quad (2.4)$$

where  $H(X_{d1,c1})$  is the Heaviside step function.  $k_{d1,c1,c2}^{(1,p1)}$  is the rate constant, while the terms in the square brackets are the influence of the other molecules in the system changing the effective rate constant.

If  $\alpha$  is a negative value, it is an indication that the flow is inhibited. It means that the compartment in which the molecule is heading to is already saturated or some other type of molecule is preventing the flow. If  $\alpha$  is zero, it means there is no influence on the flow of the molecules. Lastly, if  $\alpha$  is a positive value, there is an enhancement in the flow because of the presence of these molecules.

Let  $A_{d1,c1,0}^{(1,p1)} = A$  and  $B_{d1,c1,0}^{(1,p1)} = B$ . The rate of elimination can be approximated as

$$\begin{aligned} -\frac{d\tilde{X}_{d1,c1}^{(1)}}{dt} &= \frac{k_{d1,c1,0}^{(1,p1)} X_{d1,c1}^A}{1 + \Gamma_{d1,c1,0}^{(1,p1)} X_{d1,c1}^B} \\ &\approx \begin{cases} \frac{k_{d1,c1,0}^{(1,p1)}}{\Gamma_{d1,c1,0}^{(1,p1)}} X_{d1,c1}^{(A-B)} \sum_{n=0}^{\infty} \left[ \frac{-1}{\Gamma_{d1,c1,0}^{(1,p1)} X_{d1,c1}^B} \right]^n; & \text{if } \left| \Gamma_{d1,c1,0}^{(1,p1)} X_{d1,c1}^B \right| > 1 \\ k_{d1,c1,0}^{(1,p1)} X_{d1,c1}^A \sum_{n=0}^{\infty} \left[ -\Gamma_{d1,c1,0}^{(1,p1)} X_{d1,c1}^B \right]^n; & \text{if } \left| \Gamma_{d1,c1,0}^{(1,p1)} X_{d1,c1}^B \right| < 1. \end{cases} \end{aligned} \quad (2.5)$$

The  $\sim$  in  $\tilde{X}_{d1,c1}^{(1)}$  indicates this is only one term in equation 2.3. Equation 2.5 illustrates when the rate of elimination goes from low concentration behaviour to high concentration behaviour. In addition, if  $B > A$  then the maximum rate of flow from compartment  $c1$  to compartment 0 occurs when the amount of drug is

$$X_{d1,c1}^{M(c1,0)} = \left[ \frac{A_{d1,c1,0}^{(1,p1)}}{\Gamma_{d1,c1,0}^{(1,p1)} \left( B_{d1,c1,0}^{(1,p1)} - A_{d1,c1,0}^{(1,p1)} \right)} \right]^{1/B_{d1,c1,0}^{(1,p1)}}, \quad (2.6)$$

for a single process. This will change if two processes are involved. Concentrations greater than the threshold given in equation 2.6 will produce a larger *AUC* due to the slower elimination rate in addition to the higher concentration. The amount of molecules at the point where the low concentration behaviour transits to high concentration behaviour due to the effect of saturation on the kinetics of the molecules is expressed as

$$X_{d1,c1,c2}^{T(c1,c2)} = \left[ \frac{1}{\Gamma_{d1,c1,c2}^{(1,p1)}} \right]^{1/B_{d1,c1,c2}^{(1,p1)}}, \quad (2.7)$$

from equation 2.5.

3. The third term on the right-hand side in equation 2.1 describes the change of molecule  $d1$  in compartment  $c1$  into another type of molecule ( $d1, c1|d2, c1$ ) and vice versa. It describes the decomposition of the materials that are used in the drug preparation, and allows the molecules to become interactive with the body. This type of reaction is represented by Figure 2.4 and the differential equation is;

$$\frac{dX_{d1,c1}^{(2)}}{dt} = \sum_{d2=1}^N \sum_{p1=0}^2 \left\{ \frac{\delta_{d2|d1}^{(1,p1,d1,c1)} \bar{k}_{d2|d1}^{(2,p1,d1,c1)} X_{d2,c1}^{A_{d2|d1}^{(2,p1,d1,c1)}}}{1 + \Gamma_{d2|d1}^{(2,p1,d1,c1)} X_{d2,c1}^{B_{d2|d1}^{(2,p1,d1,c1)}}} - \frac{\delta_{d1|d2}^{(1,p1,d1,c1)} \bar{k}_{d1|d2}^{(2,p1,d1,c1)} X_{d1,c1}^{A_{d1|d2}^{(2,p1,d1,c1)}}}{1 + \Gamma_{d1|d2}^{(2,p1,d1,c1)} X_{d1,c1}^{B_{d1|d2}^{(2,p1,d1,c1)}}} \right\}. \quad (2.8)$$

There are a few changes to the notation compared to equation 2.3. In the subscripts, the indices are split by '|'. This break, '|', indicates the change from one type of molecule into another type of molecule. The  $\delta$ 's are in the model to ac-

count for different rates of change, that is they enforce conservation of mass. For example, a molecule may split into two new molecules. The effective rate constant ( $\bar{k} = \bar{k}_{d1|d2}^{(2,p1,d1,c1)}$ ) is;

$$\begin{aligned} \bar{k} &= k_{d1|d2}^{(2,p1,d1,c1)} \left[ 1 + \sum_{d3=1}^N \sum_{c2=1}^M \sum_{p2=0}^2 \frac{\alpha_{d1|d2||d3,c2}^{(2,p1,p2,d1,c1)} X_{d3,c2}^{C_{d1|d2||d3,c2}^{(2,p1,p2,d1,c1)}}}{1 + \beta_{d1|d2||d3,c2}^{(2,p1,p2,d1,c1)} X_{d3,c2}^{D_{d1|d2||d3,c2}^{(2,p1,p2,d1,c1)}}} \right] H(X_{d1,c2}) \\ &\times H \left( 1 + \sum_{d3=1}^N \sum_{c2=1}^M \sum_{p2=0}^2 \frac{\alpha_{d1|d2||d3,c2}^{(2,p1,p2,d1,c1)} X_{d3,c2}^{C_{d1|d2||d3,c2}^{(2,p1,p2,d1,c1)}}}{1 + \beta_{d1|d2||d3,c2}^{(2,p1,p2,d1,c1)} X_{d3,c2}^{D_{d1|d2||d3,c2}^{(2,p1,p2,d1,c1)}}} \right). \end{aligned} \quad (2.9)$$

In the subscripts, the indices are split by ‘|’ and ‘||’. The first break, ‘|’, indicates the change from one type of molecule into another type of molecule. The second break, ‘||’, separates the molecules involved in the reaction from the molecules interfering with the reaction.

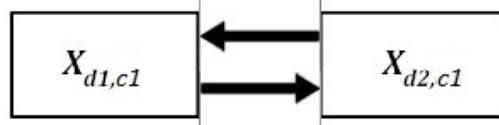


Figure 2.4: Change of molecule  $d1$  to molecule  $d2$  in compartment  $c1$ .

4. The fourth term on the right-hand side of the differential equation in equation 2.1 describes the change of one type of molecule into two new molecules. For example, the breakup of a complex molecule into a metabolite and an enzyme. The reaction is illustrated in Figure 2.5 and the differential equation is given by equation 2.10;

$$\frac{dX_{d1,c1}^{(3)}}{dt} = \sum_{d2=1}^N \sum_{d3=1}^N \sum_{p1=0}^2 \left\{ \frac{-\delta' \bar{k}_{d1|d2,d3}^{(3,p1,c1)} X_{d1,c1}^{A_{d1|d2,d3}^{(3,p1,c1)}}}{1 + \Gamma_{d1|d2,d3}^{(3,p1,c1)} X_{d1,c1}^{B_{d1|d2,d3}^{(3,p1,c1)}}} + \right.$$

$$\left. \begin{aligned} & \frac{\delta'' \bar{k}_{d_2|d_1,d_3}^{(3,p_1,c_1)} X_{d_2,d_1,d_3}^{A(3,p_1,c_1)}}{1 + \Gamma_{d_2|d_1,d_3}^{(3,p_1,c_1)} X_{d_2,c_1}^{B(3,p_1,c_1)}} + \frac{\delta''' \bar{k}_{d_2|d_3,d_1}^{(3,p_1,c_1)} X_{d_2,c_1}^{A(3,p_1,c_1)}}{1 + \Gamma_{d_2|d_3,d_1}^{(3,p_1,c_1)} X_{d_2,c_1}^{B(3,p_1,c_1)}} \end{aligned} \right\}, \quad (2.10)$$

where  $\delta'$ ,  $\delta''$ , and  $\delta'''$  represent  $\delta_{d_1|d_2,d_3}^{(2,p_1,d_1,c_1)}$ ,  $\delta_{d_2|d_1,d_3}^{(2,p_1,d_1,c_1)}$ , and  $\delta_{d_2|d_3,d_1}^{(2,p_1,d_1,c_1)}$  respectively.

The  $\delta$ 's enforce mass conservation. Note that the last two sets of sums in equation 2.10 are equivalent and one must be careful in regard to double counting. The effective rate constant ( $\bar{k} = \bar{k}_{d_1|d_2,d_3}^{(3,p_1,c_1)}$ ) is;

$$\begin{aligned} \bar{k} &= k_{d_1|d_2,d_3}^{(3,p_1,c_1)} \left[ 1 + \sum_{d_4=1}^N \sum_{c_2=1}^M \sum_{p_2=0}^2 \frac{\alpha' X_{d_4,c_2}^{C(3,p_1,p_2,c_1)}}{1 + \beta' X_{d_4,c_2}^{D(3,p_1,p_2,c_1)}} \right] \\ &\times H(X_{d_1,c_1}) H \left( 1 + \sum_{d_4=1}^N \sum_{c_2=1}^M \sum_{p_2=0}^2 \frac{\alpha' X_{d_4,c_2}^{C(3,p_1,p_2,c_1)}}{1 + \beta' X_{d_4,c_2}^{D(3,p_1,p_2,c_1)}} \right), \end{aligned} \quad (2.11)$$

where the terms  $\alpha'$  and  $\beta'$  represent  $\alpha_{d_1|d_2,d_3||d_4,c_2}^{(3,p_1,p_2,c_1)}$  and  $\beta_{d_1|d_2,d_3||d_4,c_2}^{(3,p_1,p_2,c_1)}$  respectively.

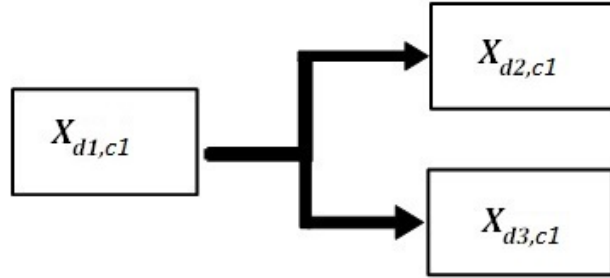


Figure 2.5: Change of molecule  $d_1$  into two molecules  $d_2$  and  $d_3$  in compartment  $c_1$ .

- The fifth term in equation 2.1 is the reverse of the previous case and describes two types of molecules combining together to form a single molecule. An example of this is the formation of a complex from a substrate binding to a ligand. This type of

reaction is illustrated in Figure 2.6 and the differential equation is;

$$\frac{dX_{d1,c1}^{(4)}}{dt} = \frac{dX_{d1,c1}^{(4,1)}}{dt} - \frac{dX_{d1,c1}^{(4,2)}}{dt} - \frac{dX_{d1,c1}^{(4,3)}}{dt}. \quad (2.12)$$

The three terms on the right-hand side of equation 2.12 represent the differential equations in equation 2.13, 2.14, and 2.15 respectively.

$$\frac{dX_{d1,c1}^{(4,1)}}{dt} = \sum_{d2,d3=1}^N \sum_{p1,p2=0}^2 \left\{ \frac{\bar{k}_{d3,d2|d1}^{(4,p1,p2,d1,c1)} X_{d3,c1}^{A(4,p1,d1,c1)} X_{d2,c1}^{A(5,p2,d1,c1)}}{1 + \Gamma_{d3,d2|d1}^{(4,p1,p2,d1,c1)} X_{d3,c1}^{B(4,p1,d1,c1)} X_{d2,c1}^{B(5,p2,d1,c1)}} \right\}. \quad (2.13)$$

$$\frac{dX_{d1,c1}^{(4,2)}}{dt} = \sum_{d2,d3=1}^N \sum_{p1,p2=0}^2 \left\{ \frac{\bar{k}_{d2,d1|d3}^{(4,p1,p2,d1,c1)} X_{d2,c1}^{A(4,p1,d1,c1)} X_{d1,c1}^{A(5,p2,d1,c1)}}{1 + \Gamma_{d2,d1|d3}^{(4,p1,p2,d1,c1)} X_{d2,c1}^{B(4,p1,d1,c1)} X_{d1,c1}^{B(5,p2,d1,c1)}} \right\}. \quad (2.14)$$

$$\frac{dX_{d1,c1}^{(4,3)}}{dt} = \sum_{d2,d3=1}^N \sum_{p1,p2=0}^2 \left\{ \frac{\bar{k}_{d1,d2|d3}^{(4,p1,p2,d1,c1)} X_{d1,c1}^{A(4,p1,d1,c1)} X_{d2,c1}^{A(5,p2,d1,c1)}}{1 + \Gamma_{d1,d2|d3}^{(4,p1,p2,d1,c1)} X_{d1,c1}^{B(4,p1,d1,c1)} X_{d2,c1}^{B(5,p2,d1,c1)}} \right\}. \quad (2.15)$$

Note that care must be exercised to not double count. The effective rate constant ( $\bar{k} = \bar{k}_{d1,d2|d3}^{(4,p1,p2,d1,c1)}$ ) is;

$$\begin{aligned} \bar{k} &= \delta_{d1,d2|d3}^{(3,p1,p2,d1,c1)} k_{d1,d2|d3}^{(4,p1,p2,c1)} H(X_{d1,c1}) H(X_{d2,c1}) \\ &\times H \left( 1 + \sum_{d4=1}^N \sum_{c2=1}^M \sum_{p3=0}^2 \frac{\alpha_{d1,d2|d3||d4,c2}^{(4,p1,p2,p3,c1)} X_{d1,d2|d3||d4,c2}^{C(4,p1,p2,p3,c1)}}{1 + \beta_{d1,d2|d3||d4,c2}^{(4,p1,p2,p3,c1)} X_{d1,d2|d3||d4,c2}^{D(4,p1,p2,p3,c1)}} \right) \\ &\times \left[ 1 + \sum_{d4=1}^N \sum_{c2=1}^M \sum_{p3=0}^2 \frac{\alpha_{d1,d2|d3||d4,c2}^{(4,p1,p2,p3)} X_{d1,d2|d3||d4,c2}^{C(4,p1,p2,p3)}}{1 + \beta_{d1,d2|d3||d4,c2}^{(4,p1,p2,p3)} X_{d1,d2|d3||d4,c2}^{D(4,p1,p2,p3)}} \right]. \end{aligned} \quad (2.16)$$

The  $\delta$ 's enforce conservation of mass.

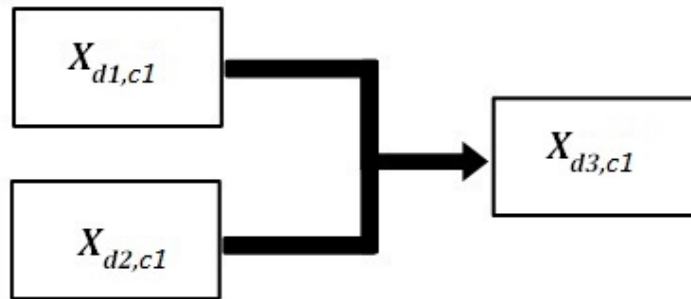


Figure 2.6: The binding of molecules  $d1$  and  $d2$  to create molecule  $d3$  in compartment  $c1$  .

### 2.1.3 PK Modelling Parameters

The PK parameters are fundamental to obtaining a better prediction of the behaviour of the molecules in the body. In order to fit the PK parameters to the data, we need the volume of distribution. Once the parameters are determined, the  $AUC$ ,  $C_{max}$  and half-life can be calculated. They include;

Volume of distribution ( $V_d$ ): The  $V_d$  is the theoretical proportionality constant between the amount of molecules contained within the body and the measured concentration of the molecules, which is typically restricted to the blood/plasma [73]. The extent at which plasma protein binds to the molecules determines the  $V_d$ . When a molecule has a lower plasma protein binding the  $V_d$  will be higher, and lower at high plasma protein binding. The mathematical expression for our model is;

$$C_{d1,c1} = \frac{X_{d1,c1}}{V_{d,d1,c1}}, \quad (2.17)$$

where  $V_{d,d1,c1}$  is the  $V_d$  for molecule  $d1$  in compartment  $c1$ ,  $X_{d1,c1}$  is the amount of molecule  $d1$  in compartment  $c1$ , and  $C_{d1,c1}$  is the concentration of molecule  $d1$  in compartment  $c1$ . The  $V_d$  in our models were obtained by minimizing the parameter along with the other PK

parameters to fit in to the clinical data.

AUC: the integral of the molecule's concentration-time curve, AUC is a numerical value that estimates the extent to which a body is exposed to a particular type of molecule. It also evaluates the bioavailability of the molecule from its dosage; i.e. the amount of drug that is readily available in the bloodstream for the target site (see equation 1.11). The main factors are the rate of elimination and the amount of dose administered. All the AUCs in our models are calculated by using the numerical estimation method (trapezoid method). The concentration-time curve considered as a discrete set of blocks and each trapezoid were determined linearly and add up together to form the AUC. Each of the trapezoid areas are expressed as:

$$AUC = \frac{1}{2}(C_1 + C_2)(t_2 - t_1), \quad (2.18)$$

Peak plasma concentration ( $C_{max}$ ) indicates the maximum concentration reached by the absorption phase of a drug, and it depends on the following events: the rate of absorption, the administered dose, and elimination. These events can be influenced by the activity of the proteins involved along the pathways. The time at which the plasma concentration reaches its peak is known as *time of peak concentration* ( $t_{max}$ ), which is used to estimate the rate of absorption and to monitor the phase change. Our models were designed using clinical data that have mainly bolus infusion. The  $C_{max}$  is attained at the end of the infusion.

Half-life: the amount of time required for a substance to decrease to half its initial value. We obtained  $t_{1/2}$  in our model numerically by determining half value of the  $C_{max}$  and find the corresponding time for this value. This gives us the accurate  $t_{1/2}$  obtained by our model.

#### 2.1.4 Numerical Modelling Tools

The origin of numerical analysis started as far back as 1945 after World War II ended. Von Neumann was one of the earliest researchers studying numerical simulations. He identified numerical fluid dynamics using computational calculations to replace classical analysis [74]. Modern numerical analysis and mathematical modelling have advanced into

processing large and complex datasets with supercomputers, such as kinetics prediction, neuron transport, non-steady multidimensional fluid dynamics, and so on [75].

The RK fourth-order method was adopted in this work for each molecules' rate equation. Nonlinear differential equations for all the compartments are solved using this numerical method. There are sets of initial numbers required in using this model, such as initial concentration values for all the molecules in all the compartments and PK parameter values. Based on the compartmental analysis, the slope increment in each compartment is treated independently. For instance, the molecule 2 (see Figure 2.2) concentration analysis in compartment 1 is analysed as a summation of the molecule's inflows and outflows in the compartment. The outflow of molecules from compartment 1 is into compartments 2, 3, and 4; while the inflows are the reversed of the outflows, from compartments 2, 3, and 4 into compartment 1. Analysing nonlinear differential equations in the RK fourth order method involves four steps [76]:

The first step functions are written as:

$$\Delta X_{d1,c1}^{(1)} = h \frac{dX_{d1,c1}}{dt}(\vec{X}, t_n), \quad (2.19)$$

where  $h$  is the time step size and  $\vec{X}$  is the array of all the different types of molecules in all the compartments.

The second step functions are written as:

$$\Delta X_{d1,c1}^{(2)} = h \frac{dX_{d1,c1}}{dt} \left( \vec{X} + \frac{\Delta \vec{X}^{(1)}}{2}, t_n + \frac{h}{2} \right). \quad (2.20)$$

The third step functions are written as:

$$\Delta X_{d1,c1}^{(3)} = h \frac{dX_{d1,c1}}{dt} \left( \vec{X} + \frac{\Delta \vec{X}^{(2)}}{2}, t_n + \frac{h}{2} \right). \quad (2.21)$$

The fourth step functions are written as:

$$\Delta X_{d1,c1}^{(4)} = h \frac{dX_{d1,c1}}{dt} \left( \vec{X} + \Delta \vec{X}^{(3)}, t_n + h \right). \quad (2.22)$$

Each increment of the function is based on the slope at the midpoint of the previous value. For instance,  $\Delta \vec{X}_{d1,c1}^{(1)}$  depends on that of the initial numbers,  $\Delta \vec{X}_{d1,c1}^{(2)}$  on the increment in previous term  $\Delta \vec{X}_{d1,c1}^{(1)}$ ,  $\Delta \vec{X}_{d1,c1}^{(3)}$  on  $\Delta \vec{X}_{d1,c1}^{(2)}$ , and  $\Delta \vec{X}_{d1,c1}^{(4)}$  on  $\Delta \vec{X}_{d1,c1}^{(3)}$ . The general solution of the amount of molecule in compartment  $c1$  at time  $t_{n+1} = t_n + h = t_o + (n+1)h$  is

$$X_{d1,c1}^{(n+1)} = X_{d1,c1}^{(n)} + \frac{1}{6} \left( \Delta X_{d1,c1}^{(1)} + 2\Delta X_{d1,c1}^{(2)} + 2\Delta X_{d1,c1}^{(3)} + \Delta X_{d1,c1}^{(4)} \right), \quad (2.23)$$

where  $X_{d1,c1}^{(n)} = X_{d1,c1}(t_n)$ .

### Variance and Optimization

The weighted percentage variance ( $S_p$ ) and the weighted variance ( $S_\sigma$ ) between the theoretical concentrations and the clinical data was minimized.  $S_p$  is given as

$$S_p = \frac{4}{N_p} \sum_{l,k,c1,d1} p_{l,d1,c1,k} \left[ \frac{X_{d1,c1}(t_k) - C_{d1,c1}^{(l)}(t_k)V_{d,d1,c1}}{X_{d1,c1}(t_k) + C_{d1,c1}^{(l)}(t_k)V_{d,d1,c1}} \right]^2, \quad (2.24)$$

where  $N_p$  is the total weight of the patients;  $X_{d1,c1}(t_k)$  is the amount of molecule  $d1$  in compartment  $c1$  at time  $t_k$  obtained from the RK fourth order method;  $C_{d1,c1}^{(l)}(t_k)$  is the concentration of molecule  $d1$  in compartment  $c1$  at time  $t_k$  from the clinical study  $l$ ; the weighting coefficient  $p_{l,d1,c1,k}$  is the number of patients attached to the formation of the mean concentration  $C_{d1,c1}^{(l)}(t_k)$ ;  $V_{d,d1,c1}$  is the distribution volume of molecule  $d1$  in compartment  $c1$ .

In order to study the sensitivity of  $S_p$  to the parameter, each one was varied while the other parameters were held constant until  $S_p$  increases by 1%. This gives an uncertainty in the parameters; denoted by  $k(\delta k)$ . The concentration of the molecules can vary over several

orders of magnitudes; hence  $S_p$  was minimized for the optimization of the parameters, since  $S_p$  gives equal weight to all the data points regardless of the absolute magnitude.  $S_p$  does not give priority to  $C_{max}$  which was seen as a deficiency because that is the essence of making a good prediction of the drug's toxicity.  $C_{max}$  of a drug is directly related to the harm it can cause to the body. This encouraged us to make use of  $S_\sigma$  starting from the results obtained from the minimisation of  $S_p$ .  $S_\sigma$  is given as:

$$S_\sigma = \frac{1}{N_p} \sum_{l,k,c1,d1} p_{l,d1,c1,k} \left[ \frac{X_{d1,c1}(t_k)}{V_{d,d1,c1}} - C_{d1,c1}^{(l)}(t_k) \right]^2. \quad (2.25)$$

The analysis with  $S_\sigma$  is given in appendix B.

### Model Algorithm with BOBYQA

Bound Optimization BY Quadratic Approximation (BOBYQA) is one of Powell's algorithms for optimization in multi-dimensions. It was developed by Michael J. D. Powell [77] and is available as an open source [78]. It is a derivative-free algorithm that solves an optimization problem using a bound constrained trust region that forms a quadratic model by interpolation [79]. The advantage of the optimizer is the constraint of lower and upper bounds that control the assign values to the function variables. The schematic drawing of the BOBYQA algorithm is shown in Figure 2.7.

BOBYQA algorithm can be accessed from Github server as one of the repositories developed by Roman Siromakha [78]. The compiling files and their functions are summarised below:

(i.) *5-Fu\_RK\_function.cpp*, containing the modelling code that solves all non-linear differential equations for all the molecules in each compartment using RK fourth-order method, and also includes the code that calculates  $S_p$  and  $S_\sigma$  between the clinical data and the numerical results. The main function part of the code "*int main()*" is written in this file, and there is a call to another executable file named "bobyqa.cpp" that returns minimized variables.

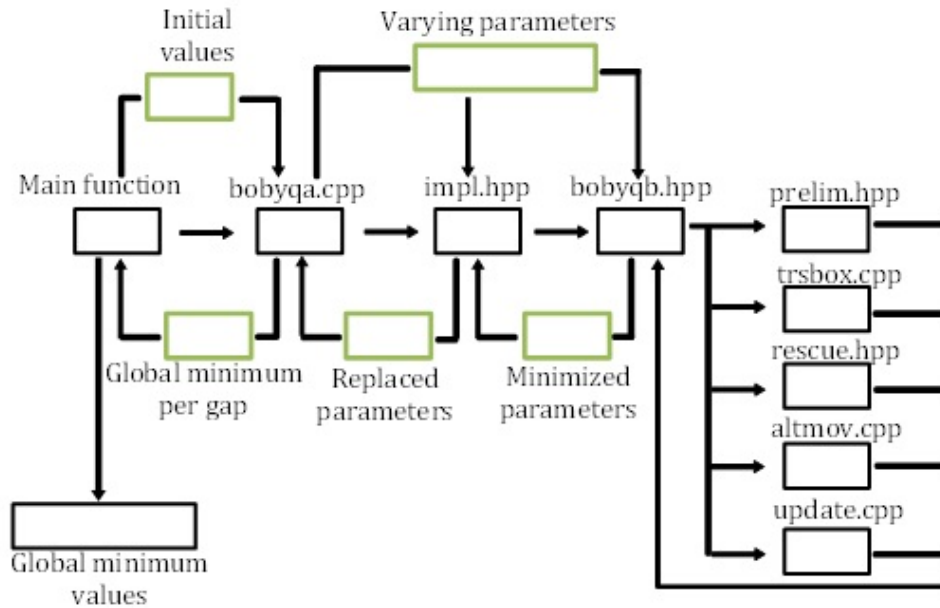


Figure 2.7: Schematic drawing of the model algorithm.

(ii.) *bobyqa.cpp* is a source file that performs the task of assigning the appropriate minimizing variable to the function by calling other source files. It serves as the organizer for the other source files. It is the only function called from the main function and links all other functions for its return values. It calls a header file named "impl.hpp" for the return of the appropriate value to assign, and implements the fitting variables.

(iii.) *impl.hpp* serves as a subroutine that searches among the several variables in a function for the global minimum value of those variables that fits into the function. It has passed components  $N$ ,  $NPT$ ,  $X$ ,  $XL$ ,  $XU$ ,  $RHOBEG$ ,  $RHOEND$ ,  $W$ , and  $MAXFUN$  from the file *bobyqa.cpp*.  $N$  is the number of variables and set to be at least two.  $NPT$  is the number of interpolation conditions. Its value is in the interval  $[N + 2, (N + 1)(N + 2)/2]$ .  $RHOBEG$  and  $RHOEND$  are the initial and final values of a trust region radius, so both must be positive with  $RHOEND$  no greater than  $RHOBEG$ . An error return occurs if any of the differences  $XU(I) - XL(I)$ ,  $I = 1, \dots, N$ , is less than  $2 * RHOBEG$ .  $MAXFUN$  is an upper bound on the number of calls of RK function. The array  $W$  represents the

working space. Its length was set to be at least  $(NPT + 5) * (NPT + N) + 3 * N * (N + 5) / 2$ . The `impl.hpp` routine makes a call to another header file "`bobyqb.hpp`" for holding and comparing variables.

(iv.) `bobyqb.hpp` is the header file that comprises arguments that are identical to such in the subroutine `bobyqa`. They hold numbers for arguments to make an adequate comparison. `bobyqb` has some function calls to four source files; `prelim`, `trsbox`, `altmov`, and `update`.

(v.) `trsbox.cpp` is a source file that comprises the corresponding arguments that are identical to subroutine `BOBYQA`. Also, additional arguments for its localized routine are: `DELTA` that seeks a small value of the quadratic model; `XOPT` is set to the displacement from `XBASE` of the trust region centre. `D` is usually `XNEW-XOPT`, known to be generated repetitively from an initial value as the trial step from `XOPT`. `XNEW` is a set value to a new vector of variables that minimizes the quadratic model. `XNEW` is regarded as `XOPT+D` after the whole loop. `GNEW` is also an argument that holds the gradient of the quadratic model at `XOPT+D` within the trust region radius, that updates whenever `D` does. `XBASE` holds a shift of origin that should reduce the contributions from rounding errors to values of the model and Lagrange functions. `XPT` is a two-dimensional array that holds the coordinates of the interpolation points relative to `XBASE`. `BMAT` holds the last `N` columns of `H`. `ZMAT` holds the factorization of the leading `NPT` by `NPT` submatrix of `H`, it provides both the correct rank and positive semi-definiteness. `NDIM` is the first dimension of `BMAT` and has the value `NPT+N`. `XBDI` represents the working space vector in this subroutine, it is set to `XBDI(I)=-1.0` or `XBDI(I)=1.0` only when the value of `I`-th variable has become fixed at a bound at `SL(I)` or `SU(I)` respectively. `SL(I)` and `SU(I)` correspond to the lower and upper bounds on moves from the updated `X`. They provide useful and exact information about components of `X` that become within distance trust region radius from their bounds. `SL` and `SU` hold the differences at lower bound `XL-XBASE` and `XU-XBASE` at the upper bound respectively.

(vi.) `altmov.cpp` is a source file that performs the movements of the index of optimal

interpolation points. It is partially comprised of similar passing arguments from subroutine BOBYQB, such as: N, NPT, XPT, XOPT, BMAT, ZMAT, NDIM, SL and SU with the same interpretations compared to that of BOBYQB. The addition arguments involved in this locality are KOPT, the optimal-interpolation-point index. KNEW, the interpolation point index that is going to be moved. ADELTA is the current trust region bound. The suitable new position for the interpolation point is labelled as XNEW. From XOPT, the step XNEW-XOPT is controlled to move along straight lines through XOPT and another interpolation point.

(vii.) *update.cpp* is the source file that updates the arrays BMAT and ZMAT mentioned in *trsbox.cpp*, this is essential for the new position of the interpolation point. The vector VLAG contains the values of the Lagrange functions at a new point X. It has N+NPT components, set on entry to the first NPT and last N components.

## 2.2 Summary

More than thirty-seven models were introduced for modelling two types of molecules within compartments progressively increasing from one-compartment to three-compartment. There are four fundamental interactions of molecules involved during the PK processes (ADME): the process of acquiring the clinically prepared drug in the active mode, the interaction of the drug with the flow of the drug from one compartment to another, the interaction of the drug with enzymes to form substrate-complex molecules, the decomposition of the substrate-complex molecules into metabolites and the enzymes, and the elimination of the molecules. The compartments are representative of events or activities. For instance, the one-compartment model unified all PK events into a single rate process, while the two-compartment models split the events into two different compartments, and likewise, the three-compartment model divides the events into three compartments. The nonlinear differential equations that describe the time course of the molecules in the body is a sum of five different processes. The processes involved are the infusion of molecules into a

compartment, the kinetic flow of molecules between compartments (inflows and outflows), the change of molecules into other molecules, the decomposition of a molecule into two molecules, and the composition of two molecules to form a single molecule.

The  $AUC$ ,  $C_{max}$ , and half-life are the quantities examined in the  $S_p$  models. The numerical modelling tools involved are: the RK fourth-order method that solves the nonlinear differential equations, and Powell's method (BOBYQA algorithm) with a bound constrained trust region that controls the searching condition for determining the parameters that minimizes the variance.

## Chapter 3

# Model Sampling Design and Analysis for 5-FU

---

*Cancer is really hard to go through  
and it's really hard to watch someone you love go through,  
and I know because I have been on both sides of the equation.*

– Cynthia Nixon

---

This chapter analyses the development of a multi-compartment model and justifies the fitness of the numerical solution of the system of nonlinear differential equations to the clinical data. The eight clinical datasets are shown in Table 3.1 were digitised to fit the PK models of 5-FU. The model sampling was designed with progressive analyses from the one-compartment model to the three-compartment model. The results were used to obtain the  $C_{max}$ ,  $AUC$ , and half-life.

Three major categories were employed for fitting the models to the clinical data. Case 1 deals with varying the parameters other than the exponents. We considered the first-order process as the primary and the subordinate cases as a combination with the zeroth- and second-order processes. Case 2 involves varying the PK parameters, including the exponents. Finally, case 3 involves the addition of interactions between the different types of molecules, along with examining the change in the effective kinetic rate constants by the presence of other molecules.

Table 3.1: The clinical datasets

Dataset	Reference	Dosage $\left(\frac{mg}{m^2}\right)$	IV Time $(min)$	Infusion $\left(\frac{\mu mol}{min.m^2}\right)$	Patients	# of data points
1	G. Bocci et al. [17]	250	1	1921	185	6
2	Di Paolo et al. [80]	370	1	2844	84	6
3	Di Paolo et al. [81]	370	2	1422	80	6
4	Di Paolo et al. [82]	370	5	568	26	6
5	G. Bocci et al. [1]	370	1	2844	20	9
6	Casale et al. [83]	400	2	1537	18	7
7	Per-Anders et al. [72]	500	2	1921	14	7
8	Heggie et al. [84]	500	1.5	2562	10	9

In all three cases, we minimised the variance for all the datasets shown in Table 3.1, but the graphs in Chapter Three illustrate only the first three datasets (1, 2, and 3) in the table to show some level of tidiness. These three datasets dominate the population of patients, three hundred and forty-nine out of four hundred and thirty-seven patients. The graphs for the other sets of clinical data are shown in appendix C.

### 3.1 One-Compartment Model

The one-compartment model has the simplest model design of all the compartment PK models. It unifies all the systemic events in the body, using a single flow rate from the stage of administration of the drug to its distribution across the body system and then to elimination, as shown in Part A of Figure 2.1. We divided the analysis of the optimised PK parameters into two: optimisation with fixed exponents and optimisation with variable exponents. The variance  $S_p$  between the theoretical and experimental results is minimised to obtain the parameter values.

### 3.1.1 Optimisation with Fixed Degree Exponents

Case 1 begins with the Michaelis-Menten model and looks at the effects of having more than one process. We assume that the Michaelis-Menten model is the dominant behaviour.

The fixed parameters involved are as follows:

$$A_{5FU,1,0}^{(0)} = B_{5FU,1,0}^{(0)} = 0; A_{5FU,1,0}^{(1)} = B_{5FU,1,0}^{(1)} = 1; \text{ and } A_{5FU,1,0}^{(2)} = B_{5FU,1,0}^{(2)} = 2.$$

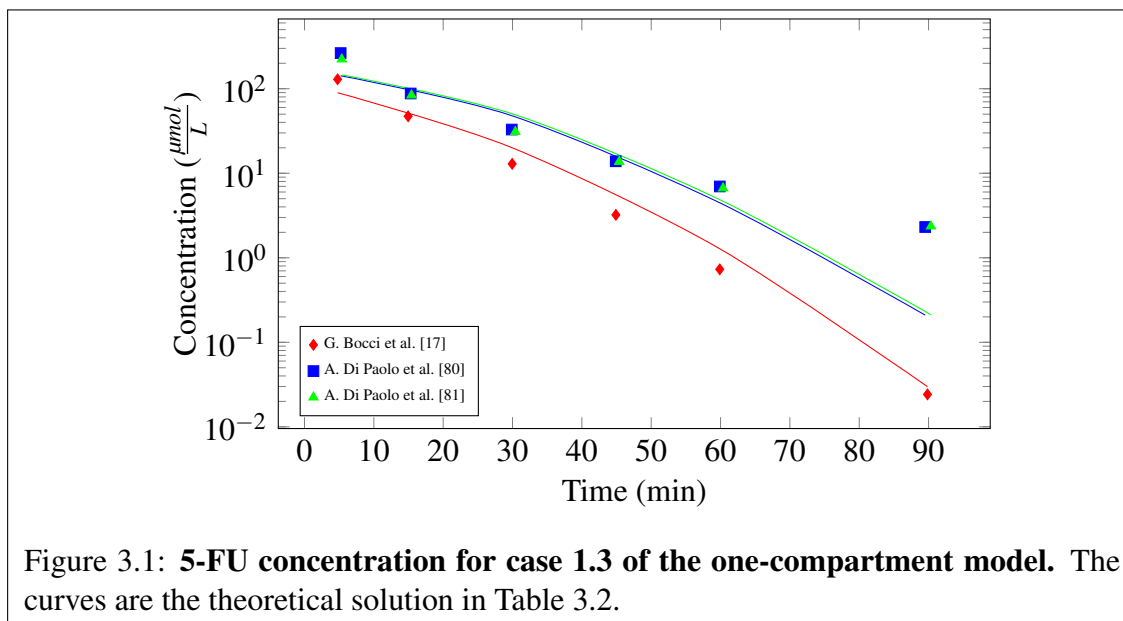
Table 3.2: 5-FU parameters for the one-compartment model with fixed exponents

Case	$p$	$k_{5FU,1,0}^{(1,p)}$	$\Gamma_{5FU,1,0}^{(1,p)}$	$V_{d,5FU,1} \left( \frac{L}{m^2} \right)$	$S_p$
1	1	0.1198(24)	0.001372(61)	16.33(17)	0.0703
1.1	0	0.0613(84)	-	16.60(98)	0.0696
	1	0.10012(57)	0.000857(32)		
1.2	1	0.1198(24)	0.001372(61)	16.33(17)	0.0703
	2	0.000000(46)	N/A*		
1.3	0	0.0613(84)	-	16.60(98)	0.0696
	1	0.10012(57)	0.000857(32)		
	2	0.000000(50)	N/A*		

\*This value is not available due to the fact that  $k$  vanishes. The S.I units for  $k_{5FU,1,0}^{(0)}$  is  $\frac{\mu\text{mol}}{m^2 \cdot \text{min}}$ ,  $k_{5FU,1,0}^{(1)}$  is  $\frac{1}{\text{min}}$ ,  $\Gamma_{5FU,1,0}^{(1)}$  is  $\frac{m^2}{\mu\text{mol}}$ ,  $k_{5FU,1,0}^{(2)}$  is  $\frac{m^2}{\mu\text{mol} \cdot \text{min}}$ , and  $\Gamma_{5FU,1,0}^{(2)}$  is  $\frac{m^4}{\mu\text{mol}^2}$ .

In addition to optimising the first-order process, we optimised the combination of zeroth-order plus first-order processes, first-order plus second-order processes, and the combination of zeroth-, first- and second-order process. The results are shown in Table 3.2. The analysis shows that there is no contribution from the second-order processes, and the zeroth-order process improves the variance by 1.1%. The dominant process is the combination of a zeroth-order and a saturable first-order process. Figure 3.1 shows the corresponding concentration vs. time graph. The theoretical curves in the graph involved the combination of the three processes, which is case 1.3 in Table 3.2. The nonlinear curves in the graph is an

indication that the process is not first order.



We obtained time, amount of molecules, and concentrations at the point of transition between low and high concentration behaviour. The results are shown in Table 3.3 for the three sets of infusion, using the four cases 1, 1.1, 1.2, and 1.3. The first transition point from low concentration behaviour to high concentration behaviour indicates that there is a slower time of transition when there is a low infusion. For instance, if we compare  $1422 \frac{\mu\text{mol}}{\text{min.m}^2}$  over two minutes with  $2844 \frac{\mu\text{mol}}{\text{min.m}^2}$  over one minute, there is 51.9% increase. Also, the transition behaviours between two different infusions over the same period indicate that the transition time is lower in the larger infusion for the first transition; whereas, the second transition point shows higher transition time for larger infusion. We can deduce from the result that the dosage of a drug influences the transition time between low and high concentration. The infusion of  $2844 \frac{\mu\text{mol}}{\text{min.m}^2}$  gives a lower transition time at the first transition point compared to  $1921 \frac{\mu\text{mol}}{\text{min.m}^2}$  and gives a higher transition time at the second transition point. There are some differences in comparing the two models, case 1 and case 1.3 of the one-compartment model. Case 1 gives a faster transition time than case 1.3 to switch from a low concentration behaviour to a high concentration behaviour; whereas, the transition from a high concentration behaviour to a low concentration behaviour is faster in

case 1.3 than case 1. See Table 3.3.

Table 3.3: 5-FU transition parameters for the one-compartment model with fixed exponents.

Case	Infusion	IV Time	$X_{5FU,1}^{T(1,0)}$	$C_{5FU,1}^{T(1,0)}$	$t_{1T(1,0)}$	$t_{2T(1,0)}$
1	1921	1	728.9	44.6	0.38	26.9
	2844	1			0.25	48.9
	1422	2			0.52	50.3
1.3	1921	1	1167	70.3	0.63	15.6
	2844	1			0.41	37.6
	1422	2			0.83	41.3

The S.I units of  $X_{5FU,1}^{g(1,0)}$  is  $\frac{\mu\text{mol}}{\text{m}^2}$  and  $C_{5FU,1}^{g(1,0)}$  is  $\frac{\mu\text{mol}}{\text{L}}$ , and  $t_{1/2}$  is *min.* where  $d$  represents DHFU and  $g$  represents T and M that symbolise transition and maximum values respectively for both concentrations and number of molecules.

### 3.1.2 Optimisation with Variable Exponents

There are several cases involved in this section; case 2 is the primary run, on which the subordinates were examined. All the PK parameters involved were varied, including the exponents. Table 3.4 shows the results, which are illustrated in Figure 3.2 (A) for case 2. The results indicate that the exponents A and B in the one-compartment model for 5-FU are approximately the same as those for the first-order process.

Table 3.4: 5-FU parameters for the one-compartment model with variable exponents

Case	$A^{(1,p)}$	$B^{(1,p)}$	$k_{5FU,1,0}^{(1,p)}$	$\Gamma_{5FU,1,0}^{(1,p)}$	$V_{d,5FU,1}$	$S_p$
2	0.9567(34)	1.2510(98)	0.1280(21)	0.0001476(90)	16.7(12)	0.0690
2.1	0.9631(29)	1.2505(90)	0.1205(16)	0.0001435(89)	16.8(14)	0.0682
	0.00(36)	0.0000*	0.023(12)	0.00(89)		
2.2	0.9631(29)	1.2505(91)	0.1204(25)	0.0001435(90)	16.8(13)	0.0682
	0.00(36)	0.0000*	0.023(12)	0.00(92)		
	2.0000*	2.0000*	0.000000(21)	N/A**		

\*The error is indeterminate since the coefficient is zero. \*\*Not relevant since  $k_{5FU,j,k}^{(p)} = 0$ . The unit of  $k_{5FU,1,0}^{(p)}$  is

$$\frac{\mu\text{mol}^{(1-A)}}{\text{m}^{(2-2A)}\text{min}}, \Gamma_{5FU,1,0}^{(p)} \text{ is } \frac{\text{m}^{2B}}{\mu\text{mol}^{(B)}}, \text{ and } V_{d,5FU,1} \text{ is } \frac{\text{L}}{\text{m}^2}$$

There is a slight change in the numbers for the exponents  $A$  and  $B$ . Considering case 2 of the one-compartment model, the value obtained for exponent  $A$  at low concentrations is 0.9567, which approximately constitutes a first-order process; however, at high concentrations, the exponent  $A - B$  is  $-0.2943$ , which is not a zeroth-order process as in the Michaelis-Menten's model. The flow rate goes to zero as the concentration becomes very large.

Case 2 has a slightly better fit when compared to case 1, as it has 1.85% reduction in  $S_p$ , and more so when the zeroth-order process is added to case 2;  $S_p$  improves by another 1.16%. These results indicate that the kinetics of 5-FU in the body has mixed exponents, although it was seen to be approximately a first-order process at low concentrations. The most significant change in going from case 1 to case 2 is the behaviour at high concentrations. The behaviour goes from being a zeroth-order process ( $A - B = 0$ ) in case 1 to mixed order ( $A - B = -0.2943$ ) in case 2. The complete set of graphs comparing the theory to the eight datasets are in appendix C.

Comparing the results shown in Figure 3.2 case 2 to case 2.2 of the one-compartment model, no obvious changes are visible in the two graphs. Part C of Figure 3.2 shows the differences between the three sets of theoretical curves, of which none reaches  $1 \frac{\mu\text{mol}}{L}$ . The curve of the graphs in Figure 3.2 A and B indicate the influences of the mixed processes involved in the kinetics of the molecules and not the combination of multiple processes. They are not wholly first-order processes; as the curves are bent and not perfect straight-line curves as in a first-order process. If we compare the combined three processes of the fixed exponents model (case 1.3) to that of the varying exponents model (case 2.2), very little change can be observed between the two models' curves. It gives an intuition that the order process of 5-FU in the body as a one-compartment model is a mixed-order process closer to a first-order process than any others. The variable exponents and multiple processes did not fix the general behaviour of the curves in the fixed exponents model; hence, a more complex model is needed.

The transition points in case 2 and case 2.2 are nearly identical, less than 0.25% differences between the cases. The lowest infusion rate of  $1422 \frac{\mu\text{mol}}{\text{min.m}^2}$  produced the longest time before the transition from low concentration behaviour to high concentration behaviour occurs; whereas the highest infusion rate:  $2844 \frac{\mu\text{mol}}{\text{min.m}^2}$  has the shortest time before the transition occurs. The results are shown in Table 3.5. The number of molecules at the maximum elimination rate for the cases are examined, the times for the amount of molecules estimated were not attainable. The numbers are higher than the available number from the numerical solution and also higher than the clinical  $C_{max}$  estimated with those infusion rates. The results for the three infusion rates are shown in Table 3.5.

Table 3.5: 5-FU transition times for the one-compartment model with variable exponents.

Parameters	Case 2			Case 2.2		
	1921	2844	1422	1921	2844	1422
IV Time	1	1	2	1	1	2
$X_{5FU,1}^{T(1,0)}$	1154	1154	1154	1184	1184	1184
$C_{5FU,1}^{T(1,0)}$	69.1	69.1	69.1	70.5	70.5	70.5
$X_{5FU,1}^{M(1,0)}$	2961	2961	2961	3114	3114	3114
$C_{5FU,1}^{M(1,0)}$	177.4	177.4	177.4	185.3	185.3	185.3
$t^{1T(1,0)}$	0.62	0.41	0.83	0.62	0.43	0.84
$t^{2T(1,0)}$	15.97	37.9	39.2	15.2	37.2	38.5
$t^{1M(1,0)}$	N/A	N/A	N/A	N/A	N/A	N/A
$t^{2M(1,0)}$	N/A	N/A	N/A	N/A	N/A	N/A

The S.I units of  $X_{5FU,1}^{g(1,0)}$  is  $\frac{\mu\text{mol}}{\text{m}^2}$  and  $C_{5FU,1}^{g(1,0)}$  is  $\frac{\mu\text{mol}}{\text{L}}$ , and  $t_{1/2}$  is *min*. where *d* represents DHFU and *g* represents T and M that symbolise transition and maximum values respectively for both concentrations and number of molecules.

The second transition point indicates that there is higher delayed time before the transition from high concentration behaviour to low concentration behaviour occurs with the highest infusion  $2844 \frac{\mu\text{mol}}{\text{min.m}^2}$  compared to  $1921 \frac{\mu\text{mol}}{\text{min.m}^2}$  over the same IV time.

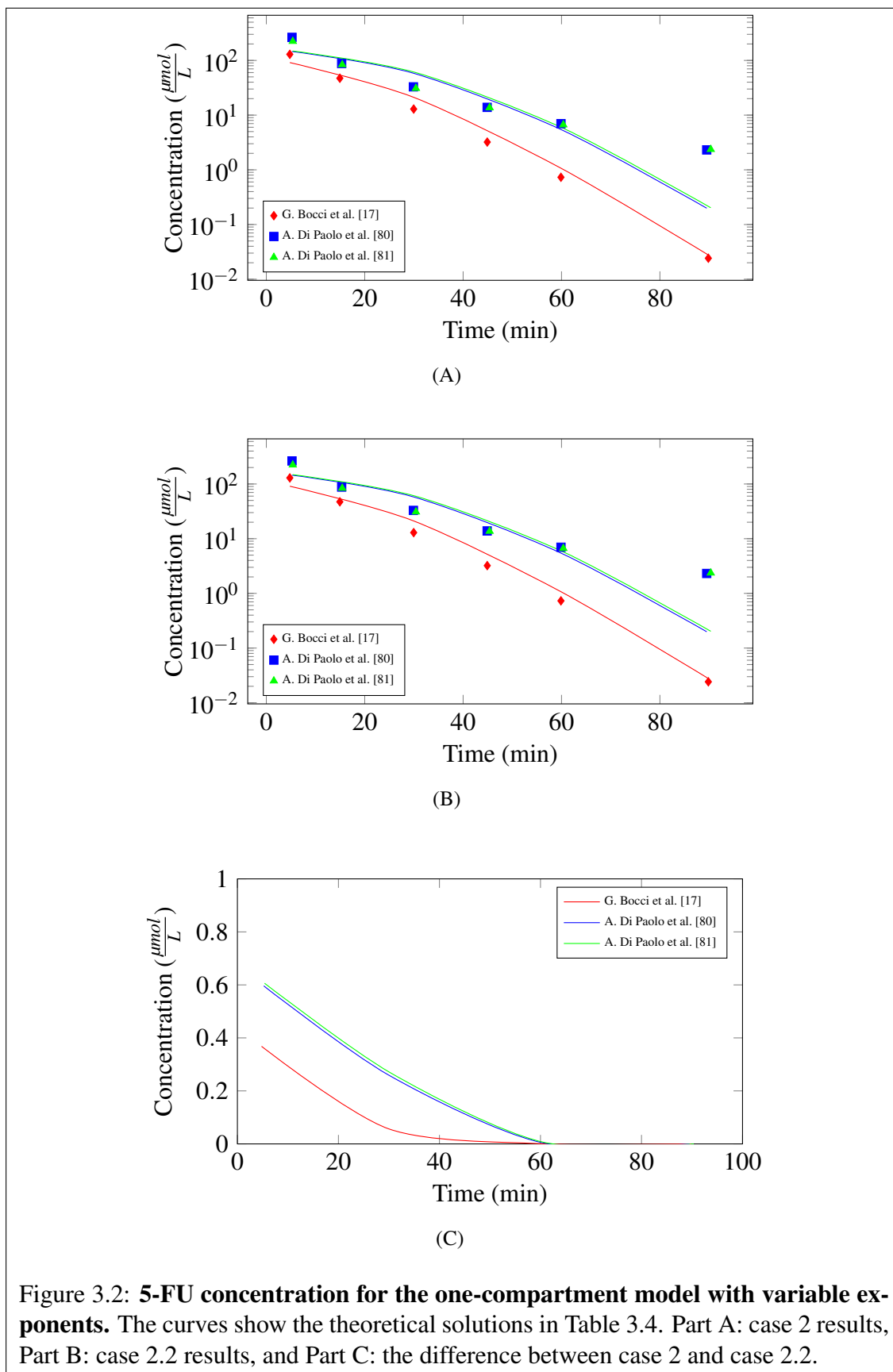


Figure 3.2: **5-FU concentration for the one-compartment model with variable exponents.** The curves show the theoretical solutions in Table 3.4. Part A: case 2 results, Part B: case 2.2 results, and Part C: the difference between case 2 and case 2.2.

## 3.2 Two-Compartment Model

We designed the two-compartment model in two different ways. Based on the differences in the route of elimination from the system, the structural designs of the flows are shown in Figures 2.1 Part B and Part C. The PK parameters of the two models were determined by minimising  $S_p$ .

### 3.2.1 Fixed Exponents with Elimination from Compartment 1

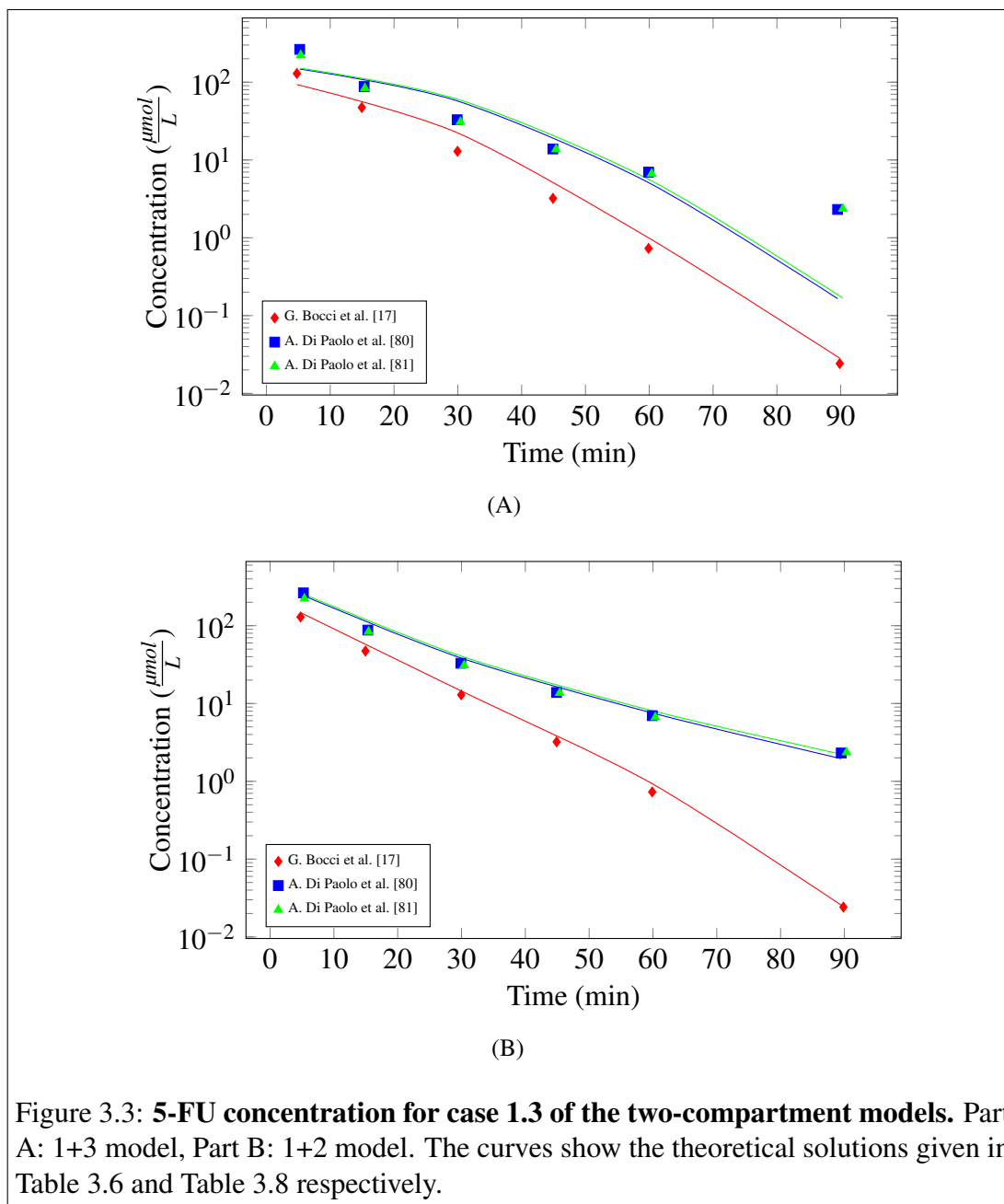
The fixed exponent system is referred to as case 1 for the (1+3) two-compartment model. The results of the minimisation of  $S_p$  are shown in Table 3.6, and Figure 3.3 Part A shows the corresponding 5-FU concentration graph fitted against the three datasets that dominated the population of patients. The graph that gives the complete set of clinical data is shown in appendix C. The results indicate that there is a slight reduction of 2.13% in  $S_p$  when the zeroth-order process is added to the first-order process. In contrast, no significant change occurs when the second-order process is added. In comparing this type of two-compartment model with the one-compartment model, there is a correlation in the behaviour of the two types of models. They behave in the same manner; their primary cases have  $S_p = 0.0703$ . The flow rates across the coupled compartments from compartment 1 to compartment 3 are too low to compare with the rate of elimination from compartment 1.

The results for the transition phase parameters are shown in Table 3.7 for the three sets of infusion, using four cases 1, 1.1, 1.2, and 1.3 of the (1+3) two-compartment model. The first transition point from a low concentration behaviour to a high concentration behaviour indicates that there is a lower transition time with the high infusion. The low infusion rate over a more extended period gives a slower transition phase between low concentration behaviours and high concentration behaviours. Both first transition (absorption phase) and second transition (elimination phase) observed to have higher transition time. When the infusion rate is high, the switch from a low concentration behaviour to a high concentration behaviour is faster.

Table 3.6: 5-FU parameters for the (1+3) two-compartment model with fixed exponents

Case	$j, k$	$k_{5FU,j,k}^{(0)}$	$k_{5FU,j,k}^{(1)}$	$\Gamma_{5FU,j,K}^{(1)}$	$k_{5FU,j,k}^{(2)}$	$\Gamma_{5FU,j,K}^{(2)}$	$V_d(\frac{L}{m^2})$	$S_p$
1	1,3	-	0.0012(20)	0.0014(42)	-	-	16.3(13)	0.0703
	1,0	-	0.1184(20)	0.001399(66)	-	-		
	3,1	-	0.00000(58)	N/A**	-	-		
1.1	1,3	0.0235(11)	0.0000(14)	N/A**	-	-	16.3(17)	0.0688
	1,0	0.0239(11)	0.1070(12)	0.001092(51)	-	-		
	3,1	0.000(11)	0.0000(62)	N/A**	-	-		
1.2	1,3	-	0.0013(21)	0.0014(34)	0.0000000(68)	N/A**	16.3(13)	0.0703
	1,0	-	0.1184(21)	0.001368(86)	0.0000000(68)	N/A**		
	3,1	-	0.00000(58)	N/A**	0.000000(38)	N/A**		
1.3	1,3	0.0235(10)	0.0000(14)	N/A**	0.0000000(67)	N/A**	16.3(15)	0.0688
	1,0	0.0239(11)	0.1070(12)	0.0011(51)	0.0000000(67)	N/A**		
	3,1	0.000(11)	0.0000(63)	N/A**	0.000000(36)	N/A**		

\*\*Not relevant since  $k_{5FU,j,k}^{(p)} = 0$ . The unit of  $k_{5FU,j,k}^{(0)}$  is  $\frac{\mu\text{mol}}{m^2 \cdot \text{min}}$ ,  $k_{5FU,j,k}^{(1)}$  is  $\frac{1}{\text{min}}$ ,  $\Gamma_{5FU,j,k}^{(1)}$  is  $\frac{m^2}{\mu\text{mol}}$ ,  $k_{5FU,j,k}^{(2)}$  is  $\frac{m^2}{\mu\text{mol} \cdot \text{min}}$ , and  $\Gamma_{5FU,j,k}^{(2)}$  is  $\frac{m^4}{\mu\text{mol}^2}$ . The fixed exponents involved are as follows:  $A_{5FU,1,3}^{(p)} = B_{5FU,1,3}^{(p)} = A_{5FU,1,0}^{(p)} = B_{5FU,1,0}^{(p)} = A_{5FU,3,1}^{(p)} = B_{5FU,3,1}^{(p)} = p$ . The values of  $p$  can be 0, 1, or 2 and represent the process order.



Case 1 gives a lower transition time when it is compared to case 1.3 at the transition from a low concentration behaviour to a high concentration behaviour; whereas case 1.3 gives lower transition time when the kinetics transit from a high concentration behaviour to a low concentration behaviour. See Table 3.7.

Table 3.7: 5-FU transition parameters for the (1+3) two-compartment model with fixed exponents.

Case	$j, k$	Inf.	$X_{5FU,1}^{1T(j,k)}$	$C_{5FU,1}^{1T(j,k)}$	$X_{5FU,1}^{2T(j,k)}$	$C_{5FU,1}^{2T(j,k)}$	$t^{1T(j,k)}$	$t^{2T(j,k)}$
1	1,0	1921	714.8	43.8	714.8	43.8	0.38	21.2
		2844					0.25	34.5
		1422					0.50	35.5
	1,3	1921	714.3	43.8	714.3	43.8	0.37	21.3
		2844					0.25	34.7
		1422					0.49	35.7
1.3	1,0	1921	909.1	55.8	909.1	55.8	0.50	15.9
		2844					0.32	30.2
		1422					0.65	31.1

The S.I units of  $X_{5FU,1}^{g(1,0)}$  is  $\frac{\mu\text{mol}}{\text{m}^2}$  and  $C_{5FU,1}^{g(1,0)}$  is  $\frac{\mu\text{mol}}{\text{L}}$ , and  $t_{1/2}$  is *min.* where  $d$  represents DHFU and  $g$  represents T and M that symbolise transition and maximum values respectively for both concentrations and number of molecules. The infusions  $1921 \frac{\mu\text{mol}}{\text{min.m}^2}$  and  $2844 \frac{\mu\text{mol}}{\text{min.m}^2}$  are administered over one minute; whereas,  $1422 \frac{\mu\text{mol}}{\text{min.m}^2}$  is administered over two minutes,

### 3.2.2 Fixed Exponents with Elimination from Compartment 2

We also designed the elimination of molecules from the body through the liver (metabolism compartment), while the other routes are designed to be negligible. This is referred to as the case 1 (1+2) two-compartment model. The comparison of both two-compartment models helps us determine the most efficient two-compartment model that will give the best fit to the clinical datasets. The exponents are all fixed, and the subordinate cases were examined in addition to the primary case. The fixed parameters are as follows:

$$A_{5FU,1,2}^{(1,p)} = B_{5FU,1,2}^{(1,p)} = A_{5FU,2,0}^{(1,p)} = B_{5FU,2,0}^{(1,p)} = A_{5FU,2,1}^{(1,p)} = B_{5FU,2,1}^{(1,p)} = p.$$

The symbol  $p$  represents the fixed-order processes 0, 1, and 2. The results for this model are shown in Table 3.8 and have a 70.84% improvement in  $S_p$  when this case 1 is compared to case 1 of the one-compartment model.

Table 3.8: 5-FU parameters for the (1+2) two-compartment model with fixed exponents

Case	$j, k$	$k_{5FU,j,k}^{(0)}$	$k_{5FU,j,k}^{(1)}$	$\Gamma_{5FU,j,K}^{(1)}$	$k_{5FU,j,k}^{(2)}$	$\Gamma_{5FU,j,K}^{(2)}$	$V_d(\frac{L}{m^2})$	$S_p$
1	1,2	-	0.1429(23)	0.000577(52)	-	-	8.60(41)	0.0205
	2,0	-	5.493(63)	0.1845(21)	-	-		
	2,1	-	0.00662(45)	0.000000(35)	-	-		
1.1	1,2	0.000(20)	0.1445(22)	0.000590(49)	-	-	8.60(35)	0.0203
	2,0	0.000(20)	5.493(64)	0.1835(22)	-	-		
	2,1	0.0035(50)	0.00675(48)	0.000000(36)	-	-		
1.2	1,2	-	0.1325(22)	0.000500(50)	0.00500(49)	0.00100(26)	8.60(34)	0.0190
	2,0	-	5.492(73)	0.1912(32)	0.000048(77)	0.0002(33)		
	2,1	-	0.00956(40)	0.000000(28)	0.000000(36)	N/A**		
1.3	1,2	0.0106(41)	0.12998(92)	0.000600(53)	0.16303(33)	0.03044(18)	8.60(31)	0.0138
	2,0	0.001(25)	5.489(61)	0.2405(26)	0.004479(55)	0.0011(25)		
	2,1	0.0229(46)	0.00858(45)	0.000000(33)	0.000000(40)	N/A**		

\*\*Not relevant since  $k_{5FU,j,k}^{(p)} = 0$ . The unit of  $k_{5FU,j,k}^{(0)}$  is  $\frac{\mu\text{mol}}{m^2 \cdot \text{min}}$ ,  $k_{5FU,j,k}^{(1)}$  is  $\frac{1}{\text{min}}$ ,  $\Gamma_{5FU,j,k}^{(1)}$  is  $\frac{m^2}{\mu\text{mol}}$ ,  $k_{5FU,j,k}^{(2)}$  is  $\frac{m^2}{\mu\text{mol} \cdot \text{min}}$ , and  $\Gamma_{5FU,j,k}^{(2)}$  is  $\frac{m^4}{\mu\text{mol}^2}$ .

The variance for case 1 of the (1+3) two-compartment model compared to case 1 of the (1+2) two-compartment model is  $S_p = 0.0703$  to  $S_p = 0.0205$ . There is a further reduction of 32.68% in  $S_p$  when both zeroth- and second-order processes are added (case 1.3 of the (1+2) two-compartment model). Figure 3.3 shows the change between the two two-compartment models. The contributions of the subordinate cases in this type of two-compartment model indicate that there are contributions from the additional terms to the values from the primary case. The primary case has  $S_p = 0.0205$ , whereas the combination with zeroth- and second-order processes improved  $S_p$  by 0.49% and 3.41% respectively. The impact of the second-order process on  $S_p$  is slightly higher than that of zeroth-order by 2.92%. The best fit in this model is the subordinate case 1.3, which comprises the combination of the primary case with the zeroth- and second-order processes. The improvement is slightly higher than that of case 1.2, with an improvement of 4.39% on  $S_p$  when compared with the primary case.

Modelling the elimination path of the molecules from the metabolism compartment gives the correct curvature for the high concentration curve as seen in Figure 3.3 when comparing Parts A and B. The amount of molecules at the transition and the time of the transition were observed in compartment two. The transition time was then used to obtain the parameters in compartment one. The results for the transition phase parameters in both compartment one and two are shown in Table 3.9 for the three sets of infusion, using four cases 1, 1.1, 1.2, and 1.3 of the (1+2) two-compartment model. There is a faster transition time when high infusion of 5-FU was administered. The transition from a low concentration behaviour to a high concentration behaviour is slower by 9.5% when we compared the infusion of  $1921 \frac{\mu\text{mol}}{\text{min.m}^2}$  to the infusion of  $2844 \frac{\mu\text{mol}}{\text{min.m}^2}$ . The impact of molecules' kinetics from compartment one to compartment two produced a large amount of the molecules at the transition point for all the cases. The elimination of molecules from compartment 2 has a more considerable influence on the transition of molecules from a low concentration to a high concentration and vice versa.

Table 3.9: 5-FU transition parameters for the (1+2) two-compartment model with fixed exponents.

Case	Inf.	$j, k$	$X_{5FU,1}^{1T(j,k)}$	$C_{5FU,1}^{1T(j,k)}$	$X_{5FU,2}^{1T(j,k)}$	$X_{5FU,1}^{2T(j,k)}$	$C_{5FU,1}^{2T(j,k)}$	$t^{1T(j,k)}$	$t^{2T(j,k)}$	
1	1921	2,0	499.1	58.0	5.42	9.52	1.11	0.26	63.5	
			2844	580.2	67.5		14.99	1.74	0.20	92.0
			1422	429.4	49.9		14.97	1.73	0.24	94.1
1.1	1921	1,2	N/A	N/A	1733	N/A	N/A	N/A	N/A	
			2844	N/A	N/A		N/A	N/A	N/A	N/A
			1422	N/A	N/A		N/A	N/A	N/A	N/A
1.1	1921	2,0	502.2	58.4	5.45	9.71	1.13	0.27	63.1	
			2844	580.2	67.5		14.98	1.74	0.20	91.9
			1422	430.2	50.0		15.01	1.50	0.29	94.1
1.1	1921	1,2	N/A	N/A	1695	N/A	N/A	N/A	N/A	
			2844	N/A	N/A		N/A	N/A	N/A	N/A
			1422	N/A	N/A		N/A	N/A	N/A	N/A
1.2	1921	2,0	435.2	50.6	5.23	7.00	0.81	0.23	64.7	
			2844	555.6	64.6		14.89	1.49	0.19	92.3
			1422	337.5	33.7		14.88	1.49	0.23	94.5
1.2	1921	1,2	N/A	N/A	2000	N/A	N/A	N/A	N/A	
			2844	N/A	N/A		N/A	N/A	N/A	N/A
			1422	N/A	N/A		N/A	N/A	N/A	N/A
1.3	1921	2,0	383.9	44.6	4.16	1.10	0.13	0.20	81.2	
			2844	446.4	51.9		14.36	1.67	0.16	92.3
			1422	313.8	35.8		14.35	1.67	0.22	94.42
1.3	1921	1,2	N/A	N/A	1667	N/A	N/A	N/A	N/A	
			2844	N/A	N/A		N/A	N/A	N/A	N/A
			1422	N/A	N/A		N/A	N/A	N/A	N/A

The S.I units of  $X_{5FU,1}^{g(1,0)}$  is  $\frac{\mu\text{mol}}{\text{m}^2}$  and  $C_{5FU,1}^{g(1,0)}$  is  $\frac{\mu\text{mol}}{\text{L}}$ , and  $t_{1/2}$  is *min*. where  $d$  represents DHFU and  $g$  represents T and M that symbolise transition and maximum values respectively for both concentrations and number of molecules. The infusions 1921  $\frac{\mu\text{mol}}{\text{min.m}^2}$ , 2844  $\frac{\mu\text{mol}}{\text{min.m}^2}$ , and 1422  $\frac{\mu\text{mol}}{\text{min.m}^2}$  were administered over one minute, one minute, and two minutes respectively.

### 3.2.3 Variable Exponents with Elimination from Compartment 1

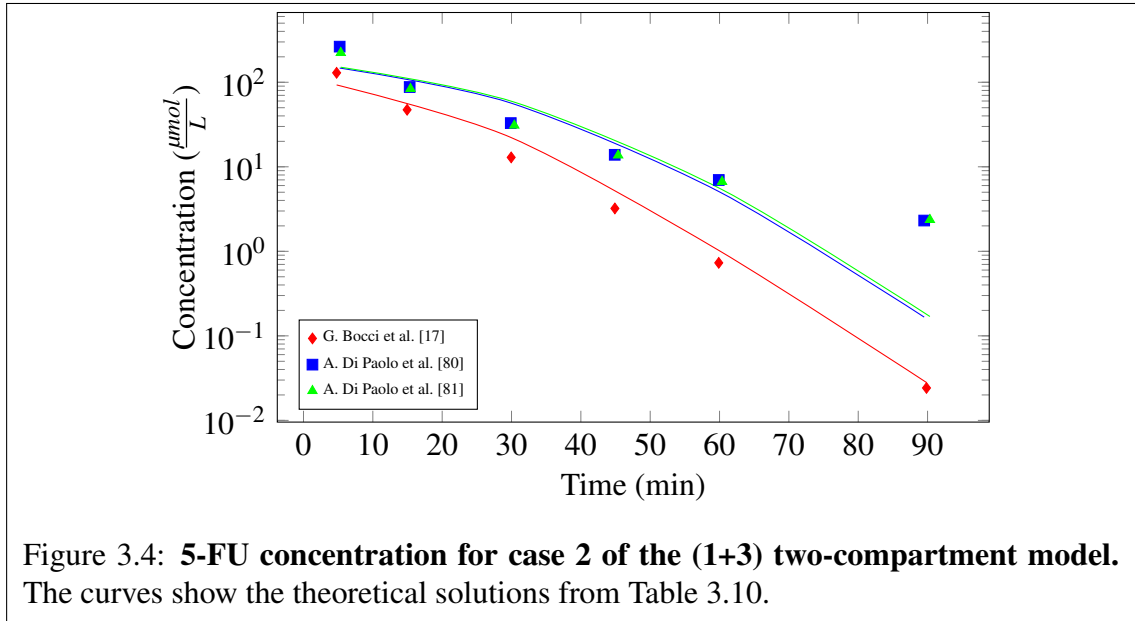
All the exponents of A and B are varied in this case. The major elimination route is considered to be through the distribution compartment. Table 3.10 shows the results obtained for this model, indicating the same behaviour observed in case 1 of the (1+3) two-compartment model. There is no considerable change when comparing it with the one-compartment model. The semi-log 5-FU concentration graph corresponding to the case 2 results are shown in Figure 3.4.

Table 3.10: 5-FU parameters for the (1+3) two-compartment model with variable exponents

Case	$j, k$	$A$	$B$	$k_{5FU,j,k}^{(p)}$	$\Gamma_{5FU,j,k}^{(p)}$	$V_d(\frac{L}{m^2})$	$S_p$
2	1,3	0.999(90)	1.00(32)	0.0033(21)	0.001(12)	16.34(63)	0.0690
	1,0	0.9908(39)	1.0053(81)	0.1185(21)	0.0012(40)		
	3,1	1.00*	N/A**	0.00000(21)	N/A**		
2.1	1,3	0.00(70)	0.0006(23)	0.006(14)	0.00001(33)	16.34(65)	0.0679
	1,3	0.998(87)	1.00(30)	0.0015(19)	0.001(11)		
	1,0	0.00(70)	0.0007(45)	0.006(14)	0.00002(32)		
	1,0	0.9896(36)	1.0060(79)	0.1174(19)	0.001135(38)		
	3,1	0.0008*	N/A**	0.000(11)	N/A**		
	3,1	1.00*	N/A**	0.00000(20)	N/A**		

\*error is indeterminate. \*\*Not relevant since  $k_{5FU,j,k}^{(p)} = 0$ . The S.I units of  $k_{5FU,j,k}^{(p)}$  is  $\frac{\mu\text{mol}^{(1-A)}}{m^{(2-2A)}\text{min}}$  and  $\Gamma_{5FU,j,k}^{(AB)}$  is  $\frac{m^{2B}}{\mu\text{mol}^B}$ .

The  $S_p$  obtained for cases 2 and 2.1 of this model are 0.0690 and 0.0679, respectively. We could not obtain results for the three-process case due to the limited number of available datasets used for fitting. We have thirty-two data points, and this case needed at least thirty-seven. In case 2.1, there is a slight improvement of 0.04% in  $S_p$  when combining the primary case with a second process. This case validates the common behaviour that we examined previously in the one-compartment and (1+3) two-compartment fixed-exponents models. At low concentration, the exponents we obtained in case 2 for the flows are approximately first-order processes, as seen by the A's in Table 3.10. We also observed non-zero



values for exponents (A-B) at the high concentration with  $A_{5FU,1,3}^{(AB)} - B_{5FU,1,3}^{(AB)} = -0.0009$  and  $A_{5FU,1,0}^{(AB)} - B_{5FU,1,0}^{(AB)} = -0.0145$ . The coupled process shows insignificant contribution to the fitting of the clinical data.

We have approximately the Michaelis-Menten model, which predicts  $A - B = 0$ . The exponents of the flow rate out of compartment one at higher concentrations are negative, which indicates a slower outflow rate compared to the inflow rate. Table 3.11 shows the amount of molecules and concentrations at the maximum elimination flow rate and the transition between low concentration behaviours and high concentration behaviours.

The (1+3) two-compartment models obtain maximum elimination rate at concentrations  $C_{5FU,1}^{M(1,0)} > 3000 \frac{\mu\text{mol}}{\text{L}}$  shown in Table 3.12. The  $X_{5FU,1}^M$  are far above what can be achieved clinically and is not realistic; none of the infusions reached the maximum elimination rate. The case 2 of the (1+3) two-compartment model gives lower transition time from a low concentration behaviour to a high concentration behaviour compared to case 2.1; whereas, from a high concentration behaviour to a low concentration behaviour, case 2.1 gives lower transition time.

Table 3.11: 5-FU transition parameters for the (1+3) two-compartment model with variable exponents.

Case	Infusion	$j, k$	$X_{5FU,1}^{1T(j,k)}$	$C_{5FU,1}^{1T(j,k)}$	$X_{5FU,1}^{2T(j,k)}$	$C_{5FU,1}^{2T(j,k)}$	$t^{1T(j,k)}$	$t^{2T(j,k)}$
2	1921	1,0	804.3	49.2	804.3	49.2	0.43	18.2
	2844						0.28	32.5
	1422						0.57	33.5
	1921	1,3	980.4	60	980.4	60	0.52	15.5
	2844						0.35	28.4
	1422						0.70	29.8
2.1	1921	1,0	846.1	51.8	846.1	51.8	0.44	16.1
	2844						0.31	29.3
	1422						0.61	30.2
	1921	1,3	980.4	60	980.4	60	0.53	13.5
	2844						0.36	26.6
	1422						0.71	27.6

The S.I units of  $X_{5FU,1}^{g(1,0)}$  is  $\frac{\mu\text{mol}}{\text{m}^2}$  and  $C_{5FU,1}^{g(1,0)}$  is  $\frac{\mu\text{mol}}{\text{L}}$ , and  $t_{1/2}$  is *min.* where  $d$  represents DHFU and  $g$  represents T and M that symbolise transition and maximum values respectively for both concentrations and number of molecules. The three infusions 1921  $\frac{\mu\text{mol}}{\text{min.m}^2}$ , 2844  $\frac{\mu\text{mol}}{\text{min.m}^2}$ , and 1422  $\frac{\mu\text{mol}}{\text{min.m}^2}$  were administered over one minute, one minute, and two minutes respectively.

Table 3.12: 5-FU transition parameters for the (1+3) two-compartment model with variable exponents.

Case	Infusion	IV Time	$A - B$	$X_{5FU,1}^{M(1,0)}$	$C_{5FU,1}^{M(1,0)}$	$t^{1M(1,0)}$	$t^{2M(1,0)}$
2	1921	1	-0.0145	53748	3289	N/A*	N/A*
	2844	1				N/A*	N/A*
	1422	2				N/A*	N/A*
2.1	1921	1	-0.0164	49823	3049	N/A*	N/A*
	2844	1				N/A*	N/A*
	1422	2				N/A*	N/A*

\*The times at the maximum elimination rates are unattainable. The S.I units of  $X_{5FU,1}^{g(1,0)}$  is  $\frac{\mu\text{mol}}{\text{m}^2}$  and  $C_{5FU,1}^{g(1,0)}$  is  $\frac{\mu\text{mol}}{\text{L}}$ , and  $t_{1/2}$  is *min.* where  $d$  represents DHFU and  $g$  represents T and M that symbolise transition and maximum values respectively for both concentrations and number of molecules.

### 3.2.4 Variable Exponents with Elimination from Compartment 2

There is a significant decrease in variance if we consider variable exponents for the two-compartment model that has the elimination of the molecules via the metabolism compartment. Table 3.13 shows the results from the minimisation of the variance for the primary case 2 and the subordinate cases.

The  $S_p$  for cases 2 and 2.1 of the (1+2) two-compartment model is 0.0127. There is no improvement in the  $S_p$  of the primary case when combined with a second process, which means that the subordinates have no contribution to the minimisation of the variance. The comparison of case 2 with case 1 shows an improvement from 0.0205 to 0.0127 (38.05% improvement in  $S_p$ ). We also obtained an approximately first-order process at a low concentration. The exponents A range from 0.8807 to 1.0973, and at high concentrations, it is observed to be  $A_{5FU,1,2}^{(AB)} - B_{5FU,1,2}^{(AB)} = 0.1158$ ,  $A_{5FU,2,0}^{(AB)} - B_{5FU,2,0}^{(AB)} = -0.3134$ , and  $A_{5FU,2,1}^{(AB)} - B_{5FU,2,1}^{(AB)} = 0.0454$ , which implies that the elimination at high concentrations is saturable.

Table 3.13: 5-FU parameters for the (1+2) two-compartment model with variable exponents

Case	$j,k$	$A$	$B$	$k_{5FU,j,k}^{(p)}$	$\Gamma_{5FU,j,k}^{(p)}$	$V_d(\frac{L}{m^2})$
2	1,2	1.0975(24)	0.9817(45)	0.1165(18)	0.00186(23)	10.000(71)
	2,0	0.8807(28)	1.19412(12)	1.6377(89)	0.00624(12)	
	2,1	1.0394(87)	0.994(34)	0.01233(47)	0.000593(22)	
2.1	1,2	0.0000*	N/A**	0.0000(30)	N/A**	10.000(71)
	2,0	0.0000*	N/A**	0.0000(28)	N/A**	
	2,1	0.00*	N/A**	0.0000(48)	N/A**	
	1,2	1.0975(24)	0.9817(45)	0.1165(18)	0.00186(23)	
	2,0	0.8807(28)	1.19412(12)	1.6377(89)	0.00624(12)	
	2,1	1.0394(87)	0.994(34)	0.01233(47)	0.000593(22)	

\*The error is indeterminate since the coefficient is zero. \*\*Not relevant since  $k_{5FU,j,k}^{(p)} = 0$ . The S.I units of  $k_{5FU,j,k}^{(p)}$  is

$$\frac{\mu\text{mol}^{(1-A)}}{m^{(2-2A)}\text{min}} \text{ and } \Gamma_{5FU,j,k}^{(AB)} \text{ is } \frac{m^{2B}}{\mu\text{mol}^B}.$$

The elimination flow rate of the molecule from compartment 2 has a negative exponent at high concentrations. The other two (A–B) remain positive, which means they do not saturate. For case 2 and case 2.1 of the (1+2) two-compartment models, we determined  $X_{5FU,2}^{M(2,0)} = 168 \frac{\mu\text{mol}}{\text{m}^2}$  when the elimination flow rate was maximum. The corresponding parameters in compartment one are shown in Table 3.14. There will be an increased *AUC* in the compartment when the number of molecules in the liver surpasses this threshold of  $X_{5FU,2}^{M(2,0)}$ . The elimination rate switches at the transition phase from a low concentration behaviour to a high concentration behaviour in the metabolism compartment when  $X_{5FU,2}^{T(2,0)} = 70.21 \frac{\mu\text{mol}}{\text{m}^2}$ . The infusion rate of the molecules into compartment 1 influences the number of molecules in the plasma which the transition phase depends upon. The results for the transition of kinetics and the maximum elimination rate are shown in Table 3.14.

The transition is slower in compartment one of the (1+2) two-compartment model compared with the one-compartment model. The results are shown in Table 3.14. Considering the infusion of  $1921 \frac{\mu\text{mol}}{\text{min.m}^2}$  in one minute, the first transition time at the absorption phase occurs at  $t = 1.17 \text{ min}$  in the (1+2) two-compartment model; whereas in the one-compartment model, it is  $t = 0.62 \text{ min}$ . Also comparing the two models, we have differences of  $t = 0.6 \text{ min}$ . and  $t = 0.48 \text{ min}$ . for  $2844 \frac{\mu\text{mol}}{\text{min.m}^2}$  over one minute and  $1422 \frac{\mu\text{mol}}{\text{min.m}^2}$  over two minutes respectively.

The first transition point from low concentration behaviour to high concentration behaviour indicates that there is a long time for a transition to occur when the infusion rate is low. The first transition of molecules at the absorption phase occurs faster when the infusion rate is high. In contrast, the second transition point indicates a slower transition time with a high infusion rate. In the three infusion rates examined, the threshold of  $C_{5FU,1}^{1T(2,0)}$  indicates the boundary where there will be a first shift from the first-order of the kinetic process of the molecule. Beyond this threshold, the process becomes a mixed-order process. On the other hand, when the transition switches back to a low concentration behaviour from a high concentration behaviour,  $C_{5FU,1}^{2T(2,0)}$  indicates the boundary where the process becomes the

first-order process.

Table 3.14: 5-FU transition parameters for the (1+2) two-compartment model with variable exponents.

Case	Inf.	$j, k$	$X_{5FU,2}^{T(j,k)}$	$X_{5FU,1}^{1T(j,k)}$	$C_{5FU,1}^{1T(j,k)}$	$X_{5FU,1}^{2T(j,k)}$	$C_{5FU,1}^{2T(j,k)}$	$t^{1T(j,k)}$	$t^{2T(j,k)}$
2	1921	1,2	604.5	882.4	88.2	80.2	8.02	10.7	36.6
	2844			1876	187.6	55.48	5.55	7.77	72.9
	1422			1920	192.0	55.42	5.54	8.05	76.0
	1921	2,0	70.21	1761	176.1	25.16	2.52	1.17	52.8
	2844			2652	265.2	23.64	2.36	1.04	88.5
	1422			1767	176.7	23.59	2.36	1.31	90.67
	1921	2,1	1764	N/A	N/A	N/A	N/A	N/A	N/A
	2844			N/A	N/A	N/A	N/A	N/A	N/A
	1422			N/A	N/A	N/A	N/A	N/A	N/A
2.1	1921	1,2	604.5	882.7	88.3	80.7	8.07	10.7	36.5
	2844			1877	187.7	55.91	5.59	7.73	72.8
	1422			1920	192.0	55.86	5.59	8.01	74.9
	1921	2,0	70.21	1761	176.1	25.38	2.54	1.17	52.7
	2844			2655	265.5	23.79	2.38	1.01	88.3
	1422			1767	176.7	23.56	2.33	1.31	90.65
	1921	2,1	1764	N/A	N/A	N/A	N/A	N/A	N/A
	2844			N/A	N/A	N/A	N/A	N/A	N/A
	1422			N/A	N/A	N/A	N/A	N/A	N/A

The S.I units of  $X_{5FU,1}^{g(1,0)}$  is  $\frac{\mu\text{mol}}{\text{m}^2}$  and  $C_{5FU,1}^{g(1,0)}$  is  $\frac{\mu\text{mol}}{\text{L}}$ , and  $t_{1/2}$  is  $\text{min}$ . where  $d$  represents DHFU and  $g$  represents T and M that symbolise transition and maximum values respectively for both concentrations and number of molecules. The three infusions 1921  $\frac{\mu\text{mol}}{\text{min.m}^2}$ , 2844  $\frac{\mu\text{mol}}{\text{min.m}^2}$ , and 1422  $\frac{\mu\text{mol}}{\text{min.m}^2}$  were administered over one minute, one minute, and two minutes respectively.

The corresponding 5-FU concentration graphs for the three datasets are shown in Figure 3.5. The complete set of graphs for the eight datasets are shown in appendix C. Case

2.1 in Table 3.13 shows that extra processes do not improve the fit.

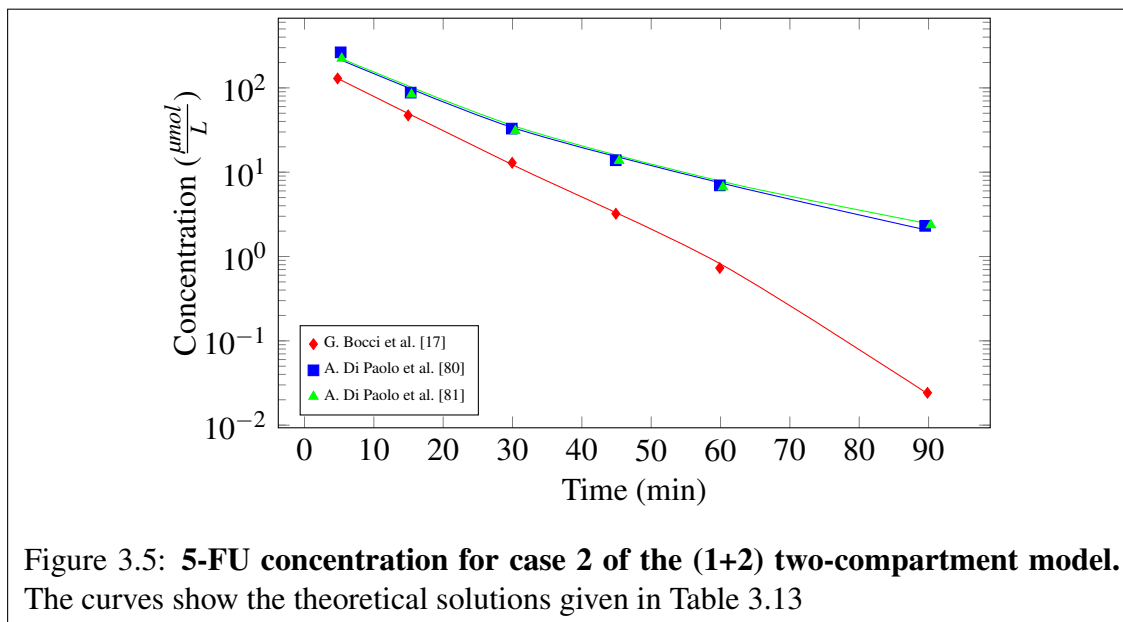


Table 3.15: 5-FU parameters at the maximum elimination rate for the (1+2) two-compartment model with variable exponents.

Case	Inf.	$X_{5FU,2}^{M(2,0)}$	$X_{5FU,1}^{1M(2,0)}$	$C_{5FU,1}^{1M(2,0)}$	$X_{5FU,1}^{2M(2,0)}$	$C_{5FU,1}^{2M(2,0)}$	$t^{1M(2,0)}$	$t^{2M(2,0)}$
2	1921	166.8	1613	161.3	33.02	3.30	2.57	50.1
	2844		2516	251.6	30.48	3.05	2.13	85.9
	1422		2557	255.7	30.47	3.05	2.49	87.9
2.1	1921	166.8	1612	161.2	33.21	3.32	2.57	50.0
	2844		2516	251.6	30.66	3.07	2.12	85.7
	1422		2557	255.7	30.66	3.07	2.49	87.8

The S.I units of  $X_{5FU,1}^{g(1,0)}$  is  $\frac{\mu\text{mol}}{\text{m}^2}$  and  $C_{5FU,1}^{g(1,0)}$  is  $\frac{\mu\text{mol}}{\text{L}}$ , and  $t_{1/2}$  is *min*. where *d* represents DHFU and *g* represents T and M that symbolise transition and maximum values respectively for both concentrations and number of molecules.

### 3.2.5 Variable Exponents and Saturation Limiting Interaction

There are additional PK parameters in the two-compartment models that analysed the interaction between molecules. These interactions produce an effective rate constant, as discussed in Chapter two. The numbers for PK parameters are shown in Table 3.16.

Table 3.16: 5-FU parameters for the (1+2) two-compartment model with saturation limiting function

Case	$j, k$	$A$	$B$	$k_{5FU,j,k}^{(AB)}$	$\Gamma_{5FU,j,k}^{(AB)}$	$C$	$D$	$\alpha_{5FU,j,k}^{(AB,p2)}$	$\beta_{5FU,j,k}^{(AB,p2)}$	$V_d(\frac{L}{m^2})$
3.0	1,2	1.0975(24)	0.9817(45)	0.1165(18)	0.00186(23)	0.0000(23)	0.0000*	-0.0003(33)	0.0000(41)	10.00(67)
	2,0	0.8807(28)	1.19412(12)	1.6377(89)	0.00624(12)	-	-	-	-	
	2,1	1.0394(87)	0.994(34)	0.01233(47)	0.000593(22)	0.0000(33)	0.0000*	-0.0003(32)	0.0000(32)	
3.1	1,2	1.1038(24)	0.9788(45)	0.1145(18)	0.00198(23)	0.00012(28)	0.00003(23)	0.0006(51)	0.0003(45)	9.997(67)
	1,2					1.9998(42)	2.0005(51)	-0.0006(45)	0.0003(34)	
	2,0	0.8720(28)	1.2144(12)	1.6390(89)	0.00510(12)	-	-	-	-	
	2,1	1.0410(87)	0.994(34)	0.01313(47)	0.000684(22)	0.00041(23)	0.00003(24)	0.0003(27)	0.00003(23)	
	2,1					2.0000(26)	2.0002(46)	0.0001(31)	0.0003(31)	

$p' = 0$ .  $p'' = 2$ . \*The error is indeterminate since the coefficient is zero. The S.I units of  $k_{5FU,j,k}^{(p)}$  is  $\frac{\mu\text{mol}^{(1-A)}}{m^{(2-2A)}\text{min}}$ ,  $\Gamma_{5FU,j,k}^{(AB)}$  is  $\frac{m^{2B}}{\mu\text{mol}^B}$ ,  $\alpha_{5FU,j,k}^{(AB,p)}$  is  $\frac{m^{2C}}{\mu\text{mol}^C}$ , and  $\beta_{5FU,j,k}^{(AB,p)}$  is  $\frac{m^{2D}}{\mu\text{mol}^D}$ .

The cases we examined with the interacting molecules involved zeroth, first, second, and the combination of the best two processes of the interacting molecules. The change in the kinetics of molecules due to the interaction involving the other molecules were observed. The constant ( $\alpha$ ), in the nonlinear differential equations supplied in Section 2.1.2, is the factor showing the impact of molecule interactions on the kinetics.

This category is tagged as case 3. Case 2 of the (1+3) two-compartment model and the (1+2) two-compartment model were used instead of the combined cases to accommodate the number of data points involved. The runs were split into two cases. The first is the impact of a single process, and the second is the combination of two processes. The results obtained for case 3 of the (1+3) two-compartment model indicate that there is no impact of  $\alpha$  on the flow of the molecules; it has zero value, and  $S_p$  remained unchanged compared with the case 2 solutions of the (1+3) two-compartment model in Table 3.10.

On the other hand, the saturation limiting interactions of molecules in the (1+2) two-compartment model are observed to have some effect on the kinetics of the molecules involved. The multi-process case of saturation limiting solution provides the best fit for the clinical data. Case 3 of the (1+2) two-compartment model has a  $S_p = 0.0125$  which is about 1.58% improvement compared to case 2 of the (1+2) two-compartment model. For case 3 of the (1+2) two-compartment model, the elimination flow rate of the molecule from compartment 2 has a negative exponent (A–B) at high concentrations, which means the elimination flow rate in the compartment obtained a maximum value at the amount of  $X_{5FU,2}^{M(2,0)} = 166.8 \frac{\mu\text{mol}}{\text{m}^2}$  in the liver. The transition phase between the low concentration and high concentration occurred at  $X_{5FU,2}^{T(2,0)} = 70.2 \frac{\mu\text{mol}}{\text{m}^2}$  in the liver. Figure 3.6 shows the 5-FU concentration for case 3.1 of the (1+2) two-compartment model.

There are slight differences between case 2 and case 3 of the (1+2) two-compartment model. The amount of molecules and concentrations at the transition point and the maximum elimination rate for the three infusion rates examined give less than 1% difference from case 2 of the (1+2) two-compartment model.

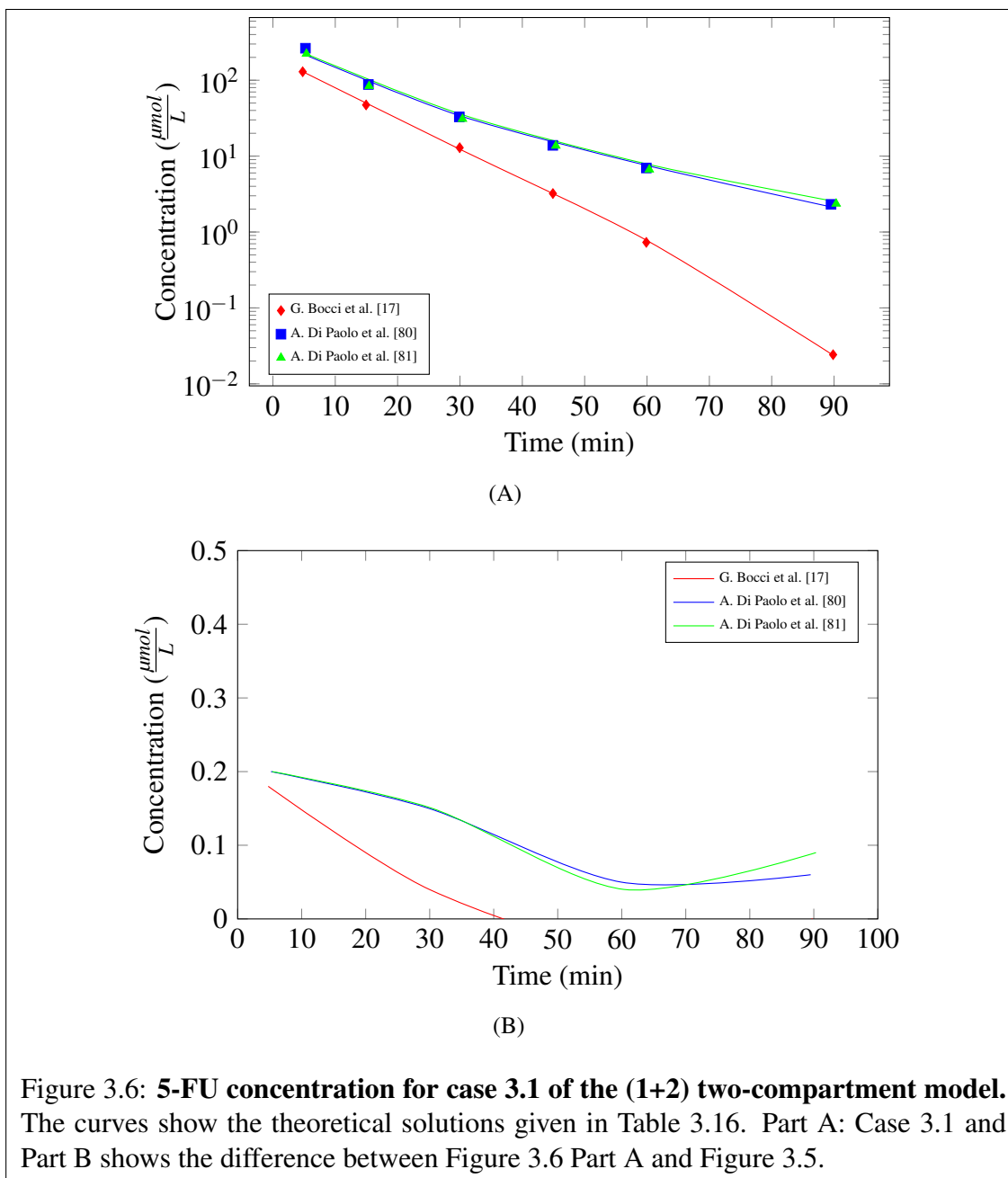


Figure 3.6: **5-FU concentration for case 3.1 of the (1+2) two-compartment model.** The curves show the theoretical solutions given in Table 3.16. Part A: Case 3.1 and Part B shows the difference between Figure 3.6 Part A and Figure 3.5.

We analysed the combination of two saturation limiting functions; labelled case 3.1, acting on each process of the (1+2) two-compartment model. We further analysed the extent to which the molecules' interactions affected the movements of the molecules. Case 3.1 shows the impact of the two processes for the interacting molecules, which improves  $S_p = 0.0127$  for case 2 of the (1+2) two-compartment model to  $S_p = 0.0125$ . The curves are not straight lines, which is an indication that the kinetics of the molecule (5-FU) is a

mixed-order process. The difference between Figure 3.6 Part A and Figure 3.5 indicates a slight change that is less than  $0.2 \frac{\mu\text{mol}}{\text{L}}$ .

The first transition point shifts from a first-order process of the molecule's kinetics to mixed-order due to the influence of the infusion rates in the plasma, the elimination rate in the liver, and inter-flows of the molecule between compartments. Whereas, the process shifts back to the first-order process from a mixed-order process when there is a switch from a high concentration behaviour to a low concentration behaviour. The transition occurred at the two phases of the kinetics of molecules (absorption phase and elimination phase), and the parameters at those points were obtained. At the absorption phase, the transition from a low concentration behaviour to a high concentration behaviour occurs at a certain amount of molecules in compartment two ( $X_{5FU,2}^{T(2,0)}$ ). The time of transitions were examined with three different infusion rates as shown in Table 3.17 ( $1921 \frac{\mu\text{mol}}{\text{min.m}^2}$ ,  $2844 \frac{\mu\text{mol}}{\text{min.m}^2}$ , and  $1422 \frac{\mu\text{mol}}{\text{min.m}^2}$ ). The impact that the inflows and outflows of molecules on the transition between low and high concentrations were examined. For instance, the outflow of 5-FU from compartment one to compartment two indicates less effect of the molecule's kinetics in the plasma compared to the impact of its elimination from the body in compartment two. It takes a longer time (nearly clinical half-life) for 5-FU to transit from a low concentration behaviour to a high concentration behaviour based on the impact of the outflows of molecules from compartment one to compartment two. Whereas, we obtained faster transition time ( $< 1.5 \text{ min.}$ ) when we consider the influence of the elimination of the molecule from the body. The impact of the inflow of 5-FU from compartment two to compartment one produced the slowest impact on the transition behaviours. The transition times are larger than the clinical half-life and unattainable with low infusion over a short time; such as  $1921 \frac{\mu\text{mol}}{\text{min.m}^2}$  administered over one minute.

The number of molecules and concentration at the elimination flow rate were examined. These values indicate the threshold for large *AUC* for the molecule in the body if they are exceeded.

Table 3.17: 5-FU transition parameters for the (1+2) two-compartment model with variable exponents.

Case	Inf.	$j, k$	$X_{5FU,2}^{T(j,k)}$	$X_{5FU,1}^{1T(j,k)}$	$C_{5FU,1}^{1T(j,k)}$	$X_{5FU,1}^{2T(j,k)}$	$C_{5FU,1}^{2T(j,k)}$	$t^{1T(j,k)}$	$t^{2T(j,k)}$
3.0	1921	1,2	604.5	895.8	89.58	80.26	8.03	10.5	35.8
			2844	1884	188.4	55.93	5.59	7.64	72.5
			1422	1927	192.7	55.87	5.59	7.93	74.6
	1921	2,0	70.2	1761	176.1	24.09	2.41	1.17	52.4
			2844	2655	265.5	22.56	2.26	1.01	88.4
			1422	1767	176.7	22.52	2.25	1.31	89.3
	1921	2,1	1764	N/A	N/A	N/A	N/A	N/A	N/A
			2844	N/A	N/A	N/A	N/A	N/A	N/A
			1422	N/A	N/A	N/A	N/A	N/A	N/A
3.1	1921	1,2	578.0	915.6	91.59	25.05	2.49	10.3	52.2
			2844	1906	190.7	55.38	5.54	7.46	73.8
			1422	1950	195.1	22.03	2.20	7.76	89.12
	1921	2,0	77.2	1750	175.0	25.05	2.49	1.28	52.2
			2844	2645	264.6	25.44	2.55	1.09	88.1
			1422	1902	190.3	22.03	2.20	1.41	89.12
	1921	2,1	1528	N/A	N/A	N/A	N/A	N/A	N/A
			2844	319.9	32.0	251.4	25.15	30.6	33.3
			1422	430.2	43.03	155.3	15.54	28.2	38.2

The S.I units of  $X_{5FU,1}^{g(1,0)}$  is  $\frac{\mu\text{mol}}{\text{m}^2}$  and  $C_{5FU,1}^{g(1,0)}$  is  $\frac{\mu\text{mol}}{\text{L}}$ , and  $t_{1/2}$  is *min*. where *d* represents DHFU and *g* represents T and M that symbolise transition and maximum values respectively for both concentrations and number of molecules.

The two models, case 3.0 and case 3.1, have nearly identical number of molecules with less than 0.1% difference. The results are shown in Table 3.18. The concentrations at the first phase of the maximum elimination rate are higher than the maximum concentrations estimated from the clinical trials. For the infusions of 1921  $\frac{\mu\text{mol}}{\text{min.m}^2}$  and 2844  $\frac{\mu\text{mol}}{\text{min.m}^2}$  over one

minute, and  $1422 \frac{\mu\text{mol}}{\text{min.m}^2}$  over two minutes, the clinical estimates are reduced by 20.27%, 3.81%, and 13.06% respectively. The time at which the maximum elimination rate occurs is shorter in larger infusion,  $1921 \frac{\mu\text{mol}}{\text{min.m}^2}$  produced the largest maximum elimination rate time by 53 sec compared to the  $2844 \frac{\mu\text{mol}}{\text{min.m}^2}$  infusion.

Table 3.18: 5-FU parameters at the maximum elimination rate for the (1+2) two-compartment model with variable exponents.

Case	Inf.	$X_{5FU,2}^{M(2,0)}$	$X_{5FU,1}^{1M(2,0)}$	$C_{5FU,1}^{1M(2,0)}$	$X_{5FU,1}^{2M(2,0)}$	$C_{5FU,1}^{2M(2,0)}$	$t^{1M(2,0)}$	$t^{2M(2,0)}$
3.0	1921	166.8	1614	161.4	31.9	3.19	2.54	50.6
	2844		2519	251.9	29.40	2.94	2.11	85.6
	1422		2561	256.1	29.34	2.93	2.43	85.4
3.1	1921	166.7	1613	161.4	33.21	3.32	2.57	50.1
	2844		2516	251.6	31.89	3.19	2.13	85.6
	1422		2557	255.7	30.66	3.07	2.49	87.7

The S.I units of  $X_{5FU,1}^{g(1,0)}$  is  $\frac{\mu\text{mol}}{\text{m}^2}$  and  $C_{5FU,1}^{g(1,0)}$  is  $\frac{\mu\text{mol}}{\text{L}}$ , and  $t_{1/2}$  is min. where  $d$  represents DHFU and  $g$  represents T and M that symbolise transition and maximum values respectively for both concentrations and number of molecules.

### 3.3 Three-Compartment Model

Considering the paths of elimination designed in the two-compartment models, the (1+2) two-compartment model gives a better fit to the clinical data than the (1+3) two-compartment model. The elimination of the molecules in the three-compartment model is designed using the analogue of the (1+2) two-compartment model. Part D of Figure 2.1 shows the three-compartment model, splitting the kinetic rate constant of metabolism events from the events occurring in the healthy and tumour cells. Compartment one represents distribution events in the plasma; compartment two represents metabolism events in the liver; while compartment three stands for the tumour cells and the healthy cells. The two types of processes were examined for both fixed and variable exponents of the model. See part C of Figure 2.1.

### 3.3.1 Fixed Exponents Minimisation for the Three-Compartment Model

The fixed first-degree exponents' optimisation is the primary case examined, and the subordinates involved adding another order process to the primary case. All the exponents are fixed parameters. The final results are shown in Table 3.19, and Figure 3.7 shows the corresponding concentration-time curves. There is an indication that case 1 of the three-compartment model is an improvement of 10.24% in the variance  $S_p$  compared with case 1 of the (1+2) two-compartment model. There is a slight improvement of 1.09% in  $S_p$  observed in the subordinate case 1.1 compared to case 1; on the other hand, case 1.3 has an improvement of 1.63% in  $S_p$  when compared to case 1. However, case 2 of the (1+2) two-compartment model has a better fit to the clinical data than case 1.3 of the three-compartment model.

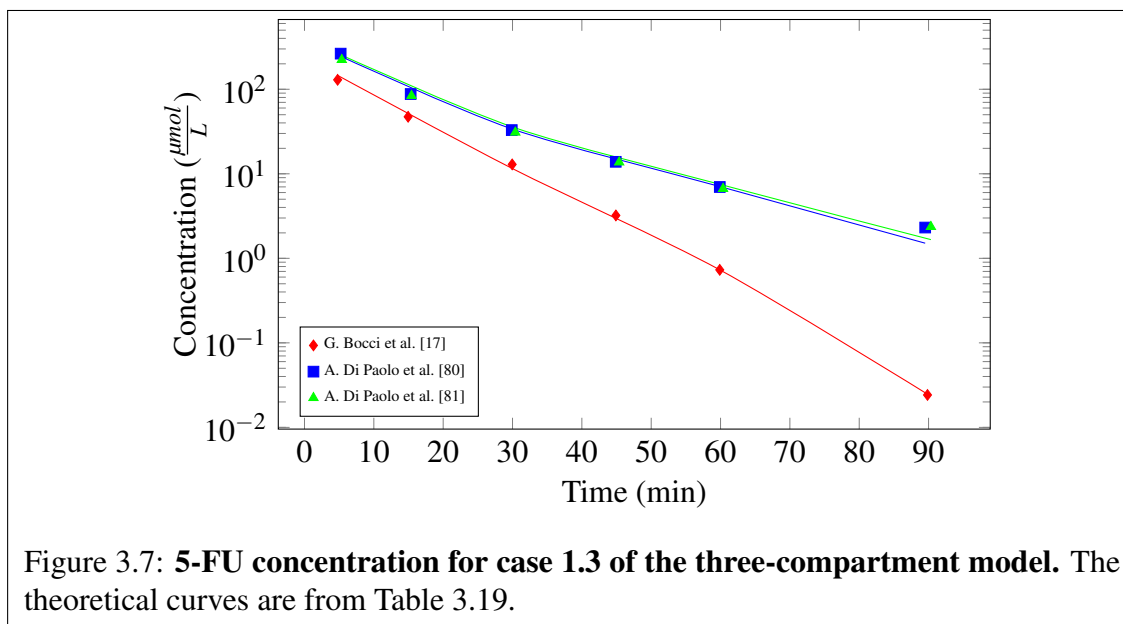
The transition between low and high concentration behaviours was examined using three fixed exponential cases of three-compartment model: cases 1, 1.1, and 1.3. The results are shown in Table 3.20 for the three sets of infusion. The first transition point from low concentration behaviour to high concentration behaviour indicates that there is a longer transition time for a low infusion rate. There is a difference of 19.1% between the transition times of the  $1921 \frac{\mu\text{mol}}{\text{min.m}^2}$  and  $2844 \frac{\mu\text{mol}}{\text{min.m}^2}$  infusions. The infusion time also influences the parameters obtained for the transition behaviours and maximum elimination rate.

The infusion of  $1422 \frac{\mu\text{mol}}{\text{min.m}^2}$  administered over two minutes exhibits a slower transition from high concentration behaviour to low concentration behaviour by 2.2% when compared with the higher infusion  $2844 \frac{\mu\text{mol}}{\text{min.m}^2}$  over one minute. We can conclude from our results that the dosage of a drug has an impact on transition time and concentration of a drug in the plasma. The combined cases 1.1 and 1.3 depicted a slightly smaller number of molecules compared with case 1 at the transition point in compartment two by 2.5%. Case 1 of the three-compartment model gives a higher number of molecules at the first and second transition points compared to case 1.3.

Table 3.19: 5-FU parameters for the three-compartment model with fixed exponents

Case	$j, k$	$k^{(0)}(\frac{\mu\text{mol}}{\text{m}^2\text{min}})$	$k^{(1)}(\frac{1}{\text{min}})$	$\Gamma^{(1)}(\frac{\text{m}^2}{\mu\text{mol}})$	$k^{(2)}(\frac{\text{m}^2}{\mu\text{mol}\cdot\text{min}})$	$\Gamma^{(2)}(\frac{\text{m}^4}{\mu\text{mol}^2})$	$V_d(\frac{L}{\text{m}^2})$	$S_p$
1	1,2	-	1.1791(34)	0.00095(15)	-	-	8.60(74)	0.0184
	1,3	-	0.04120(54)	0.0240(41)	-	-		
	2,0	-	5.493(92)	0.1939(86)	-	-		
	2,1	-	0.01021(79)	0.000000(82)	-	-		
	3,1	-	0.0006(52)	0.000(14)	-	-		
1.1	1,2	0.0017(21)	1.1815(44)	0.00097(64)	-	-	8.60(66)	0.0182
	1,3	0.0022(34)	0.0530(37)	0.0302(21)	-	-		
	2,0	0.0007(12)	5.492(55)	0.1950(38)	-	-		
	2,1	0.0000(52)	0.0105(49)	0.00000(46)	-	-		
	3,1	0.0000(24)	0.0007(52)	0.0000(45)	-	-		
1.3	1,2	0.0038(10)	1.1817(42)	0.00097(64)	0.00000(23)	N/A**	8.60(69)	0.0181
	1,3	0.0052(21)	0.0525(36)	0.0285(20)	0.0002(51)	0.0000(13)		
	2,0	0.0002(23)	5.493(49)	0.1949(31)	0.00022(13)	0.00016(41)		
	2,1	0.0005(45)	0.0107(50)	0.00000(45)	0.00005(32)	0.000198(28)		
	3,1	0.0000(24)	0.0007(50)	0.00000(11)	0.0002(47)	0.00019(22)		

\*\*Not relevant because  $k_{SFU,j,k}^{(p)} = 0$ .  $\Gamma^{(0)}$  has no contribution in fixed exponents.



The impact of the inflows and outflows of molecules influences the transition of the molecules' kinetics between a low concentration behaviour and a high concentration behaviour. We examined the impact of outflows from compartment one to compartment two and compartment three, and the elimination from compartment two. The outflow of 5-FU from compartment one to compartment two has the least impact on the transition time of the molecules, the transition time falls within the range of clinical half-life, and is unattainable with low infusion over a short time; such as  $1921 \frac{\mu\text{mol}}{\text{min.m}^2}$  administered over one minute. The transition time with the impact of the outflow from compartment one to compartment three is observed to be a little higher than that of outflow from compartment one to compartment two. Whereas, the elimination of the molecules from compartment two to compartment zero (external) has the greatest influence on the transition time and the amount of molecules at the point. The amount of molecules at the transition is smallest when we considered the elimination of molecules from compartment two compared to the outflow from compartment one. Likewise, the period before the first transition occurs is shortest when we considered the elimination of 5-FU from compartment two and longest before the second transition from a high concentration behaviour to a low concentration behaviour.

Table 3.20: 5-FU transition parameters for the three-compartment model with fixed exponents.

Case	Inf.	$j, k$	$X_{5FU,2}^{T(j,k)}$	$X_{5FU,1}^{1T(j,k)}$	$C_{5FU,1}^{1T(j,k)}$	$X_{5FU,1}^{2T(j,k)}$	$C_{5FU,1}^{2T(j,k)}$	$t^{1T(j,k)}$	$t^{2T(j,k)}$
1	1921	1,2	1053	N/A	N/A	N/A	N/A	N/A	N/A
	2844			1337	155.5	71.68	8.34	12.2	55.0
	1422			1382	160.7	71.16	8.27	12.5	56.8
	1921	1,3	41.67	1482	172.3	8.72	1.01	0.80	62.4
	2844			1854	215.6	8.70	1.01	0.66	92.6
	1422			1206	140.2	8.71	1.01	0.89	94.4
	1921	2,0	5.16	455.9	53.01	6.35	0.74	0.22	64.2
	2844			570.3	66.31	6.40	0.74	0.19	94.4
	1422			398.4	46.33	6.40	0.74	0.27	96.1
1.1	1921	1,2	1031	N/A	N/A	N/A	N/A	N/A	N/A
	2844			1369	159.2	69.86	8.12	11.9	55.8
	1422			1413	164.3	69.36	8.07	12.1	57.6
	1921	1,3	33.11	1324	154.0	8.61	1.00	0.74	64.9
	2844			1622	188.6	8.25	0.96	0.59	93.0
	1422			1057	122.9	8.26	0.96	0.78	94.7
	1921	2,0	5.13	450.9	52.43	6.21	0.72	0.21	64.9
	2844			564.5	65.64	6.40	0.74	0.19	94.3
	1422			392.8	45.67	6.26	0.73	0.26	96.4
1.3	1921	1,2	1031	N/A	N/A	N/A	N/A	N/A	N/A
	2844			1369	159.2	69.86	8.12	11.9	55.8
	1422			1413	164.3	69.36	8.07	12.1	57.6
	1921	1,3	35.09	1335	155.2	8.33	0.97	0.72	62.7
	2844			1708	198.6	8.34	0.97	0.60	92.9
	1422			1120	130.2	8.37	0.97	0.81	94.6
	1921	2,0	5.13	450.9	52.43	6.21	0.72	0.21	64.9
	2844			564.5	65.64	6.40	0.74	0.19	94.3
	1422			392.8	45.67	6.26	0.73	0.26	96.4

The S.I units of  $X_{5FU,1}^{g(1,0)}$  is  $\frac{\mu\text{mol}}{m^2}$  and  $C_{5FU,1}^{g(1,0)}$  is  $\frac{\mu\text{mol}}{L}$ , and  $t_{1/2}$  is *min.* where *d* represents DHFU and *g* represents T and M that symbolise transition and maximum values respectively for both concentrations and number of molecules.

### 3.3.2 Variable Exponents' Minimisation for the Three-Compartment Model

There is validation that the kinetics of 5-FU metabolism is approximately first-order through all the compartments that were modelled. In comparing the one-compartment model to the three-compartment model, the order processes were observed to be nearly first-order at low concentration. The results are shown in Table 3.21.

Table 3.21: 5-FU parameters for the three-compartment model with variable exponents.

Parameters	j,k				
	1,2	1,3	2,0	2,1	3,1
<i>A</i>	1.0901(21)	0.99995(21)	0.88183(76)	1.0414(70)	1.0002(52)
<i>B</i>	0.9817(41)	0.9999(32)	1.19466(72)	0.995(15)	1.0001*
$k_{5FU,j,k}^{(AB)}$	0.1264(23)	0.00025(51)	1.6384(80)	0.0127(14)	0.00325(13)
$\Gamma_{5FU,j,k}^{(AB)}$	0.00194(10)	0.0009(19)	0.00630(14)	0.00057(24)	0.00000(36)
$V_d \left(\frac{L}{m^2}\right)$	9.999(88)				
$S_p$	0.0126				

\*No uncertainty error. The S.I units of  $k_{5FU,j,k}^{(p)}$  is  $\frac{\mu mol^{(1-A)}}{m^{(2-2A)}min}$  and  $\Gamma_{5FU,j,k}^{(AB)}$  is  $\frac{m^{2B}}{\mu mol^B}$ .

The variance  $S_p$  shows an insignificant change between case 2 of the three-compartment model ( $S_p = 0.0126$ ) and case 2 of the (1+2) two-compartment model with  $S_p = 0.0127$ . The two models were observed to be the best fit to the clinical data. Case 2 of the three-compartment model can be best used for predicting the molecules' kinetics in the body. It splits the rate constant into three different compartments that represent three different rates of distribution, metabolism, and interaction with healthy and tumour cells. The splitting of the rate constant is an advantage over case 2 of the (1+2) two-compartment model that can only predict three different kinetics at a time. The two-compartment model unifies the kinetic rate of elimination with and the healthy and tumour cells; however, the advantage of the two-compartment model is the reduced number of parameters to analyse. The three-compartment concentration-time curves are shown in Figure 3.8. The curvature of the graph

indicates a mixed-order process. The detailed graph for all eight datasets are shown in Figure C.9 in the appendix C.

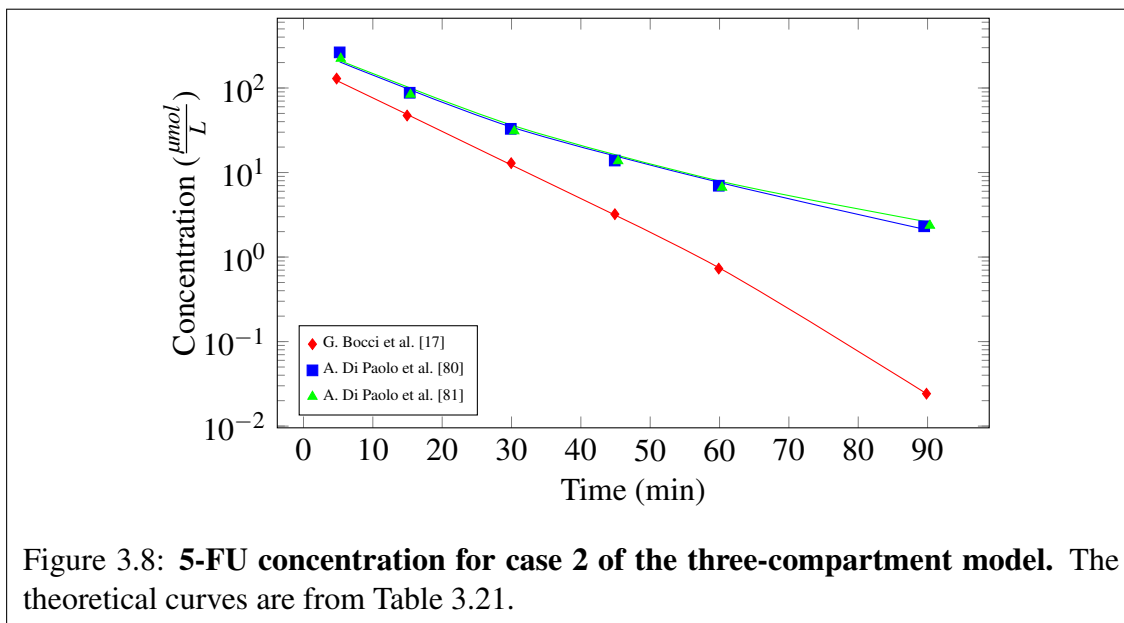


Figure 3.8: **5-FU concentration for case 2 of the three-compartment model.** The theoretical curves are from Table 3.21.

The elimination flow rate of the molecule from compartment 2 has a negative exponent ( $A-B$ ) at high concentration, which means it has a maximum elimination rate at  $X_{5FU,2}^{M(2,0)} = 165.5 \frac{\mu\text{mol}}{\text{m}^2}$ . The  $AUC$  becomes large when the number of molecules in compartment 2 is higher than the threshold of  $X_{5FU,2}^{M(2,0)}$ . The transition between a low concentration behaviour and a high concentration behaviour were examined with the influence of three sets of infusions rate, inflows and outflows in compartment one, and elimination rates from compartment two. The estimates of the parameters in the plasma at the transition points and the maximum elimination rate are shown in Table 3.22. The elimination rates shift the first-order process to mixed-order process when there is a transit from a low concentration behaviour to a high concentration behaviour and vice versa.

We had limitations in the number of cases investigated. Some cases were not examined in the three-compartment model because the number of varying PK parameters would exceed the total number of clinical data points available.

Table 3.22: 5-FU transition parameters for the three-compartment model with variable exponents.

Inf.	$j, k$	$X_{5FU,2}^{T(j,k)}$	$X_{5FU,1}^{1T(j,k)}$	$C_{5FU,1}^{1T(j,k)}$	$X_{5FU,1}^{2T(j,k)}$	$C_{5FU,1}^{2T(j,k)}$	$t^{1T(j,k)}$	$t^{2T(j,k)}$
1921	1,2	579.1	929.2	92.9	72.69	7.27	10.08	37.7
2844			1910	190.1	54.45	5.45	7.47	73.9
1422			1954	195.4	54.40	5.44	7.76	76.0
1921	1,3	1111	N/A	N/A	N/A	N/A	N/A	N/A
2844			1124	112.4	83.65	8.37	15.9	55.3
1422			1173	117.3	82.64	8.26	16.0	57.4
1921	2,0	22.04	966.5	96.66	18.80	1.88	0.52	55.0
2844			1206	120.6	17.99	1.80	0.43	90.7
1422			805.7	8.06	18.00	1.80	0.59	92.8
1921	2,1	182	1587	158.7	33.12	3.31	2.81	49.9
2844			2492	249.2	31.03	3.10	2.33	85.7
1422			2534	253.4	27.30	2.73	2.68	89.3

The S.I units of  $X_{5FU,1}^{g(1,0)}$  is  $\frac{\mu\text{mol}}{\text{m}^2}$  and  $C_{5FU,1}^{g(1,0)}$  is  $\frac{\mu\text{mol}}{\text{L}}$ , and  $t_{1/2}$  is *min.* where  $d$  represents DHFU and  $g$  represents T and M that symbolise transition and maximum values respectively for both concentrations and number of molecules.

Table 3.23: 5-FU transition parameters for the three-compartment model with variable exponents.

Inf.	$X_{5FU,2}^{M(2,0)}$	$X_{5FU,1}^{1M(2,0)}$	$C_{5FU,1}^{1M(2,0)}$	$X_{5FU,1}^{2M(2,0)}$	$C_{5FU,1}^{2M(2,0)}$	$t^{1M(2,0)}$	$t^{2M(2,0)}$
1921	165.5	1616	161.6	31.76	3.18	1.55	50.4
2844		2519	251.9	29.87	2.99	2.13	86.1
1422		2557	255.7	29.90	2.99	2.48	88.3

The S.I units of  $X_{5FU,1}^{g(1,0)}$  is  $\frac{\mu\text{mol}}{\text{m}^2}$  and  $C_{5FU,1}^{g(1,0)}$  is  $\frac{\mu\text{mol}}{\text{L}}$ , and  $t_{1/2}$  is *min.* where  $d$  represents DHFU and  $g$  represents T and M that symbolise transition and maximum values respectively for both concentrations and number of molecules.

### 3.4 Summary

Optimising progressively from the one-compartment model to the three-compartment model enabled us to establish the connection of the multi-compartment model and the kinetics of molecules in the body. The model validates this in our analysis: the three-compartment model is better than the one-compartment model (see Sections 3.1 and 3.2).

The two different two-compartment models were also examined for the best elimination route to fit the clinical data. It was confirmed that having the elimination modelled in the metabolism compartment has more effect on achieving our goal than having the elimination route via the plasma distribution compartment. The behaviour of the (1+3) two-compartment model with the elimination route via the central compartment behaves in the same manner as the one-compartment model. The three-compartment model was seen to be the model with the best fit to the clinical data (see Sections 3.1 , 3.2 , and 3.3).

The first-degree fixed exponent in combination with other degree exponents (zeroth, second, and the combination) was examined. The insignificant impact of these subordinate runs on each case model was validated. We also observed that all the cases at a low concentration approximately obeyed the first-order process in the same manner as with the Michaelis-Menten model; however, in the high concentration regions, there were non-zeroth order processes. The rate of elimination decreased with large concentrations and can have the effect of increasing *AUC* for concentrations above the threshold.

## Chapter 4

# Model Sampling Design and Analysis for DHFU

---

*More than 10 million Americans are living with cancer,  
and they demonstrate the ever-increasing possibility of  
living beyond cancer.*

– Sheryl Crow

---

The sampling and analysis of the multi-compartment models for DHFU have been examined in this chapter. The datasets used comprise of 433 patients and 48 data points. Still, we used 42 data points for the fitting to accommodate regular weight on each data point and also to maintain the same time frame for the kinetics of DHFU. The clinical details are shown in Table 4.1.

We split the analysis into two categories based on the number of types of molecules varied at a time: (i.) one-molecule model, we use the results for 5-FU in chapter three as fixed parameters to obtain the PK parameters for DHFU, and (ii.) two-molecule model involved varying the two types of molecules (5-FU and DHFU) together to obtain the PK parameters for both DHFU and 5-FU. We considered these two approaches to examine the kinetics of the interaction between 5-FU and DPYD that forms DHFU. We examined the models using one-compartment model analysis by unifying the kinetic rate constants of the molecule involved from the point of administration to elimination as a homogenous system. We also used the (1+2) two-compartment model to solve for the best fit of DHFU to the clinical data, and this involved splitting the metabolism and central compartment into two

interconnected compartments with elimination from the metabolism compartment.

Table 4.1: The clinical datasets of DHFU

Dataset	Reference	Dosage	IV Time	Infusion	Patients	Data points
		5-FU	5-FU	5-FU		DHFU
1	G. Bocci et al. [17]	250	1	1921	185	6
2	Di Paolo et al. [80]	370	1	2844	84	6
3	Di Paolo et al. [81]	370	2	1422	80	6
4	Di Paolo et al. [82]	370	5	568	26	6
5	G. Bocci et al. [1] <sup>a</sup>	250	1	1921	20	8
6	G. Bocci et al. [1] <sup>b</sup>	370	1	2844	20	9
7	Casale et al. [83]	400	2	1537	18	7

<sup>a</sup> and <sup>b</sup> represent the study from G. Bocci et al. [1] with low dosage and high dosage infusion of 1921  $\frac{\mu\text{mol}}{\text{min.m}^2}$  and 2844 over one minute respectively. Dosage measures in  $\frac{\text{mg}}{\text{m}^2}$ . IV time measures in *min*. Infusion measures in  $\frac{\mu\text{mol}}{\text{min.m}^2}$ .

## 4.1 One-Compartment DHFU Model

### 4.1.1 Fixed Degree Exponents, One-Molecule Model

The minimisation of the variance involves variable PK parameters with fixed exponents for DHFU. We make use of the PK parameters for 5-FU from chapter three, which are held constant. Table 4.2 shows the set of fixed parameters in case 1 and case 1.3 for the one-compartment model optimisation of DHFU. The 5-FU rate constant splits into two with the elimination rate possessing 20% of the rate constant and the formation of the 5-FU-enzyme complex taking 80% [67]. In Chapter two, we discussed the formation of the complex, which involves the amount of 5-FU and DPYD. The exponent of 5-FU corresponding to a first-order process and the enzyme is a zeroth-order process at low concentrations. The  $S_p$  obtained for cases 1, 1.1, 1.2, and 1.3 are 0.00213, 0.00211, 0.00211, and 0.00207 respectively. The graphs in this chapter represent the DHFU concentrations for G. Bocci et al. [17], Di Paolo et al. [80], and Di Paolo et al. [81] experimental datasets that dominate

the subject population.

Table 4.2: DHFU parameters for the one-molecule one-compartment model with fixed exponents

Case	$A_{d,j,k}^{(p)}$	$B_{d,j,k}^{(p)}$	5FU,1 → 5FU,0		5FU,1 → CMPX,1		$V_d(\frac{L}{m^2})$
			$k_{5FU,1,0}^{(p)}$	$\Gamma_{5FU,1,0}^{(p)}$	$k_{CMPX,1,1}^{(p)}$	$\Gamma_{CMPX,1,1}^{(p)}$	
1	1.000	1.000	0.0240	0.0013	0.0958	0.0013	16.3274
1.1	0.0000	0.0000	0.01226	N/A*	0.0490	N/A*	16.5487
	1.0000	1.0000	0.02002	0.0009	0.0801	0.0009	
1.2	1.0000	1.0000	0.02396	0.0014	0.0958	0.0014	16.3278
	2.0000	2.0000	0.0000	N/A**	0.0000	N/A**	
1.3	0.0000	0.0000	0.0209	N/A*	0.0836	N/A*	16.5678
	1.0000	1.0000	0.0194	0.0008	0.0776	0.0008	
	2.0000	2.0000	0.0000	N/A**	0.0000	N/A**	

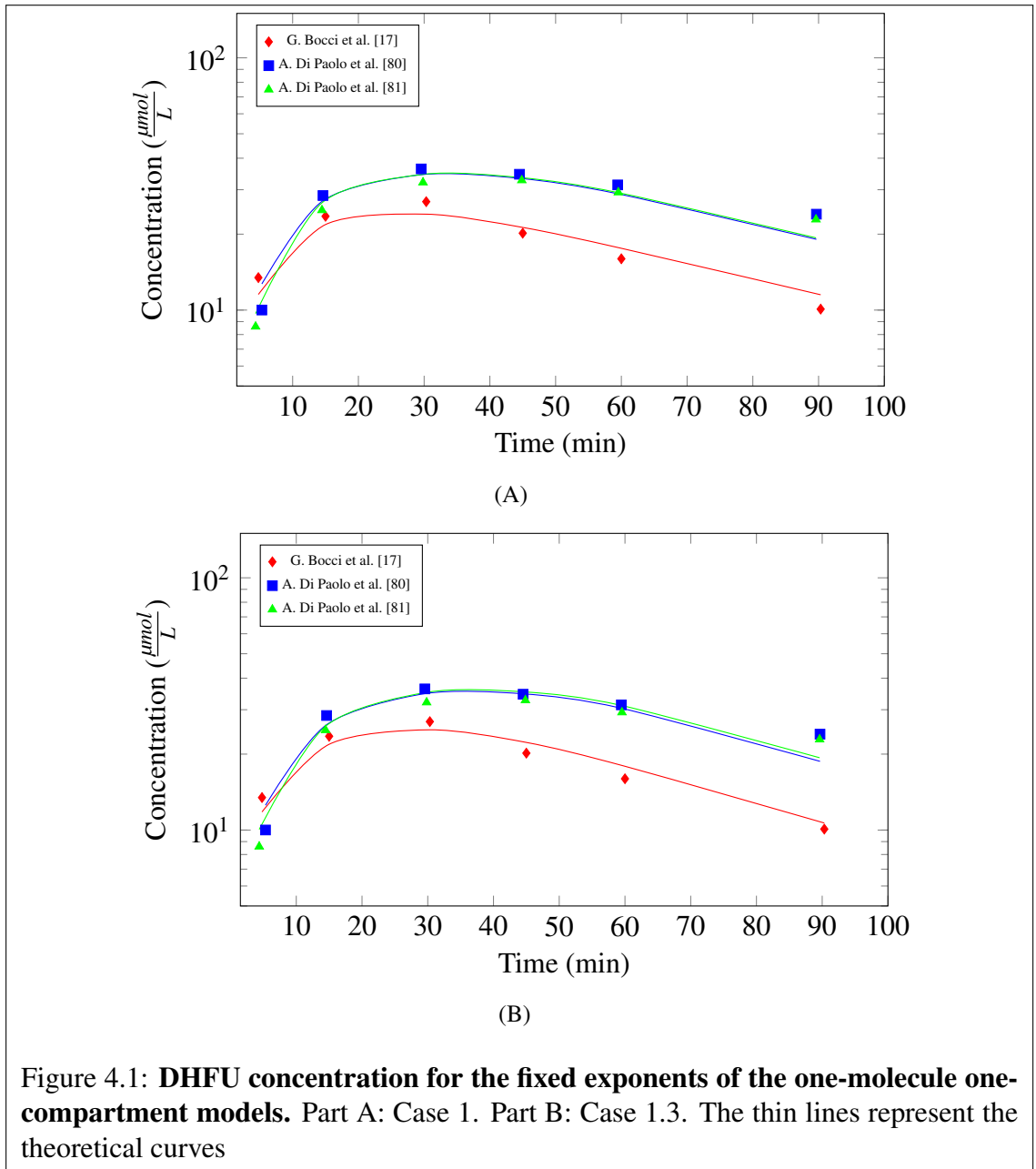
  

Case	$A_{d1,j,k}^{(p)}$	$B_{d1,j,k}^{(p)}$	DHFU,1 → DHFU,0		CMPX,1 → DHFU,1		$V_d(\frac{L}{m^2})$
			$k_{DHFU,1,0}^{(p)}$	$\Gamma_{DHFU,1,0}^{(p)}$	$k_{CMPX,1,1}^{(p)}$	$\Gamma_{CMPX,1,1}^{(p)}$	
1	1.0000	1.0000	0.3254(23)	0.00774(23)	0.0141(34)	0.00021(10)	5.09(43)
1.1	0.0000	0.0000	0.0006(31)	N/A*	0.0003(27)	N/A*	5.10(72)
	1.0000	1.0000	0.3726(22)	0.00889(21)	0.0132(28)	0.00015(33)	
1.2	1.0000	1.0000	0.3257(22)	0.00769(21)	0.0140(28)	0.00019(33)	5.09(72)
	2.0000	2.0000	0.0000(27)	N/A**	0.0000(12)	N/A**	
1.3	0.0000	0.0000	0.0003(31)	N/A*	0.0002(27)	N/A*	5.10(72)
	1.0000	1.0000	0.3093(22)	0.00863(21)	0.0125(28)	0.00015(33)	
	2.0000	2.0000	0.0042(27)	0.00097(23)	0.0000(12)	N/A**	

\*\*Not relevant since  $k_{d1,j,k}^{(p)} = 0$ .  $p = A_{d1,j,k}^{(p)} = B_{d1,j,k}^{(p)}$ . \* $\Gamma^{(0)}$  is irrelevant in fixed exponents. The units for  $k_{d1,j,k}^{(0)}$  is  $\frac{\mu mol}{m^2 min}$ ;  $k_{d1,j,k}^{(1)}$  is  $\frac{1}{min}$ ; and  $k_{d1,j,k}^{(2)}$  is  $\frac{m^2}{\mu mol \cdot min}$ .  $\Gamma_{d1,j,k}^{(1)}$  unit is  $\frac{m^2}{\mu mol}$ ;  $\Gamma_{d1,j,k}^{(2)}$  unit is  $\frac{m^4}{\mu mol^{-2}}$ , where  $d1$  represents DHFU, complex. Values without errors are fixed values.

The complete graphs for all datasets are shown in Figure C.10 of appendix C. The

results for DHFU show slight differences in  $S_p$  between cases 1, 1.1, 1.2, and 1.3. The  $S_p$  in case 1.3 was observed to be reduced by 5.00% compared with the primary case. The DHFU concentration graph for both case 1 and case 1.3 are shown in Figure 4.1 Parts A and B, respectively.



The transition of molecules between low concentration behaviours and high concentration behaviours for cases 1 and 1.3 indicates that the number of molecules at this point can

not be reached with the two models when  $1921 \frac{\mu\text{mol}}{\text{min.m}^2}$  is administered over one minute. With cases 1.1 and 1.3, the infusion  $1921 \frac{\mu\text{mol}}{\text{min.m}^2}$  has attainable transition times that are shown in Table 4.3.

Table 4.3: DHFU transition parameters for the one-compartment model with fixed exponents.

Case	Infusion	IV Time	$X_{DHFU,1}^{T(1,0)}$	$C_{DHFU,1}^{T(1,0)}$	$t^{1T(1,0)}$	$t^{2T(1,0)}$
1	1921	1	129.2	25.38	N/A	N/A
	2844	1			12.5	71.4
	1422	2			12.9	71.9
1.1	1921	1	112.5	22.05	14.9	43.9
	2844	1			10.21	80.5
	1422	2			10.62	81.0
1.2	1921	1	130.0	25.55	N/A	N/A
	2844	1			12.7	71.0
	1422	2			13.1	71.5
1.3	1921	1	115.9	22.72	16.2	41.2
	2844	1			10.6	78.6
	1422	2			11.1	79.1

The S.I units of  $X_{DHFU,1}^{g(1,0)}$  is  $\frac{\mu\text{mol}}{\text{m}^2}$  and  $C_{DHFU,1}^{g(1,0)}$  is  $\frac{\mu\text{mol}}{\text{L}}$ , and  $t_{1/2}$  is *min.* where  $g$  represents T that symbolise transition for both concentrations and number of molecules.

#### 4.1.2 Variable Exponents, One-Molecule, One-Compartment Model

The minimisation of the variance for DHFU in this section involved all the parameters of DHFU being varied, including the exponents. The fixed 5-FU variables for case 2 are shown in Table 4.4. The elimination rate constant of the one-compartment model for 5-FU is held constant, with it being split into two rate constants; 20% of the rate constant becomes the direct elimination of 5-FU, and 80% of the rate constant represents the interaction of 5-FU with the enzymes to form the complex that converts into DHFU.

Table 4.4: DHFU parameters for the one-molecule one-compartment model with variable exponents

<i>old</i> → <i>new</i>	$A_{d1,j,k}^{(p)}$	$B_{d1,j,k}^{(p)}$	$k_{d1,j,k}^{(p)}$	$\Gamma_{d1,j,k}^{(p)}$	$V_d(\frac{L}{m^2})$
F,1 → F,0	0.9567	1.2510	0.0256	0.0002	16.6951
F,1 → C,1	-	-	0.1024	0.0002	
<i>old</i> → <i>new</i>	$A_{d1,j,k}^{(p)}$	$B_{d1,j,k}^{(p)}$	$k_{d1,j,k}^{(p)}$	$\Gamma_{d1,j,k}^{(p)}$	$V_d(\frac{L}{m^2})$
D,1 → D,0	1.0099(23)	1.0089(35)	0.3323(29)	0.0083(38)	5.100(37)
E,1 → C,1	1.0010(34)	0.9990(31)	-	-	
C,1 → D,1	1.0074(27)	1.0164(42)	0.0135(33)	0.0002(41)	

F,1→F,0 represents the flows 5FU,1→5FU,0. E,1→C,1 represents the composition 5FU+DPYD,1→CMPX,1.

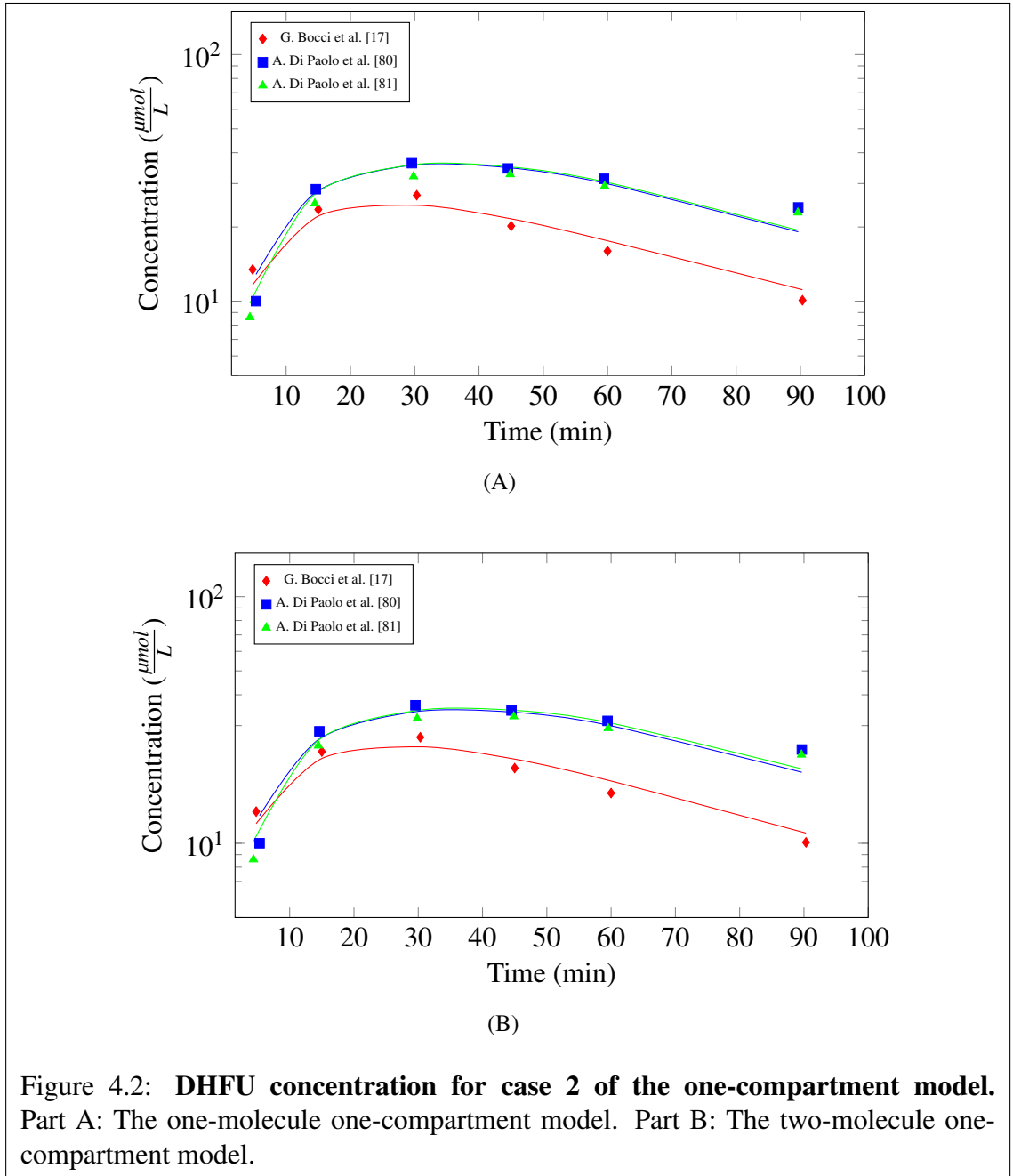
C,1→D,1 represents decomposition CMPX,1→DHFU+DPYD,1. D,1 → D,0 represents the elimination

DHFU,1→DHFU,0. The S.I units of  $k_{d1,j,k}^{(p)}$  and  $\Gamma_{d1,j,k}^{(p)}$  are  $\frac{\mu mol^{(1-A)}}{m^{(2-2A)}min}$  and  $\frac{m^{2B}}{\mu mol^B}$  respectively, where *d*1

represents 5-FU, DHFU, DPYD, or CMPX. Values without errors are fixed values.

The DHFU is formed from the complex-substrate, and the elimination rate of DHFU was found to be approximately a first-order process at low concentration ( $A= 1.0099$  for DHFU elimination flow, 1.0010 for the complex-substrate formation, and 1.0074 for the complex-substrate decomposition); whereas, at high concentrations, the reactions are nearly a zeroth-order process ( $(A-B) = 0.001$  for DHFU elimination flow, 0.0020 for the complex-substrate formation, and  $-0.009$  for the complex-substrate decomposition). The negative exponent value obtained at high concentrations in the formation of DHFU indicates that the rate of formation has a maximum value at a finite concentration. At higher concentrations, the conversion rate to DHFU becomes slower. The results for DHFU, DPYD, and complex substrate are shown in Table 4.4 for case 2, of which the  $S_p$  is 0.0020. The DHFU concentration graph is shown in Figure 4.2.

Three kinetic events in the body influence the formation of the DHFU model. First, the rate at which 5-FU reacts with DPYD to form the complex-substrate. Second, the decomposition of the complex-substrate and the formation of DHFU.



The third reaction involved is the elimination rate of DHFU from the body. The fit is slightly better in case 2 when compared to case 1 of the one-compartment model. Case 1 has  $S_p = 0.00214$  and case 2 has  $S_p = 0.00205$ , an improvement in  $S_p$  by 4.39%. The kinetic processes of DHFU are mixed, but approximately first-order processes. It is an indication that the model produces a slight improvement to the Michaelis-Menten model analysis for DHFU. The complete set of graphs for case 2 are shown in Figure C.11 in

appendix C. The transition times were obtained using the three infusions shown in Table 4.5. The exponent,  $A - B$ , for high concentrations is positive, which means there is no maximum to the elimination flow rate.

Table 4.5: DHFU transition parameters for the one molecule one-compartment model with variable exponents.

Infusion	IV Time	$X_{DHFU,1}^{T(1,0)}$	$C_{DHFU,1}^{T(1,0)}$	$t^{1T}$	$t^{2T}$
1921	1	115.5	22.65	16.12	41.73
2844	1			10.67	79.21
1422	2			11.02	80.17

The S.I units of  $X_{5FU,1}^{T(1,0)}$  is  $\frac{\mu\text{mol}}{\text{m}^2}$  and  $C_{5FU,1}^{T(1,0)}$  is  $\frac{\mu\text{mol}}{\text{L}}$ , and  $t_{1/2}$  is *min*. where  $d$  represents DHFU and T symbolises transition. infusion measures in  $\frac{\mu\text{mol}}{\text{min.m}^2}$ .

## 4.2 Variable Exponents, the Two-Molecule One-Compartment Model

We examined the two-molecule one-compartment models as another approach to observe the interactions between the varying PK parameters of 5-FU and DPYD to produce a better fit to the clinical data. The results are shown in Table 4.6. The PK parameters of the two molecules, 5-FU and DHFU, were minimised simultaneously for fitting the theoretical curves to the clinical data to obtain the best fit. In Table 4.6, F,1→F,0 represents the flow from 5FU,1 to 5FU,0; F,1IE,1→C,1 represents the formation of the complex 5FU+DPYD,1→CMPX,1; C,1→D,1IE, 1 represents the decomposition of the complex-substrate CMPX,1→DHFU,1+DPYD,1; D,1 → D,0 represents the elimination of the metabolite DHFU,1 to DHFU,0.

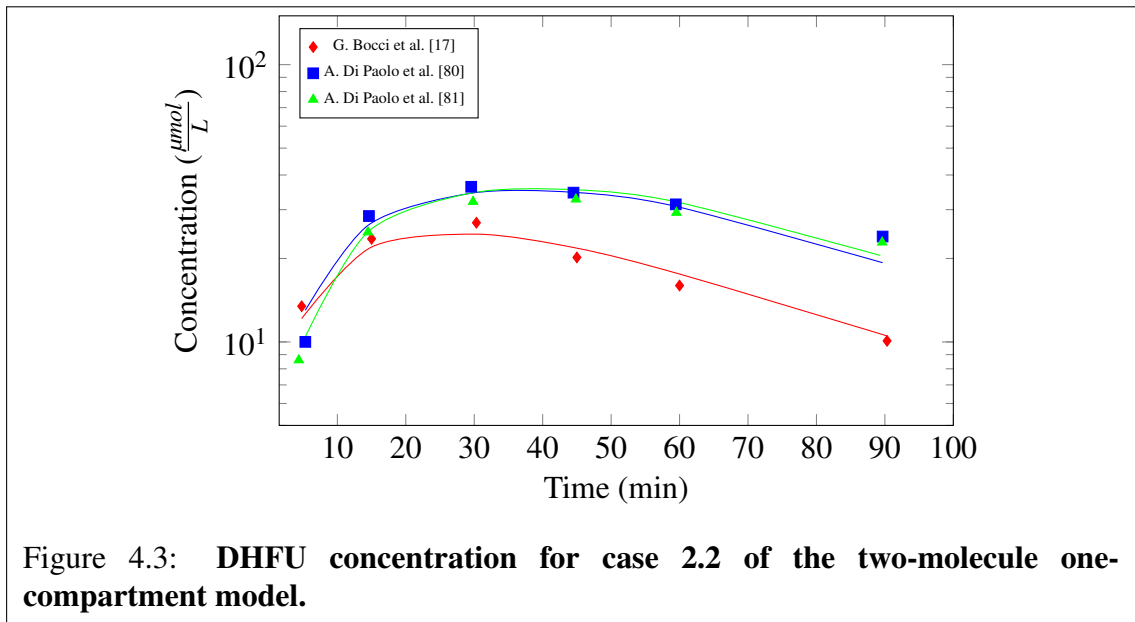
The  $S_p$  obtained for cases 2, 2.1, and 2.2 are approximately 0.0020 with insignificant changes below  $10^{-5}$ . There is little improvement between case 2 of the one-molecule one-compartment model and case 2 of the two-molecule one-compartment model. The two-molecule one-compartment model is observed to have a slightly better fit to the clinical data than the one-molecule one-compartment model.

Table 4.6: DHFU parameters for the two-molecule one-compartment model with variable exponents

Case	<i>old</i> → <i>new</i>	$A_{d1,j,k}^{(p)}$	$B_{d1,j,k}^{(p)}$	$k_{d1,1,0}^{(p)}$	$\Gamma_{d1,1,0}^{(p)}$	$V_d$
2	F,1→F,0	0.9560(24)	1.2505(33)	0.0191(16)	0.0004(54)	5.101(43)
	F,1E,1→C,1	1.0007(32)	0.9987*	1.0181(12)	0.0000(56)	
	C,1→D,1E,1	1.0180(24)	1.0237(31)	0.0159(21)	0.0003(34)	
	D,1→D,0	1.0134(31)	1.0427(25)	0.3724(12)	0.0082(33)	
2.1	F,1→F,0	0.0001*	N/A**	0.0000(15)	N/A**	5.101(42)
	F,1→F,0	0.9561(21)	1.2505(32)	0.0191(17)	0.0004(51)	
	F,1E,1→C,1	0.0000*	N/A**	0.0000(16)	N/A**	
	F,1E,1→C,1	1.0007(32)	0.9988*	1.0181(12)	0.000(56)	
	C,1→D,1E,1	0.0000*	N/A**	0.0000(16)	N/A**	
	C,1→D,1E,1	1.0180(24)	1.0237(31)	0.0159(21)	0.0003(34)	
	D,1→D,0	0.0000(23)	0.0000(32)	0.0001(15)	0.000002(24)	
	D,1→D,0	1.0135(33)	1.0523(24)	0.3822(15)	0.0082(32)	
2.2	F,1→F,0	0.0004(24)	0.0001(33)	0.0036(16)	0.0006(17)	5.101(43)
	F,1→F,0	2.0000(24)	2.0000(33)	0.0015(16)	0.0001(26)	
	F,1→F,0	0.9559(24)	1.2505(33)	0.0191(16)	0.0010(54)	
	F,1E,1→C,1	0.0001(24)	0.0009*	0.0192(16)	0.00000(34)	
	F,1E,1→C,1	1.9959(32)	2.0000(22)	0.0009(16)	0.0001(33)	
	F,1E,1→C,1	1.0007(32)	0.9987*	1.0180(12)	0.0000(56)	
	C,1→D,1E,1	0.0001(24)	0.00014(33)	0.0002(16)	0.0001(25)	
	C,1→D,1E,1	2.0000*	N/A**	0.0000(16)	N/A**	
	C,1→D,1E,1	1.0180(24)	1.0237(31)	0.0159(21)	0.0003(34)	
	D,1→D,0	0.0003(24)	0.0004(33)	0.0001(16)	0.0004(41)	
	D,1→D,0	2.0000(31)	2.0000(25)	0.0027(16)	0.0019(22)	
	D,1→D,0	1.0140(31)	1.0444(25)	0.3729(12)	0.0090(33)	

\*\*Not relevant since  $k_{SFU,j,k}^{(p)} = 0$ . \*The value and error are indeterminate. The units of  $k_{d1,j,k}^{(p)}$  is  $\frac{\mu\text{mol}^{(1-A)}}{m^{(2-2A)}\text{min}}$ , and  $\Gamma_{d1,j,k}^{(p)}$  is  $\frac{m^{2B}}{\mu\text{mol}^B}$ .

$S_p$  improves from 0.0021 to 0.0020, which is about a 6.67% reduction. The elimination rate of 5-FU is reduced by 25% compared to the one-molecule one-compartment model, which compensates for the increase in the conversion rate for the complex formation from 80% of the total kinetics rate of elimination of 5-FU to over 90%. The results also show that the model is a saturable system. The exponents at high concentrations for the elimination rate of 5-FU are negative, so are the decomposition rate of the complex and the DHFU elimination rate. Figure 4.2 shows there is little change between the one-molecule case 2 results and two-molecule case 2 results.



The exponent at high concentrations is less than zero and we determined  $X_{DHFU,1}^{M(1,0)}$  for case 2, case 2.1, and case 2.2 of the two-molecule one-compartment model. The maximum elimination rate could not be reached because the value is larger than the maximum concentrations achieved for these infusions. The results are shown in Table 4.7. The kinetics of molecules switches at the transition point between a low concentration behaviour and a high concentration behaviour at the times given in Table 4.7. The high infusion rate gives a faster transition time from low concentration behaviour to high concentration behaviour.

Table 4.7: DHFU transition times for the two-molecule one-compartment models with variable exponents.

Inf.	case	$X_{DH,1}^{T(1,0)}$	$C_{DH,1}^{T(1,0)}$	$X_{DH,1}^{M(1,0)}$	$C_{DH,1}^{M(1,0)}$	$t^{1T(1,0)}$	$t^{2T(1,0)}$	$t^{1M(1,0)}$	$t^{2M(1,0)}$
1921	2	100.2	19.6	2997	587.5	12.75	52.85	N/A	N/A
2844						9.02	88.02	N/A	N/A
1422						9.32	90.1	N/A	N/A
1921	2.1	96.05	18.8	2133	418.2	10.73	56.11	N/A	N/A
2844						8.53	92.4	N/A	N/A
1422						8.83	94.5	N/A	N/A
1921	2.2	90.95	17.8	2613	512.2	9.61	60.16	N/A	N/A
2844						7.94	98.2	N/A	N/A
1422						8.24	100.3	N/A	N/A

The S.I units of  $X_{d,1}^{g(1,0)}$  is  $\frac{\mu\text{mol}}{\text{m}^2}$  and  $C_{d,1}^{g(1,0)}$  is  $\frac{\mu\text{mol}}{\text{L}}$ , and  $t$  is *min*. where  $g$  represents subscript T and M that symbolise transition and maximum values respectively for both concentrations and number of molecules. DH represents DHFU. Inf. represents infusion which measures in  $\frac{\mu\text{mol}}{\text{min.m}^2}$ .

### 4.3 (1+2) Two-Compartment DHFU Model

#### 4.3.1 Fixed Exponents, One-Molecule Two-Compartment Model

In the one-molecule two-compartment model, the 5-FU parameters were held constant. We used the case 1 (fixed exponents) of the two-compartment model results for 5-FU as fixed numbers to minimise the PK parameters for DHFU. Table 4.8 shows the fixed PK parameters of 5-FU for the first-order process; as well as, the DHFU PK parameters.

The rate constant  $k_{5FU,2,0}$  splits into two in the ratio 4:1 between the enzymatic reaction and the elimination of 5-FU. We varied the parameters of the complex-substrates along with that of DHFU and compared the results of case 1 of the one-molecule one-compartment model in Table 4.2 to case 1 of the one-molecule two-compartment model in Table 4.8. The semi-log graph for DHFU concentration is demonstrated in Figure 4.4 for the three datasets

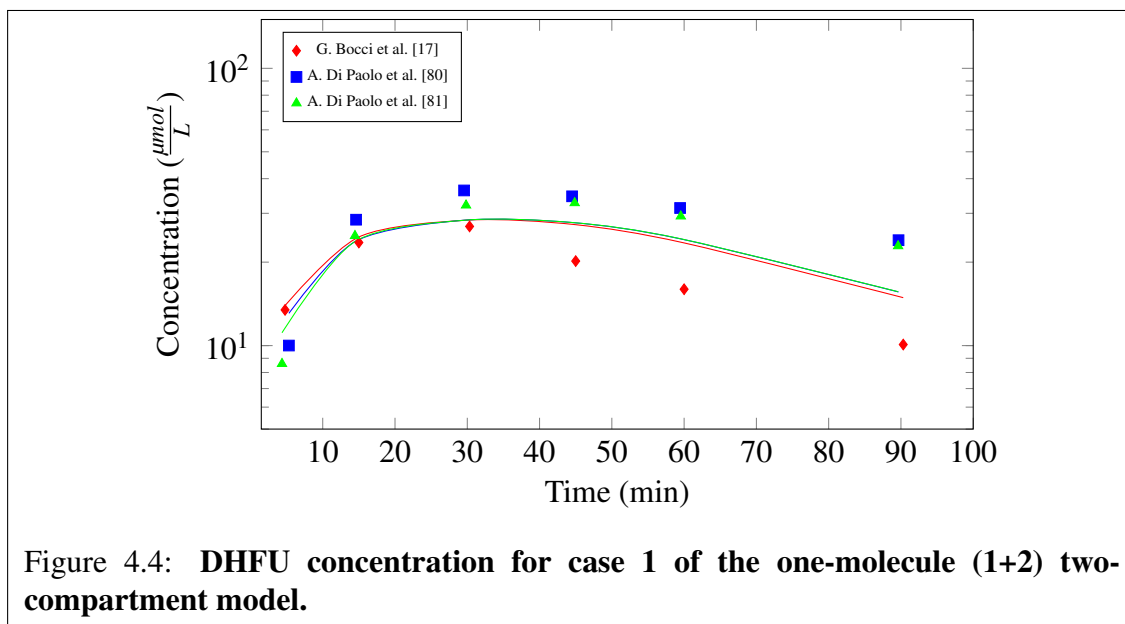
that dominate the population.

Table 4.8: DHFU parameters for the one-molecule two-compartment model with fixed exponents.

Case	$j, k$	5FU, $j \rightarrow$ 5FU, $k$		5FU, $j \rightarrow$ CMPX, $k$		$V_d$
		$k_{5FU,j,k}^{(p)}$	$\Gamma_{5FU,j,k}^{(p)}$	$k_{CMPX,j,k}^{(p)}$	$\Gamma_{CMPX,j,k}^{(p)}$	
1	1,2	0.1429	0.0006	-	-	16.3274
	2,0	1.0986	0.1845	-	-	
	2,1	0.0066	0.0000	-	-	
	2,2	-	-	4.3945	0.1845	
Case	$j, k$	DHFU, $j \rightarrow$ DHFU, $k$		CMPX, $j \rightarrow$ DHFU, $k$		$V_d$
		$k_{DHFU,j,k}^{(p)}$	$\Gamma_{DHFU,j,k}^{(p)}$	$k_{CMPX,j,k}^{(p)}$	$\Gamma_{CMPX,j,k}^{(p)}$	
1	1,2	0.1997(27)	0.0024(31)	-	-	5.09(56)
	2,0	0.7919(33)	0.0009(45)	-	-	
	2,1	0.0993(57)	0.0041(45)	-	-	
	2,2	-	-	0.0309(55)	0.0000(45)	

\*\*Not relevant since  $k_{d,j,k}^{(p)} = 0$ .  $p = A_{d,j,k}^{(p)} = B_{d,j,k}^{(p)}$ . The units for  $k_{d,j,k}^{(0)}$  is  $\frac{\mu\text{mol}}{\text{m}^2 \cdot \text{min}}$ ;  $k_{d,j,k}^{(1)}$  is  $\frac{1}{\text{min}}$ ; and  $k_{d,j,k}^{(2)}$  is  $\frac{\text{m}^2}{\mu\text{mol} \cdot \text{min}}$ .  $\Gamma_{d,j,k}^{(1)}$  unit is  $\frac{\text{m}^2}{\mu\text{mol}}$ ;  $\Gamma_{d,j,k}^{(2)}$  unit is  $\frac{\text{m}^4}{\mu\text{mol}^2}$ , where  $d$  represents DHFU, complex. Values without errors are fixed values.

The results show that there is a reduction in  $S_p$  by 74.07%. The unification of the rate constants in a single compartment model seems to have an impact on the faster rate of 5-FU conversion than what we observed in the two-compartment model. This can be analysed as the molecule will undergo three different kinetic rate constants across compartments to convert to its metabolite, and the metabolite flows back to the central compartment where it is observed. Maintaining the consistent proportion between the rate constants for elimination and formation of the complex molecule can be slower when compared to the homogeneous system of the one-compartment model. The complete set of graphs for all the datasets are shown in Figure C.13 within appendix C.



#### 4.3.2 Variable Exponents, One-Molecule Two-Compartment Model

The fitting of the PK parameters to the clinical data in this section involved the exponents varying along with the other PK parameters. The parameters for Case 2 of the (1+2) two-compartment model for 5-FU are fixed with the rate constant of 5-FU elimination split into 80% and 20%. The 80% goes into the formation of the complex. Table 4.9 shows the fixed PK parameters for 5-Fu and the results of fitting the PK parameters for DHFU to the clinical data. There is an improvement in  $S_p$  by 32% when this model is compared to the fixed exponent one-molecule two-compartment model, which was reduced from 0.0081 to 0.0055. The model with variable exponents A and B provides a better fit to the clinical data. See Figures 4.4 and 4.5.

When we compare the variable exponent one-molecule one-compartment model to the variable exponent one-molecule two-compartment model, it shows that the one-molecule one-compartment model has a better fit. There is about 63% improvement in the variance when case 2 of the one-molecule two-compartment model is compared to case 2 of the one-molecule one-compartment model. This encouraged us to design further the two-molecule two-compartment model. The exponents for DHFU at high concentration are greater than

zero; therefore, we cannot obtain the number of molecules at the maximum elimination rate.

Table 4.9: DHFU parameters for the one-molecule two-compartment model with variable exponents.

$old \rightarrow new$	$A_{d1,j,k}^{(p)}$	$B_{d1,j,k}^{(p)}$	$k_{d1,j,k}^{(p)}$	$\Gamma_{d1,j,k}^{(p)}$	$V_d$
F,1→F,2	1.0975	0.9817	0.1165	0.00186	10.000
F,2→F,0	0.8807	1.1941	0.3275	0.00624	
F,2→F,1	1.0394	0.994	0.01233	0.00059	
F,2IE,1→C,2	0.9940(23)	1.00045(32)	1.3102	0.00624	
C,2→D,2IE,2	1.0321(33)	1.0004*	0.0050(21)	0.00000(34)	
D,1→D,2	1.0882(34)	0.9985(42)	0.2671(52)	0.00178(23)	5.10(61)
D,2→D,0	1.0416(42)	1.0398(23)	0.8031(43)	0.0066(52)	
D,2→D,1	1.0540(41)	1.0017*	0.1855(23)	0.0000(34)	

Values without errors or stars are fixed numbers. \*The error is indeterminate because the coefficient is zero. \*\*Not relevant because  $k_{d,j,k}^{(p)} = 0$ . The S.I units of  $k_{d1,j,k}^{(p)}$  is  $\frac{\mu mol^{(1-A)}}{m^{(2-2A)} min}$  and  $\Gamma_{d1,j,k}^{(p)}$  is  $\frac{m^{(2B)}}{\mu mol^B}$ , where  $d1$  represent 5-FU, DHFU, DPYD, or CMPX. F,k represents 5FU in compartment k. C,k represents complex-substrate in compartment k. D,k represents DHFU in compartment k. E,k represents DPYD in compartment k.

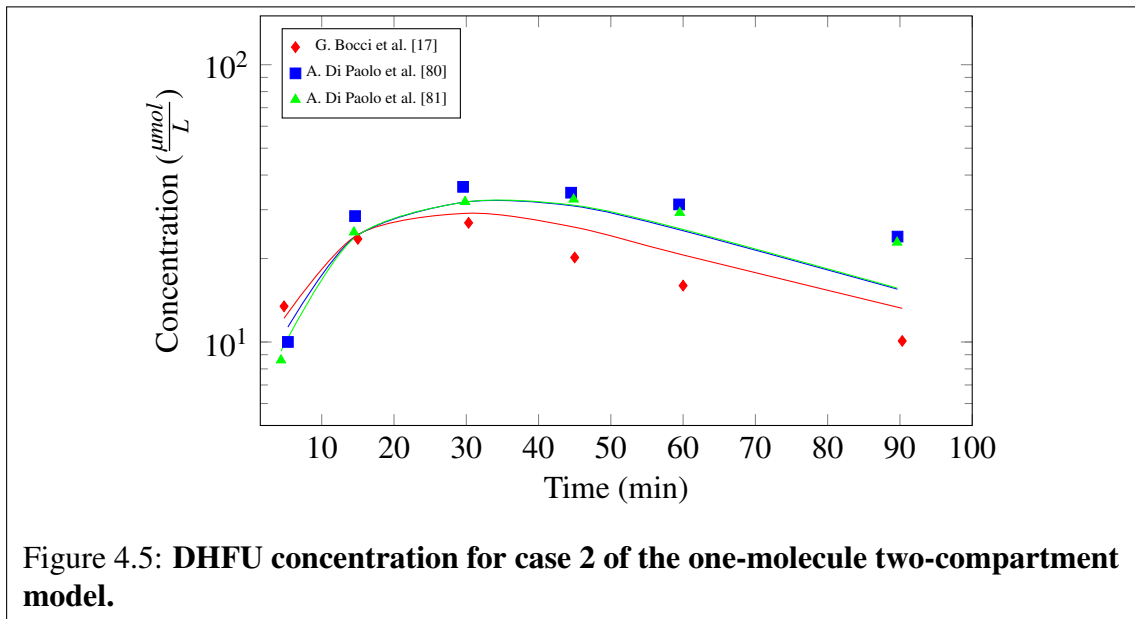


Figure 4.5: DHFU concentration for case 2 of the one-molecule two-compartment model.

The transition behaviours were examined using three infusions: 1921  $\frac{\mu\text{mol}}{\text{min.m}^2}$  and 2844  $\frac{\mu\text{mol}}{\text{min.m}^2}$  over one minute, and 1422  $\frac{\mu\text{mol}}{\text{min.m}^2}$  over two minutes. The transition occurs slightly faster in the high infusion rate. The amount of molecules, concentrations and transition times were observed to have less than 1.00% deviation from each diffusion rate observed. The results are shown in Table 4.10.

Table 4.10: DHFU transition times for the one-molecule two-compartment models with variable exponents.

Inf.	$j, k$	$X_{d,1}^{1T(j,k)}$	$C_{d,1}^{1T(j,k)}$	$X_{d,2}^{T(j,k)}$	$X_{d,1}^{2T(j,k)}$	$C_{d,1}^{2T(j,k)}$	$t^{1T(j,k)}$	$t^{2T(j,k)}$
1921	1,2	N/A	N/A	567.2	N/A	N/A	N/A	N/A
2844		N/A	N/A		N/A	N/A	N/A	N/A
1422		N/A	N/A		N/A	N/A	N/A	N/A
1921	2,0	58.51	11.47	125.03	93.09	18.27	5.41	68.5
2844		57.91	11.36		93.23	18.28	5.32	78.8
1422		58.12	11.40		93.20	18.28	5.36	79.4

The S.I units of  $X_{d,1}^{g(j,k)}$  is  $\frac{\mu\text{mol}}{\text{m}^2}$  and  $C_{d,1}^{g(j,k)}$  is  $\frac{\mu\text{mol}}{\text{L}}$ , and  $t_{1/2}$  is *min.* where  $d$  represents DHFU and  $g$  represents subscript T that symbolise transition between low and high concentration behaviours. Inf. represents infusion which measures in  $\frac{\mu\text{mol}}{\text{min.m}^2}$ .

The other factors that influence the transition of a molecule’s kinetics between the two concentration behaviours are the inflow and outflow of molecules between compartments, and the elimination rate of molecules from the body. For the one-molecule two-compartment model, the inflow from compartment two to compartment one produces no impact on the transition of molecules because  $\Gamma_{DHFU,2,1}^{(p)}$  is zero. The outflow of the molecule from compartment one to compartment two does not influence the transition of DHFU, because none of the infusion could reach the amount of molecule expected at the transition point. The transition of molecules produced as a result of the influence of the elimination of molecules from compartment two has a significant impact on the transition process.

#### 4.4 Two-Molecule (1+2) Two-Compartment DHFU Model

The two-molecule two-compartment model was examined, which allowed the interaction between 5-FU and DPYD to be varied to obtain the suitable position for the enzymatic reaction and, in turn, produce a better fit of the theoretical curve to the experimental data. This can help identify the ideal proportion of 5-FU, which goes to direct elimination and conversion to DHFU. The results are shown in Table 4.11.

Table 4.11: 5-FU and DHFU PK parameters for the two-molecule two-compartment model with variable exponents.

<i>old</i> → <i>new</i>	$A_{d1,j,k}^{(p)}$	$B_{d1,j,k}^{(p)}$	$k_{d1,1,0}^{(p)}$	$\Gamma_{d1,1,0}^{(p)}$	$V_d$
F,1→F,2	2.4640(33)	2.6330(21)	0.1526(27)	0.0028(42)	9.999(55)
F,2→F,0	0.8780(32)	1.1929(23)	0.0242(30)	0.0233(22)	
F,2→F,1	1.0359(38)	0.9976(31)	0.0079(28)	0.0020(25)	
F,2IE,1→C,2	0.9967(27)	0.9994*	0.1898(25)	0.00000(56)	
C,2→D,2IE,2	0.9812(54)	1.0140(45)	0.0165(42)	0.00007(43)	
D,1→D,2	1.1084(32)	0.9921*	0.2729(24)	0.00000(46)	3.222(25)
D,2→D,0	1.0223(23)	1.1200(65)	0.5426(38)	0.0075(12)	
D,2→D,1	1.0432(27)	0.9681(55)	0.2955(21)	0.0042(18)	

The S.I units of  $k_{d1,j,k}^{(p)}$  is  $\frac{\mu\text{mol}^{(1-A)}}{m^{(2-2A)}\text{min}}$  and  $\Gamma_{d1,j,k}^{(p)}$  is  $\frac{m^{(2B)}}{\mu\text{mol}^B}$ , where *d1* represents 5-FU, DHFU, DPYD, or CMPX. *F,k* represents 5FU in compartment *k*. *C,k* represents complex-substrate in compartment *k*. *D,k* represents DHFU in compartment *k*. *E,k* represents DPYD in compartment *k*.

All the PK parameters were varied for 5-FU. The result shows a slight improvement in  $S_p$  compared to the one-molecule two-compartment model. The  $S_p$  obtained in case 2 of the one-molecule one-compartment model is 0.0021, and it is reduced to 0.0020 in case 2 of the two-molecule one-compartment model. Case 2 of the two-molecule two-compartment model has the same variance as in case 2 of the two-molecule one-compartment model (0.0020). In examining the model, it indicates that the influence of varying PK parameters of 5-FU adds to the fitness of DHFU to the clinical data. The exponent A of 5-FU

flowing from compartment 1 to compartment 2 is approximately a second-order process ( $A = 2.4639$ ) at low concentrations. The semi-log graphs are shown in Figure 4.6.

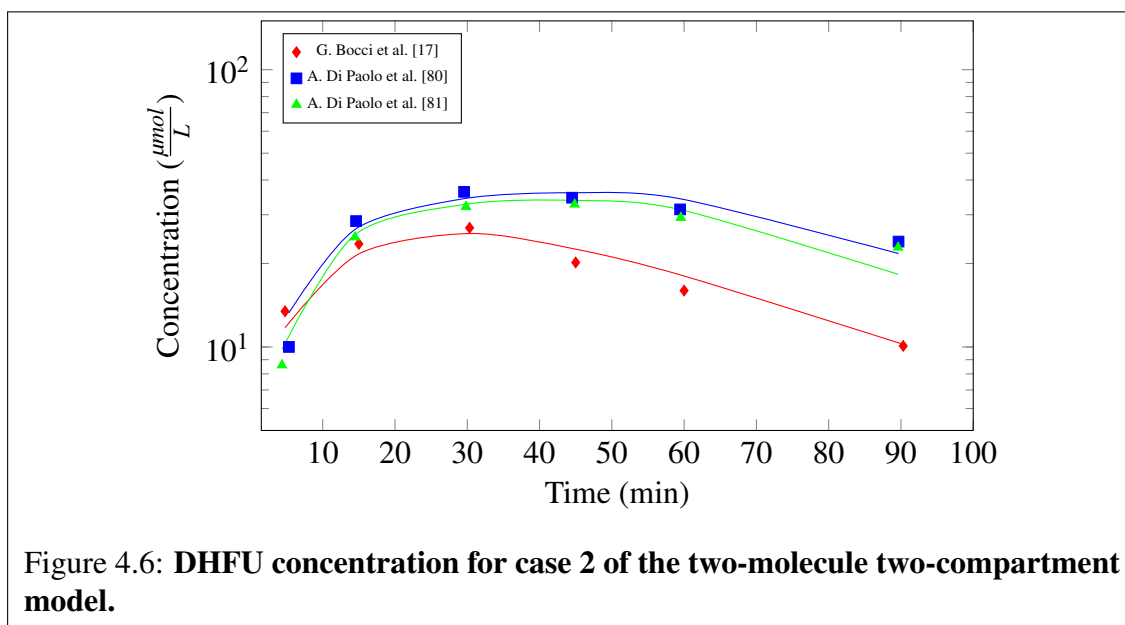


Table 4.12: DHFU transition times for the two-molecule two-compartment models with variable exponents.

Inf.	$j, k$	$X_{d,1}^{1T(j,k)}$	$C_{d,1}^{1T(j,k)}$	$X_{d,2}^{T(j,k)}$	$X_{d,1}^{2T(j,k)}$	$C_{d,1}^{2T(j,k)}$	$t^{1T(j,k)}$	$t^{2T(j,k)}$
1921	2,0	41.42	12.86	78.93	54.87	17.03	6.40	65.30
2844		33.22	10.31		55.78	17.31	4.15	99.8
1422		34.46	10.70		55.64	17.27	4.72	93.2
1921	2,1	N/A	N/A	238.1	N/A	N/A	N/A	N/A
2844		104.9	32.56		109.6	34.02	23.4	62.9
1422		106.2	32.98		108.8	33.77	28.9	50.45

The S.I units of  $X_{d,1}^{T(j,k)}$  is  $\frac{\mu\text{mol}}{\text{m}^2}$  and  $C_{d,1}^{T(j,k)}$  is  $\frac{\mu\text{mol}}{\text{L}}$ , and  $t_{1/2}$  is *min.* where  $d$  represents DHFU and subscript T symbolises transition between low and high concentration behaviours. Inf. represents infusion which measures in  $\frac{\mu\text{mol}}{\text{min.m}^2}$ .

The transition concentrations of the molecules' kinetics between a low concentration behaviour and a high concentration behaviour and the transition times are measured for both the absorption phase and the elimination phase of the molecules' kinetics. The two

sides of the transition were obtained (switching from low concentration behaviour to high concentration behaviour and vice-versa). Table 4.12 shows the amount of molecules and concentrations at the transition between the two types of behaviour.

The model is saturable for DHFU, and the elimination exponents are negative at high concentrations, with  $(A-B)$  equal to  $-0.0958$ . The number of molecules obtained at the maximum elimination rate of DHFU is unreachable with the three infusion sets used for the analysis, which indicates that before the threshold can be reached there needs to be an infusion rate larger than  $2844 \frac{\mu\text{mol}}{\text{min.m}^2}$  or for a longer time period. The results are shown in Table 4.13.

Table 4.13: DHFU maximum elimination times for the two-molecule two-compartment models.

Inf.	$X_{d,1}^{1M(2,0)}$	$C_{d,1}^{1M(2,0)}$	$X_{d,2}^{M(2,0)}$	$X_{d,1}^{2M(2,0)}$	$C_{d,1}^{2M(2,0)}$	$t^{1M(2,0)}$	$t^{2M(2,0)}$
1921	N/A	N/A	642.2	N/A	N/A	N/A	N/A
2844	N/A	N/A		N/A	N/A	N/A	N/A
1422	N/A	N/A		N/A	N/A	N/A	N/A

The S.I units of  $X_{d,1}^{g(j,k)}$  is  $\frac{\mu\text{mol}}{\text{m}^2}$  and  $C_{d,1}^{g(j,k)}$  is  $\frac{\mu\text{mol}}{\text{L}}$ , and  $t_{1/2}$  is *min.* where  $d$  represents DHFU and  $g$  represents subscript M that symbolise maximum elimination rate.

## 4.5 Summary

The models that were designed for DHFU in this chapter were in two categories: the one-molecule models and the two-molecule models. In one-molecule models, case 2 of the one-compartment model has the best fit with a variance  $S_p = 0.0021$ , while in two-molecule models, case 2 of the two-compartment model has the best fit with variance  $S_p = 0.0020$ . The  $S_p$  of the one-molecule two-compartment model plateaued at a higher value compared to the one-compartment model. In all, the one-molecule one-compartment model gives a better fit than the one-molecule two-compartment model. This suggests that the unification of the rate constant makes the flow rate faster and the higher the number of compartments

involved; the slower the rate of reaction becomes. The limitations observed in the modelling of DHFU have to do with the one-molecule model that involved the PK parameters of 5-FU held constant. The best fit for DHFU to the clinical data is case 2 of the two-molecule two-compartment model. The two-molecule model was solved by varying the PK parameters of 5-FU and DHFU simultaneously. Moreover, we also identify the variable-exponent models as giving better  $S_p$  values than the fixed-exponent models.

The maximum elimination flow rate and transition times were used to observed the amount of molecules and their concentrations at these times. We identify the influence of the infusion rates on the transition times and the elimination flow rate for all our models. The higher the infusion rates, the faster the first transition point from a low concentration behaviour to a high concentration behaviour; whereas, at the second transition point the higher infusion rate produces a slower transition from a high concentration behaviour to a low concentration behaviour.

# Chapter 5

## Results and Applications

---

*You beat cancer by how you live,  
why you live and in the manner in which you live.*

– Stuart Scott

---

The agreement between the numerical solutions and experimental data encourages us to calculate several observable quantities:  $AUC$ ,  $C_{max}$ , and  $t_{1/2}$  for both 5-FU and DHFU, and these were compared with the experimental estimates. The best fit for the 5-FU model was found in the variable-exponent three-compartment model, and for DHFU, the best fit was obtained from the two-molecule two-compartment model. The gender and age influence on 5-FU and DHFU were examined using the study of G. Bocci et al. [17], the study examined 185 patients treated with an infusion of  $1921 \frac{\mu\text{mol}}{\text{min.m}^2}$  of 5-FU over one minute. The data set has six data points. Furthermore, we compared the result of our best fit models for 5-FU and DHFU with the study from J. G. Maring et al. [2] with a bolus infusion of  $1633 \frac{\mu\text{mol}}{\text{min.m}^2}$  over two minutes [2] for the treatment of liver-metastasis and non-liver metastasis patients. The weighted averages of the the observable quantities were obtained to determine the varying degree of each quantity.

### 5.1 AUC, $C_{max}$ , and Half-life for 5-FU

The *AUC* was calculated using case 2 and case 3 of the (1+2) two-compartment model, and case 2 of the three-compartment model for the eight clinical datasets shown in Table 5.1. There are correlations between the theoretical numbers and the clinical data we examined, considering the factors that could influence each component of the experimental data. It is shown that the theoretical numbers obtained are in reasonable agreement with the clinical estimates.

Table 5.1: Comparison of the *AUC* of the 5-FU theoretical models to the clinical estimates.

datasets	Clinical AUC	C2.1Cp	C2.2Cp	C3.2Cp	C2.3Cp
G. Bocci et al. [1]	6278	4231	4444	4430	4444
F. Casale et al. [83]	5346	3268	3441	3428	3448
G. Bocci et al. [17]	1730	1416	1490	1475	1474
G. D. Heggie et al. [84]	7127	6958	7305	7284	7345
L. Per-Anders et al. [72]	6158	6489	6835	6820	6877
A. Di Paolo et al. [80]	3649	3068	3276	3277	3276
A. Di Paolo et al. [80]	6269	4275	4501	4503	4500
A. Di Paolo et al. [81]	3690	3183	3769	3771	3770
Weighted Average		2721	2949	2942	2945

*AUC* measures in  $\frac{\text{min} \cdot \mu\text{mol}}{\text{L}}$ . The  $S_p$  for case 2 of one-compartment model, case 2 and case 3 of the (1+2) two-compartment model and case 2 of the three-compartment model are 0.0690, 0.0127, 0.0125, and 0.0126 respectively. C2.1Cp represents case 2 of the one-compartment model. C2.2Cp represents case 2 of the two-compartment model. C3.2Cp represents case 3 of the two-compartment model. C2.3Cp represents case 2 of the three-compartment model.

The *AUC* tells the extent to which a body is exposed to the molecule. The best agreement between the theoretical *AUC* and the experimental estimates is for case 2 of the (1+2) two-compartment model and A. Di Paolo et al. [81] with a 2.17% deviation; whereas G. Bocci et al. [17] and A. Di Paolo et al. [80], have deviations of 13.8% and 10.2% respectively. There is a slight deviation in case 2 of the three-compartment model when compared

with case 2 of the (1+2) two-compartment model; we observed 1.0%, 0.0%, and 0.002% for G. Bocci et al. [17], A. Di Paolo et al. [80], and A. Di Paolo et al. [81] respectively. Case 2 of the one-compartment model has the largest deviation from the clinical estimates, they are 18.2%, 15.9%, and 13.7% deviations from G. Bocci et al. [17], A. Di Paolo et al. [80], and A. Di Paolo et al. [81] respectively.

The  $C_{max}$  is the maximum concentration attained by the molecules in the plasma. It is controlled by the rate at which the molecules are administered, absorbed, distributed, metabolized and eliminated. The  $C_{max}$  provides a measure of the toxicity of the active molecules. The  $C_{max}$  obtained by the theoretical models show some deviations from the clinical estimates. Table 5.2 shows the comparison between the models and the clinical estimates.

Table 5.2: Comparison of the  $C_{max}$  of the 5-FU theoretical models to the clinical estimates.

datasets	Clinical $C_{max}$	C2.1Cp	C2.2Cp	C3.2Cp	C2.3Cp
G. Bocci et al. [1]	372.2	186.4	275.5	275.5	275.4
F. Casale et al. [83]	426.2	198.7	283.9	283.9	283.8
G. Bocci et al. [17]	128.69	107.8	178.1	178.1	178
G. D. Heggie et al. [84]	419.8	243.1	360.3	360.4	361.2
L. Per-Anders et al. [72]	134	239.8	357.7	357.8	359.6
A. Di Paolo et al. [80]	242	160.5	265.6	265.7	266.7
A. Di Paolo et al. [80]	430.3	146.6	239.8	239.8	244.1
A. Di Paolo et al. [81]	222.3	160.2	261.8	261.8	263.1
Weighted Average		144.5	214.3	214.4	233.4

The  $C_{max}$  measures in  $\frac{\mu\text{mol}}{L}$ . The  $S_p$  for case 2 of one-compartment model, case 2 and case 3 of the (1+2) two-compartment model and case 2 of the three-compartment model are 0.0690, 0.0127, 0.0125, and 0.0126 respectively. C2.1Cp represents case 2 of the one-compartment model. C2.2Cp represents case 2 of the two-compartment model. C3.2Cp represents case 3 of the two-compartment model. C2.3Cp represents case 2 of the three-compartment model.

Cases 2 and 3 of the (1+2) two-compartment model and case 2 of the three-compartment

model have very close  $C_{max}$  that range between 0.0% and 1.8% deviations. Using case 2 of the (1+2) two-compartment model to compare with the clinical estimates, there is a 10.20% deviation from the value obtained in the study of A. Di Paolo et al. [80], 18.38% deviation when it is compared with A. Di Paolo et al. [81], and 28.32% when compared with G. Bocci et al. [17]. For case 2 of the three-compartment model, the estimated  $C_{max}$  for G. Bocci et al. [17] is below the weighted average by 23.3%, A. Di Paolo et al. [80] and A. Di Paolo et al. [81] have a  $C_{max}$  that are above the weighted average by 14.3% and 12.7% respectively. Case 2 of the one-compartment model was observed to have the largest deviations from the clinical estimates ranging from 16.2% to 65.9%.

The half-life  $t_{1/2}$  indicates how long it takes the molecules in the plasma to reduce to half the initial amount. Moreover, it can be influenced by the rate at which the molecule is administered, absorbed, and eliminated. The  $t_{1/2}$  obtained from the models are shown in Table 5.3.

Table 5.3: Comparison of the  $t_{1/2}$  of the theoretical models to the clinical estimates.

datasets	Clinical $t_{1/2}$	C2.1Cp	C2.2Cp	C3.2Cp	C2.3Cp
G. Bocci et al. [1]	12.6	16.12	12.86	12.86	12.84
F. Casale et al. [83]	19.2	18.65	15.06	15.06	15.03
G. Bocci et al. [17]	10.2	14.95	9.63	9.64	9.6
G. D. Heggie et al. [84]	12.6	18.67	16.91	16.9	17.96
L. Per-Anders et al. [72]	13.2	19.41	17.39	17.35	18.32
A. Di Paolo et al. [80]	21.6	21.1	17.43	17.42	17.01
A. Di Paolo et al. [80]	16.2	19.55	16.84	16.82	16.88
A. Di Paolo et al. [81]	23.4	22.2	18.36	18.39	18.25

The  $t_{1/2}$  measures in *minute*. The  $S_p$  for case 2 of one-compartment model, case 2 and case 3 of the (1+2) two-compartment model and case 2 of the three-compartment model are 0.0690, 0.0127, 0.0125, and 0.0126 respectively. C2.1Cp represents case 2 of the one-compartment model. C2.2Cp represents case 2 of the two-compartment model. C3.2Cp represents case 3 of the two-compartment model. C2.3Cp represents case 2 of the three-compartment model.

With respect to the clinical values, the  $t_{1/2}$  obtained in case 2 of the (1+2) two-compartment model has a deviation of 21.5% from A. Di Paolo et al. [81] compared with 22.01% deviation of the three-compartment model. For G. Bocci et al. [17], case 2 of the (1+2) two-compartment model and case 2 of the three-compartment model deviated from clinical  $t_{1/2}$  estimates by 5.88%. For A. Di Paolo et al. [80] we observed a 19.3% deviation in case 2 of the (1+2) two-compartment model and a 21.25% deviation compared to case 2 of the three-compartment model.

## 5.2 AUC, $C_{max}$ , and Half-life for DHFU

The  $AUC$ ,  $C_{max}$ , and half-life were calculated using several of our models. The details and the comparison of the numbers between the clinical values and the theoretical models are presented in Table 5.4.

Table 5.4: Comparison of the  $AUC$  of the DHFU theoretical models to the clinical estimates.

datasets	Clinical AUC	C2.1M.1C	C2.2M.1C	C2.1M.2C	C2.2M.2C
G. Bocci et al. [1] <sup>a</sup>	2448	1724	1637	1888	1728
G. Bocci et al. [1] <sup>b</sup>	3974	2581	2467	2177	2615
F. Casale et al. [83]	2698	2868	2768	2289	2660
G. Bocci et al. [17]	1653	1890	1805	2046	1765
A. Di Paolo et al. [80]	5864	2726	2617	2317	2746
A. Di Paolo et al. [82]	4774	2814	2707	2427	2615
A. Di Paolo et al. [81]	5964	2875	2766	2420	2636
Weighted Average		2355	2257	2199	2242

<sup>a</sup> and <sup>b</sup> represent the study from G. Bocci et al. [1] with low dosage and high dosage infusion of  $1921 \frac{\mu\text{mol}}{\text{min.m}^2}$  and 2844 over one minute respectively.  $AUC$  measures in  $\frac{\text{min.}\mu\text{mol}}{L}$ . The  $S_p$  for case 2 of the one-molecule one-compartment and two-compartment models are 0.0021 and 0.0055 respectively. For case 2 of the two-molecule one-compartment and two-compartment models are 0.0021 and 0.0020 respectively. C2 represents case 2. 1M and 2M represent one- and two-molecule respectively. 1C and 2C represent one- and two-compartment respectively.

There are correlations between the theoretical numbers and the experimental estimates. The results from A. Di Paolo et al. [80] and A. Di Paolo et al. [81] are seen to have the largest deviation of the *AUC* when it is compared to the theoretical solutions. They both have 53.2% and 55.8% deviations compared with case 2 of the two-molecules two-compartment model respectively. The A. Di Paolo et al. [80] study expressed that the *AUC* of DHFU was observed to be almost identical to 5-FU. In our theoretical solutions there are some identifiable differences. For example, the comparison between the *AUC* for 5-FU and DHFU for case 2 of the two-compartment model has a difference of  $530 \frac{\text{min.}\mu\text{mol}}{L}$  (see Table 5.4 and 5.1). G. Bocci et al. [17] and F. Casale et al. [83] have the closest values of *AUC* to the theoretical solutions, 6.8% and 1.4% when compared with the results from case 2 of the two-molecule two-compartment model. Comparing case 2 of the two-molecule one-compartment model to case 2 of the two-molecule two-compartment model, there are differences of  $40 \frac{\text{min.}\mu\text{mol}}{L}$ ,  $129 \frac{\text{min.}\mu\text{mol}}{L}$ , and  $130 \frac{\text{min.}\mu\text{mol}}{L}$  for G. Bocci et al. [17], A. Di Paolo et al. [80], and A. Di Paolo et al. [81] infusions respectively.

The closest  $C_{max}$  estimated in the clinical trials to the theoretical solutions was found between case 2 of the two-molecule two-compartment model and A. Di Paolo et al.'s [81] study with a difference of 1.5%. The largest deviation in  $C_{max}$  was found between the value estimated in F. Casale et al.'s [83] study and case 2 of the two-molecule two-compartment model with a 23.2% difference. The  $C_{max}$  estimated for G. Bocci et al. [17] using case 2 of the two-molecule two-compartment model is lower by 12.2%. The  $C_{max}$  comparison between the clinical and theoretical values also indicates that there are considerable correlations (see Table 5.5). The comparison between the one-compartment models and two-compartment models are observed to have slight differences. Case 2 of the two-molecule two-compartment model are identified as the best fit to the clinical estimates. The slight differences between the DHFU models ranges between 0.2% and 15.5%. The average value for  $C_{max}$  putting the weight of each dataset into account are between  $30.16 \frac{\mu\text{mol}}{L}$  and  $31.00 \frac{\mu\text{mol}}{L}$ , which is closest to the highest weighted estimate obtained from G. Bocci et al. [17]

(28.09  $\frac{\mu\text{mol}}{\text{L}}$ ).

Table 5.5: Comparison of the  $C_{max}$  of the theoretical models to the clinical estimates for DHFU.

datasets	Clinical $C_{max}$	C2.1M.1C	C2.2M.1C	C2.1M.2C	C2.2M.2C
G. Bocci et al. [1] <sup>a</sup>	27.25	24.81	24.73	29.14	24.67
G. Bocci et al. [1] <sup>b</sup>	39.82	35.40	34.76	32.45	36.02
F. Casale et al. [83]	47.16	38.91	38.01	33.41	36.23
G. Bocci et al. [17]	28.09	24.81	24.73	29.14	24.67
A. Di Paolo et al. [80]	N/A	35.40	34.76	32.46	36.02
A. Di Paolo et al. [82]	N/A	36.20	35.49	33.42	34.34
A. Di Paolo et al. [81]	33.39	35.95	35.25	32.54	33.90
Weighted Average		30.68	30.28	31.00	30.16

<sup>a</sup> and <sup>b</sup> represent the study from G. Bocci et al. [1] with low dosage and high dosage infusion of 1921  $\frac{\mu\text{mol}}{\text{min.m}^2}$  and 2844 over one minute respectively.  $C_{max}$  measures in  $\frac{\mu\text{mol}}{\text{L}}$ . The  $S_p$  for case 2 of the one-molecule one-compartment and two-compartment models are 0.0021 and 0.0055 respectively. For case 2 of the two-molecule one-compartment and two-compartment models are 0.0021 and 0.0020 respectively. C2 represents case 2. 1M and 2M represent one- and two-molecule respectively. 1C and 2C represent one- and two-compartment respectively.

The corresponding distribution  $t_{1/2}$  obtained in the theoretical models indicate comparability to the clinical estimates (see Table 5.6). The closest  $t_{1/2}$  to the low dosage study of G. Bocci et al. [1]<sup>a</sup> is case 2 of one-molecule two-compartment model by 8.3%, followed by case 2 of the one-molecule one-compartment model, by 20.6%. The high dosage study of G. Bocci et al. [1]<sup>b</sup> has the closest deviation from case 2 of the one-molecule two-compartment model by 3.3%, followed by a deviation from case 2 of the one-molecule one-compartment model of 8.7%. The half-life  $t_{1/2}$  indicates the amount of time needed for the molecules in the plasma to be reduced to half  $C_{max}$ . This can be influenced by the rate at which the molecule is administered, absorbed, and eliminated. The infusion of different dosages administered over the same period of time in our models resulted in different  $t_{1/2}$  (compare G. Bocci et al. [1]<sup>a</sup> and G. Bocci et al. [1]<sup>b</sup> in Table 5.6), The  $t_{1/2}$  obtained from

the low dosage study is lower by 19.5% compared to the high dosage study.

Table 5.6: Comparison of the  $t_{1/2}$  of the theoretical models to the clinical estimates for DHFU.

datasets	Clinical $t_{1/2}$	C2.1M.1C	C2.2M.1C	C2.1M.2C	C2.2M.2C
G. Bocci et al. [1] <sup>a</sup>	7.80	6.19	5.99	7.15	6.13
G. Bocci et al. [1] <sup>b</sup>	8.40	7.67	7.63	8.12	7.61
F. Casale et al. [83]	40.80	8.52	8.55	8.45	7.93
G. Bocci et al. [17]	45.00	5.21	5.01	6.15	5.13
A. Di Paolo et al. [80]	N/A	7.66	7.64	8.12	7.62
A. Di Paolo et al. [82]	N/A	9.41	9.30	8.38	8.71
A. Di Paolo et al. [81]	64.20	8.13	8.07	8.18	7.61

<sup>a</sup> and <sup>b</sup> represent the study from G. Bocci et al. [1] with low dosage and high dosage infusion of  $1921 \frac{\mu\text{mol}}{\text{min.m}^2}$  and 2844 over one minute respectively.  $t_{1/2}$  measures in *min*. The  $S_p$  for case 2 of the one-molecule one-compartment and two-compartment models are 0.0021 and 0.0055 respectively. For case 2 of the two-molecule one-compartment and two-compartment models are 0.0021 and 0.0020 respectively. C2 represents case 2. 1M and 2M represent one- and two-molecule respectively. 1C and 2C represent one- and two-compartment respectively.

### 5.3 The Theoretical Solutions Compared to the Clinical Data for 5-FU

#### 5.3.1 Comparison to the 5-FU Results From G. Bocci et al. [81]

The results obtained in cases 2 and 3 of the two-compartment model, and case 2 of the three-compartment model were used for comparison between our models and the experimental datasets from G. Bocci et al. [1]. The study has 20 patients who are treated with 5-FU at a low dose level of  $250 \frac{\text{mg}}{\text{m}^2}$ . This study was not part of the data used to determine the parameters in our models. The comparison of the three models to the clinical dataset indicates a considerable agreement between the theoretical solutions and the experimental trials. G. Bocci et al. [1] used a bolus infusion of  $1921 \frac{\mu\text{mol}}{\text{min.m}^2}$  for one minute. Table 5.7 provides a comparison of the quantities obtained from the theoretical solutions and the clinical estimates. Figure 5.1 shows the concentration curves for the three models. We obtained  $S_p$

to be 0.0127 and 0.0126 for two-compartment and three-compartment models respectively. Case 2 of the three-compartment model gives the best prediction out of the three models used to predict the time course of 5-FU in the body. The *AUC* obtained with this solution is about 4.16% deviation from the value of the *AUC* calculated by G. Bocci et al. [1]. For case 2 of the (1+2) two-compartment and case 3 of the (1+2) two-compartment models, the *AUC* obtained have a deviation of 5.74% and 5.00% from the G. Bocci et al.'s calculation [1].

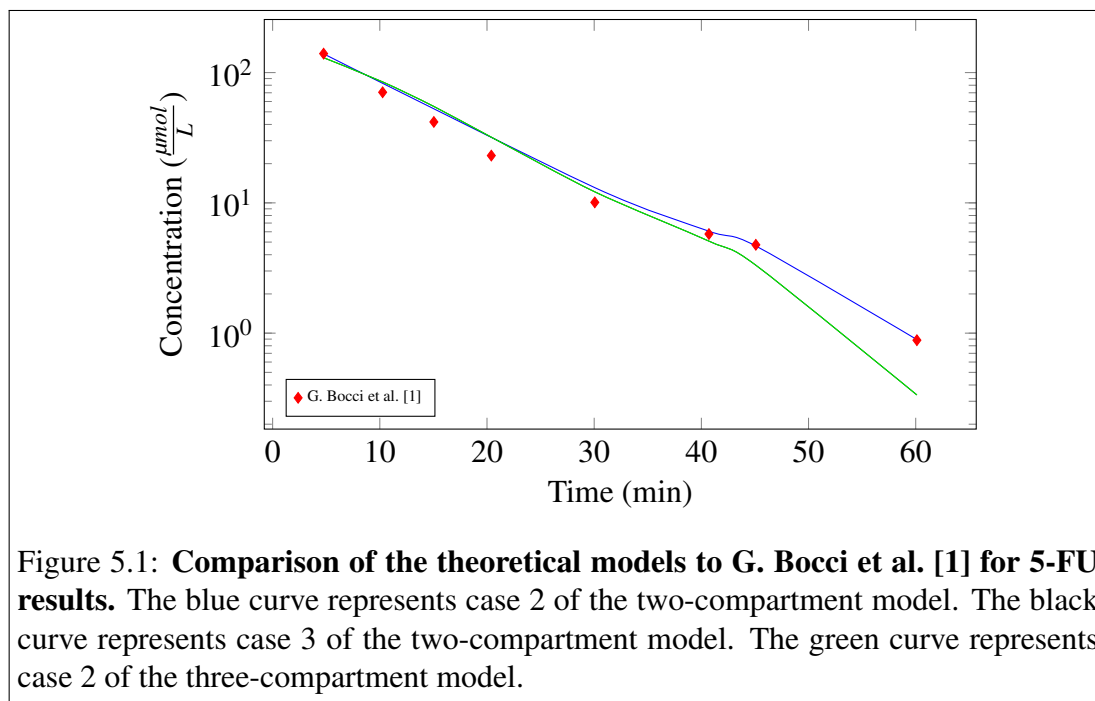
Table 5.7: Comparison of the theoretical models to G. Bocci et al. [81]

Quantities	G. Bocci et al.'s results	C2.2C	C3.2C	C2.3C
$AUC \left( \frac{\text{min.}\mu\text{mol}}{L} \right)$	2486	2628	2610	2589
$C_{max} \left( \frac{\mu\text{mol}}{L} \right)$	139.5	182.0	183.5	180.2
$t_{1/2} \text{ (min.)}$	10.2	9.63	9.78	10.0

The  $S_p$  for case 2 and case 3 of the (1+2) two-compartment model and case 2 of the three-compartment model are 0.0127, 0.0125, and 0.0126 respectively. C2.2C represents case 2 of the two-compartment model. C3.2C represents case 3 of the two-compartment model. C2.3C represents case 2 of the three-compartment model.

The  $C_{max}$  is  $139.5 \frac{\mu\text{mol}}{L}$  according to G. Bocci et al. [1]. They obtained the  $C_{max}$  at 5 minutes while the infusion lasted for one minute. We obtained the  $C_{max}$  from the theoretical solution at 1 *minute*. When we used case 2 of the (1+2) two-compartment model we got 30.5% increase compared to the clinical estimate.  $C_{max}$  was 31.5% and 29.2% higher using case 3 of the (1+2) two-compartment and case 2 of the three-compartment models. There is a small difference between the results for the three models. The concentration we obtained at 5 minutes for case 2 of the two-compartment model, case 3 of the two-compartment model, and case 2 of the three-compartment model are  $139.4 \frac{\mu\text{mol}}{L}$ ,  $130.1 \frac{\mu\text{mol}}{L}$ , and  $130.1 \frac{\mu\text{mol}}{L}$  compared to  $139.8 \frac{\mu\text{mol}}{L}$  estimated by G. Bocci et al. [1].

The  $t_{1/2}$  obtained in the theoretical solution of case 2 of the (1+2) two-compartment model is 9.63 *min.* compared to G. Bocci et al.'s [1]  $t_{1/2} = 10.20 \text{ min.}$  The  $t_{1/2}$  for case 3 of the (1+2) two-compartment model is  $t_{1/2} = 9.78 \text{ min.}$  and for case 2 of the three-



compartment model it is  $t_{1/2} = 10.04 \text{ min}$ . The deviations observed in the three models, cases 2 and 3 of the (1+2) two-compartment model and case 2 of the three-compartment model compared to G. Bocci et al. [1] are 5.59%, 4.12%, and 1.57%. The best agreement to the clinical estimate was found to be case 2 of the three-compartment model. The  $S_p$  obtained for cases 2 and 3 of the (1+2) two-compartment models are 0.0134 and 0.0057, while case 2 of the three-compartment model is 0.0057.

### 5.3.2 Comparison to the 5-FU Results From J. G. Maring et al. [84]

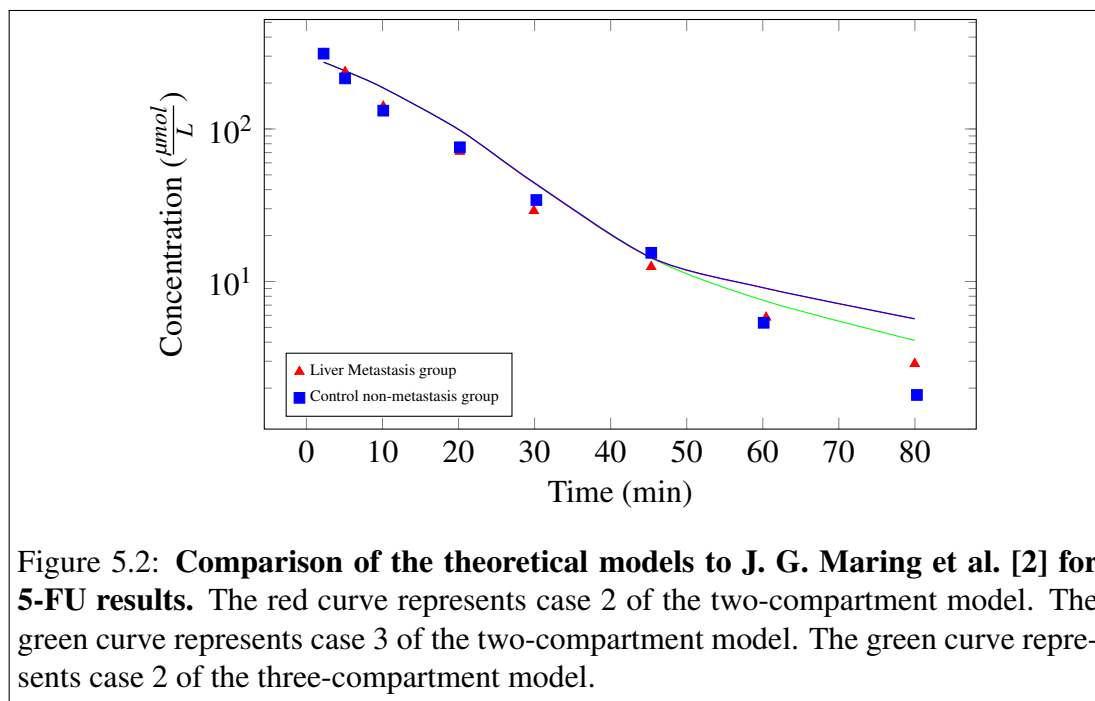
We examined the study by J. G. Maring et al. [2] using the three models as in the case of G. Bocci et al. [1]: cases 2 and 3 of the (1+2) two-compartment model and case 2 of the three-compartment model. This study involved 18 patients with liver metastases, who received a bolus infusion of  $1633 \frac{\mu\text{mol}}{\text{min}\cdot\text{m}^2}$  over two minutes [2]. The  $AUC$  in the study is  $4659 \frac{\text{min}\cdot\mu\text{mol}}{\text{L}}$  [2]. The study recorded the apparent effect of the liver metastases on the PK of 5-FU. Table 5.8 shows the comparison of the quantities obtained from the theoretical models and J. G. Maring et al.'s [2] study. The three theoretical models correlate with the study (see Figure 5.2). The  $S_p$  obtained using case 2 of the three-compartment model for liver

metastasis group is 0.1271, while for non-liver metastasis group it is 0.1173. This indicates little difference between the two groups, there is about 8.35% increase in  $S_p$  obtained in the liver metastasis group compared liver metastasis group. The  $S_p$  obtained in case 2 and 3 of the (1+2) two-compartment models are; for the metastasis group the variances are 0.3515 and 0.1273 respectively; and for the non-metastasis group the variances are 0.2141 and 0.1176 respectively. The  $AUC$  we obtained using the case 2 (1+2) two-compartment model has a deviation of 16.98% from the value J. G. Maring et al. [2] obtained. The case 3 of the (1+2) two-compartment model and the case 2 of the three-compartment model have values of 16.81% and 11.83% deviations respectively. 5-FU is an active drug that needs no hepatic metabolism to remain active. The study indicates that the dysfunction or reduction in DPYD capacity does not affect the flow rate of 5-FU clearance [2]. The elimination rate of 5-FU majorly depends on the hepatic blood flow, which compensates for the defect activities of DPYD [2] in the formation of DHFU. Figure 5.2 shows that the theoretical solution of our model is able to predict the time course of 5-FU in the body with any dosage. The purpose of obtaining the  $AUC$ ,  $C_{max}$  and  $t_{1/2}$  is to verify how our model can predict the PK quantities of the drug in the body.

Table 5.8: Comparison of the  $AUC$  of the 5-FU theoretical models to J. G. Maring et al. [84].

Quantities	Clinical estimates	C2.2C	C3.2C	C2.3C
$AUC$ ( $\frac{min.\mu mol}{L}$ )	4659	5450	5442	5210
$C_{max}$ ( $\frac{\mu mol}{L}$ )	N/A	302.9	301.8	306.7
$t_{1/2}$ (min.)	N/A	13.7	13.9	12.9

The  $S_p$  for case 2 and case 3 of the (1+2) two-compartment model and case 2 of the three-compartment model are 0.0127, 0.0125, and 0.0126 respectively. C2.2C represents case 2 of the two-compartment model. C3.2C represents case 3 of the two-compartment model. C2.3C represents case 2 of the three-compartment model.



#### 5.4 Comparison to the DHFU Results from J. G. Maring et al. [84]

The results obtained for our models were used for comparison between our models and the two experimental datasets from J. G. Maring et al. [2]. The study has a liver metastatic cancer group of 16 patients and a controlled non-liver metastatic cancer group of 18 patients. Both datasets are not part of the data used for the minimisation of the variance. Both groups have the same bolus infusion of  $1633 \frac{\mu\text{mol}}{\text{min.m}^2}$  over two minutes [2]. Table 5.9 shows the comparison of the quantities obtained from the theoretical models and J. G. Maring et al.'s [2] study for DHFU. Figure 5.3 shows the two separate groups.

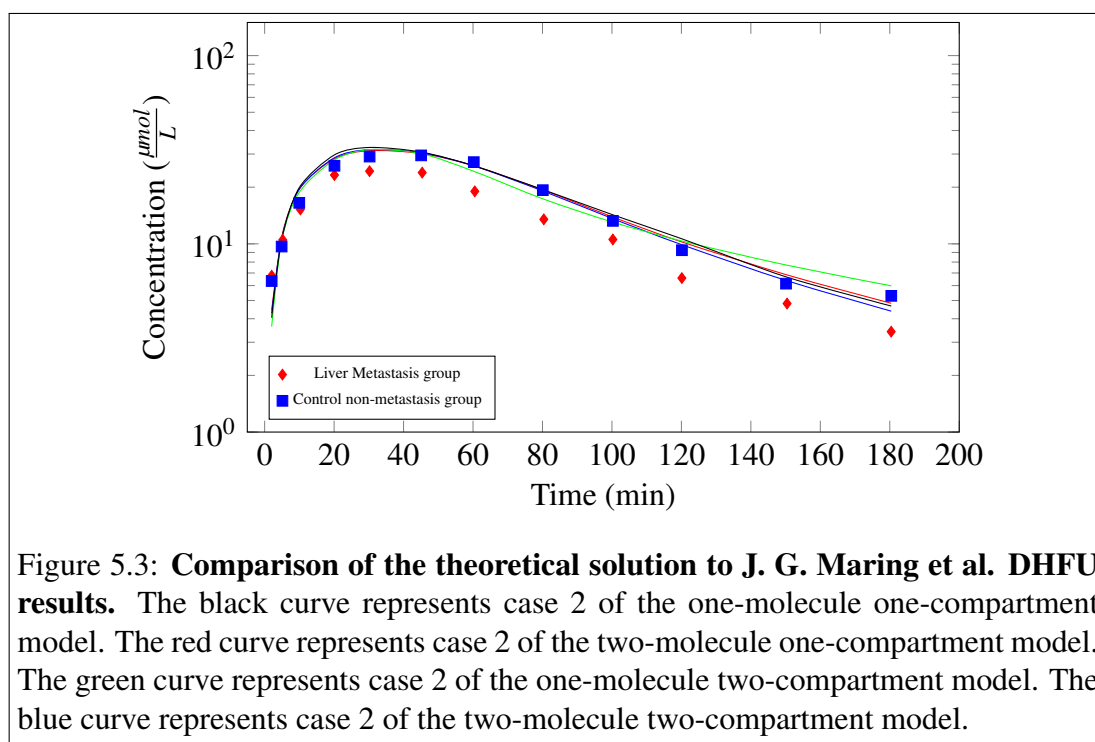
The comparisons were done to investigate the influence of liver metastases on the PK of 5-FU and its metabolite DHFU, and also to investigate the predictive power of our models. J. G. Maring et al. [2] suggested that there was no effect of liver metastases on the clearance of 5-FU, but they observed the effect of the metastasis on the formation of DHFU. In the comparison of DHFU in the study to the theoretical models, it is seen that there is a better fit to the non-liver metastatic cancer control group than the metastasis group.

Table 5.9: The quantities of the theoretical models compared to the clinical estimates for DHFU.

Quantities	Clinical estimates	C2.1M.1C	C2.2M.1C	C2.1M.2C	C2.2M.2C
$AUC (\frac{min \cdot \mu mol}{L})$	2543	3105	3233	2952	3033
$C_{max} (\frac{\mu mol}{L})$	N/A	31.85	33.42	33.76	31.75
$t_{1/2} (min.)$	N/A	7.64	7.34	8.03	7.62

The  $S_p$  for case 2 of the one-molecule one-compartment model is 0.0021, case 2 of the one-molecule two-compartment model is 0.0055, and case 2 of the two-molecule one-compartment model is 0.0021, and case 2 of the two-molecule two-compartment model is 0.0020 respectively. C2 represents case 2. dM represents d-molecule. dC represents d-compartment.

This supports the suggestion about the influence of liver metastasis on DHFU formation. The reduction in the activeness of the liver has an effect on DPYD since DPYD is the main hepatic enzyme that catalyses the formation of DHFU, and indirectly slows down the catalytic reaction of the formation of DHFU.



The  $AUC$  values were compared to the value from J. G. Maring et al. [2], the case 2 two-molecule two-compartment model is 29.09% deviated from the clinical result. The clinical

*AUC* comprises the entire combination of the two groups treated in the study; on the other hand, our theoretical model is a better fit to the control non-metastasis cancer group than the liver metastasis group (see Figure 5.3). The  $S_p$  obtained for the two groups are 0.0641 and 0.1807 respectively. Figure 5.3 shows our theoretical solution has a better fit to the non-metastasis group of patients and supports the idea that states "there is a reduction in liver DPYD capacity due to liver metastases" by J. G. Maring et al. [2]. The metabolism of 5-FU to DHFU completely depends on the activeness of DPYD as an enzyme that catalyses the reaction. When DPYD is dysfunctional or has reduced capacity due to the liver metastasis, there is a dramatic influence on the formation of DHFU. We can conclude there is a considerable influence of liver metastasis on the PK of DHFU. The  $C_{max}$  was also examined to support this conclusion. The theoretical  $C_{max}$  from the case 2 two-molecule two-compartment model is comparable to the non-metastasis group; whereas, the metastasis group is significantly lower by 23.5%, indicating the poorer performance of DPYD due to the liver metastasis.

## 5.5 The Influence of Gender and Age

We investigated the effect of gender and age on the PK of 5-FU and DHFU. The behaviour of the proteins responsible for the variation in each category were examined. We calculated our results and compared them with the estimation made in the clinical study. It allowed us to identify the responsible PK parameters for each specific deviation obtained in the different categories.

The influence of gender on the PK of 5-FU and DHFU was examined. The only clinical dataset used for the comparison is from G. Bocci et al. [17], where a total of 185 patients (by gender: 99 men and 86 women, and by age: 116 young adult and 69 old age) were administered bolus infusions of  $1921.94 \frac{\mu\text{mol}}{\text{m}^2\text{min}}$  [17] over one minute.

### 5.5.1 The PK Parameters Responsible for Gender Influence on 5-FU

We performed three separate calculations for the PK parameters with women, men, and combined patients using case 2 of the (1+2) two-compartment model. The PK parameters results shown in Table 3.13 were used as the initial numbers to minimize the PK parameters responsible for gender influence on 5-FU. The results are tabulated in Table 5.10 and the corresponding graph is in Figure 5.4.

Table 5.10: PK values for gender influence on 5-FU

Case	$j, k$	$A_{5FU,j,k}^{(AB)}$	$B_{5FU,j,k}^{(AB)}$	$k_{5FU,j,k}^{(AB)}$	$\Gamma_{5FU,j,k}^{(AB)}$	$V_d(\frac{L}{m^2})$	$S_p$
2	1,2	1.0975	0.9817	0.1165	0.00186	10.000	0.0127
	2,0	0.8807	1.19412	1.6377	0.00624		
	2,1	1.0394	0.994	0.01233	0.000593		
<b>Gender</b>							
men	1,2	1.0975(33)	0.98173(38)	0.1165(22)	0.00186(33)	10.29(27)	0.0062
	2,0	0.6489(28)	0.88425(53)	1.4435(20)	0.00508(21)		
	2,1	1.0394(38)	0.99435(46)	0.0123(28)	0.00059(23)		
women	1,2	1.0975(28)	0.98173(31)	0.1165(29)	0.00186(30)	11.36(23)	0.0031
	2,0	0.6523(33)	1.0038(45)	0.6833(28)	0.000004(24)		
	2,1	1.0394(39)	0.99436(42)	0.0123(38)	0.00059(33)		
combined	1,2	1.0975(30)	0.98173(31)	0.1165(31)	0.00186(31)	10.63(33)	0.0045
	2,0	0.5680(35)	0.85604(49)	1.3531(26)	0.00122(19)		
	2,1	1.0394(35)	0.99436(41)	0.0123(35)	0.00059(34)		

The values without errors are fixed values. The unit of  $k_{5FU,j,k}^{(AB)}$  and  $\Gamma_{5FU,j,k}^{(AB)}$  are  $\frac{\mu\text{mol}^{(1-A)}}{m^{(2-2B)}\text{min}}$  and  $\frac{m^2B}{\mu\text{mol}^{(B)}}$  respectively. The weighted average for exponent A is 0.9679

The main gender influence on 5-FU is observed in the elimination of 5-FU. This indicates total clearance routes of 5-FU, that involve the conversion of 5-FU into DHFU and direct elimination of 5-FU from the body. Comparing men and women, Table 5.10 shows that the elimination rate constant in men is 52% higher than that of women. The higher  $V_d$

observed in women (10.40% higher) compensates for the lower observable  $C_{max}$  obtained in women compared to men. The tissue binding rate seemed to be higher in women, which indirectly influenced the conversion rate of 5-FU to form DHFU. At low concentration, the exponent A of the elimination process in both men and women is a little higher than the mid point between the zeroth and the first order process; whereas, the exponents (A-B) at high concentrations for both genders are negatives, -0.2354 and -0.3515 respectively. The  $AUC$  in men is slightly greater than that in women by 3.27%. See Table 5.11.

We obtained a small difference between the PK of 5-FU administered to the two groups. The  $C_{max}$  attained in men is slightly higher by 7.87% than that in women. The half-life of 5-FU in men is also slightly higher than the half-life of the molecule in women: 9.67 *min.* compared to 9.20 *min.* At high concentrations the exponents obtained at the elimination are negative for both groups: (A-B) is -0.2354 for men and -0.3515 for women. The values for the observable quantities and the graph are shown in Tables 5.11 and Figure 5.4.

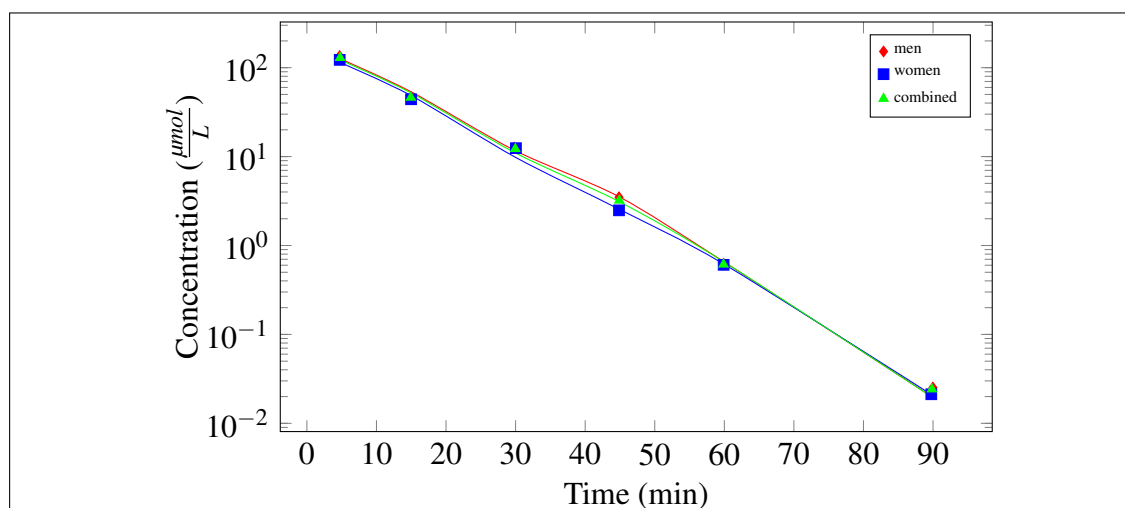


Figure 5.4: **Concentration versus time curve for 5-FU comparing the effects of gender.** The clinical data set is from G. Bocci et al. [17]. The thin red curve represents the theoretical solution for men. The thin blue curve represents the theoretical solution for women. The thin green curve represents the theoretical solution for the combined patients.

Comparing the case 2 of the (1+2) two-compartment model obtained in chapter three, there is correlation in the PK parameters to those we obtained in the model that examined

the gender influence on 5FU. The main PK parameters responsible for the gender influence on 5-FU are the PK parameters responsible for clearance of 5-FU. The combined group of gender study indicates lower elimination rate constant compare with case 2 of the two-compartment model in chapter three by 17.38%. This could be as a result of several datasets from different sources were involved in chapter three, and G. Bocci et al. [17] study was only used for gender influence on 5-FU. The factors such as: races, genes, and type of cancers can also play an important role in the differences. The exponent at low concentration also dropped by 35.51%; whereas, at higher concentration the exponents (A–B) in the combined case increases from -0.3134 to -0.2880, which indicates an increase in the elimination rate.

### 5.5.2 AUC, $C_{max}$ , and Half-life for Gender Differences

Tables 5.11 shows the comparison between the observable quantities of the theoretical solution for our model to the clinical dataset from G. Bocci et al. [17]. They are split into gender and age groups, and there are correlations between the results. Both theoretical and the experimental studies suggested that the *AUC* in men is higher when compared to women by 3.27% and 1.64% respectively. The  $C_{max}$  is estimated higher in men than in women, both the theoretical solution and the experimental study show an agreement with 7.90% and 10.34% respectively. The average value obtained from all the groups by involving the weight of each dataset; the *AUC* of 5-FU is  $1780 \frac{\text{min.}\mu\text{mol}}{\text{L}}$  and *AUC* of *DHFU* is  $1717 \frac{\text{min.}\mu\text{mol}}{\text{L}}$ .

### 5.5.3 The PK Parameters Responsible for Gender Influence on DHFU

The number of PK parameters varied for the gender influence on DHFU is six.  $k_{5FU,2,0}^{(AB)}$ ,  $k_{5FU,2,1}^{(AB)}$ ,  $k_{DPYD,2,2}^{(AB)}$ ,  $k_{complex,2,2}^{(AB)}$ ,  $k_{DHFU,2,0}^{(AB)}$ , and  $k_{DHFU,2,1}^{(AB)}$ . We used the best fit that was obtained in case 2 of the two-molecule two-compartment model.

Table 5.11: Comparison of the theoretical results and clinical results for gender difference using the PK parameters shown in Table 5.10.

<i>Parameter</i>	Clinical			Theoretical		
	<i>All patients</i>	<i>Men</i>	<i>Women</i>	<i>All patients</i>	<i>Men</i>	<i>Women</i>
5-FU						
<i>AUC (min.μmolL<sup>-1</sup>)</i>	1720	1734	1706	1795	1865	1683
<i>C<sub>max</sub> (μmolL<sup>-1</sup>)</i>	129.0	134.9	122.2	173.7	179.2	163.6
<i>t<sub>1/2</sub> (min)</i>	9.60	9.35	9.60	9.24	9.24	9.21
DHFU						
<i>AUC (min.μmolL<sup>-1</sup>)</i>	1679	1623	1748	1697	1685	1754
<i>C<sub>max</sub> (μmolL<sup>-1</sup>)</i>	28.52	27.6	29.52	27.17	26.53	28.11
<i>t<sub>1/2</sub> (min)</i>	45	45	45.6	76.21	77.26	78.15

The combined patients comprise 185 men and women. Men group comprises of 99 patients. Women group constitutes 86 patients.

The results obtained are shown in Table 5.12, and the corresponding graphical analysis is shown in Figure 5.5. Using case 2 of the two-molecule two-compartment model, the exponent ( $A-B$ ) at high concentration is a negative value and remains fixed for both genders. The models for all the categories were designed as saturable models. The exponent ( $A-B$ ) is  $-0.3149$  for 5-FU and  $-0.0959$  for DHFU.

There are considerable differences in the PK parameters of both 5-FU and DHFU in both the men and women categories. The *AUC* for DHFU in men is lower than that in women by 3.93%. This is comparable with the clinical study, which has *AUC* for men lower by 7.15% when compared with the women group. Likewise, the *C<sub>max</sub>* for DHFU is higher in women than in men by 5.96% in the theoretical results, while the experimental study recorded a 6.97% higher *C<sub>max</sub>* in women. See Table 5.11. The elimination rate of DHFU in relation to the conversion rate of 5-FU to DHFU was seen to be faster in men than women as shown in Table 5.12.

Table 5.12: PK values for gender influence on DHFU

case	parameter	old $\rightarrow$ new							
		F,1 $\rightarrow$ F,2	F,2 $\rightarrow$ F,0	F,2 $\rightarrow$ F,1	F,2 E,2 $\rightarrow$ C,2	C,2 $\rightarrow$ D,2 E,2	D,1 $\rightarrow$ D,2	D,2 $\rightarrow$ D,0	D,2 $\rightarrow$ D,1
C2.2M.2C	$A_{d,j,k}^{(p)}$	2.4639	0.8780	1.0359	0.9967	0.9814	1.1123	1.0235	1.0432
	$B_{d,j,k}^{(p)}$	2.6330	1.1929	0.9976	0.6407	1.0140	0.9921	1.1194	0.9681
	$k_{d,j,k}^{(p)}$	0.1526	0.0242	0.0079	0.5426	0.2955	0.2729	0.1898	0.0165
	$\Gamma_{d,j,k}^{(p)}$	0.0028	0.0233	0.0020	0.0000	0.00007	0.0000	0.0075	0.0043
men	$k_{d,j,k}^{(p)}$	N/A	0.0681(33)	0.0385(21)	0.6285(37)	0.7773(23)	N/A	0.3433(31)	0.0180(29)
women	$k_{d,j,k}^{(p)}$	N/A	0.0585(24)	0.0305(41)	0.5561(31)	0.8088(23)	N/A	0.2614(30)	0.0169(22)
combined	$k_{d,j,k}^{(p)}$	N/A	0.0632(31)	0.0258(40)	0.5344(34)	0.6896(27)	N/A	0.3014(32)	0.0176(26)

The values without errors are fixed values.  $k_{d,1,0}^{(AB)}$  unit is  $\frac{\mu\text{mol}^{(1-A)}}{m^{(2-2A)}\text{min}}$ ;  $\Gamma_{d,1,0}^{(AB)}$  is  $\frac{m^2B}{\mu\text{mol}^B}$ . The  $V_d$  that was used is  $3.2216 \frac{L}{m^2}$ . The  $S_p$  obtained for men, women, and combined groups are 0.0007, 0.0020, and 0.0010 respectively. F,k represents 5FU in compartment k. C,k represents complex-substrate in compartment k. D,k represents DHFU in compartment k. E,k represents DPYD in compartment k. Combined group comprises 185 men and women. Men group comprises of 99 patients. Women group constitutes 86 patients.

The half-life from the theoretical solution is about 71.3% higher than the experimental estimate. The women's group has a higher  $t_{1/2}$  compared to the men's group by 0.89 *min.* It is correlated with the experimental data that has a 0.6 *min.* difference.

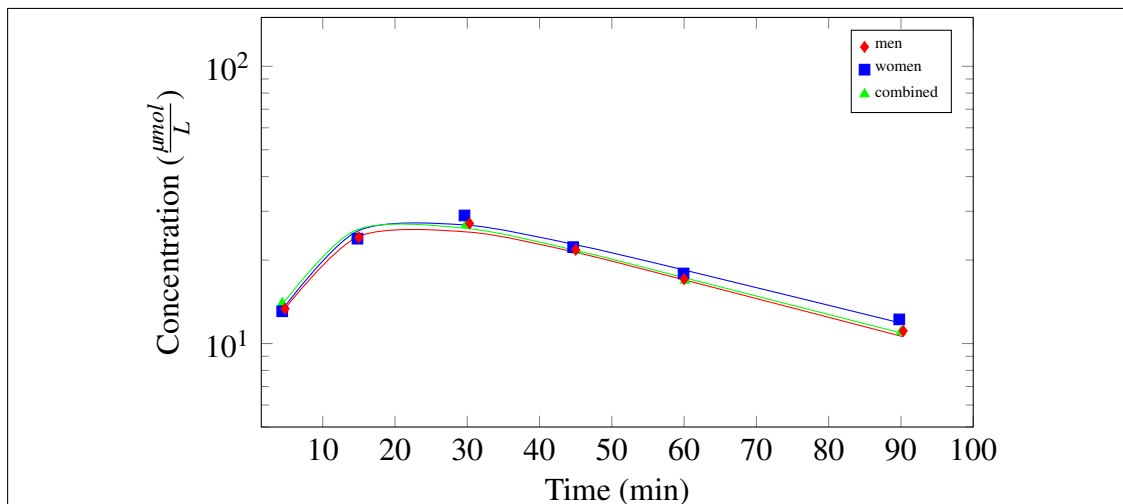


Figure 5.5: **Concentration versus time curve for DHFU comparing the effect of gender.** The clinical data set is from G. Bocci et al. [17]. The thin red curve represents the theoretical solution for men. The thin blue curve represents the theoretical solution for women. The thin green curve represents the theoretical solution for the combined patients.

There is a slower rate of elimination of DHFU in the women's group. The elimination rate constant of DHFU in the men's group is higher by 31.3% compared to the women's group. Likewise, the liver seems to retain more DHFU in women than in men. Considering the rate of inflow of DHFU from compartment 1 to 2 remains the same, the rate of outflow of DHFU from compartment 2 to 1 is still slower in women by 6.11% than in men, of which this could enhance the toxic effect of the molecule in the body. We also examined the ratio of the rate constant of DHFU formation from the complex-substrate to its elimination for the two groups. In men we obtained 2:1 while in women it is 3:1. There is a tendency for women to retain more DHFU in the body than men and are prone to a higher  $C_{max}$  when compared with men under the same dosage.

It can be suggested that the three enzymes along the path of DHFU elimination: dihydrofluorouracil, alpha-fluoro-beta-ureidopropionate, and alpha-fluoro-beta-alanine appear

to be more active and/or more numerous in men than in women. The activities of these three enzymes determine the fate of DHFU in the body. As a result of this, women are more responsive to the toxic effect of DHFU than men using the same 5-FU dosage.

### 5.5.4 The PK Parameters Responsible for Age Influence on 5-FU

The clinical dataset available for age comparison is from G. Bocci et al. [17] with an infusion of  $1921.94 \frac{\mu\text{mol}}{\text{m}^2\text{min}}$  over one minute. The study has 185 patients and six data points available for the minimisation of the PK parameters. The results are shown in Table 5.13.

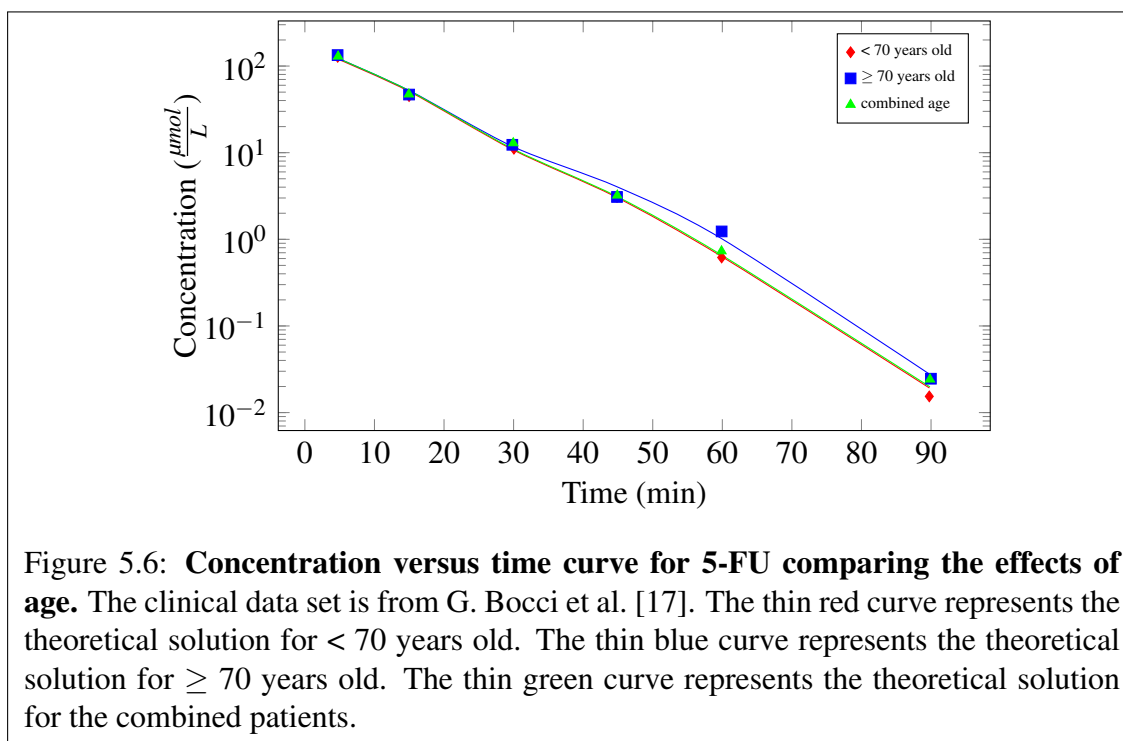
Table 5.13: PK values for age influence on 5-FU

case	$j, k$	$A_{5FU, j, k}^{(AB)}$	$B_{5FU, j, k}^{(AB)}$	$k_{5FU, j, k}^{(AB)}$	$\Gamma_{5FU, j, k}^{(AB)}$	$V_d(\frac{L}{m^2})$	$S_p$
2	1,2	1.0975	0.9817	0.1165	0.00186	10.000	0.0127
	2,0	0.8807	1.19412	1.6377	0.00624		
	2,1	1.0394	0.994	0.01233	0.000593		
Age							
< 70 yrs	1,2	1.0975(33)	0.98173(38)	0.1165(22)	0.00186(33)	10.85(27)	0.0031
	2,0	0.5229(28)	0.89528(53)	1.6169(20)	0.00050(21)		
	2,1	1.0394(38)	0.99436(46)	0.0123(28)	0.00059(23)		
$\geq$ 70 yrs	1,2	1.0975(35)	0.98173(42)	0.1165(32)	0.00186(43)	10.59(21)	0.0073
	2,0	0.6494(25)	0.89521(46)	1.3798(25)	0.00050(27)		
	2,1	1.0394(32)	0.99436(41)	0.0123(21)	0.00059(33)		
combined	1,2	1.0975(30)	0.98173(31)	0.1165(31)	0.00186(31)	10.63(33)	0.0045
	2,0	0.5680(35)	0.85604(49)	1.3531(26)	0.00122(19)		
	2,1	1.0394(35)	0.99436(41)	0.0123(35)	0.00059(34)		

The values without errors are fixed values. The units of  $k_{5FU, j, k}^{(AB)}$  and  $\Gamma_{5FU, j, k}^{(AB)}$  are  $\frac{\mu\text{mol}^{(1-A)}}{m^{(2-2B)}\text{min}}$  and  $\frac{m^{2B}}{\mu\text{mol}^{(B)}}$  respectively.  $S$  represents  $S_p$  and  $S_\sigma(\frac{\mu\text{mol}^2}{L^2})$ . The weighted average for exponent A is 0.5701. Combined group comprises 185 young adult and old age patients. Old age group comprises 69 patients older than or equal to 70 years old. Young adult age group comprises 116 patients with lesser age than 70 years old.

The category of age was grouped into two: the young adult age range from 37–69,

tagged as an age group that is less than 70 years old, and the ages of those greater than or equal to 70 years range from 70 to 80. The two groups are constituted of both men and women. Accordingly, there are 116 young adult patients and 69 old age patients. These two categories were modelled and examined alongside their combination. Figure 5.6 shows the graphical illustration.



The  $V_d$  is higher in the young adult group than in the old age group. This indicates that the organs are more active in younger people. There is a higher degree of reception of the drug at the site of action (tissues). The general idea of a smaller volume of distribution in  $\geq 70$  years patients is that the drug molecules stay more in the blood plasma and do not effectively flow to the organs. The rate of elimination in the older group shows a slightly lower value when compared to the young adult age group by 14.7%. At a low concentration, the exponent A is approximately a first order process for both age groups and correlated with the result we had from the entire population in chapter three. At high concentrations, the exponent (A-B) of the elimination rate for both groups are negative:  $-0.3724$  for < 70 years old group and  $-0.6494$  for  $\geq 70$  years old group. This shows that the model is

saturable and correlated with what we observed in chapter three.

We compared the effects of the two age groups on 5-FU, see Table 5.14. The *AUC* has a little gap between the two groups, and we confirmed a higher *AUC* of 5-FU in the old age group compared to the young age group by 5.06%.

Table 5.14: Comparison of the theoretical results and clinical estimates for age difference.

<i>Parameter</i>	Clinical estimates			Theoretical estimates		
	<i>All patients</i>	$\geq 70$ y	$< 70$ y	<i>All patients</i>	$\geq 70$ y	$< 70$ y
5-FU						
<i>AUC</i> ( $\text{min.}\mu\text{molL}^{-1}$ )	1720.52	1845.06	1683.62	1795	1826	1738
<i>C<sub>max</sub></i> ( $\mu\text{molL}^{-1}$ )	129.00	133.84	127.62	173.7	174.4	169.2
<i>t<sub>1/2</sub></i> ( <i>min</i> )	9.60	10.20	9.60	9.24	9.25	9.24
DHFU						
<i>AUC</i> ( $\text{min.}\mu\text{molL}^{-1}$ )	1679	1909.64	1540.62	1697	2028	1601
<i>C<sub>max</sub></i> ( $\mu\text{molL}^{-1}$ )	28.52	31.98	26.6	27.17	30.88	25.14
<i>t<sub>1/2</sub></i> ( <i>min</i> )	45	48	43.2	76.21	81.01	76.01

The combined patients: comprises 185 young adult and old age patients. Old age group comprises 69 patients older than than or equal to 70 years old. Young adult age group comprises 116 patients with lesser age than 70 years old. The weighted average for *AUC* of 5-FU is 1770; The weighted average for *AUC* of DHFU is 1760.

There is a tendency for a faster elimination rate in the young age group compared to the old age group. We also observed a slightly higher *C<sub>max</sub>* for 5-FU in the old age group by approximately 2.65%. We compared the *AUC* and *C<sub>max</sub>* from the theoretical solution to the value obtained by G. Bocci et al. [17]. For the old age group, there was 1.03% difference in *AUC* and 30.30% in *C<sub>max</sub>*; meanwhile, for the young age group, we have 3.27% difference in *AUC* and 32.58% difference in *C<sub>max</sub>* compared to the clinical estimates.

### 5.5.5 The PK Parameters Responsible for Age Influence on DHFU

The number of data points available for the age influence on DHFU is six. We use the best fit model for DHFU: case 3 of the two-molecule two-compartment model. The varied PK parameters are:  $k_{5FU,2,0}^{(AB)}$ ,  $k_{5FU,2,1}^{(AB)}$ ,  $k_{DPYD,2,2}^{(AB)}$ ,  $k_{complex,2,2}^{(AB)}$ ,  $k_{DHFU,2,0}^{(AB)}$ ,  $k_{DHFU,2,1}^{(AB)}$ . The three categories were examined: < 70 years old,  $\geq$  70 years old, and combined age. The results obtained are shown in Table 5.15, and the corresponding graphical analysis is shown in Figure 5.7.

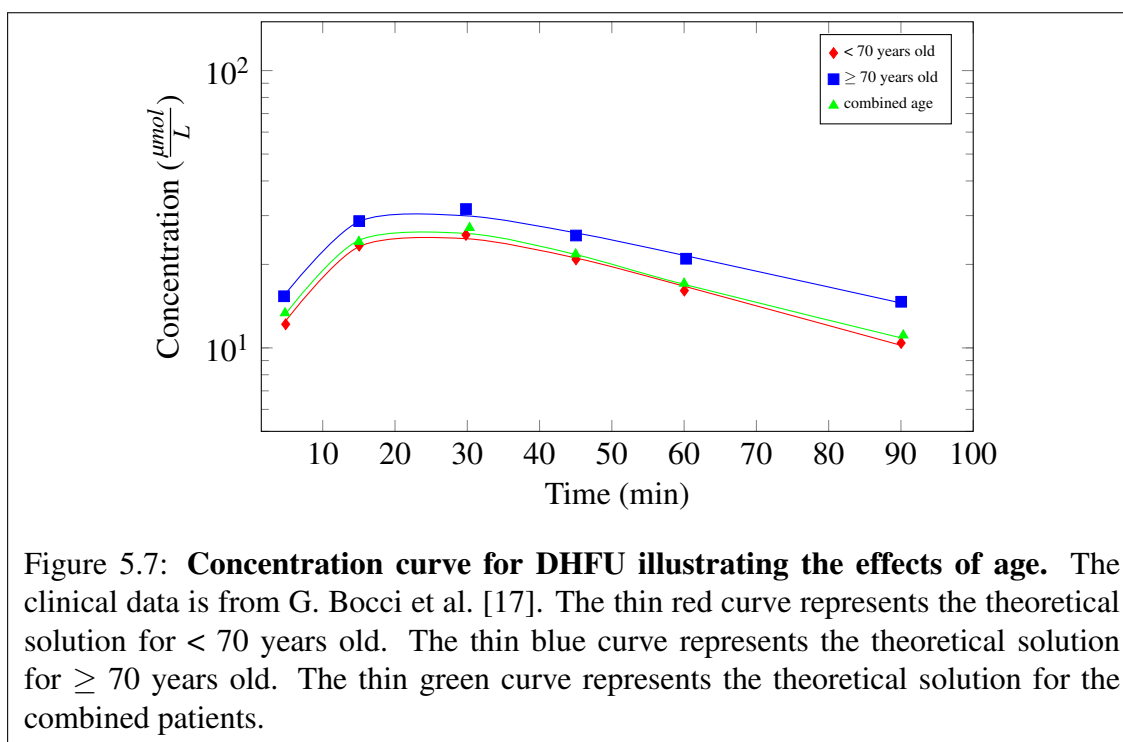
The exponent (A–B) is fixed for all three groups and is negative, which indicates that the models for the three categories (< 70 years old,  $\geq$  70 years old, and combined patients) are saturable at high concentrations. The exponent (A–B) is  $-0.3149$  for 5-FU and  $-0.0959$  for DHFU. There are significant differences in the PK parameters of both 5-FU and DHFU between the younger age group and the older age group. The elimination rate constant of 5-FU in the older age group is reduced by 59.0% when compared with the younger age group, which enhanced the  $C_{max}$  that was observed in older age group. And coupled with the slower 5-FU flow from the metabolism compartment to the central compartment. The theoretical solution indicated that the  $AUC$  and the  $C_{max}$  for 5-FU obtained in the older age group are higher by 5.06% and 3.07% respectively, when they are compared with the younger age group. There are correlations with the clinical data from the G. Bocci et al. study [17], where they obtained 9.63% and 4.87% higher in  $AUC$  and  $C_{max}$  in older age group. The  $AUC$  for DHFU kinetics in the younger age group is lower than the older age group by 21.06%. This is comparable with the study from G. Bocci et al. [17], which has the  $AUC$  for younger age group lower by 19.33% compared with older age group. Likewise, the  $C_{max}$  for DHFU is higher in the older age group compared to the younger age group by 22.83% in the theoretical solution, and 20.23% in the clinical estimate (see Table 5.14). The higher  $AUC$  can also be enhanced by the slower flow rate from compartment 2 to 1, about 2.83% slower in the older age group compared to the younger age group (see Table 5.15).

Table 5.15: PK values for age influence on DHFU

case	parameter	old $\rightarrow$ new							
		F,1 $\rightarrow$ F,2	F,2 $\rightarrow$ F,0	F,2 $\rightarrow$ F,1	F,2 E,2 $\rightarrow$ C,2	C,2 $\rightarrow$ D,2 E,2	D,1 $\rightarrow$ D,2	D,2 $\rightarrow$ D,0	D,2 $\rightarrow$ D,1
C2.2M.2C	$A_{d,j,k}^{(p)}$	2.4639	0.8780	1.0359	0.9967	0.9814	1.1123	1.0235	1.0432
	$B_{d,j,k}^{(p)}$	2.6330	1.1929	0.9976	0.6407	1.0140	0.9921	1.1194	0.9681
	$k_{d,j,k}^{(p)}$	0.1526	0.0242	0.0079	0.5426	0.2955	0.2729	0.1898	0.0165
	$\Gamma_{d,j,k}^{(p)}$	0.0028	0.0233	0.0020	0.0000	0.00007	0.0000	0.0075	0.0043
< 70 years	$k_{d,j,k}^{(p)}$	0.1526	0.0743(21)	0.0519(24)	0.4835(15)	0.5768(19)	0.2729	0.2955(22)	0.0177(16)
$\geq$ 70 years	$k_{d,j,k}^{(p)}$	0.1526	0.0305(27)	0.0132(30)	0.6151(32)	0.8978(25)	0.2729	0.3588(29)	0.0172(22)
combined	$k_{d,j,k}^{(p)}$	0.1526	0.0632(31)	0.0258(40)	0.5344(34)	0.6896(27)	0.2729	0.3014(32)	0.0176(26)

The values without errors are fixed values.  $k_{d,1,0}^{(AB)}$  unit is  $\frac{\mu\text{mol}^{(1-A)}}{m^{(2-2A)}\text{min}}$ ;  $\Gamma_{d,1,1}^{(AB)}$  is  $\frac{m^{2B}}{\mu\text{mol}^B}$ . The  $S_p$  for < 70 yrs,  $\geq$  70 yrs, and combined groups 0.00010, 0.0007, and 0.0010. F,k represents 5FU in compartment k. C,k represents complex-substrate in compartment k. D,k represents DHFU in compartment k. E,k represents DPYD in compartment k. Combined group comprises 185 young adult and old age patients. Old age group comprises 69 patients older than or equal to 70 years old. Young adult age group comprises 116 patients with lesser age than 70 years old.

In Table 5.15, we examined the ratio of DHFU formation to its elimination from the body. The elimination rate of DHFU compared to its formation from the complex-substrate was seen to be faster in the young age group (see Table 5.15). Approximately 2:1 in the younger age group and for the older group it is 3:1. As a result of this, the DHFU stays longer in the older age group with about 6.58% higher  $t_{1/2}$ . There is tendency for the older age group to retain more 5-FU and DHFU in the body compared with the younger group under the same treatment. More so, they are more prone to the toxic effect of both 5-FU and DHFU. For every single value increase in the conversion rate of the complex-substrate, the elimination rate of DHFU in the older group is increased by 13.52%, while in the young age group, we have a 27.34% increase. The DPYS and UPB1 are the major enzymes transforming DHFU, which might be weaker or insufficient in the old age group compared to the young age group.



## 5.6 Summary

We obtained the physical quantities  $AUC$ ,  $C_{max}$ , and half-life for all the models. Case 2 of the three-compartment model obtained the best fit to the clinical data for 5-FU, while case 2 of the two-molecule two-compartment model gave the best fit to the clinical data for DHFU. The best  $AUC$  for 5-FU compared with the clinical estimate has a deviation of 0.53% and for DHFU, we obtained a deviation of 6.29% to the clinical estimate. The best fitted theoretical  $C_{max}$  has a deviation of 10.20% for 5-FU and 7.12% for DHFU. The closest  $t_{1/2}$  of the theoretical solution to the clinical data has a 5.88% deviation.

We determined the amount of molecules  $X_{d1,c1}^{M(j,k)}$  and the concentration  $C_{d1,1}^{M(j,k)}$  at maximum elimination. This occurs at high concentration, when the exponent (A-B) is negative and the system becomes saturable. At concentrations above this threshold, the elimination rate of the molecule from the body is reduced. This gave us the idea about the threshold of the amount of molecules  $X_{d1,c1}^{M(j,k)}$  and the corresponding concentration  $C_{d1,1}^{M(j,k)}$  that determine the increased in  $AUC$  due to the slower elimination.

A comparison of the theoretical solution to the clinical data using the results of our model supports the studies conducted by J. G. Maring et al. [2], which examined the influence of liver metastasis on 5-FU and DHFU, where our numerical model supports that the formation of DHFU is influenced by the metastasis of liver (see Figure 5.3). The application of gender and age influence on 5-FU and DHFU were also examined, and we were able to analyse the influence of these variances on the PK parameters. We discovered that the elimination of DHFU compared to the formation of the molecule from 5-FU is slower in women compared to men, and this suggests the three enzymatic reactions along the pathway from DHFU to FBAL that leads to excretion are more active in men than in women. Likewise, the activeness of these enzymes are shown to be weaker in the older age group than in the younger age group.

# Chapter 6

## Conclusion

---

*Every successful cancer treatment includes  
the following three ingredients:  
thorough detoxification,  
a change of diet and mental or spiritual work.*

– Lothar Hirneise

---

The PK parameters were obtained progressively from the one-compartment model to the three-compartment model for 5-FU. The clinical data used involves eight datasets that contained four hundred and thirty-seven patients and thirty-two data points. The best fit obtained in modelling 5-FU is the variable-exponent three-compartment model with  $S_p = 0.0126$ . The model was developed for DHFU from the one-molecule one- and two-compartment models to the two-molecule one- and two-compartment models. The clinical data involves seven datasets representing four hundred and thirty-three patients with forty-two data points. The best fit obtained for the DHFU model is the variable-exponents two-molecule two-compartment model with  $S_p = 0.0020$ . The results obtained show some level of agreement between the models and the empirical clinical data for 5-FU and DHFU. The theoretical curve approximately overlaps the data points from each experimental dataset using the specific infusion that produced the ideal fit for the data.

The three datasets that dominate the population in the clinical datasets are: G. Bocci et al. [17], A. Di Paolo et al. [80], and A. Di Paolo et al. [81]. They were examined as the main driver of the variance minimization to fit the model into the clinical data. The

G. Bocci et al. [17] paper used a test dose level of  $250 \text{ mg}/\text{m}^2$  administered by IV bolus two weeks before starting the major 5-FU treatment of  $370 \text{ mg}/\text{m}^2$  plus  $100 \text{ mg}/\text{m}^2/\text{day}$  of L-folinic acid for five consecutive days every four weeks. The study of A. Di Paolo et al. [80] has a dosage of  $370 \text{ mg}/\text{m}^2$  of 5-FU that was administered in one minute for the treatment of colorectal cancer in 110 patients. The patients were grouped in two based on the level of toxicities according to WHO criteria. The none or mild toxicity (WHO grade  $\leq 1$ ) and moderate-to-severe toxicity (WHO grade  $\geq 2$ ). And lastly, the studies of A. Di Paolo et al. [81] that treated colorectal cancer with a dosage of  $370 \text{ mg}/\text{m}^2$  of 5-FU in two minutes.

The simplest model we studied was the one-compartment model with fixed exponents, as it comprises the smallest number of PK parameters (three for 5-FU and five for DHFU) that were to be varied. The higher the number of PK parameters involved, the more complex the model design and analysis becomes. Designing the two-compartment model with a saturation limiting function seems to be the most complex and time-consuming to minimise. The best 5-FU fit of our models was obtained for case 2 of the three-compartment model. It has a slight improvement when compared to case 2 of the (1+2) two-compartment model. On the other hand, we got the best fit for DHFU from case 2 of the two-molecule one-compartment and two-compartment models. For 5-FU the idea of multi-compartment PK model is more realistic than a single compartment model. Whereas, for DHFU model there is unnoticeable change between the one-compartment model and the two-compartment model.

We also examined different modelling designs and realized that there are some models that cannot be used to fit the clinical data. The models that have their elimination routes via the central compartment are observed to be far from giving a good fit to the clinical data. This design is incorporated into the one-compartment model and the (1+3) two-compartment model. There was no significant change in the results between these two models. We found the models that have their elimination route via compartment 2

(metabolism compartment) are a better design that gives a close fit to the clinical data. All the multi-compartment models we designed in this research were based on this type of model for minimisation.

We obtained the  $AUC$ ,  $C_{max}$ , and  $t_{1/2}$  for all our models and they are agreeable with the clinical results. Case 2 of the three-compartment model has the best fit for 5-FU, with  $AUC$  having a 14.8% deviation from G. Bocci et al.'s estimate [17], 10.2% deviated from A. Di Paolo et al. [80], and 2.17% deviated from A. Di Paolo et al. [80]. The  $C_{max}$  we obtained in our model for the three studies: G. Bocci et al. [17], A. Di Paolo et al. [80], and A. Di Paolo et al. [81] are 38.3% , 10.2%, and 15.1% deviation from the clinical estimates, respectively. We also obtained the half-life for the three experimental datasets with our theoretical solution for case 2 of the three compartment model. The deviation from the clinical estimates are: 5.9% for G. Bocci et al. [17], 21.3% for A. Di Paolo et al. [80], and 22.0% for A. Di Paolo et al. [81]. The theoretical curves and the parameters give the best fit over the entire population of 437 patients for 5-FU. The deviation in the values can be a result of the factors that could influence the experimental data, such as the method and environment, race, gender, age, stage and type of cancer, and the health history of patients involved. Our model found the best fit for the PK parameters that can be used to make precise predictions of the molecules' kinetics within the body. Case 3 of the two-compartment and Case 2 of the three compartment models are ranked equal for providing the best predictions. The three-compartment model is a better model for studying the activities of the molecules within the body in detail.

We investigated the influence of gender (men and women) and age ( $< 70$  and  $\geq 70$  years old) differences on 5-FU and DHFU. This helped to identify the responsible PK parameters for the variations. The gender differences had little influence on 5-FU. However, influence of the difference was clearly observed on DHFU. Women have slower elimination of DHFU from the body compared to men. Therefore, we can suggest that DPYD is more active in women and has a higher conversion rate compared to that of the other two enzymes (DPYS

and UPB1) along the pathway. Retaining DHFU more than the conversion rate capacity of DPYS and UPB1 can lead to inadequate elimination of DHFU, which can result in toxic effects. The age influence analysis on 5-FU and DHFU indicates that the old age group has a slower elimination of both molecules. The old age group tends to hold more molecules in the plasma with a slower elimination rate. It can be suggested that the old age group is more prone to toxic effects than young people due to weakened enzymatic reaction [17] and cell functions. Our suggestion can also be validate by the values we obtained for the half-life of the two categories, the theoretical solution indicates that the older group has a higher half-life compared to the young group for both 5-FU and DHFU. It is an indication that the two molecules are retained longer in the body of the older group.

The aim of the research determined the physical quantities  $AUC$ ,  $C_{max}$ , and  $t_{1/2}$  using the theoretical solution that gave the best fit to the clinical data (case 2 of the three-compartment model). We also determined the influence of gender and age on 5-FU and DHFU, of which we realized that women suffer from the toxic effects of DHFU more than men when administered the same dosage. Likewise, the theoretical model indicate that old age patients are more prone to the side-effects of both 5-FU and DHFU compared to younger patients. Overall, the model predictions correlate with the experimental data.

**Future work:** We designed the model for gender and age differences using a dataset of 185 patients from G. Bocci et al. [17]. This could be biased based on factors associated with the treatment such as the type of cancer, race, and gene formations, which may influence the experimental data. Further work is encouraged with multiple datasets that split gender and age differences for better prediction. Furthermore, there is a need for advancement in combining 5-FU with other drugs for the treatment of cancer, such as 5-FU in combination with leucovorin (LV); with cyclophosphomide and methotrexate (CMF); with cisplatin; with thymoquinone; docetaxel and so on. The usage of the monotherapy for the treatment of cancer is fading, and the combination of chemotherapeutic drugs take the credit for the most effective chemotherapy.

# Bibliography

- [1] Guido Bocci, Romano Danesi, Antonello Di Paolo, Federico Innocenti, Giacomo Allegrini, Alfredo Falcone, Alessandro Melosi, Mario Battistoni, Gemma Barsanti, Pier Franco Conte, and Mario Del Tecca. Comparative pharmacokinetic analysis of 5-fluorouracil and its major metabolite 5-fluoro-5,6-dihydrouracil after conventional and reduced test dose in cancer patients. *Clinical Pharmacology and Therapeutics*, 6(8):3032–3037, 2000.
- [2] Jan G. Maring, Henk Piersma, Albert V. Dalen, Harry J. M. Groen, Donald R. A. Uges, and Elisabeth G. E. DeVries. Extensive hepatic replacement due to liver metastases has no effect on 5-fluorouracil pharmacokinetics. *Cancer Chemother Pharmacol*, 51:167–173.
- [3] Vincent T. DeVita Jr. and Edward Chu. A history of cancer chemotherapy. *Cancer Research*, 68(21):8643–8653, 2008.
- [4] T. Velkov, P. Bergen, J. Lora-Tamayo, C. B. Landersdorfer, and J. Li. PK/PD models in antibacterial development. *Current Opinion in Microbiology*, 16(5):573–9, 2013.
- [5] Adjuvant chemotherapy. Retrieved from: <https://chemoth.com/adjuvant>. (Accessed on 12/31/2019).
- [6] Lei L. Chen, Xinjian Chen, Haesun Choi, Hongxun Sang, Leo C. Chen, Hongbo Zhang, Launce Gouw, Robert H. Andtbacka, Benjamin K. Chan, Christopher K. Rodesch, Arnie Jimenez, Pedro Cano, Kimberly A. Jones, Caroline O. Oyedeji, Tom Martins, Harry R. Hill, Jonathan Schumacher, Carlynn Willmore, Courtney L. Scaife, John H. Ward, Kathryn Morton, R. Lor Randall, Alexander J. Lazar, Shreyaskumar Patel, Jonathan C. Trent, Marsha L. Frazier, Patrick Lin, Peter Jensen, and Robert S. Benjamin. Exploiting antitumor immunity to overcome relapse and improve remission duration. *Cancer Immunology, Immunotherapy*, 61(7):1113–1124, 2012.
- [7] F. M. Schabel. Concepts for systemic treatment of micrometastases. *Cancer*, 35:15–24, 1975.
- [8] Robert Duschinsky, Edward Plevin, and Charles Heidelberger. The synthesis of 5-fluoropyrimidines. *Journal of the American Chemical Society*, 79(16):4559–4560, 1957.
- [9] D.B. Longley, D.P. Harkin, and P.G. Johnston. 5-fluorouracil: mechanisms of action and clinical strategies. *Nat Rev Cancer*, 3(5):330–338, 2003.

- [10] R.D. Petty and J. Cassidy. Novel fluoropyrimidines: improving the efficacy and tolerability of cytotoxic therapy. *Curr Cancer Drug Targets*, 4(2):191–204, 2004.
- [11] Robert B Diasio and Barry E. Harris. Clinical pharmacology of 5-fluorouracil. *Clinical Pharmacokinetics*, 16(4):215–237, 1989.
- [12] National Center for Biotechnology Information. Pubchem database. 5-fluorouracil. Retrieved from <https://pubchem.ncbi.nlm.nih.gov/compound/3385>. (Accessed on 08/24/2019).
- [13] C. Focaccetti, A. Bruno, E. Magnani, D Bartolini, E Principi, and K. Dallaglio. Effects of 5-fluorouracil on morphology, cell cycle, proliferation, apoptosis, autophagy and ros production in endothelial cells and cardiomyocytes. *PLoS ONE*, 10(2):1–25, 2015.
- [14] Sarah M. Gressett, Brad L. Stanford, and Fred Hardwicke. Management of hand-foot syndrome induced by capecitabine. *Journal of Oncology Pharmacy Practice*, 12(13):131–141, 2016.
- [15] Christine C. Meyer, Karim A. Calis, Laurie B. Burke, Cynthia A. Walawander, and Thaddeus H. Grasela. Symptomatic cardiotoxicity associated with 5-fluorouracil. *Pharmacotherapy: The Journal of Human Pharmacology and Drug Therapy*, 17(4):729–736, 2012.
- [16] Søren Astrup Jensen and Jens Benn Sørensen. Risk factors and prevention of cardiotoxicity induced by 5-fluorouracil or capecitabine. *Cancer Chemotherapy and Pharmacology*, 58(4):487–493, 2006.
- [17] Guido Bocci, Cecilia Barbara, Francesca Vannozzi, Antonello Di Paolo, Alessandro Melosi, Gemma Barsanti, Giacomo Allegrini, Alfredo Falcone, Mario Del Tecca, and Romano Danesi. A pharmacokinetic-based test to prevent severe 5-fluorouracil toxicity. *Clinical Pharmacology and Therapeutics*, 80:384–395, 2006.
- [18] Jesus Anampa, Della Makower, and Joseph A. Sparano. Progress in adjuvant chemotherapy for breast cancer: an overview. *BMC Medicine*, 13(1):195, 2015.
- [19] Gianni Bonadonna, Ercole Brusamolino, Pinuccia Valagussa, Anna Rossi, Luisa Brugnattelli, Cristina Brambilla, Mario De Lena, Gabriele Tancini, Emilio Bajetta, Renato Musumeci, and Umberto Veronesi. Combination chemotherapy as an adjuvant treatment in operable breast cancer. *New England Journal of Medicine*, 294(8):405–410, 1976. PMID: 1246307.
- [20] Kenneth J.E. Vos, Angela G. Martin, Maxine G. Trimboli, Lindsay Forestell, Khaled Barakat, and Jack A. Tuszynski. A multi-compartment pharmacokinetic model of the interaction between paclitaxel and doxorubicin. *EPJ Nonlinear Biomedical Physics*, 2:13, 2014.
- [21] Yolanda Smith. Pharmacokinetics. Retrieved from <https://www.news-medical.net/health/Pharmacokinetics.aspx>. (Accessed on 08/24/2019).

- [22] John G. Wagner. History of pharmacokinetics. *Pharmacology and Therapeutics*, 12(3):537 – 562, 1981.
- [23] Eino Nelson. Kinetics of drug absorption, distribution, metabolism, and excretion. *Journal of Pharmaceutical Sciences*, 50(3):181 – 192, 1961.
- [24] Kenneth A. Johnson and Roger S. Goody. The original michaelis constant: Translation of the 1913 michaelis-menten paper. *Biochemistry*, 50(39):8264–8269, 2011.
- [25] E Widmark and J. Tandberg. Uber die bedingungen f'tir die akkumulation indifferenter narkoliken theoretische bereckerunger. *Biochem*, 147:358–369, 1924. Cited in: John G. Wagner. History of pharmacokinetics. *Pharmacology and Therapeutics*, 12(3):537-562, 1981.
- [26] John G. Wagner. A modern view of pharmacokinetics. *Journal of Pharmacokinetics and Biopharmaceutics*, 1(5):363–401, 1973.
- [27] F. Lundquist and M. Wolthers. The kinetics of alcohol elimination in man. *Acta pharm. tox.*, 14:365–289, 1953. Cited in: John G. Wagner. History of pharmacokinetics. *Pharmacology and Therapeutics*, 12(3):537-562, 1981.
- [28] John G. Wagner. Linear pharmacokinetic models and vanishing exponential terms: Implications in pharmacokinetics. *Journal of Pharmacokinetics and Biopharmaceutics*, 4(5):395–425, 1976.
- [29] Steve Abel. Pharmacokinetics of alcohol - addictive behavior. Retrieved from <https://www.doctorabel.us/addictive-behavior/pharmacokinetics-of-alcohol.html>. (Accessed on 08/24/2019).
- [30] R. Dominguez. Studies of renal excretion of creatinine. ii. volume of distribution. *Proceedings of the Society for Experimental Biology and Medicine*, 31(9):1146–1149, 1934. Cited in: John G. Wagner. History of pharmacokinetics. *Pharmacology and Therapeutics*, 12(3):537-562, 1981.
- [31] R. Dominguez and E. Pomerene. Studies of renal excretion of creatinine i. on the functional relation between the rate of output and the concentration in the plasma. *The Journal of Biological Chemistry*, 104(3):449–471, 1934.
- [32] R. Dominguez, H. Goldblatt, and E. Pomerene. Kinetics of the elimination of substances injected intravenously (experiments with creatinine). *American Journal of Physiology*, 114:240–254, 1935. Cited in: John G. Wagner. History of pharmacokinetics. *Pharmacology and Therapeutics*, 12(3):537-562, 1981.
- [33] R. Dominguez and E. Pomerene. Kinetics of the disappearance of galactose from the plasma after a rapid intravenous injection. *American Journal of Physiology*, 141:368–381, 1944. Cited in: John G. Wagner. History of pharmacokinetics. *Pharmacology and Therapeutics*, 12(3):537-562, 1981.

- [34] Rafael Dominguez and Elizabeth Pomerene. Calculation of the rate of absorption of exogenous creatinine. *Proceedings of the Society for Experimental Biology and Medicine*, 60:173–181, 1945. Cited in: John G. Wagner. History of pharmacokinetics. *Pharmacology and Therapeutics*, 12(3):537-562, 1981.
- [35] Rafael Dominguez and Elizabeth Pomerene. Recovery of creatinine after ingestion and after intravenous injection in man. *Proceedings of the Society for Experimental Biology and Medicine*, 58(1):26–28, 1945. Cited in: John G. Wagner. History of pharmacokinetics. *Pharmacology and Therapeutics*, 12(3):537-562, 1981.
- [36] R. Dominguez, A. C. Corcoran, and I. H. Page. Mannitol: Kinetics of distribution, excretion and utilization in human beings. *Journal of Laboratory and Clinical Medicine*, 32(1):1192–1202, 1947. Cited in: John G. Wagner. History of pharmacokinetics. *Pharmacology and Therapeutics*, 12(3):537-562, 1981.
- [37] R. Dominguez, H. Goldblatt, and E. Pomerene. Kinetics of the excretion and utilization of xylose. *American Journal of Physiology*, 119(3):429–438, 1947. Cited in: John G. Wagner. History of pharmacokinetics. *Pharmacology and Therapeutics*, 12(3):537-562, 1981.
- [38] R. Dominguez. Kinetics of elimination, absorption and volume of distribution in the organism. In Medical Physics II, editor, *This is the yearbook*. Yearbook Publishers, Chicago, 1950. Cited in: John G. Wagner. History of pharmacokinetics. *Pharmacology and Therapeutics*, 12(3):537-562, 1981.
- [39] T. Teorell. Kinetics of distribution of substances administered to the body i. the extravascular modes of administration. *Archs. int. Pharmacodyn. Ther.*, 57:205–255, 1937. Cited in: John G. Wagner. History of pharmacokinetics. *Pharmacology and Therapeutics*, 12(3):537-562, 1981.
- [40] T. Teorell. Kinetics of distribution of substances administered to the body ii. the intravascular modes of administration. *Archs. int. Pharmacodyn. Ther.*, 57:226–240, 1937. Cited in: John G. Wagner. History of pharmacokinetics. *Pharmacology and Therapeutics*, 12(3):537-562, 1981.
- [41] John G. Wagner and Eino Nelson. Per cent absorbed time plots derived from blood level and/or urinary excretion data. *Journal of Pharmaceutical Sciences*, 52(6):610–611, 1963.
- [42] J. G. Wagner. Application of the loo-riegelman absorption method. *Journal of Pharmacokinetics and Biopharmaceutics*, 3(1):51 – 67, 1975.
- [43] J. C. K. Loo and S. Riegelman. New method for calculating the intrinsic absorption rate of drugs. *Journal of Pharmaceutical Sciences*, 57(6):918–928, 1968.
- [44] A. H. BECKETT and M. ROWLAND. Urinary excretion kinetics of amphetamine in man. *Journal of Pharmacy and Pharmacology*, 17(10):628–639, 1965.

- [45] Milo Gibaldi and Howard Weintraub. Some considerations as to the determination and significance of biologic half-life. *Journal of Pharmaceutical Sciences*, 60(4):624–626, 1981. Cited in: John G. Wagner. History of pharmacokinetics. *Pharmacology and Therapeutics*, 12(3):537-562, 1981.
- [46] Jim E. Riviere. *Introduction: Comparative Pharmacokinetics*, chapter 1, pages 3–11. John Wiley and Sons, Ltd, 2011.
- [47] Pharmacology. Five routes of drug administration. Retrieved from <http://www.pharmacology.org/news/routes-administration/>, 2011.
- [48] Jim E. Riviere. *Principles of Drug Movement in the Body*, pages 13–25. Wiley-Blackwell, 2011.
- [49] Jianghong Fan and Ines A.M. de Lannoy. Pharmacokinetics. *Biochemical Pharmacology*, 87(1):93 – 120, 2014. Special Issue: Pharmacology in 21st Century Biomedical Research.
- [50] Ravikiran Panakanti and Ajit S. Narang. Impact of excipient interactions on drug bioavailability from solid dosage forms. *Pharmaceutical Research*, 29(10):2639–2659, 2012.
- [51] Gary G. Liversidge and Kenneth C. Cundy. Particle size reduction for improvement of oral bioavailability of hydrophobic drugs: I. absolute oral bioavailability of nanocrystalline danazol in beagle dogs. *International Journal of Pharmaceutics*, 125(1):91 – 97, 1995.
- [52] Yukinobu Kodama, Shintaro Fumoto, Junya Nishi, Mikiro Nakashima, Hitoshi Sasaki, Junzo Nakamura, and Koyo Nishida. Absorption and distribution characteristics of 5-fluorouracil (5-fu) after an application to the liver surface in rats in order to reduce systemic side effects. *Biological and Pharmaceutical Bulletin*, 31(5):1049–1052, 2008.
- [53] Frances J. Sharom. The p-glycoprotein multidrug transporter. *Essays In Biochemistry*, 50:161–178, 2011.
- [54] G. Gordon Gibson and Paul Skett. *Pathways of Drug Metabolism*, chapter 2, pages 1–14. Chapman and Hall, 1986.
- [55] Carlo Barnaba, Katherine Gentry, Nirupama Sumangala, and Ayyalusamy Ramamoorthy. The catalytic function of cytochrome p450 is entwined with its membrane-bound nature. *F1000Research*, 6:662, 2017.
- [56] Paul R. Ortiz de Montellano and John T. Groves. *Models and Mechanisms of Cytochrome P450 Action*, pages 1–10. Springer, Boston, MA, 2005.
- [57] Ilia G. Denisov, Thomas M. Makris, Stephen G. Sligar, and Ilme Schlichting. Structure and chemistry of cytochrome p450. *Chemical Reviews*, 105(6):2253–2278, 2005. PMID: 15941214.

- [58] Irwin H. Segel. *Introduction - Enzymes as biological catalysts*. Wiley classics library. Wiley-Interscience, 1975.
- [59] Bee Chin Chen, Rowani Mohd Rawi, Rutger Meinsma, Judith Meijer, Raoul C.M. Hennekam, and André B.P. Van Kuilenburg. Dihydropyrimidine dehydrogenase deficiency in two malaysian siblings with abnormal mri findings. *Mol Syndromol*, 5:299–303, 2014.
- [60] Etienne-Grimaldi M-C, Boyer J-C, Beroud C, Mbatchi L, van Kuilenburg A, and Bobin-Dubigeon C. New advances in dpyd genotype and risk of severe toxicity under capecitabine. *PLoS ONE*, 12:5, 2017.
- [61] National Cancer Institute and National Institutes of Health. Common terminology criteria for adverse events (CTCAE). Retrieved from [https://ctep.cancer.gov/protocoldevelopment/electronic\\_applications/docs/CTCAE\\_v5\\_Quick\\_Reference\\_8.5x11.pdf](https://ctep.cancer.gov/protocoldevelopment/electronic_applications/docs/CTCAE_v5_Quick_Reference_8.5x11.pdf).
- [62] Yolanda Smith. Drug excretion / elimination. Retrieved from <https://www.news-medical.net/health/Drug-Excretion-Elimination.aspx>, 2019. (Accessed on 11/26/2019).
- [63] Pavan Vajjah, Geoffrey K. Isbister, and Stephen B. Duffull. *Introduction to Pharmacokinetics in Clinical Toxicology*, volume 929, pages 289–312. Humana Press, Totowa, NJ, 2011. Cited in: Brad Reisfeld, Arthur N. Mayeno (auth.), Brad Reisfeld, Arthur N. Mayeno (eds.). *Computational Toxicology: Methods in Molecular Biology (Methods and Protocols)*, 613–625 Humana Press, 2013.
- [64] Nuventra Pharma Sciences. What is noncompartmental pk analysis? Retrieved from <https://www.nuventra.com/resources/blog/what-is-nca/>, 2019. (Accessed on 11/26/2019).
- [65] Nuventra Pharma Sciences. The difference between pbpk and population pk modeling. Retrieved from <https://www.nuventra.com/resources/blog/difference-pbpk-poppk-modeling/>, 2019. (Accessed on 11/26/2019).
- [66] Par Victor Henri. Lois générales de l’action des diastases. *American Chemical Society*, 25:780–782, 1903.
- [67] Caroline F. Thorn, Sharon Marsh, Michelle Whirl Carrillo, Howard L McLeod, Teri E. Klein, and Russ B. Altman. Pharmgkb summary: fluoropyrimidine pathways. *Pharmacogenetics and genomics*, 21(4):237–242, 2011.
- [68] Eric M. Koehn and Amnon Kohen. Flavin-dependent thymidylate synthase: a novel pathway towards thymine. *Archives of biochemistry and biophysics*, 493(1):96–102, 2009.

- [69] Muhammad W. Saif, Kostas N. Syrigos, and Nikos A. Katirtzoglou. S-1: a promising new oral fluoropyrimidine derivative. *Expert Opinion on Investigational Drugs*, 18(3):335–348, 2009.
- [70] M. Boisdron-Celle, G. Remaud, S. Traore, A.L. Poirier, L. Gamelin, A. Morel, and E. Gamelin. 5-fluorouracil-related severe toxicity: A comparison of different methods for the pretherapeutic detection of dihydropyrimidine dehydrogenase deficiency. *ScienceDirect, Elsevier Ireland Ltd*, 249:271–282, 2007.
- [71] Glimelius B., Hoffman K., Graf W., Pählman L., and Sjöden PO. Quality of life during chemotherapy in patients with symptomatic advanced colorectal cancer. the nordic gastrointestinal tumor adjuvant therapy group. *Cancer*, 73(3):556–562, 1994.
- [72] Per-Anders Larsson, Göran Carlsson, Bengt Gustavsson, Wilhelm Graf, and Bengt Glimelius. Different intravenous administration techniques for 5-fluorouracil: Pharmacokinetics and pharmacodynamics effects. *Acta Oncologica*, 35(2):207–212, 1996.
- [73] Richard A. Sams and William W. Muir. Chapter 9 - principles of drug disposition and drug interaction in horses. In William W. Muir and John A.E. Hubbell, editors, *Equine Anesthesia (Second Edition)*, pages 171 – 184. W.B. Saunders, Saint Louis, second edition edition, 2009.
- [74] Garrett Birkhoff. Fluid dynamics, reactor computations, and surface representation. *Association for Computing Machinery*, pages 63–87, 1990.
- [75] Stephen G. Nash. History of scientific computing. *Association for Computing Machinery*, pages 88–105, 1990.
- [76] Greeks for Greeks: A computer science portal for greeks. Runge-kutta 4th order method to solve differential equation. Retrieved from: <https://www.geeksforgeeks.org/runge-kutta-4th-order-method-solve-differential-equation/>. (Accessed on 12/02/2019).
- [77] Roman Siromakha. Bobyqa-cpp: C++ implementation of bobyqa algorithm with c interface. Retrieved from: <https://github.com/elsid/bobyqa-cpp>. (Accessed on 08/24/2019).
- [78] Roman Siromakha. Repositories - github. Retrieved from: <https://github.com/elsid?tab=repositories>. (Accessed on 08/24/2019).
- [79] Michael J. D. Powell. The bobyqa algorithm for bound constrained optimization without derivatives. Retrieved from: [http://www.damtp.cam.ac.uk/user/na/NA\\_papers/NA2009\\_06.pdf](http://www.damtp.cam.ac.uk/user/na/NA_papers/NA2009_06.pdf). (Accessed on 08/25/2019).
- [80] A. Di Paolo, R. danesi, A. Falcone, L. Cionini, F. Vannozzi. G. Masi, and G. Alleg. Relationship between 5-fluorouracil disposition, toxicity and dihydropyrimidine dehydrogenase activity in cancer patients. *Annals of Oncology*, 12:1301–1306, 2001.

- [81] Antonello Di Paolo, Romano Danesi, Francesca Vannozzi, Alfredo Falcone, Enrico Mini, Luca Cionini, Toni Ibrahim, Dino Amadori, and Mario del Tecca. Limited sampling model for the analysis of 5-fluorouracil pharmacokinetics in adjuvant chemotherapy for colorectal cancer. *Clinical Pharmacology and Therapeutics*, 72(6):627–637, 2002.
- [82] A. Di Paolo, R. danesi, A. Falcone, L. Cionini, F. Vannozzi. G. Masi, and G. Alleg. Relationship between 5-fluorouracil disposition, toxicity and dihydropyrimidine dehydrogenase activity in cancer patients. *Annals of Oncology*, 12:1301–1306, 2001.
- [83] Federico Casale, Roberto Canaparo, Loredana Serpe, Elisabetta Muntoni, Carlo Della Pepa, Mario Costa, Lorenza Mairone, Gian Paolo Zara, Gianni Fornari, and Mario Eandi. Plasma concentrations of 5-fluorouracil and its metabolites in colon cancer patients. *Pharmacological Research*, 50(2):173–179, 2004.
- [84] Glen D. Heggie, Jean-Pierre Sommadossi, David S. Cross, William J. Huster, and Robert B. Diasio. Clinical pharmacokinetics of 5-fluorouracil and its metabolites in plasma, urine, and bile. *Cancer Research*, 47(8):2203–2206, 1987.
- [85] Quora. What is chemical affinity? Retrieved from `\protect\unhbox\voidb@x\penalty\@M\https://www.quora.com/What-is-Chemical-Affinity`, 2019. (Accessed on 12/31/2019).
- [86] The Editors of Encyclopaedia Britannica. Antimetabolite. Retrieved from `https://www.britannica.com/science/antimetabolite`, 2017. (Accessed on 12/31/2019).
- [87] CHEBI. amino acid. Retrieved from `https://www.ebi.ac.uk/chebi/searchId.do?chebiId=33709`. (Accessed on 12/13/2019).
- [88] Wikipedia. Area under the curve (pharmacokinetics). Retrieved from `https://en.wikipedia.org/wiki/Area_under_the_curve_(pharmacokinetics)`. (Accessed on 12/31/2019).
- [89] Wikipedia. Biotransformation. Retrieved from `\protect\unhbox\voidb@x\penalty\@M\https://en.wikipedia.org/wiki/Biotransformation`, 2019. (Accessed on 12/31/2019).
- [90] C Case-Lo. About intravenous medication administration. Retrieved from `\protect\unhbox\voidb@x\penalty\@M\https://www.healthline.com/health/intravenous-medication-administration-what-to-know#standard-iv-lines`, 2019. (Accessed on 12/31/2019).
- [91] Berg Sabrina. `https://prezi.com/uqf6mw0dy0up/cancer/`. Retrieved from `\protect\unhbox\voidb@x\penalty\@M\https://prezi.com/uqf6mw0dy0up/cancer/`, 2019. (Accessed on 12/31/2019).

- [92] U.S. National Library of Medicine. Capecitabine. Retrieved from =<https://pubchem.ncbi.nlm.nih.gov/compound/Capecitabine>. (Accessed on 12/31/2019).
- [93] The Free Dictionary. cardiotoxic glycosides. Retrieved from =[https://medical-dictionary.thefreedictionary.com/cardiotoxic glycosides](https://medical-dictionary.thefreedictionary.com/cardiotoxic+glycosides). (Accessed on 12/31/2019).
- [94] MedicineNet. Definition of cell cycle. Retrieved from: =<https://www.medicinenet.com/script/main/art.asp?articlekey=7107>. (Accessed on 12/31/2019).
- [95] University of Nottingham. Drug elimination. Retrieved from: =<https://www.nottingham.ac.uk/nursing/sonet/rlos/bioproc/kidneydrug/>. (Accessed on 12/31/2019).
- [96] Toxtutor - chemical reactions. Retrieved from: =<https://toxtutor.nlm.nih.gov/12-002.html>. (Accessed on 12/31/2019).
- [97] Global minimum. Retrieved from: =<http://mathworld.wolfram.com/GlobalMinimum.html>. (Accessed on 12/31/2019).
- [98] Diren Beyoğlu, Sandrine Imbeaud, Olivier Maurhofer, Paulette Bioulac-Sage, Jessica Zucman-Rossi, Jean-François Dufour, and Jeffrey R. Idle. Tissue metabolomics of hepatocellular carcinoma: Tumor energy metabolism and the role of transcriptional classification. *Hepatology*, 58(1):229–238, 2013.
- [99] Low white blood cell count. Retrieved from: =<https://www.mayoclinic.org/symptoms/low-white-blood-cell-count/basics/definition/sym-20050615>, Nov 2018. (Accessed on 12/31/2019).
- [100] Minimization. Retrieved from =<https://www.thefreedictionary.com/minimization>. (Accessed on 08/24/2019).
- [101] Anne Marie Helmenstine. Learn chemical reaction orders using kinetics. Retrieved from: =<https://www.thoughtco.com/chemical-reaction-orders-608182>, Aug 2019. (Accessed on 08/24/2019).
- [102] Nci dictionary of cancer terms. Retrieved from: =<https://www.cancer.gov/publications/dictionaries/cancer-terms>. (Accessed on 08/24/2019).
- [103] W. Sun, P. E. Sanderson, and W Zheng. Drug combination therapy increases successful drug repositioning. *Drug discovery today*, 21(7):1189–1195, 2016.
- [104] Maximum concentration. Retrieved from: =[https://medical-dictionary.thefreedictionary.com/Maximum Concentration](https://medical-dictionary.thefreedictionary.com/Maximum+Concentration). (Accessed on 12/31/2019).

- [105] P. De Paepe, F.M. Belpaire, and W.A. Buylaert. Pharmacokinetic and pharmacodynamic considerations when treating patients with sepsis and septic shock. *Clin Pharmacokinet*, 41:1135–1151, 2002.
- [106] A. Chen, M. L. Yarmush, and T. Maguire. Physiologically based pharmacokinetic models: integration of in silico approaches with micro cell culture analogues. *Current drug metabolism*, 13(6):863–880, 2012.
- [107] Center for Drug Evaluation and Research. Route of administration. Retrieved from: [=https://www.fda.gov/drugs/data-standards-manual-monographs/route-administration](https://www.fda.gov/drugs/data-standards-manual-monographs/route-administration). (Accessed on 08/24/2019).
- [108] Boundless. Boundless anatomy and physiology. Retrieved from: [=https://courses.lumenlearning.com/boundless-ap/chapter/physiology-of-the-kidneys/](https://courses.lumenlearning.com/boundless-ap/chapter/physiology-of-the-kidneys/). (Accessed on 08/24/2019).
- [109] Variance: Simple definition, step by step examples. Retrieved from: [=https://www.statisticshowto.datasciencecentral.com/probability-and-statistics/variance/](https://www.statisticshowto.datasciencecentral.com/probability-and-statistics/variance/). (Accessed on 08/24/2019).
- [110] Nathan Teuscher. Certara. Retrieved from: [=https://www.certara.com/2010/06/05/understanding-volume-of-distribution/](https://www.certara.com/2010/06/05/understanding-volume-of-distribution/), Nov 2017. (Accessed on 08/24/2019).

# Appendix A

## Dictionary

<b>adjuvant chemotherapy</b>	This is therapy that is given in addition to the primary or initial therapy to maximize its effectiveness [12].
<b>affinity</b>	The extent to which one substance tends to combine with another[85].
<b>alpha-fluoro-beta-alanine</b>	An inactive end product of 5-fluorouracil [12].
<b>antineoplastic</b>	Acting to prevent, inhibit or halt the development of a tumour [12].
<b>antimetabolite</b>	A substance that competes with, replaces, or inhibits a specific metabolite of a cell and thereby interferes with the cell's normal metabolic functioning [86].
<b>antitumour</b>	Acting to prevent, inhibit or halt the development of a tumour [10].
<b>amino acid</b>	Organic compounds containing amine (-NH <sub>2</sub> ) and carboxyl (-COOH) functional groups, along with a side chain (R group) specific to each amino acid [87].
<b>area under the curve</b>	The definite integral in a plot of drug concentration vs. time [88].
<b>beta-ureidopropionase</b>	The enzyme that convert fluoro-beta-ureidopropionate to alpha-fluoro-beta-alanine [12].
<b>biliary excretion</b>	The elimination of drugs and drug metabolites in bile [62].
<b>bioavailability</b>	The degree and rate at which an administered drug is absorbed by the body's circulatory system, the systemic circulation [50].
<b>biopharmaceutics</b>	The study of the chemical and physical properties of drugs and the biological effects they produce [26].
<b>biotransformation</b>	The alteration of a substance, such as a drug, within the body [89].
<b>bloodstream</b>	The blood circulating through the body of a person or animal [89].

---

<b>bolus injection</b>	Rapid injection of a relatively large volume of fluid or dose of a drug or test substance given indirectly into the bloodstream [90].
<b>cancer</b>	Uncontrolled growth of abnormal cells in the human body with the ability to migrate from the original site and spread to distant sites [91].
<b>capecitabine</b>	An antineoplastic drug that is converted into 5-fluorouracil in the body, used in the treatment of colorectal cancer and metastatic breast cancer [92].
<b>cardiotoxicity</b>	A drug-induced poisonous or deleterious effect upon the heart muscle or its conduction system [93].
<b>cell cycle</b>	The sequence of events within the cell between mitotic (cell) divisions [94].
<b>chemotherapy</b>	Treatment of disease by means of a chemical that binds to and specifically kills microbes or tumour cells [94].
<b>clearance</b>	The elimination of a drug from the body, primarily by the kidneys into the urine, but other routes for elimination include bile, sweat, saliva, breast milk, and exhaled air [95].
<b>compartment</b>	Different sections of a body or different events within a body that are assumed to be a homogeneous entity [64].
<b>compartment models</b>	A type of mathematical model used for describing the way drugs are transmitted among the compartments of a system [64].
<b>conjugation reactions</b>	Phase II reactions that involve covalent attachment of small hydrophilic endogenous molecule such as glucuronic acid, sulfate, or glycine to form water-soluble compounds, that are more hydrophilic [96].
<b>cyclophosphamide</b>	A prodrug that is classified as an alkylating agent that is used to treat many types of cancer by damaging the cell's DNA [18, 19].
<b>cytochrome P450</b>	A group of enzymes involved in drug metabolism into less toxic forms that are easier for the body to excrete and they are found in high levels within the liver [54].
<b>cytochrome b5</b>	A membrane bound hemoprotein which functions as an electron carrier for several membrane bound oxygenases [57].
<b>dihydrofluorouracil</b>	A metabolite of 5-fluorouracil as formed by the reaction with dihydropyrimidine dehydrogenase [12].
<b>dihydropyrimidinase</b>	The enzyme that converts dihydrofluorouracil to fluoro-beta-ureidopropionate [12].

---

<b>dihydropyrimidine dehydrogenase</b>	It is the enzyme that converts 5-fluorouracil to dihydrofluorouracil [12].
<b>efflux</b>	The flowing out of a particular substance or particle [53].
<b>endocytosis</b>	The incorporation of substances into a cell by phagocytosis or pinocytosis [53].
<b>fluoro-beta-ureidopropionate</b>	The second stage of metabolites of 5-fluorouracil from dihydrofluorouracil catalyzed by dihydropyrimidinase [12].
<b>5-fluoro-deoxyuridine</b>	An intermediate metabolite between the drug 5-fluorouracil and the metabolite 5-Fluorodeoxyuridine monophosphate [12].
<b>5-fluoro-deoxyuridine monophosphate</b>	One of the three active metabolites created from 5-fluorouracil that inhibits thymidylate synthase [12].
<b>5-fluorodeoxyuridine triphosphate</b>	One of the three active metabolites created from 5-fluorouracil that is incorporated into DNA [12].
<b>5-fluorouridine triphosphate</b>	One of the three active metabolites created from 5-fluorouracil that incorporated into RNA [12].
<b>5-fluoroxyuridine monophosphate</b>	The metabolite that is largely converted from 5-fluorouracil either directly by uridine monophosphate synthase and glutamine phosphoribosylpyrophosphate amino transferase or indirectly via fluorouridine by uridine phosphorylase 1 and 2 and uridine-cytidine kinase 1 and 2 [12].
<b>fluoropyrimidine</b>	An antimetabolite [12].
<b>5-fluorouracil</b>	An antimetabolite drug used to treat cancers of the breast, colon, rectum, stomach, and pancreas, it inhibits cells from making DNA and may kill cancer cells [12].
<b>fluorouridine</b>	An intermediate metabolite between the drug 5-fluorouracil and the metabolite 5-Fluoroxyuridine monophosphate [12].
<b>global minimum</b>	An absolute minimum, the smallest overall value of a set, function, etc., over its entire range [97].
<b>glomerular filtration</b>	The process that the kidneys use to filter excess fluid and waste products out of the blood into the urine collecting tubules of the kidney, so they may be eliminated from the body [63].
<b>glucuronic acid</b>	A uronic acid that was first isolated from urine, and is important for the metabolism of microorganisms, plants and animals [54].
<b>glutamine phosphoribosylpyrophosphate amino transferase</b>	An enzyme responsible for catalysing the conversion of 5-phosphoribosyl-1-pyrophosphate (PRPP) into 5-phosphoribosyl-1-amine (PRA), using the ammonia group from a glutamine side-chain [12].

---

<b>hepatoma metabolism</b>	The chemical processes that occur within a cancer of the cells of the liver in order to maintain life [98].
<b>heterozygous mutation carrier</b>	A person or other organism that has inherited a mutation affecting only one allele but usually does not display that trait or show symptoms of the disease [59].
<b>homozygous mutation carrier</b>	A person or other organism that has inherited an identical mutation of both the paternal and maternal alleles [59].
<b>hydrolysis</b>	A chemical reaction that uses water to break down a compound [54].
<b>infusion</b>	The slow therapeutic introduction of fluid other than blood into the bloodstream [72].
<b>intravenous</b>	A way of giving a drug or other substance through a needle or tube inserted into a vein [50].
<b>isoforms</b>	Any of two or more functionally similar proteins that have a similar but not identical amino acid sequence and are either encoded by different genes or by RNA transcripts from the same gene which have had different exons removed [55].
<b>kinetics</b>	The study of motion and its causes [21].
<b>leukopenia</b>	A reduction in the number of white cells in the blood, typical of various diseases [99].
<b>mean residence time</b>	The average time the drug stays at the site of action [49].
<b>membrane</b>	A very thin layer of tissue that covers a surface [48].
<b>metabolism</b>	The chemical changes that take place in a cell or an organism (biotransformation) [54].
<b>metabolite</b>	A substance made or used when the body breaks down food, drugs or chemicals, or its own tissue (for example, fat or muscle tissue) [54].
<b>methotrexate</b>	A chemotherapy agent and immune system suppressant. It is used to treat cancer [19].
<b>micrometastases</b>	A small collection of cancer cells that have been shed from the original tumour and spread to another part of the body [3].
<b>minimization</b>	To reduce to the smallest possible amount, extent, size, or degree [100].
<b>mixed-order kinetics</b>	The process order changes for different concentrations of the chemical species involved [101].
<b>monotherapy</b>	The use of a single drug to treat a disease or condition [102].

---

<b>multi-drug therapy</b>	The use of combination of drugs to treat a disease or condition [103].
<b>murine-S37</b>	A model for cancer chemotherapy screening developed by the National Cancer Institute [3].
<b>nausea</b>	A feeling of sickness or discomfort in the stomach that may come with an urge to vomit. Nausea is a side effect of some types of cancer therapy [102].
<b>non-compartment model</b>	The model is based on the assumption that the drugs or metabolites follow linear kinetics [64].
<b>oxidation</b>	A chemical reaction that takes place when a substance comes into contact with oxygen or another oxidizing substance [102].
<b>passive diffusion</b>	The transport across the cell membrane that does not require energy [51].
<b>peak plasma concentration</b>	The maximum (or peak) serum concentration that a drug achieves in a specified compartment or test area of the body after the drug has been administered and before the administration of a second dose [104].
<b>pharmacodynamic</b>	The study of how a drug affects an organism [105].
<b>pharmacokinetics</b>	The study of how the organism affects the drug [105].
<b>physiologically based models</b>	A mathematical modelling technique for predicting the absorption, distribution, metabolism and excretion (ADME) of synthetic or natural chemical substances in humans and other animal species [106].
<b>pyrimidine</b>	One of two chemical compounds that cells use to make the building blocks of DNA and RNA [12].
<b>radiotherapy</b>	The treatment of disease, especially cancer, using radiation [102].
<b>receptor</b>	A molecule inside or on the surface of a cell that binds to a specific substance and causes a specific effect in the cell [49].
<b>rectal administration</b>	An administration that uses the rectum as a route for medication and other fluids, which are absorbed by the rectum's blood vessels, and flow into the body's circulatory system [47].
<b>route of administration</b>	The path by which a drug, fluid, or other substance is taken into the body [107].
<b>screening</b>	Checking for disease when there are no symptoms [3].

<b>stomatitis</b>	Inflammation or irritation of the mucous membranes in the mouth [102].
<b>transcellular transport</b>	The transportation of solutes by a cell through a cell [51].
<b>transplantation</b>	A surgical procedure in which tissue or an organ is transferred from one area of a person's body to another area, or from one person (the donor) to another person (the recipient) [51].
<b>transporter</b>	A protein that serves the function of moving other materials within an organism [51].
<b>tubular secretion</b>	The transfer of materials from peritubular capillaries to the renal tubular lumen [108].
<b>tumour</b>	An abnormal mass of tissue that results when cells divide more than they should or do not die when they should. Tumours may be benign (not cancer), or malignant (cancer) [102].
<b>thymidine kinase</b>	An enzyme that catalyses the phosphorylation of thymidine in a pathway leading to DNA synthesis, that is active especially in tissues undergoing growth or regeneration, and that is the key enzyme mediating replication in certain viruses [12].
<b>thymidylate phosphorylase</b>	An enzyme that catalyses the reversible phosphorylation of thymidine, deoxyuridine, and their analogs (except deoxycytidine) to their respective bases (thymine/uracil) and 2-deoxyribose 1-phosphate [12].
<b>uracil</b>	A chemical compound that is used to make one of the building blocks of RNA [12].
<b>uridine-cytidine kinase</b>	An enzyme that in humans is encoded by the UCK2 gene [12].
<b>uridine monophosphate synthase</b>	The enzyme that catalyses the formation of uridine monophosphate (UMP), an energy-carrying molecule in many important biosynthetic pathways [12].
<b>uridine phosphorylase</b>	An enzyme that catalyses the chemical reaction uridine + phosphate → uracil + alpha-D-ribose 1-phosphate [12].
<b>variance</b>	A numerical value used to indicate how widely individuals in a group vary [109]. This is also known as least squares.
<b>volume of distribution</b>	The theoretical volume that would be necessary to contain the total amount of an administered drug at the same concentration that is observed in the blood plasma [110].
<b>zero-order process</b>	The process at a fixed rate of reaction and independent of the concentration of the reacting substances within the body [101].

# Appendix B

## Weighted Variance

### B.1 Effects of $S_\sigma$ Results Compared to the $S_p$ Results

Using the results obtained from  $S_p$  minimization for the initial PK parameters for minimization of  $S_\sigma$  will provide a better set of parameters for calculating accurate  $C_{max}$  without having a huge effect on the lower concentration. The fixed and variable exponents parameters were obtained for the one, two (1+2), and three-compartment models.

#### B.1.1 One-Compartment Model Optimization with $S_\sigma$

There are four cases to examine using  $S_\sigma$  for the one-compartment optimization. Fixed first degree exponents (case 1); fixed zeroth, first, and second-degree exponents (case 1.4); variable exponents, and the combination of variable exponents with saturation limiting function (cases 2.2) respectively. Final results are shown in Table B.1.

Table B.1: The PK values for cases 1, 1.4, 2, and 2.2, one-compartment model with  $S_\sigma$  minimization.

Case	A	B	$k_{5FU,1,0}^{(p)}$	$\Gamma_{5FU,1,0}^{(AB)}$	$V_d(\frac{L}{m^2})$	$S_\sigma(\frac{\mu mol^2}{L^2})$
1	1.0000	1.0000	0.1084(65)	0.00000(23)	6.445(45)	115.1
1.4	0.0000	0.0000	0.0000(58)	-	6.445(45)	115.1
	1.0000	1.0000	0.1084(65)	0.0000 (23)		
	2.0000	2.0000	0.0000(61)	-		
2	1.3377(34)	1.0025(44)	0.02400(58)	0.000000(18)	3.283(63)	74.14
2.2	0.0001*	N/A**	0.0000(89)	-	3.272(64)	71.97
	1.3587(22)	1.024(31)	0.0242(33)	0.0001(31)		
	1.9995*	N/A**	0.0000(55)	-		

The S.I units of  $k_{5FU,j,k}^{(p)}$  is  $\frac{\mu mol^{(1-A)}}{m^{(2-2A)} min}$  and  $\Gamma_{5FU,j,k}^{(AB)}$  is  $\frac{m^{2B}}{\mu mol^B}$ .

The 5-FU concentration graphs for case 1 and case 2.2 of the one-compartment model are shown in Figure B.1 part A and part B respectively. Observing the graphs compared with the corresponding one-compartment model with  $S_p$  minimized (see Figure 3.1 and Figure 3.2), there is a better fit to the  $C_{max}$  of 5-FU.

Considering the contribution of subordinates to the primary cases. In case 1.4, there is no contribution from the zeroth-order and second order process to case 1. With the variable exponents cases, the processes are mixed exponents but nearly first order process

at the low concentration,  $A^{(2)} = 1.3377$  and  $A^{(2.2)} = 1.3387$ . In case 2.2, we have no impact from the second-order processes. At high concentrations  $(A - B)^{(2)} = 0.3352$  and  $(A - B)^{(2.2)} = 0.3367$ . They are not zero values unlike the Michaelis-Mentens model.

### B.1.2 (1+2) Two-Compartment Model with $S_\sigma$ Minimization

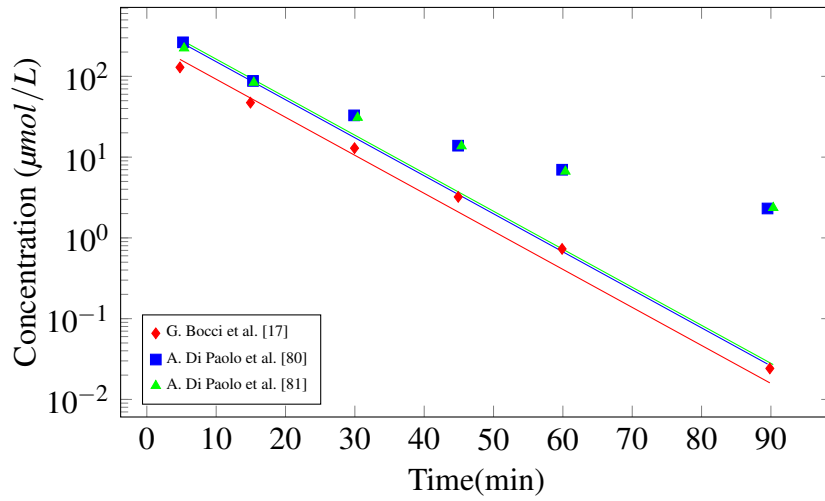
The model optimization with  $S_\sigma$  were examined for cases 1, 1.4, 2, and 3.3 for the (1+2) two-compartment model. The model has a slightly better fit than the case 2 for the one-compartment model. The case 2 of the two-compartment model has the best fit with  $S_\sigma = 73.534 \frac{\mu\text{mol}^2}{L^2}$ , which it is better than case 1 of the two-compartment model by 25.57%. The numbers are shown in Table B.2.

Table B.2: Cases 1, 1.4, 2, and 3.3 of the (1+2) two-compartment model with  $S_\sigma$  minimized

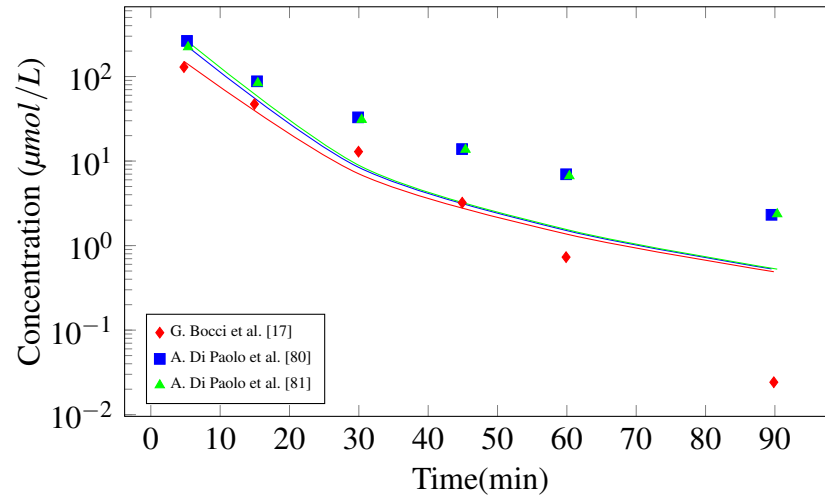
Case	$p$	$j, k$	$A$	$B$	$k_{5FU, j, k}^{(p)}$	$\Gamma_{5FU, j, k}^{(p)}$	$V_d (\frac{L}{m^2})$	$S_\sigma$
1	1	1,2	1.0000	1.0000	0.1336(54)	0.00000(15)	6.107(34)	98.80
		2,0	1.0000	1.0000	0.1276(41)	0.0017(56)		
		2,1	1.0000	1.0000	0.015(52)	0.0000(18)		
1.3	0	1,2	0.0000	0.0000	0.0000(13)	-	6.107(25)	98.76
		2,0	0.0000	0.0000	0.0000(23)	-		
		2,1	0.0000	0.0000	0.0000 (55)	-		
	1	1,2	1.0000	1.0000	0.1336(53)	0.00000(15)		
		2,0	1.0000	1.0000	0.1276(41)	0.0012(56)		
		2,1	1.0000	1.0000	0.0153(53)	0.0000(17)		
	2	1,2	2.0000	2.0000	0.0002(11)	0.0002(28)		
		2,0	2.0000	2.0000	0.0000(34)	-		
		2,1	2.0000	2.0000	0.0000(41)	-		
2	AB	1,2	1.7138(28)	1.182(32)	0.0029(11)	0.0003(24)	4.54(36)	72.69
		2,0	1.7121(32)	1.1818(21)	0.0116(37)	0.0064(42)		
		2,1	1.000(83)	0.9999*	0.0115(24)	0.00000(10)		
3.3	AB	1,2	1.7119(28)	1.182(32)	0.0044(11)	0.0015(24)	4.54(36)	54.87
		2,0	1.7120(32)	1.1819(21)	0.0056(37)	0.0037(42)		
		2,1	1.002(83)	1.0004*	0.0199(24)	0.00000(10)		
$p2$		$j, k$	C	D	$\alpha_{5FU, j, k}^{(AB, p2)}$	$\beta_{5FU, j, k}^{(AB, p2)}$		
1		1,2	1.0005	0.99981	0.0032	0.0000		
		2,1	1.00013	1.0002	0.0061	0.0005		
2		1,2	1.9999	1.9995	-0.0003	0.0005		
		2,1	2.0001	2.0002	-0.0007	0.0002		

The S.I units of  $k_{5FU, j, k}^{(p)}$  is  $\frac{\mu\text{mol}^{(1-A)}}{m^{(2-2A)}\text{min}}$ ,  $\Gamma_{5FU, j, k}^{(p)}$  is  $\frac{m^{2B}}{\mu\text{mol}^B}$ ,  $\alpha_{5FU, j, k}^{(AB, p)}$  is  $\frac{m^{2C}}{\mu\text{mol}^C}$ ,  $\beta_{5FU, j, k}^{(AB, p)}$  is  $\frac{m^{2D}}{\mu\text{mol}^D}$ , and  $S_\sigma$  is  $\frac{\mu\text{mol}^2}{L^2}$ .

Case 3.3 involves the saturation limiting function and adds no considerable changes to case 2. The values for  $\alpha$  remained zero, which implies that there is no influence on the flow of the molecules. The 5-FU concentration graphs for the three datasets are shown in Figure B.2.

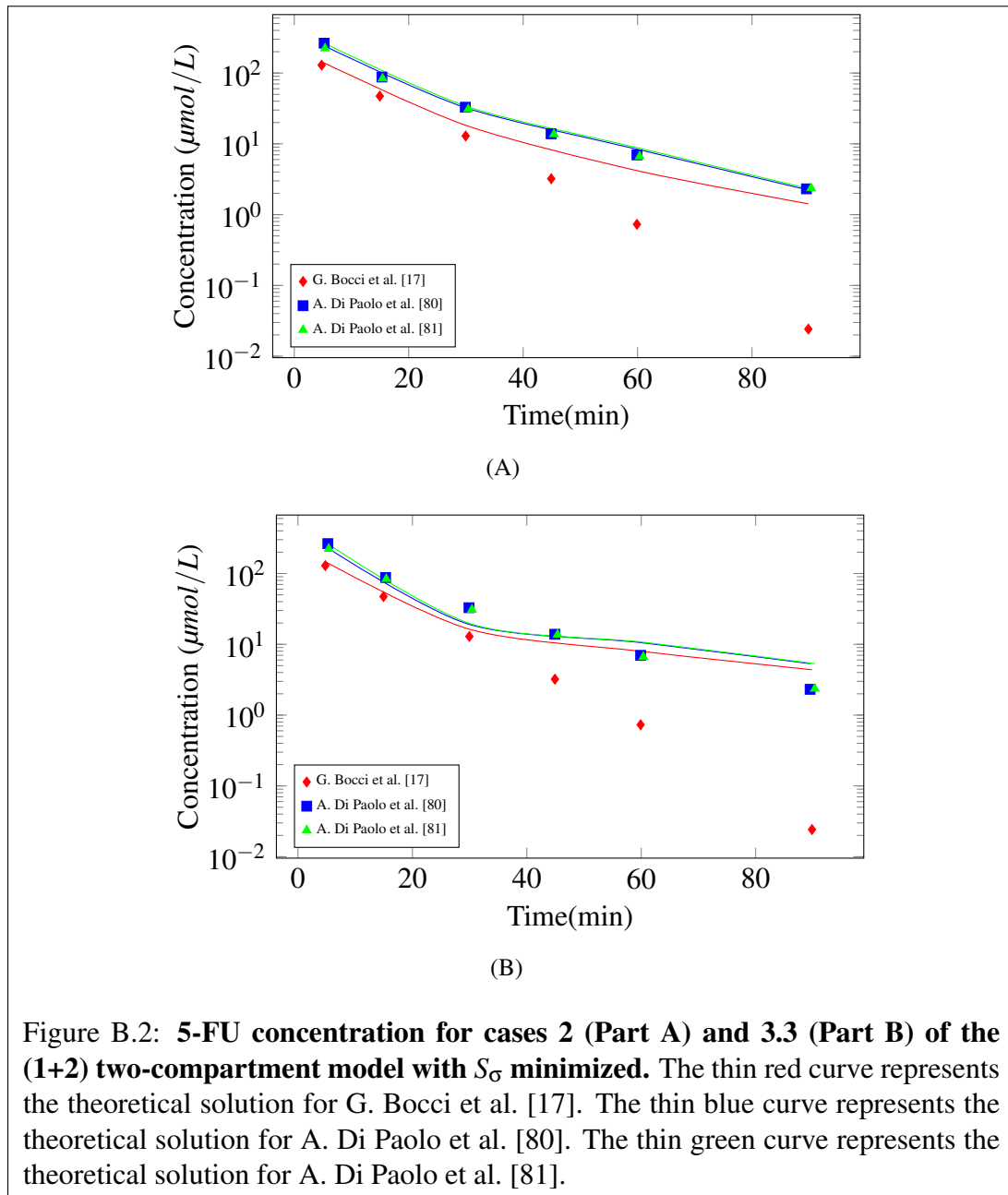


(A)



(B)

Figure B.1: **5-FU concentration for case 1.4 (Part A) and case 2.2 (Part B) of the one-compartment model with  $S_{\sigma}$  minimized.** The thin red curve represents the theoretical solution for G. Bocci et al. [17]. The thin blue curve represents the theoretical solution for A. Di Paolo et al. [80]. The thin green curve represents the theoretical solution for A. Di Paolo et al. [81].



At low concentration, the exponents  $A$  are shown to be mixed order, while from compartment 2 to compartment 1 is first-order. The numbers were stable in-between the first and second-order process. Whereas at high concentration, the exponents ( $A-B$ ) are non-zeroth order process 0.530 except for the elimination from compartment 2 which is zeroth-order process.

### B.1.3 Three-Compartment Model with $S_{\sigma}$ Minimization

The minimization of  $S_{\sigma}$  for case 2 of the three-compartment model was examined. The best fit results are shown in Table B.3. Comparing the three-compartment model with  $S_{\sigma}$  minimized to the (1+2) two-compartment model indicates that the three-compartment model has a slight improvement in  $S_{\sigma}$  of 0.12%. The order process  $A$  at low concentration remained to be the mixed-order process that is closer to second order process for two of the five  $A$ 's, see Table B.3, exponents  $A$  is ranging from  $A = 1.000$  to 1.7138; meanwhile, at the high concentration, the order process ( $A - B$ ) is observed to be non-zero values ranging from 0.0001 to 0.5318, and some are closer to zero. (1,3), (2,1), and (3,1) flows look like Michaelis-Menten processes. Figure B.3 shows the graphs of the results.

Table B.3: The PK values for case 2 of the three-compartment model

<i>Parameter</i>	1,2	1,3	2,0	2,1	3,1
$A$	1.7138(65)	1.07(25)	1.71(30)	1.000(55)	1.073(12)
$B$	1.182(14)	0.98(49)	1.18(33)	0.9999*	0.984(34)
$k_{5FU,j,k}^{(AB)}$	0.0029(83)	0.002(23)	0.012(56)	0.0115(13)	0.0013(12)
$\Gamma_{5FU,j,k}^{(AB)}$	0.00028(13)	0.008(86)	0.006(21)	0.0000(15)	0.0005(21)
$V_d \frac{L}{m^2}$	4.54(39)				
$S_{\sigma}$	72.59				

The S.I units of  $k_{5FU,j,k}^{(p)}$  is  $\frac{\mu mol^{(1-A)}}{m^{(2-2A)} min}$ ,  $\Gamma_{5FU,j,k}^{(p)}$  is  $\frac{m^{2B}}{\mu mol^B}$ , and  $S_{\sigma}$  is  $\frac{\mu mol^2}{L^2}$ .

## B.2 $AUC$ , $C_{max}$ , and $t_{1/2}$ for 5-FU

In examining the differences observed between  $S_p$  and  $S_{\sigma}$ , we observed that  $S_{\sigma}$  has a higher  $AUC$  and  $C_{max}$  in all the model tested. Whereas, we have a shorter  $t_{1/2}$  in  $S_{\sigma}$  than in  $S_p$ . In case 2 and case 3 of the (1+2) two-compartment model, the  $AUC$  has increase by 43.6% and 43.8% respectively, and in case 2 of the three compartment, the  $AUC$  is higher in  $S_{\sigma}$  by 44.7%. The higher  $C_{max}$  in  $S_{\sigma}$  is at the average of 15% (see Table B.4). The results indicates that there is more consideration for the higher concentrations than the lower ones in  $S_{\sigma}$ , while in  $S_p$  shows equal weights for all data points.

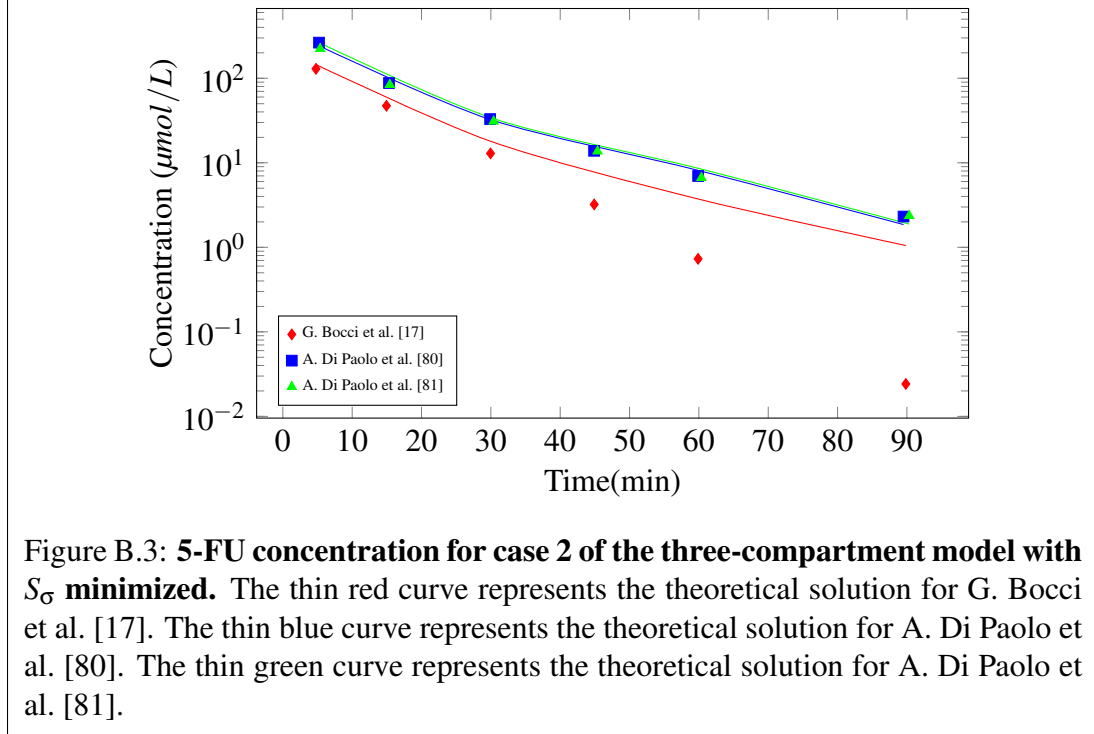


Figure B.3: **5-FU concentration for case 2 of the three-compartment model with  $S_\sigma$  minimized.** The thin red curve represents the theoretical solution for G. Bocci et al. [17]. The thin blue curve represents the theoretical solution for A. Di Paolo et al. [80]. The thin green curve represents the theoretical solution for A. Di Paolo et al. [81].

Table B.4: The observable quantities in comparing  $S_p$  and  $S_\sigma$

Case	$S_p$ Optimization			$S_\sigma$		
	$AUC$	$C_{max}$	$t_{1/2}$	$AUC$	$C_{max}$	$t_{1/2}$
2 (1+2) two-compartment	1490	178.1	9.63	2140	205.2	5.23
3 (1+2) two-compartment	1475	178.1	9.64	2121	205.8	5.19
2 (1+2) three-compartment	1474	178.0	9.60	2133	206.5	5.30

The S.I units of  $AUC$  is  $\frac{min.\mu mol}{L}$ ,  $C_{max}$  is  $\frac{\mu mol}{L}$ , and  $t_{1/2}$  is  $min.$ .

### B.3 Minimization of the Weighted Variance ( $S_\sigma$ ) for DHFU

The results obtained from  $S_p$  for DHFU are used as the starting point to determine the best parameters to minimize  $S_\sigma$ . This method enhances the fitness to the clinical data by prioritizing the  $C_{max}$  and  $AUC$  variation.

#### B.3.1 $S_\sigma$ Minimization for Case 2 of the One-Compartment Model

The result obtained shows that there is a considerable effect of minimized  $S_\sigma$  on the data, the  $C_{max}$  attained a better fit than minimized  $S_p$ . See Table B.5. Comparing the kinetics of DHFU in  $S_\sigma$  to  $S_p$  minimization, we observed that the process in the two techniques are approximately first order process at low concentration, the exponent  $A$  in this case is 1.0107, while exponents  $(A - B) = 0.0077$  a non zero kinetics at high concentration. The concentration-time curve is in Figure B.4. Complete graph for all the datasets are in appendix C.

Table B.5: The DHFU PK values for case 2, one-compartment model

$d$	$j,k$	$A_{d,j,k}^{(AB)}$	$B_{d,j,k}^{(AB)}$	$k_{d,j,k}^{(AB)}$	$\Gamma_{d,j,k}^{(AB)}$	$V_d(\frac{L}{m^2})$	$S_\sigma$
DH	1,0	1.0107(19)	1.0030(32)	0.3305(29)	0.00843(21)	5.10(13)	0.6772
en	1,1	1.0(10)	0.9989	0.1089	0.0000		
com	1,1	1.0049(12)	1.0007(39)	0.01474(19)	0.000203(11)		

$k_{d,j,k}^{(AB)}$  unit is  $\frac{\mu\text{mol}^{(1-A)}}{m^{(2-2A)}\text{min}}$ ;  $\Gamma_{d,j,k}^{(AB)}$  unit is  $\frac{m^{2B}}{\mu\text{mol}^B}$ , where  $A = A_{d,j,k}^{(AB)}$  and  $B = B_{d,j,k}^{(AB)}$ ; and DH, en, and com represent DHFU, enzymes, and complex substrate respectively.  $S_\sigma$  is  $\frac{\mu\text{mol}^2}{L^2}$

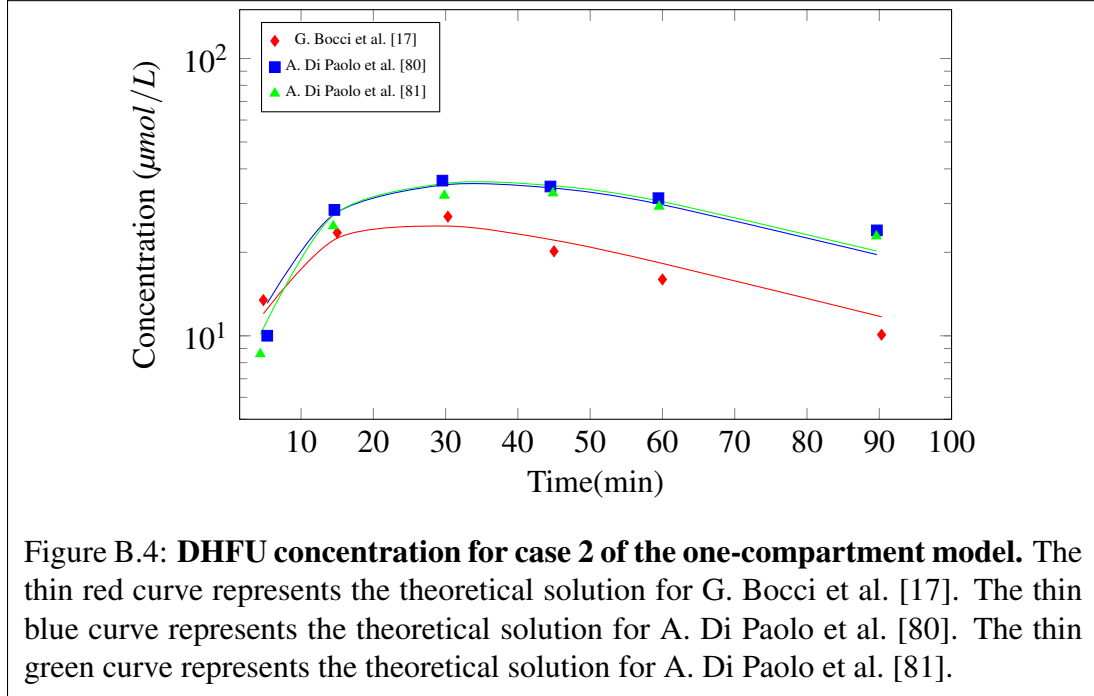


Figure B.4: **DHFU concentration for case 2 of the one-compartment model.** The thin red curve represents the theoretical solution for G. Bocci et al. [17]. The thin blue curve represents the theoretical solution for A. Di Paolo et al. [80]. The thin green curve represents the theoretical solution for A. Di Paolo et al. [81].

The uncertainty numbers show to what extent the deviation of each parameter from global minimum can influence the variance to deviate by 1.00%. The deviation in  $\Gamma_{complex,1,1}^{(AB)}$  seemed to be the very sensitive to the system as the shortest range ( $10^{-6}$ ) from global minimum to influence the variance by 1.00%.  $A_{enzymes,1,1}^{(AB)}$  has highest tolerance for the uncertainty variation values; it has  $10^{-1}$  of value to effect the change.

Table B.6: PK values for gender influence on 5-FU

Gender	$A_{5FU,1,0}^{(AB)}$	$B_{5FU,1,0}^{(AB)}$	$k_{5FU,1,0}^{(AB)}$	$\Gamma_{5FU,1,0}^{(AB)}$	$V_d(\frac{L}{m^2})$	$S_p$
men	1.050(22)	1.293(43)	0.1398(37)	0.00022(28)	10.49(55)	14.489
women	1.0164(23)	1.134(31)	0.1098(26)	0.00021(24)	10.56(61)	5.1027
combined	0.9967(33)	1.148(41)	0.1414(23)	0.00033(27)	10.70(59)	13.259

The unit of  $k_{5FU,1,0}^{(AB)}$  and  $\Gamma_{5FU,1,0}^{(AB)}$  are  $\frac{\mu\text{mol}^{(1-A)}}{m^{(2-2B)}\text{min}}$  and  $\frac{m^{2B}}{\mu\text{mol}^{(-B)}}$  respectively.  $S$  represents  $S_p$  and  $S_\sigma(\frac{\mu\text{mol}^2}{L^2})$ . Var represents variance.

Table B.7: PK values for gender influence on DHFU

Variance	Parameters	men	women	combined
$S_{\sigma}$	$k_{D,1,0}^{(AB)}$	0.3590(21)	0.4780(23)	0.4009(23)
	$\Gamma_{D,1,0}^{(AB)}$	0.0074(34)	0.0117(32)	0.0093(30)
	$k_{cmp,1,1}^{(AB)}$	0.0186(16)	0.0264(13)	0.0177(15)
	$\Gamma_{cmp,1,1}^{(AB)}$	0.0002(33)	0.0005(40)	0.0002(38)
	$V_d(\frac{L}{m^2})$	5.002(34)	5.193(29)	5.193(35)
	$S_{\sigma}$		0.2826	1.0001

A and B are represent corresponding order process for DHFU and complex:  $A_{D,1,0}^{(AB)}$ ,  $B_{D,1,0}^{(AB)}$ ,  $A_{cmp,1,0}^{(AB)}$  and  $B_{cmp,1,0}^{(AB)}$  respectively. D and cmp represent DHFU and complex-substrate respectively;  $k_{d1,1,0}^{(AB)}$  unit is  $\frac{\mu mol^{(1-A)}}{m^{(2-2A)} min}$ ;  $\Gamma_{d1,1,1}^{(AB)}$  is  $\frac{m^{2B}}{\mu mol^B}$ ;  $S_{\sigma}$  measured in  $\frac{\mu mol^2}{L^2}$ .

Table B.8: PK values for age influence on 5-FU

Var	Age	$A_{5FU,1,0}^{(AB)}$	$B_{5FU,1,0}^{(AB)}$	$k_{5FU,1,0}^{(AB)}$	$\Gamma_{5FU,1,0}^{(AB)}$	$V_d(\frac{L}{m^2})$	S
$S_{\sigma}$	< 70 yrs	0.980(23)	1.163(24)	0.1688(39)	0.00024(51)	10.14(44)	9.418
	≥ 70 yrs	1.011(21)	1.1443(27)	0.1334(27)	0.00029(66)	10.26(48)	6.7112
	combined	0.997(23)	1.1482(22)	0.1414(29)	0.00030(57)	10.68(53)	13.260

The unit of  $k_{5FU,1,0}^{(AB)}$  and  $\Gamma_{5FU,1,0}^{(AB)}$  are  $\frac{\mu mol^{(1-A)}}{m^{(2-2B)} min}$  and  $\frac{m^{2B}}{\mu mol^{(-B)}}$  respectively. S represents  $S_p$  and  $S_{\sigma}(\frac{\mu mol^2}{L^2})$ . Var represent Variance

Table B.9: PK values for age influence on DHFU

Variance	Parameters	< 70 yrs	≥ 70 yrs	combined
$S_{\sigma}$	$k_{D,1,0}^{(AB)}$	0.3219(27)	0.3286(24)	0.4009(30)
	$\Gamma_{D,1,0}^{(AB)}$	0.0074(33)	0.0067(30)	0.0093(40)
	$k_{cmp,1,1}^{(AB)}$	0.0114(17)	0.0237(21)	0.0177(19)
	$\Gamma_{cmp,1,1}^{(AB)}$	0.0001(42)	0.0004(55)	0.0002(48)
	$V_d(\frac{L}{m^2})$	5.099(33)	5.090(47)	5.193(37)
	$S_{\sigma}$		0.1434	1.3382

A and B are represent corresponding order process for DHFU and complex:  $A_{D,1,0}^{(AB)}$ ,  $B_{D,1,0}^{(AB)}$ ,  $A_{cmp,1,0}^{(AB)}$  and  $B_{cmp,1,0}^{(AB)}$  respectively. D and cmp represent DHFU and complex-substrate respectively;  $k_{d1,1,0}^{(AB)}$  unit is  $\frac{\mu mol^{(1-A)}}{m^{(2-2A)} min}$ ;  $\Gamma_{d1,1,1}^{(AB)}$  is  $\frac{m^{2B}}{\mu mol^B}$ ;  $S_{\sigma}$  measured in  $\frac{\mu mol^2}{L^2}$ .

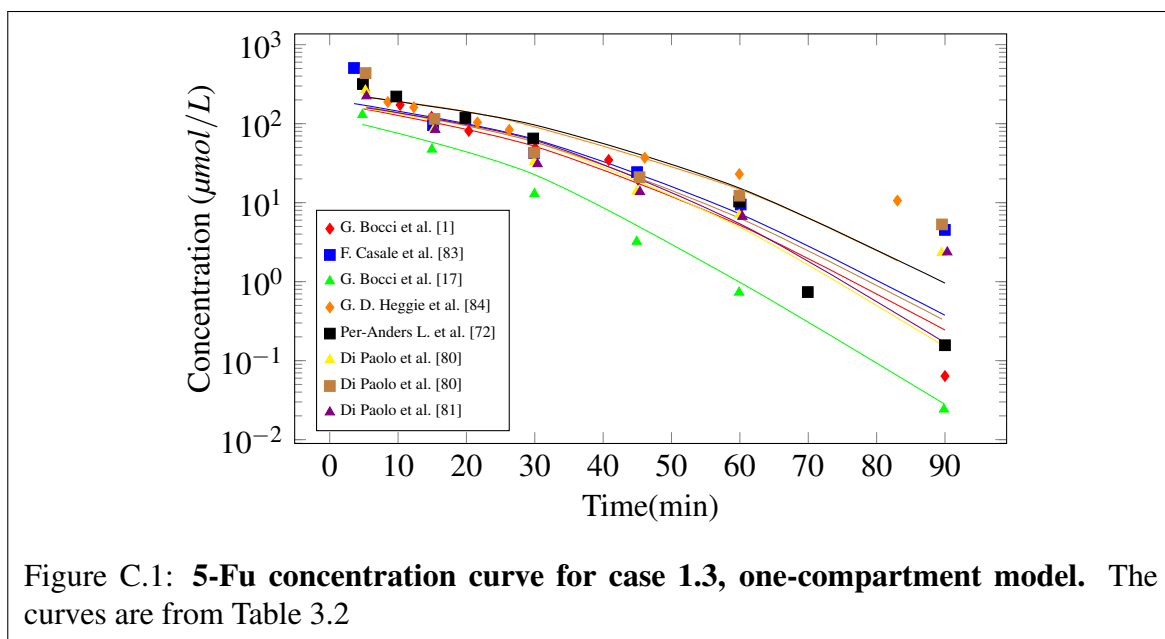
We examined comparison between the theoretical solution and experimental results using  $S_{\sigma}$ , there is correlation between the numbers 28.34% for young age and 13.87% for old age group. Comparing the  $AUC$  and the  $C_{max}$  for DHFU between the two groups, we obtained from our theoretical solution  $2277 \frac{min \cdot \mu mol}{L}$  and  $31.22 \frac{\mu mol}{L}$  for old age group and  $1918 \frac{min \cdot \mu mol}{L}$  and  $25.94 \frac{\mu mol}{L}$  for young age group respectively, compared to the experimental values of  $1910 \pm 1061 \frac{min \cdot \mu mol}{L}$  and  $31.98 \pm 16.91 \frac{\mu mol}{L}$  for old age group and  $1541 \pm$

$788.8 \frac{\text{min.}\mu\text{mol}}{\text{L}}$  and  $26.60 \pm 12.15 \frac{\mu\text{mol}}{\text{L}}$  for young age group respectively. See Table 5.14 and Table 5.11.

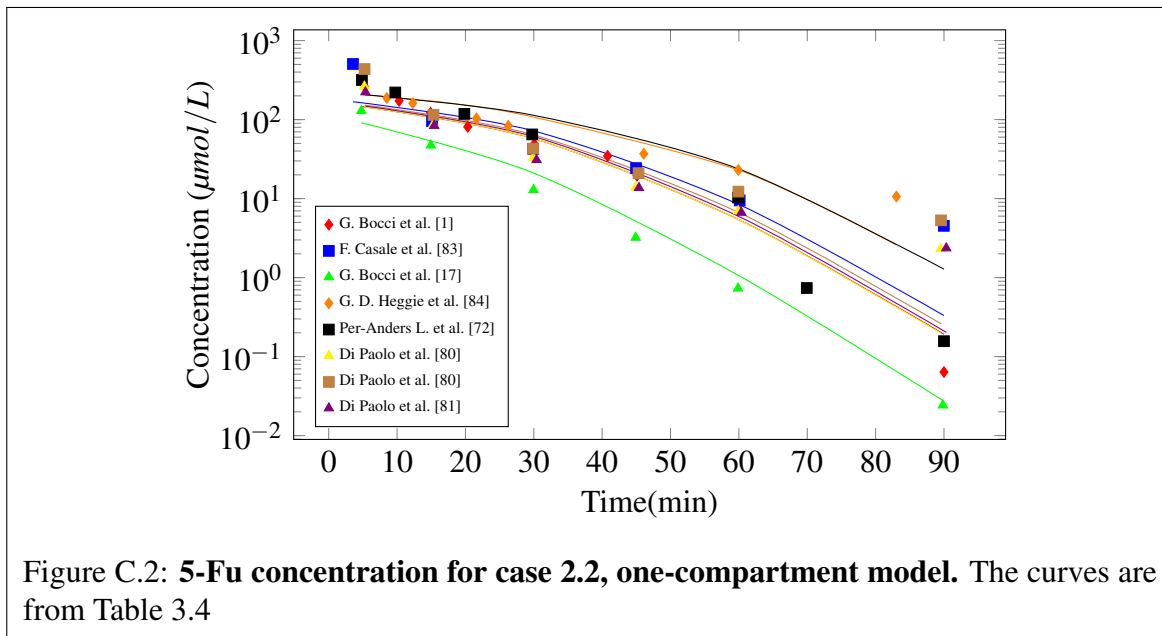
# Appendix C

## Graphs

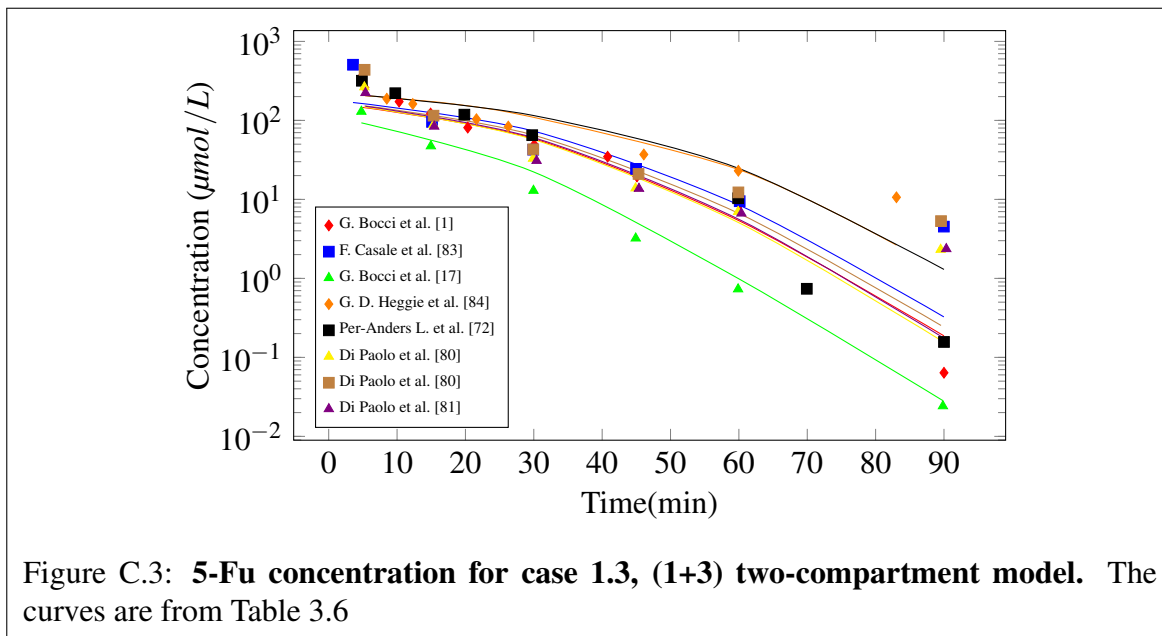
The complete graphical analyses for comparison between the theoretical solution and experimental data. It involved all the eight datasets that are plotted in semi-log. The experimental data are from the studies shown in Table 3.1 for 5-Fu model with 437 patients and 32 data points for the entire studies. Whereas, Table 4.1 shows the clinical data used for DHFU minimization. There are 433 patients and 42 data points in the data for DHFU modelling. The PK parameters are shown in Table 3.2.



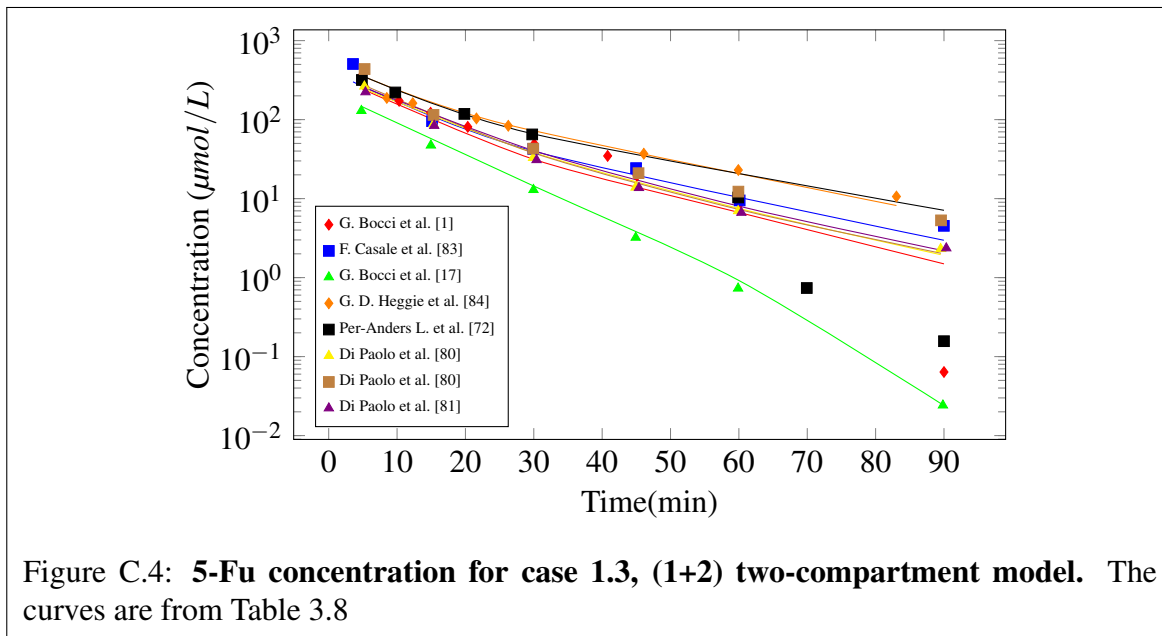
Case 1.3 is the best fit we obtained in the fixed exponents minimization of the one-compartment model for 5-Fu. The  $S_p$  obtained is 0.0696. Figure C.1 is the graph that comprises all the eight datasets that were minimized. The  $C_{max}$  seemed to be lower in the theoretical solution compared to all the clinical estimates.



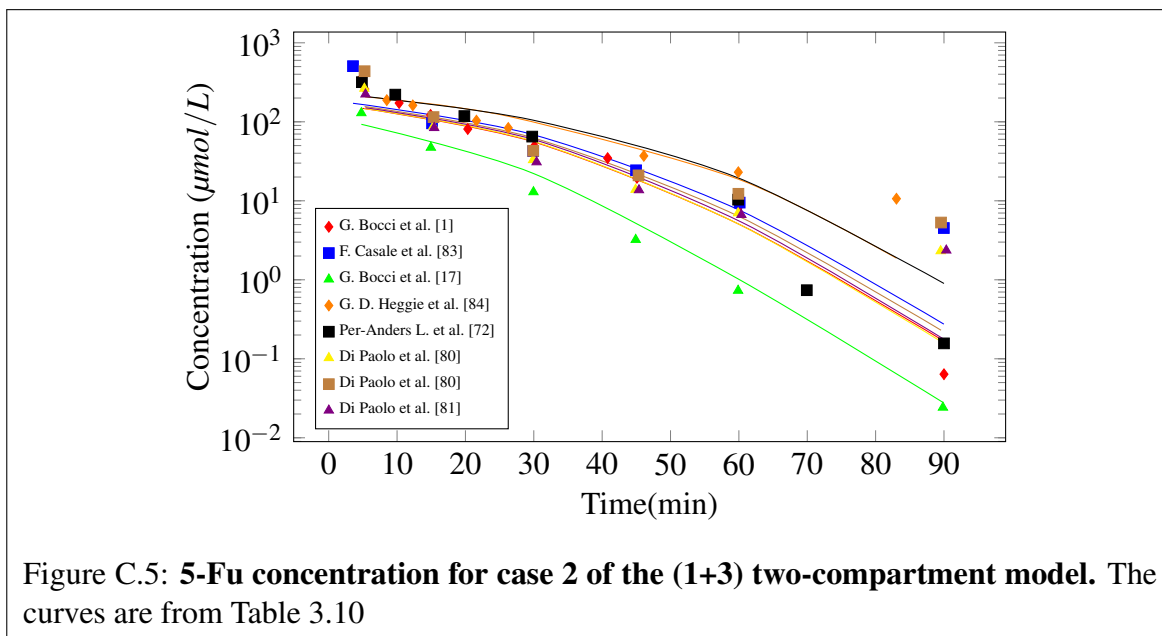
Case 2.2 is the best fit we obtained in the variable exponents minimization of the one-compartment model for 5-Fu. The  $S_p$  obtained is 0.0682. It has a better fit compare to case 1.3 of one-compartment model by 2.01%. Figure C.2 shows the graph that comprises all the eight datasets that were minimized.



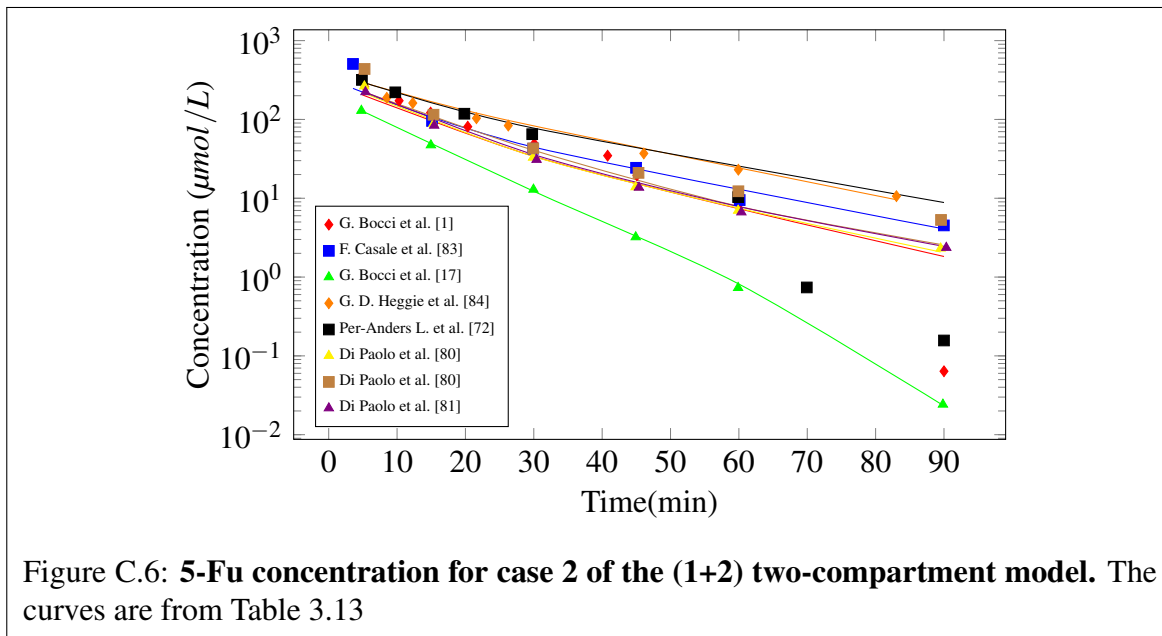
Case 1.3 is the best fit we obtained in the fixed exponents minimization of the (1+3) two-compartment model for 5-Fu. The  $S_p$  obtained is 0.0688. It has a better fit compare to case 1.3 of one-compartment model by 1.15%. Figure C.3 shows the graph that comprises all the eight datasets that were minimized.



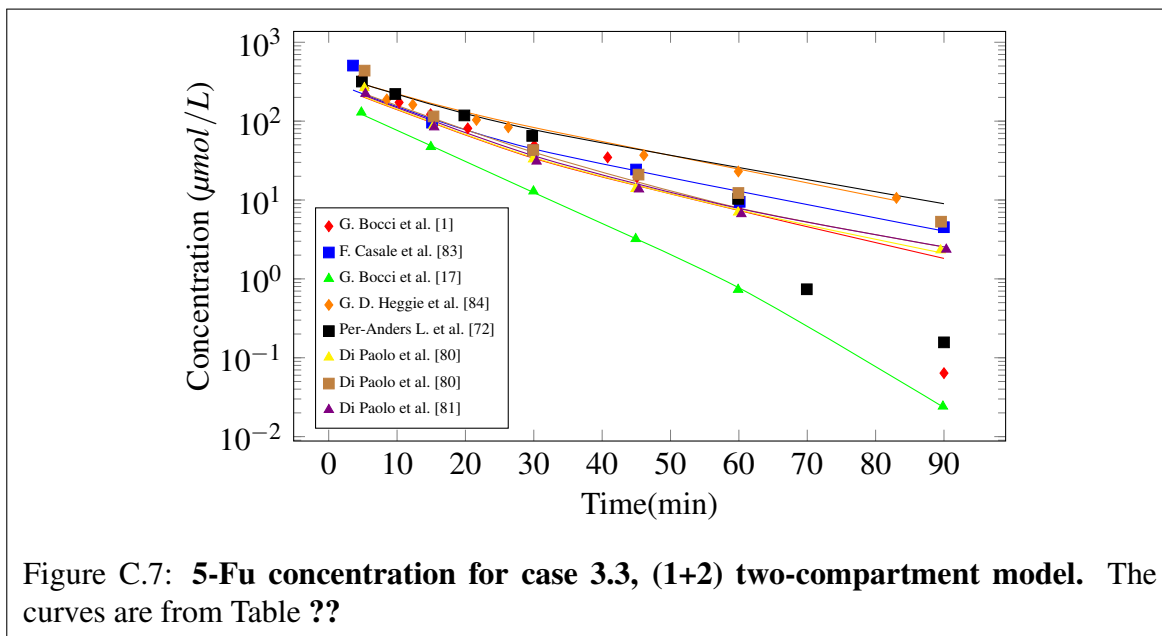
Case 1.3 has the best fit in the fixed exponents minimization of the two-compartment model for 5-Fu. The  $S_p$  obtained is 0.0138. It has a better fit compare to case 1.3 of one-compartment model by 80.17%. Figure C.4 shows the graph that comprises all the eight datasets that were minimized.



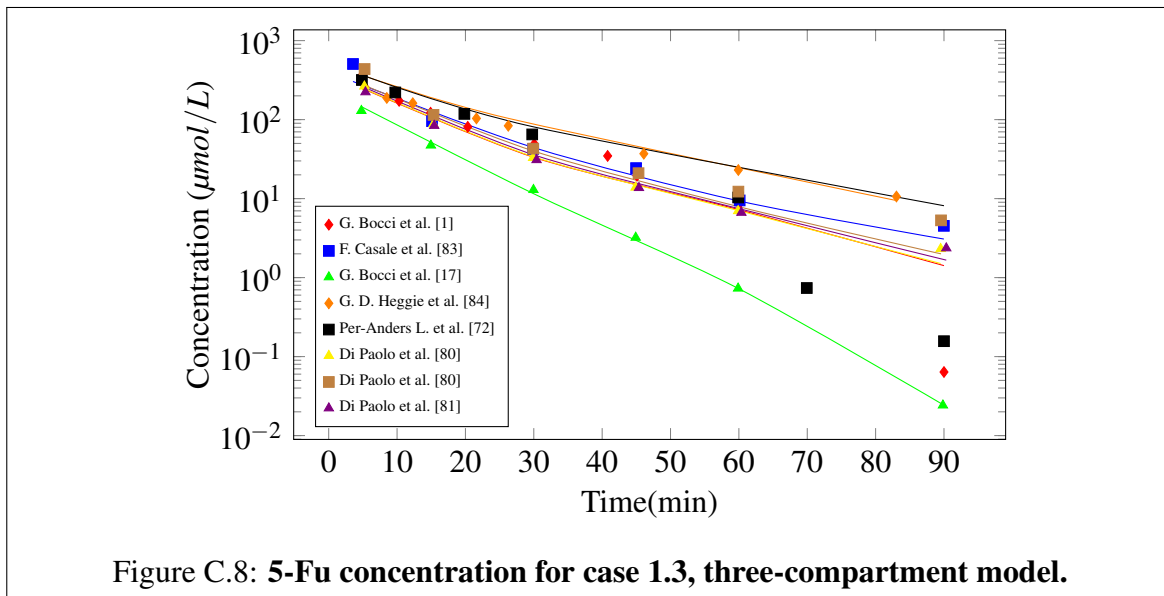
In the variable exponents minimization, case 1.3 has the best fit for the two-compartment model for 5-Fu. The  $S_p$  obtained is 0.0679. It has a better fit compare to case 2 of one-compartment model by 1.30%. Figure C.5 shows the graph that comprises all the eight datasets that were minimized.



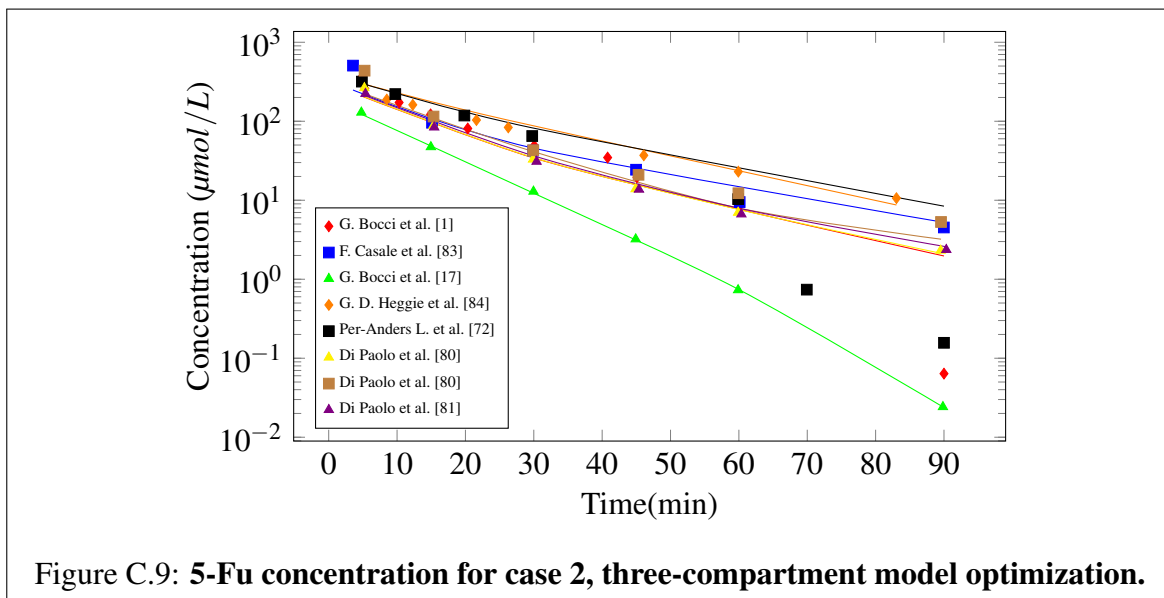
The  $S_p$  obtained in case 2 of the (1+2) two-compartment model has a better fit when it is compared to case 1.3 of (1+2) two compartment model by 0.69%. There were insignificant contributions from the subordinate cases. Figure C.6 shows the graph that comprises all the eight datasets that were minimized.



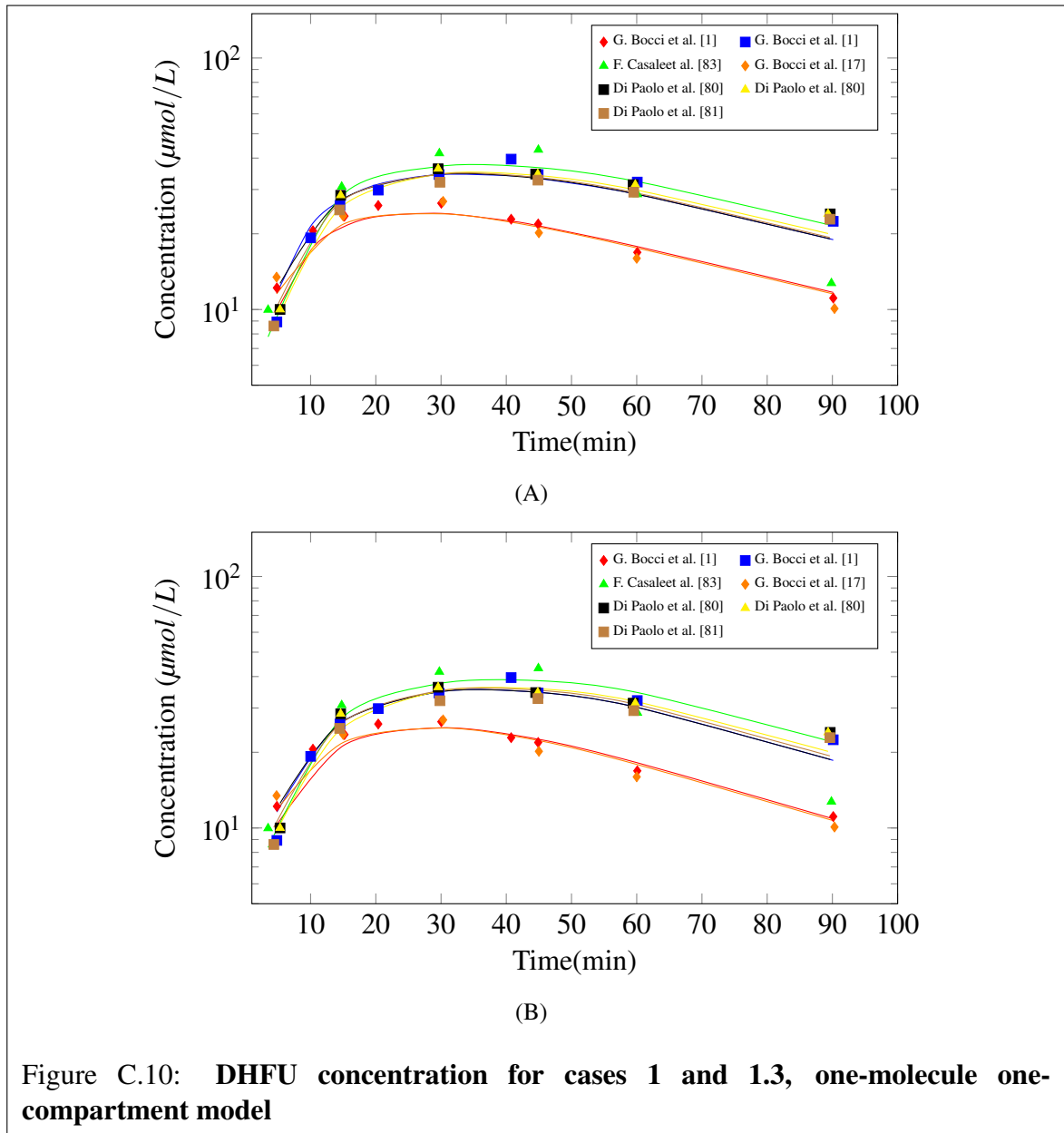
The addition of the saturation limiting function to the model function was examined and indicated that there is insignificant contribution from the additional function. The  $S_p$  obtained is the same as we have it in case 2 of the (1+2) two-compartment model as a better fit with  $S_p = 0.0127$ . There were insignificant contributions from the subordinate cases. Figure C.7 shows the graph that comprises all the eight datasets that were minimized.



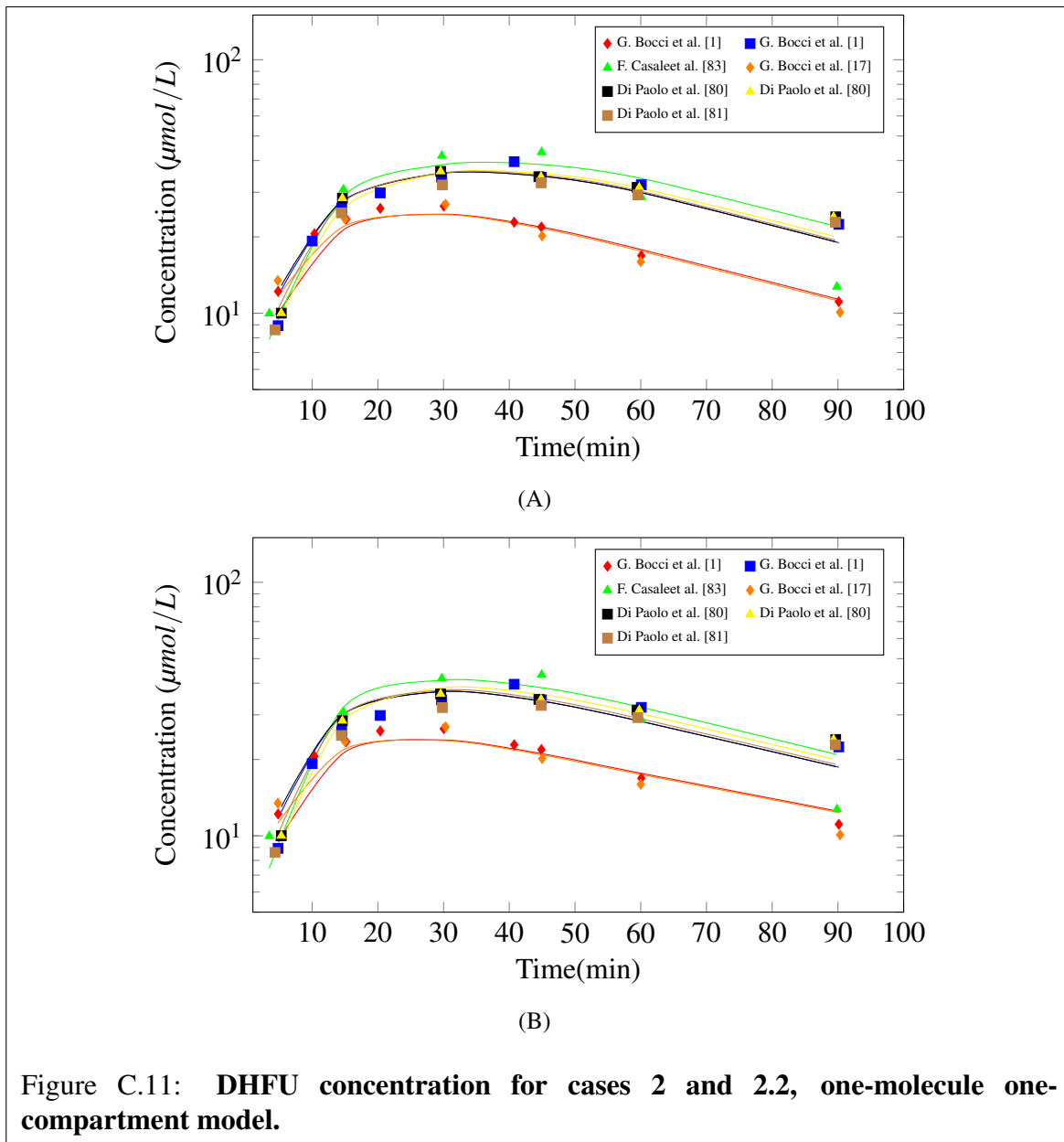
In the fixed exponents of the three compartment model, there is no improvement in  $S_p$  when it is compared with case 2 of the (1+2) two-compartment model. The  $S_p$  obtained is the same as we have it in case 2 of the (1+2) two-compartment model as a better fit with  $S_p = 0.0127$ . There were insignificant contributions from the subordinate cases as well. Figure C.8 shows the graph that comprises all the eight datasets that were minimized.



In the variable exponents of the three compartment model shows no improvement in  $S_p$  when it is compared with case 2 of the (1+2) two-compartment model. The  $S_p$  obtained is nearly the same as we have it in case 2 of the (1+2) two-compartment model as a better fit with  $S_p = 0.0127$ . There were insignificant contributions from the subordinate cases as well. Figure C.9 shows the graph that comprises all the eight datasets that were minimized.

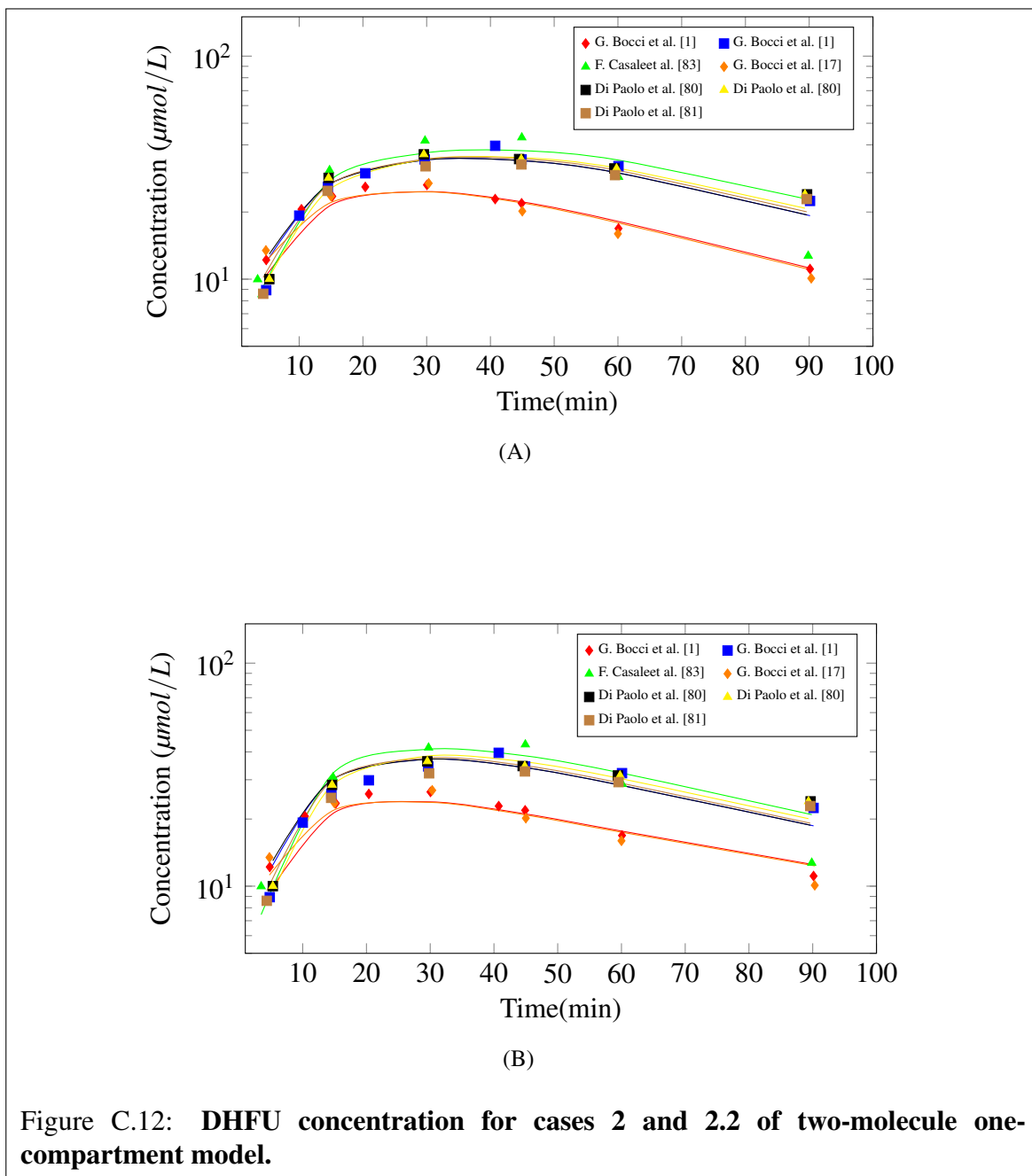


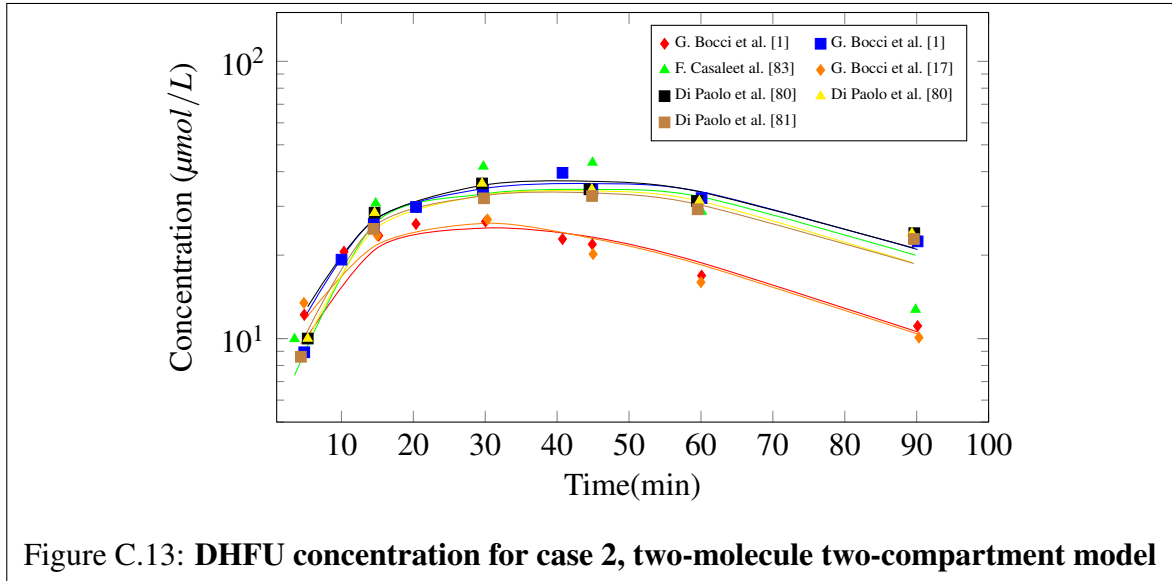
In the fixed exponents of the one-compartment model for DHFU, there is no improvement in  $S_p$  when it is compared with case 1 and case 1.3 of the one-compartment model. The  $S_p$  obtained is 0.0021. Figure C.10 shows the graph that comprises all the eight datasets that were minimized for both cases 1 and 1.3.



In the variable exponents of the one-molecule one-compartment model for DHFU, there is a slight improvement in  $S_p$  when it is compared with case 1 of the one-molecule one-compartment model. The  $S_p$  obtained is 0.0020. Figure C.11 shows the graph that comprises all the eight datasets that were minimized for cases 2 and 2.2.

Examining variable exponents minimization for the two-molecule one-compartment model for DHFU, there is an improvement 4.76% in  $S_p$  when we compare case 2 of the two-molecule one-compartment model to case 2 of the one-molecule one-compartment model. The  $S_p$  obtained is 0.0020. Figure C.12 shows the graph that comprises all the eight datasets that were minimized.





Case 2 of the two-molecule two-compartment model for DHFU, there is no significant improvement observed in  $S_p$ . The  $S_p$  obtained is 0.0020. Figure C.13 shows the graph that comprises all the eight datasets that were minimized.

# Appendix D

## Tables

The tables that are shown in this chapter comprises of the data points of clinical datasets used for minimization.

Table D.1: Digitized clinical datasets for 5-Fu

Datasets	<i>Time(min)</i>	$C_{5FU,1} (\frac{\mu mol}{L})$	Datasets	<i>Time(min)</i>	$C_{5FU,1} (\frac{\mu mol}{L})$
1. Guido Bocci et al. [17]	4.639175258	129.2948226	2. Di Paolo et al. [80]	5.217305866	263.9189696
	14.84536082	47.23054479		15.31392264	87.84886076
	29.92268041	12.91576701		29.89290276	32.88896851
	45.00324221	3.21621629		44.88651623	13.86275827
	60.07731959	0.73043655		59.89192022	6.981399137
	90.69587629	0.02418641		89.51364098	2.312660603
3. Di Paolo et al. [81]	5.376804492	223.0982557	4. Di Paolo et al. [80]	5.250712344	436.9871144
	15.43262637	83.79124709		15.33160842	114.7298073
	30.40597477	30.87920474		29.91058854	42.95269156
	45.38425106	13.68653968		45.32080045	20.99700229
	60.36499128	6.652750947		59.92925687	12.26605663
	90.33731305	2.35922139		89.56866341	5.306577728
5. Bocci G. et al. [1]	4.92110094	370.4530848	8. Heggie et al. [84]	5.30203011	257.2463768
	10.30149084	177.2985581		8.50023112	187.6811594
	14.90676606	125.4062972		12.30092111	163.0434783
	20.34185778	85.04564981		21.61182436	103.5746395
	30.07310778	51.8922609		26.26820585	83.56528932
	40.80189222	37.47774399		46.09342971	37.01945553
	45.09030966	23.06322707		59.92016399	23.01578739
	60.1142202	12.97306523		83.04671486	10.63199914
	90.00051606	2.882903384		118.2004531	0.219243356
7. Per-Anders et al. [72]	4.855428782	317.5384615	6. Casale et al. [83]	3.554315987	506.2867474
	9.738373206	220.80021350		15.11682247	95.6538572
	19.8437247	118.1538462		29.91689076	42.56984718
	29.76883327	64.98461538		44.95940447	24.34237439
	59.88949577	10.33846154		60.11873151	9.486656234
	69.93332352	0.738461538		89.98212588	4.521919462
			120.0029822	0.0071243	

Table D.2: Digitized clinical datasets for DHFU

Datasets	Time(min)	$C_{DHFU,1}$ ( $\frac{\mu\text{mol}}{\text{L}}$ )	Datasets	Time(min)	$C_{DHFU,1}$ ( $\frac{\mu\text{mol}}{\text{L}}$ )
1. Guido Bocci et al. [17]	4.787203944	13.66709752	2. Di Paolo et al. [80]	4.649446494	10.16648565
	14.99990569	23.91742066		14.61254613	28.9065798
	30.31895831	27.33419504		29.55719557	36.8584957
	44.99971707	20.50064628		44.50184502	35.10988662
	59.99962276	16.22967831		59.44649446	31.85760096
	90.31858107	10.25032314		89.66789668	24.38473731
			179.6678967	9.922400717	
3. Di Paolo et al. [81]	4.364067205	8.737925026	4. Di Paolo et al. [80]	4.317343173	10.16648565
	14.45967516	25.28039793		14.61254613	28.21256805
	29.82869555	32.57496081		29.55719557	35.97356814
	44.85708174	33.21644364		44.83394834	35.97356814
	59.54088433	29.74336366		59.77859779	31.85760096
	89.6085175	23.22911753		89.33579336	22.1259396
179.4697955	8.987304524	179.6678967	2.25329104		
5. Bocci G. et al. [1]	4.83452737	12.38887977	6. Bocci G. et al. [1]	4.83452737	9.07042983
	10.35970151	20.90623461		10.01437812	19.57885463
	15.19422888	23.89283955		14.50358211	26.32636951
	20.37407963	26.32636951		20.37407963	30.30850943
	30.04313437	26.8794445		29.69781099	34.95433935
	40.74815926	23.22914957		40.74815926	40.26385925
	44.89203986	22.23361458		44.89203986	34.95433935
	60.08626874	17.14532468		60.08626874	32.63142439
	90.12940311	11.28272979		90.12940311	22.78668957
	120.5178609	7.189974865		120.5178609	14.93302472
	180.2588062	3.539679934		180.6041296	6.526284878
240.3450749	1.880454965	239.9997516	2.544144952		
			7. Casale et al. [83]	3.487174392	10.1338422
				14.76920919	31.27513368
				29.74354629	42.45730438
				44.92301129	43.85507571
				60.10247629	29.17847667
				89.84602258	12.92938487
			119.9998247	8.910792276	

Table D.3: Digitized clinical datasets for 5-Fu comparison

Datasets	$Time(min)$	$C_{5FU,1} (\frac{\mu mol}{L})$	Datasets	$Time(min)$	$C_{5FU,1} (\frac{\mu mol}{L})$
1. Guido Bocci et al. [17]	4.755782401	139.8208141	2. Maring J. G. et al. [?]	2.260773485	311.7524674
	10.26334152	70.6311329		5.086045997	236.524728
	15.04199509	41.80209906		10.10699436	140.6480248
	20.40224835	23.06322707		20.17065037	71.06941227
	30.05814705	10.09016184		29.90566123	29.08272646
	40.70771417	5.765806767		45.32781229	12.48709331
	45.08360253	4.765806767		60.43912124	5.814838439
	60.11035017	0.882903384		79.97540988	2.887980321

Table D.4: Digitized clinical datasets for DHFU comparison from Maring J. G. et al.[79]

Datasets	$Time(min)$	$C_{DHFU,1} (\frac{\mu mol}{L})$	Datasets	$Time(min)$	$C_{DHFU,1} (\frac{\mu mol}{L})$
1. Control metastasis group	2.023399452	6.346290004	2. Liver metastasis group	2.027355686	6.771861707
	4.891201479	9.674072892		5.211934161	10.49130987
	9.976438642	16.51673289		10.28728074	15.22909474
	20.10932875	25.98759826		20.10240534	23.1972687
	30.22144862	29.08173211		30.21056898	24.32779861
	45.064445	29.51001371		45.36737462	23.89698007
	60.2172944	27.16573465		60.51132251	19.0095436
	80.09112972	19.27960347		80.38515783	13.49113019
	100.2787743	13.24542228		100.2649275	10.5537603
	120.1516206	9.249013433		120.1308503	6.578207014
	150.1266961	6.14481371		150.4276476	4.817128683
	180.433384	5.292487594		180.4066794	3.414992273